Comparison of the modes of action of Apremilast and Roflumilast

by

Nicola Margaret Walsh B.Sc., M.Res.

A thesis submitted in fulfilment of the requirements for the degree of Doctor of Philosophy

Institute of Cardiovascular and Medical Sciences
College of Medical, Veterinary and Life Sciences
University of Glasgow
November 2015

Abstract

The phosphodiesterase 4 (PDE4) family are cAMP specific phosphodiesterases that play an important role in the inflammatory response and is the major PDE type found in inflammatory cells. A significant number of PDE4 specific inhibitors have been developed and are currently being investigated for use as therapeutic agents. Apremilast, a small molecule inhibitor of PDE 4 is in development for chronic inflammatory disorders and has shown promise for the treatment of psoriasis, psoriatic arthritis as well as other inflammatory diseases. It has been found to be safe and well tolerated in humans and in March 2014 it was approved by the US food and drug administration for the treatment of adult patients with active psoriatic arthritis. The only other PDE4 inhibitor on the market is Roflumilast and it is used for treatment of respiratory disease. Roflumilast is approved in the EU for the treatment of COPD and was recently approved in the US for treatment to reduce the risk of COPD exacerbations. Roflumilast is also a selective PDE4 inhibitor, administered as an oral tablet once daily, and is thought to act by increasing cAMP within lung cells. As both (Apremilast and Roflumilast) compounds selectively inhibit PDE4 but are targeted at different diseases, there is a need for a clear understanding of their mechanism of action (MOA). Differences and similarity of MOA should be defined for the purposes of labelling, for communication to the scientific community, physicians, and patients, and for an extension of utility to other diseases and therapeutic areas. In order to obtain a complete comparative picture of the MOA of both inhibitors, additional molecular and cellular biology studies are required to more fully elucidate the signalling mediators downstream of PDE4 inhibition which result in alterations in pro- and anti-inflammatory gene expression. My studies were conducted to directly compare Apremilast with Roflumilast, in order to substantiate the differences observed in the molecular and cellular effects of these compounds, and to search for other possible differentiating effects. Therefore the main aim of this thesis was to utilise cutting-edge biochemical techniques to discover whether Apremilast and Roflumilast work with different modes of action.

In the first part of my thesis I used novel genetically encoded FRET based cAMP sensors targeted to different intracellular compartments, in order to monitor cAMP levels within specific microdomains of cells as a consequence of challenge

with Apremilast and Roflumilast, which revealed that Apremilast and Roflumilast do regulate different pools of cAMP in cells.

In the second part of my thesis I focussed on assessing whether Apremilast and Roflumilast cause differential effects on the PKA phosphorylation state of proteins in cells. I used various biochemical techniques (Western blotting, Substrate kinase arrays and Reverse Phase Protein array and found that Apremilast and Roflumilast do lead to differential PKA substrate phosphorylation. For example I found that Apremilast increases the phosphorylation of Ribosomal Protein S6 at Ser240/244 and Fyn Y530 in the S6 Ribosomal pathway of Rheumatoid Arthritis Synovial fibroblast and HEK293 cells, whereas Roflumilast does not. This data suggests that Apremilast has distinct biological effects from that of Roflumilast and could represent a new therapeutic role for Apremilast in other diseases.

In the final part of my thesis, Phage display technology was employed in order to identify any novel binding motifs that associate with PDE4 and to identify sequences that were differentially regulated by the inhibitors in an attempt to find binding motifs that may exist in previously characterised signalling proteins. Petide array technology was then used to confirm binding of specific peptide sequences or motifs. Results showed that Apremilast and Roflumilast can either enhance or decrease the binding of PDE4A4 to specific peptide sequences or motifs that are found in a variety of proteins in the human proteome, most interestingly Ubiquitin-related proteins. The data from this chapter is preliminary but may be used in the discovery of novel binding partners for PDE4 or to provide a new role for PDE inhibition in disease.

Therefore the work in this thesis provides a unique snapshot of the complexity of the cAMP signalling system and is the first to directly compare action of the two approved PDE4 inhibitors in a detailed way.

Table of Contents

Abstract....2
List of Tables....7
List of Figures....8
Acknowledgement....17
Author's Declaration....18
Definitions/Abbreviations....19
1 Introduction....24
1.1 Cyclic 3' 5'- adenosine monophosphate (cAMP) signalling....24
1.1.1 cAMP generation....25
1.1.2 cAMP Compartmentalisation....29
1.2 Measurement of cAMP gradients using FRET....32
1.3 cAMP degradation by Phosphodiesterases....35
1.3.1 PDE Catalytic and Regulatory Domains....37
1.4 Phosphodiesterase 4 (PDE4)....39
1.4.1 N-terminal Region....39
1.4.2 Upstream conserved regions (UCRs)....39
1.4.3 Conserved Catalytic Domain....41
1.4.4 Unique C terminal Region....41
1.5 PDE4 and the Inflammatory Response....42
1.5.1 The PDE4/PKA signalling Pathway....42
1.5.2 Role of PDE4 in Psoriasis and Psoriatic Arthritis....44
1.6 PDE4 inhibitors and their use in Inflammatory Disease....45
1.6.1 Structural basis of Inhibitor binding to PDE4....46
1.6.2 The main chemical classes of PDE 4 inhibitors....47
1.6.3 Rolipram....49
1.6.4 Cilomilast....50
1.6.5 Roflumilast....51
1.6.6 Apremilast....52
1.6.7 Comparing Apremilast and Roflumilast....54
1.7 Thesis aims....58
2 Materials and Methods....60
2.1 Mammalian Cell Culture....60
2.1.1 HEK293 cells....60
2.1.2 Jurkat T and U937 cells....60
2.1.3 Rheumatoid Arthritis Synovial Fibroblasts....61

2.1.4 Transfection of cells for FRET analysis 61
2.1.5 PDE4 inhibitor treatments for western blotting analysis 62
2.1.6 Preparation of whole cell lysates..... 63
2.1.7 Protein Assay 63
2.2 Western Blot 63
2.2.1 SDS- PAGE 63
2.2.2 Western Immunoblotting..... 64
2.3 Fluorescence Resonance Energy Transfer (FRET) imaging..... 66
2.3.1 FRET based imaging..... 66
2.3.2 Fret Sensors 67
2.3.3 FRET Imaging Set up 67
2.3.4 Fret imaging acquisition 68
2.4 CelluSpots™ tyrosine kinase substrate arrays..... 71
2.5 Reverse Phase Protein Array preparation of cells 72
2.6 Phage Display 86
2.7 Solid Phase Peptide Array and overlay experiments..... 86
2.8 Basic Local Alignment Search Tool (BLAST) 87
2.9 Multiple Em for Motif Elicitation (MEME) 87
2.10 Statistical analysis..... 87
3 FRET imaging for real time cAMP dynamics in cells..... 88
3.1 Introduction..... 88
3.2 Specific Aims..... 90
3.3 Experimental Procedure 90
3.4 Results 91
3.5 Discussion 99
4 Profiling Signalling differences between Apremilast and Roflumilast..... 105
4.1 Comparing effects of Apremilast and Roflumilast on PKA phosphorylation states in cells 105
4.1.1 Introduction..... 105
4.1.2 Specific aims..... 106
4.1.3 Results 107
4.1.4 Discussion 110
4.2 CelluSpots™ - Kinase Substrate Arrays to potentially identify signalling differences 115
4.2.1 Results 116
4.2.2 Discussion 119
4.3 Reverse Phase Protein Array 121
4.3.1 Results 122
4.3.2 Discussion 136

5 Phage Display 139
5.1 Introduction 139
5.2 Discussion 148
6 Final Discussion and Future Perspectives 152
6.1 Final Conclusion 157
7 List of References 159

List of Tables

TABLE 1-1 REGULATORY PROPERTIES OF MEMBRANE-BOUND ACS. (SADANA AND DESSAUER 2009)..... 26
TABLE 1-2 TISSUE DISTRIBUTION OF ACS. ADAPTED FROM (SADANA AND DESSAUER 2009)..... 27
TABLE 1-3 SUMMARY OF THE CHARACTERISTICS OF THE 11 PDE FAMILIES. 36
TABLE 1-4 CLASSIFICATION OF PDE4 ISOFORMS 40
TABLE 1-5 IC_{50} VALUES OF THE COMPOUNDS AGAINST EXAMPLE PDE4 ISOFORMS FROM EACH OF THE FOUR PDE4 SUB-FAMILIES (STUDY BPS BIOSCIENCE CELGENE_PDE4_1001)..... 56
TABLE 1-6 . INHIBITION OF THE LOW AFFINITY AND HIGH AFFINITY FORMS OF PDE4A4 EXPRESSED IN COS7 CELLS..... 57
TABLE 2-1 LIST OF PRIMARY ANTIBODIES, THEIR SOURCE AND WORKING DILUTIONS. 65
TABLE 2-2 LIST OF SECONDARY ANTIBODIES, THEIR SOURCE AND WORKING DILUTIONS. 66
TABLE 2-3 TABLE OF AGONIST AND INHIBITOR TREATMENTS USED IN EXPERIMENTS..... 71
TABLE 2-4 TABLE OF ANTIBODIES USED IN RPPA 86
TABLE 3-1 TOP SCORING GENE TRANSCRIPT BIOGROUPS REGULATED CONCORDANTLY BY PDE4 INHIBITORS IN LPS-STIMULATED MONOCYTES (SCHAFER, PARTON ET AL. 2014)..... 101
TABLE 3-2 TOP-SCORING TRANSCRIPT BIOGROUPS REGULATED DISCORDANTLY BY APREMILAST VERSUS OTHER PDE4 INHBITORS IN LPS-STIMULATED MONOCYTES (SCHAFER, PARTON ET AL. 2014)..... 101
TABLE 4-1 PEPTIDE SEQUENCE INFORMATION OF PHOSPHORYLATED PEPTIDES ON TYROSINE KINASE SUBSTRATE ARRAYS FOLLOWED BY TREATMENT OF APREMILAST AND ROFLUMILAST IN RHEUMATOID ARTHRITIS SYNOVIAL FIBROBLASTS. 118
TABLE 5-1 BLAST SEARCH RESULTS FROM SELECTED BINDING SPOTS FROM PHAGE ARRAY DATA. THE NUMBER OF TIMES EACH PARTICULAR SEQUENCE IS BOUND TO PDE4A4 ALONE OR PDE4A4 BOUND TO APREMILAST OR ROFLUMILAST IS SHOWN IN THE LEFT HAND COLUMNS..... 145
TABLE 5-2 BLAST RESULTS FROM IDENTIFIED BINDING MOTIFS. 148

List of Figures

FIGURE 1-1 STRUCTURE OF THE SECOND MESSENGER CYCLIC ADENOSINE 3'5'-MONOPHOOSPHATE (CAMP). THE 3' BOND IS HYDROLYSED BY PHOSPHODIESTERASE (PDE) ENZYMES INDICATED BY THE ARROW (BENDER AND BEAVO 2006). 25

FIGURE 1-2 AN OVERVIEW OF CAMP SIGNALLING IN CELLS. CAMP IS PRODUCED FOLLOWING STIMULATION OF 7-TRANSMEMBRANE DOMAIN RECEPTORS (GPCRS) AT THE PLASMA MEMBRANE. THESE RECEPTORS COUPLE TO G-PROTEINS, WHICH ACTIVATE ADENYLYL CYCLASES LEADING TO THE CONVERSION OF ATP INTO CAMP. THE EFFECTS OF CAMP WITHIN THE CELL ARE MEDIATED BY THREE DISTINCT EFFECTOR PROTEINS: PKA, EPAC AND CYCLIC NUCLEOTIDE-CHANNELS. CAMP IS DEGRADED BY PHOSPHODIESTERASE ENZYMES. 7-TM, 7-TRANSMEMBRANE DOMAIN RECEPTOR; G, G-PROTEIN; AC, ADENYLYL CYCLASE; PKA, CAMP DEPENDENT PROTEIN KINASE A; PDE, PHOSPHODIESTERASE. 28

FIGURE 1-3 CONVERSION OF ATP TO CYLIC ADENOSINE 3'5'-MONOPHOSPHATE (CAMP) BY ADENYLYL CYCLASE ENZYMES. ADENYLYL CYCLASES CATALYSE THE CONVERSION OF ATP TO PYROPHOSPHATE (PPI) AND 3'5-CAMP, WHICH ACTS AS A SECOND MESSENGER IN CELLS. PDE HYDROLYSE THE CATALYTIC CLEAVAGE OF CAMP TO 5'AMP, TERMINATING THE CAMP SIGNAL (SECTION 1.3, (FIGURE 1-1). 28

FIGURE 1-4 ACTIVATION OF THE CAMP-DEPENDENT PROTEIN KINASE (PKA) IN RESPONSE TO INCREASED CAMP LEVELS. WHEN CAMP IS LOW, PKA EXISTS AS AN INACTIVE HETEROTETRAMER WITH AND R_2C_2 CONFORMATION. THE TWO CATALYTIC SUBUNITS ARE MAINTAINED IN AN INHIBITED STATE BY THE REGULATORY SUBUNITS. WHEN CAMP LEVELS ARE RAISED, CAMP BINDS TO THE R-SUBUNITS WITH 2:1 STOICHOMETRY. ACTIVE C-SUBUNITS ARE THEN RELEASED TO GO ON TO PHOSPHORYLATE THEIR DOWNSTREAM TARGETS WHICH ARE INVOLVED IN A DIVERSE RANGE OF BIOLOGICAL PROCESSES. ... 30

FIGURE 1-5 GENETIC ENGINEERING OF DIFFERENT FRET SENSORS TO MONITOR REAL TIME CHANGES IN CAMP LEVELS WITHIN CELLS. 34

FIGURE 1-6 DOMAIN STRUCTURES OF PDE FAMILIES 1-11. ADAPTED FROM (CONTI AND BEAVO 2007). THE 11 PDE FAMILIES SHOWN ARE GROUPED ACCORDING

TO THEIR DIFFERING STRUCTURES, KINETICS, TISSUE DISTRIBUTIONS AND MODES OF REGULATION..... 38
FIGURE 1-7 DOMAIN STRUCTURES OF PDE4 ISOFORMS (HOUSLAY 2010). 41
FIGURE 1-8 THE PDE4/PKA SIGNALLING PATHWAY. ADAPTED FROM (SCHAFER, PARTON ET AL. 2010). 44
FIGURE 1-9 CLASSIFICATION OF THE ACTIVE SITE OF PDES 47
FIGURE 1-10 STRUCTURES OF A, B, C AND D (MODIFIED FROM (DAL PIAZ AND GIOVANNONI 2000). 49
FIGURE 1-11 CHEMICAL STRUCTURES OF THE PDE4 INHIBITORS APREMILAST, ROLIPRAM, CILOMILAST AND ROFLUMILAST 53
FIGURE 1-12 AN OVERVIEW OF PROPOSED MECHANISM OF ACTION OF APREMILAST IN VARIOUS CELL TYPES DERIVED FROM *IN VITRO* STUDIES. BY BLOCKING PDE4 ACTIVITY, APREMILAST AFFECTS SEVERAL CELL TYPES IN THE IMMUNE SYSTEM INCLUDING MONOCYTES, DENDRITIC CELLS , NEUTROPHILS, T CELLS, NATURAL KILLER CELLS AND MACROPHAGES (SAMRAO, BERRY ET AL. 2012). 54
FIGURE 1-13 INTRACELLULAR CAMP LEVELS IN PGE2-STIMULATED PBMC TREATED WITH VARIOUS PDE4 INHIBITORS (N=3) (DATA COURTESY OF CELGENE) 55
FIGURE 1-14 . SELECTIVITY OF APREMILAST AND ROFLUMILAST AGAINST RECOMBINANT HUMAN PDE ENZYMES (DATA COURTESY OF CELGENE) 55
FIGURE 1-15 COLOCALIZATION OF PDE4A4B (PDE46) WITH THE KINASE LYN (MCPHEE, YARWOOD ET AL. 1999). 57
FIGURE 3-1 PKA-RI AND PKA-RII LOCALIZING PROBES BASED ON THE AKAP-BINDING DOMAIN OF PKA-RIA OR PKA-RIIB, FUSED TO THE CAMP-BINDING DOMAIN OF EPAC. (DI BENEDETTO, ZOCCARATO ET AL. 2008) EPAC1 CAMPS CYTOSOLIC LOCALIZING PROBE AND EPAC 1-NLS NUCLEAR LOCALIZING PROBE (NIKOLAEV, BUNEMANN ET AL. 2004). 89
FIGURE 3-2 APREMILAST STIMULATION OF HEK 293 CELLS INDUCES HIGHER CONCENTRATIONS OF CAMP IN THE CYTOSOL COMPARED TO ROFLUMILAST. (A-B) ARE REPRESENTATIVE IMAGES OF HEK CELLS TRANFECTED WITH THE CYTOSOLIC EPAC1-CAMPS SENSOR. (C) SUMMARY OF EXPERIMENTS PERFORMED N=18. ERROR BARS REPRESENT SEM * P <0.05. (D-E) REPRESENTATIVE KINETICS OF % FRET CHANGES GENERATED IN THE CYTOSOL UPON STIMULATION OF EITHER 10 µM APREMILAST OR 10 µM ROFLUMILAST FOLLOWED BY 100µM IBMX AND 25µM FORSKOLIN. VALUES ARE NORMALISED

TO THE RATIO VALUE AT TIME T=0 (R_O). D) SUMMARY OF EXPERIMENTS PERFORMED N=18. ERROR BARS REPRESENT SEM * P <0.05. (SCALE BAR 10μM). 92
FIGURE 3-3 APREMILAST STIMULATION OF HEK 293 CELLS INDUCES HIGHER CONCENTRATIONS OF CAMP IN THE PKA-R1 COMPARTMENT (CYTOSOLIC) COMPARED TO ROFLUMILAST. (A-B) ARE REPRESENTATIVE IMAGES OF HEK CELLS TRANFECTED WITH THE CYTOSOLIC ASSOCIATED R1-EPAC SENSOR. (C) SUMMARY OF EXPERIMENTS PERFORMED N=12. ERROR BARS REPRESENT SEM * P <0.05. (D-E) REPRESENTATIVE KINETICS OF % FRET CHANGES GENERATED IN THE CYTOSOL UPON STIMULATION OF EITHER 10 μM APREMILAST OR 10 μM ROFLUMILAST FOLLOWED BY 100μM IBMX AND 25μM FORSKOLIN. VALUES ARE NORMALISED TO THE RATIO VALUE AT TIME T=0 (R_O). D) SUMMARY OF EXPERIMENTS PERFORMED N=12. ERROR BARS REPRESENT SEM * P <0.05. (SCALE BAR 10μM). 93
FIGURE 3-4 ROFLLUMILAST STIMULATION OF HEK 293 CELLS INDUCES HIGHER CONCENTRATIONS CAMP IN THE PKA-R11 COMPARTMENT (MEMBRANE ASSOCIATED) COMPARED TO APREMILAST. (A-B) ARE REPRESENTATIVE IMAGES OF HEK CELLS TRANFECTED WITH THE MEMBRANE ASSOCIATED R11-EPAC SENSOR. (C) SUMMARY OF EXPERIMENTS PERFORMED N=14. ERROR BARS REPRESENT SEM * P <0.05. (D-E) REPRESENTATIVE KINETICS OF % FRET CHANGES GENERATED IN THE CYTOSOL UPON STIMULATION OF EITHER 10 μM APREMILAST OR 10 μM ROFLUMILAST FOLLOWED BY 100μM IBMX AND 25μM FORSKOLIN. VALUES ARE NORMALISED TO THE RATIO VALUE AT TIME T=0 (R_O). D) SUMMARY OF EXPERIMENTS PERFORMED N=14. ERROR BARS REPRESENT SEM * P <0.05. (SCALE BAR 10μM). 94
FIGURE 3-5 ROFLUMILAST STIMULATION OF JURKAT T CELLS INDUCES HIGHER CONCENTRATIONS OF CAMP IN THE CYTOSOL COMPARED TO APREMILAST. (A-B) ARE REPRESENTATIVE IMAGES OF JURKAT T CELLS TRANFECTED WITH THE CYTOSOLIC EPAC1-CAMPS SENSOR. (C) SUMMARY OF EXPERIMENTS PERFORMED N=14. ERROR BARS REPRESENT SEM * P <0.05. (D-E) REPRESENTATIVE KINETICS OF % FRET CHANGES GENERATED IN THE CYTOSOL UPON STIMULATION OF EITHER 10 μM APREMILAST OR 10 μM ROFLUMILAST FOLLOWED BY 100μM IBMX AND 25μM FORSKOLIN. VALUES ARE NORMALISED TO THE RATIO VALUE AT TIME T=0 (R_O). D) SUMMARY OF EXPERIMENTS

PERFORMED N=14. ERROR BARS REPRESENT SEM * P <0.05. (SCALE BAR 10μM). 96
FIGURE 3-6 APREMILAST STIMULATION OF RHEUMATOID ARTHRITIS SYNOVIAL FIBROBLAST CELLS INDUCES HIGHER CONCENTRATIONS OF CAMP IN THE CYTOSOL COMPARED TO ROFLUMILAST. (A-B) ARE REPRESENTATIVE IMAGES OF HEK CELLS TRANFECTED WITH THE CYTOSOLIC EPAC1-CAMPS SENSOR. (C) SUMMARY OF EXPERIMENTS PERFORMED N=18. ERROR BARS REPRESENT SEM * P <0.05. (D-E) REPRESENTATIVE KINETICS OF % FRET CHANGES GENERATED IN THE CYTOSOL UPON STIMULATION OF EITHER 10 μM APREMILAST OR 10 μM ROFLUMILAST FOLLOWED BY 100μM IBMX AND 25μM FORSKOLIN. VALUES ARE NORMALISED TO THE RATIO VALUE AT TIME T=0 (R_0). D) SUMMARY OF EXPERIMENTS PERFORMED N=18. ERROR BARS REPRESENT SEM **P <0.005. (SCALE BAR 10μM). 97
FIGURE 3-7 APREMILAST STIMULATION OF RHEUMATOID ARTHRITIS SYNOVIAL FIBROBLAST (RASF) CELLS HAS NO EFFECT ON CAMP PRODUCTION IN THE NUCLEUS WHEREAS ROFLUMILAST DOES STIMULATE CAMP PRODUCTION IN THE NUCLEUS. (A-B) ARE REPRESENTATIVE IMAGES OF RASF CELLS TRANSFECTED WITH THE NUCLEAR LOCALISED EPAC1-NLS CAMPS SENSOR. (C) SUMMARY OF EXPERIMENTS PERFORMED N=12. ERROR BARS REPRESENT SEM * P <0.05. (D-E) REPRESENTATIVE KINETICS OF % FRET CHANGES GENERATED IN THE CYTOSOL UPON STIMULATION OF EITHER 10 μM APREMILAST OR 10 μM ROFLUMILAST FOLLOWED BY 100μM IBMX AND 25μM FORSKOLIN. VALUES ARE NORMALISED TO THE RATIO VALUE AT TIME T=0 (R_0). D) SUMMARY OF EXPERIMENTS PERFORMED N=12. ERROR BARS REPRESENT SEM ***P <0.0005. (SCALE BAR 10μM). 98
FIGURE 4-1 EFFECT OF APREMILAST AND ROFLUMILAST ON CREB PHOSPHORYLATION. A-C WESTERN BLOT ANALYSIS OF CREB PROTEIN SER133 PHOSPHORYLATION IN A) U937 CELLS B) HEK 293 CELLS AND C) JURKAT T CELLS. A REPRESENTATIVE WESTERN BLOT IS PRESENTED WITH EACH GRAPH. ALL TREATMENT GROUPS WERE COMPARED WITH DMSO BY ONE-WAY ANOVA FOLLOWED BY DUNN'S MULTIPLE COMPARISON POST- TEST (N=3. NO STATISTICALLY SIGNIFICANT DIFFERENCES WERE OBSERVED BETWEEN APREMILAST AND ROFLUMILAST. *P<0.05 VERSUS DMSO, **P<0.01 VERSUS DMSO, 30-MINUTE STIMULATION WITH DRUG..... 108

FIGURE 4-2 EFFECT OF APREMILAST AND ROFLUMILAST ON PKA PHOSPHORYLATION. WESTERN BLOT ANALYSIS OF PKA SUBSTRATE PHOSPHORYLATION (R-X-X-P S/T) IN JURKAT T CELLS. A REPRESENTATIVE WESTERN BLOT IS PRESENTED WITH GRAPH. ALL TREATMENT GROUPS WERE COMPARED WITH DMSO BY ONE-WAY ANOVA FOLLOWED BY DUNN'S MULTIPLE COMPARISON POST- TEST (N=3). NO STATISTICALLY SIGNIFICANT DIFFERENCES WERE OBSERVED BETWEEN APREMILAST AND ROFLUMILAST. 30-MINUTE STIMULATION WITH DRUG. 109
FIGURE 4-3 EFFECT OF APREMILAST AND ROFLUMILAST ON THE PHOSPHORYLATION OF VASP AT SER157. A-B WESTERN BLOT ANALYSIS OF VASP PHOSPHORYLATION AT SER133 IN A) U937 CELLS AND B) HEK 293 CELLS. A REPRESENTATIVE WESTERN BLOT IS PRESENTED WITH EACH GRAPH. ALL TREATMENT GROUPS WERE COMPARED WITH DMSO BY ONE-WAY ANOVA FOLLOWED BY DUNN'S MULTIPLE COMPARISON POST- TEST (N=3). NO STATISTICALLY SIGNIFICANT DIFFERENCES WERE OBSERVED BETWEEN APREMILAST AND ROFLUMILAST IN U937 CELLS. *P<0.05 VERSUS DMSO, **P<0.01 VERSUS DMSO ***P<0.001 VERSUS DMSO, 30-MINUTE STIMULATION WITH DRUG. 110
FIGURE 4-4 CELLUSPOTS™ - KINASE SUBSTRATE ARRAYS ILLUSTRATION. READY TO SCREEN KINASE ARRAYS WITH TYROSINE- AND SERINE/THREONINE-KINASE SUBSTRATES FROM ANNOTATED PHOSPHORYLATION SITES. (INTAVIS BIOANALYTICAL INSTRUMENTS)..... 116
FIGURE 4-5 CELLUSPOTS™ TYROSINE KINASE SUBSTRATE ARRAYS. A) N=1-3 TYROSINE KINASE SUBSTRATE ARRAYS OVERLAID WITH LYSATES FROM RASF CELLS EITHER UNTREATED OR TREATED WITH APREMILAST 10μM OR ROFLUMILAST 10μM INCLUDES AN ANTIBODY ONLY CONTROL. EACH BLACK SPOT CORRESPONDS TO A KNOWN PEPTIDE SEQUENCE THAT HAS BEEN PHOSPHORYLATED BY KINASES IN THE LYSATE. NON-PHOSPHORYLATED SEQUENCES APPEAR AS NEGATIVE (NO SPOT) B) DENSITOMETRY ANALYSIS OF THE ARRAYS NORMALISED TO ANTIBODY ONLY CONTROL. DATA IS SHOWN AS SEM FOR THREE EXPERIMENTS * P <0.05 AND ** P<0.01..... 117
FIGURE 4-6 EFFECT OF APREMILAST AND ROFLUMILAST ON THE PHOSPHORYLATION OF FYN AT Y530 (A) AND SRC Y416 (B) IN RHEUMATOID ARTHRITIS SYNOVIAL FIBROBLASTS (RASFS). A) WESTERN BLOT ANALYSIS OF PHOSPHORYLATION OF FYN (Y530) IN RASF CELLS (N=4) AND

REPRESENTATIVE BLOT FOR GRAPH. B) WESTERN BLOT ANALYSIS OF PHOSPHORYLATION OF SRC (Y416) (N=3) ALONG WITH REPRESENTATIVE BLOT. STUDENT'S T- TEST WAS USED TO COMPARE TREATMENTS WITH THE UNTREATED CELLS. NO STATISTICALLY SIGNIFICANT DIFFERENCES WERE OBSERVED BETWEEN UNTREATED, APREMILAST AND ROFLUMILAST ON PHOSPHORYLATION OF SRC (Y416) IN RASFS. STATISTICAL SIGNIFICANT DIFFERENCES WERE FOUND BETWEEN UNTREATED AND APREMILAST TREATED CELLS AS WELL AS A SIGNIFICANT DIFFERENCE BETWEEN APREMILAST AND ROFLUMILAST IN THE PHOSPHORYLATION OF FYN (Y530) *P<0.05. 30 MINUTES STIMULATION WITH 10 μM APREMILAST OR ROFLUMILAST. 119

FIGURE 4-7 SCHEMATIC REPRESENTATION OF REVERSE PHASE PROTEIN ARRAY PLATFORM. CELL LYSATES ARE ARRAYED ONTO NITROCELLULOSE-COATED SLIDES AND SUBSEQUENTLY INCUBATED WITH PRIMARY AND SECONDARY VALIDATED ANTIBODIES. THE SLIDES ARE THEN SCANNED AND ANALYSED ON A LICOR ODDYSSEY SCANNER..... 122

FIGURE 4-8 REVERSE PHASE PROTEIN ARRAY. A-B SHOW ALL HITS FROM RPPA, OVER 150 ANTIBODIES WERE TESTED (SEE MATERIALS AND METHOD SECTION). ARRAYS WERE SCANNED ON LICOR ODDYSSEY SCANNER AND INTENSITIES OF SPOTS WERE QUANTIFIED (BRYAN SERRELS EDINBURGH CANCER RESEARCH CENTRE). 123

FIGURE 4-9 REVERSE PHASE PROTEIN ARRAY IMAGES. SELECTION OF IMAGES OF INTERESTING RPPA HITS. 124

FIGURE 4-10 EFFECT OF APREMILAST AND ROFLUMILAST ON THE PHOSPHORYLATION OF AKT AT THR 308 AND SER 473 IN RHEUMATOID ARTHRITIS SYNOVIAL FIBROBLASTS (RASF). A-B WESTERN BLOT ANALYSIS OF AKT PHOSPHORYLATION IN RASF CELLS A) PAKT (THR308) B)PAKT (SER473). C) REPRESENTATIVE WESTERN BLOTS FOR EACH GRAPH. STUDENT'S T- TEST WAS USED TO COMPARE TREATMENTS WITH THE UNTREATED CELLS. NO STATISTICALLY SIGNIFICANT DIFFERENCES WERE OBSERVED BETWEEN APREMILAST AND ROFLUMILAST ON PHOSPHORYLATION OF AKT (SER473) IN RASFCELLS. *P<0.05. 30 MINUTES STIMULATION WITH 10 μM APREMILAST OR ROFLUMILAST..... 125

FIGURE 4-11 EFFECT OF APREMILAST AND ROFLUMILAST ON RPS6 IN RASF CELLS. A-B WESTERN BLOT ANALYSIS OF A) PHOSPHORYLATION OF S6 RIBOSOMAL PROTEIN AT SER 240/244 B) TOTAL RPS6. C) REPRESENTATIVE WESTERN

BLOTS FOR EACH GRAPH. STUDENT'S T-TEST WAS USED TO COMPARE TREATMENTS WITH UNTREATED CELLS (N=3) SIGNIFICANT DIFFERENCES WERE FOUND BETWEEN APREMILAST AND ROFLUMILAST ON THE PHOSPHORYLATION OF RPS6 SER240/244. * P<0.05 126
FIGURE 4-12 TCR SIGNALLING PATHWAYS LEADING TO RIBOSOMAL RPS6 PHOSPHORYLATION (SALMOND, EMERY ET AL. 2009). A) TCR INDUCED ACTIVATION OF LCK AND FYN RESULTS IN DOWNSTREAM ACTIVATION OF MEK AND PI3K, AND UPTAKE OF AMINO ACIDS (AA) FROM THE EXTRACELLULAR ENVIRONMENT. MEK ACTIVATES ITS DOWNSTREAM EFFECTOR ERK THAT IN TURN ACTIVATES RSK. PI3K AND AA SIGNALLING FACILITATES ACTIVATION OF MTOR. MTOR IS CRITICAL FOR PHOPHORYLATION OF S6K AT RESIDUE T389, WHEREAS BOTH MTOR AND MEK – DEPENDENT SIGNALS ARE REQUIRED FOR PHOSPHORYLATION OF S6K T421/S424. RSK AND S6K BOTH CONTRIBUTE TO MAXIMAL PHOSPHORYLATION OF RPS6 AT RESIDUES SER235/236. B) UPSTREAM SIGNALS REQUIRED FOR RPS6 SER 240/244 PHOSPHORYLATION ARE SIMILAR FOR RPS6 SER 235/236 AS DESCRIBED IN A. HOWEVER RSK PLAYS A MINOR ROLE IN SER240/244 AND MTOR-DEPENDENT S6K ACTIVITY IS DOMINANT FOR RPS6240/244 PHOSHORYLATION. FURTHERMORE, MEK MAY ALSO BE AN INHIBITORY PATHWAY, DECREASING RPS6 PHOSPHORYLATION. 128
FIGURE 4-13 TCR SIGNALLING PATHWAY LEADING TO RPS6 PHOSPHORYLATION. INDICATED POINTS OF INHIBITION SHOWN ON THE PATHWAY BY AVAILABLE PHARMACOLOGICAL INHIBITORS. ADAPTED FROM (SALMOND, EMERY ET AL. 2009)..... 129
FIGURE 4-14 EFFECT OF INHIBITION OF PKA BEFORE STIMULATION WITH APREMILAST AND ROFLUMILAST ON THE S6 RIBOSOMAL PATHWAY. HEK 293 CELLS WERE PRETREATED WITH +/- H-89 FOR 30 MINS BEFORE STIMULATION WITH APREMILAST AND ROFLUMILAST 10μM FOR 30 MINS. A-F) WESTERN BLOT ANALYSIS OF PHOSPHORYLATION OF RPS6 SER240/244, SER235/236, TOTAL RPS6, S6 KINASE P70 (T421/S424), PI3K P85 AND FYN Y506. G) REPRESENTATIVE BLOTS AND LOADING CONTROL. VALUES REPRESENT THE MEAN OF 3 EXPERIMENTS, ERROR BARS REPRESENT SE. *P<0.05,***P<0.001. 132
FIGURE 4-15 EFFECT OF INHIBITION OF MTOR BEFORE STIMULATION WITH APREMILAST AND ROFLUMILAST ON THE S6 RIBOSOMAL PATHWAY. HEK 293

CELLS WERE PRE-TREATED WITH +/- H-89 FOR 30 MINS BEFORE STIMULATION WITH APREMILAST AND ROFLUMILAST 10μM FOR 30 MINS. A-D) WESTERN BLOT ANALYSIS OF PHOSPHORYLATION OF RPS6 SER240/244, S6 KINASE P70 T421/S424, TOTAL RPS6 AND TOTAL S6 KINASE P70. E) REPRESENTATIVE BLOTS AND LOADING CONTROL. VALUES REPRESENT THE MEAN OF 3 EXPERIMENTS, ERROR BARS REPRESENT SE. *P<0.05. 133
FIGURE 4-16 EFFECT OF INHIBITION OF MEK1/2 BEFORE STIMULATION OF APREMILAST AND ROFLUMILAST ON THE S6 RIBOSOMAL PATHWAY. HEK 293 CELLS WERE PRETREATED WITH +/- H-89 FOR 30 MINS BEFORE STIMULATION WITH APREMILAST AND ROFLUMILAST 10μM FOR 30 MINS. A-F) WESTERN BLOT ANALYSIS OF PHOSPHORYLATION OF RPS6 SER240/244, SER235/236, P90 RSK, TOTAL RPS6 AND TOTAL P90 RSK. G) REPRESENTATIVE BLOTS AND LOADING CONTROL. VALUES REPRESENT THE MEAN OF 3 EXPERIMENTS, ERROR BARS REPRESENT SE. *P<0.05. 135
FIGURE 5-1 BIOPANNING. THE PROCESS FOR AFFINITY SELECTION OF PHAGE-DISPLAYED PEPTIDE OR PROTEIN: STEP 1, TARGET IS IMMOBILIZED AND PHAGE LIBRARY IS ADDED.STEP 2,WASHING TO REMOVE UNBOUND PHAGE. STEP 3, ELUTION OF BOUND PHAGE AS THE RESULT OF CONFORMATIONAL CHANGES TO THE BINDING SITE CAUSED BY PH CHANGE OR OTHER MEANS WHICH DISRUPTS THE INTERACTION BETWEEN DISPLAYED LIGAND AND THE TARGET. STEP 4, AMPLIFICATION OF ELUTED PHAGE FOR NEXT ROUND OF BIOPANNING. 141
FIGURE 5-2 IDENTIFICATION OF 12MER PEPTIDE SEQUENCES THAT BOUND PDE 4A4 ALONE OR IN ITS LIGAND BOUND STATE WITH EITHER APREMILAST OR ROFLUMILAST. SELECTION OF SOME OF THE SEQUENCES IDENTIFIED, WHERE BINDING AFFINITY WAS EITHER INCREASED OR DECREASED WHEN APREMILAST OR ROFLUMILAST WAS BOUND TO PDE4A4 AND ANY DIFFERENCES NOTED BETWEEN THE INIHIBITORS. 143
FIGURE 5-3 PEPTIDE ARRAY CONTAINING PHAGE DISPLAY SEQUENCES IDENTIFIED FROM ANALYSIS. A) PEPTIDE ARRAY WAS OVERLAID WITH EITHER PURIFIED PDE4A4-MBP PROTEIN OR AS A CONTROL MBP ONLY AND PROBED USING ANTI-MBP ANTIBODY. POSITIVELY INTERACTING PEPTIDES GENERATE DARK SPOTS ON THE ARRAY. B) BAR CHART REPRESENTS DENSITOMETRY ANALYSIS OF ARRAY SHOWN AS % OF THE MAXIMUM SPOT DENSITY. 145

FIGURE 5-4 IDENTIFICATION OF CONSENSUS SITE MOTIFS (A) 1000 PEPTIDES THAT WERE IDENTIFIED AS BINDING TO PDE4A4 WERE PROCESSED USING MEME (B) TO IDENTIFY CONSENSUS MOTIFS (HTTP://MEME.NBCR.NET/MEME/CGI-BIN/MEME.CGI). THE PANEL IN A) REPRESENTS DATA FROM THE ONE OF THE CORE MOTIFS IDENTIFIED FROM THE 12MER PEPTIDE LIBRARY AS GYMPVVS WHICH IS ALSO SHOWN IN B). EXAMPLE OF A CONSENSUS SITE MOTIF THAT CAN BE DEVELOPED FROM THE DEEP SEQUENCING USING MEME. 147
FIGURE 5-5 PDE4A4 BINDING TO PEPTIDE ARRAYS CONSISTING OF PEPTIDE SPOTS CONTAINING IDENTIFIED MOTIFS. POSITIVELY INTERACTING PEPTIDES GENERATE DARK SPOTS, WHILE THOSE THAT DO NOT INTERACT LEAVE BLANK SPOTS. POSITIVE INTERACTIONS WERE IDENTIFIED ON MOTIFS 1,2,4,7 AND 8 ON THE ARRAY. 147

Acknowledgement

Firstly I would like to thank my supervisor Professor George Baillie for all his advice, support and supervision throughout this project. I would also like to thank Peter Schafer (Celgene corporation) for providing me with this project and for all his valuable input.

I would also like to thank all the past and present members of the Gardiner Lab for all their help on a day to day basis.

Lastly I would like to thank all my family and in particular my Husband Brian and my parents who have supported me throughout this process.

Author's Declaration

I hereby declare that the following thesis is my own composition and that it is a record of my own work. It has not been presented in any previous application for a higher degree.

Nicola Margaret Walsh

Definitions/Abbreviations

aa	amino acid
Ab	Antibody
AC	Adenylyl cyclase
AKAP	A-kinase anchoring protein
AKAR	A-kinase activity reporter
AMP	Adenosine monophosphate
AR	Adrenergic receptor
ATP	Adenosine triphosphate
AC	adenylyl cyclases
AKAP	A Kinase anchoring protein
ANOVA	analysis of variance
ATP	adenosine triphosphate
β-AR	ß-adrenergic receptor
BSA	Bovine serum albumin
C	PKA catalytic subunit
cAMP	3', 5' cyclic adenosine monophosphate
cGMP	3', 5' cyclic guanosine monophosphate

CCD	charged-coupled device
CFP	cyan fluorescent protein
cGMP	3', 5' cyclic guanosine monophosphate
CBD	cyclic nucleotide binding domains
CNB	Cyclic nucleotide-binding domains
CNG	Cyclic nucleotide-Gated Channels
CRE	cAMP response element
CREB	CRE binding protein
COPD	Chronic obstructive pulmonary disease
DAG	diacylglycerol
DEP	Dishevelled, Egl-10, and Pleckstrin
DMEM	Dulbecco's modified Eagle's medium
DMSO	Dimethylsulfoxide
ECC	excitation-contraction coupling
ECL	Enhanced chemiluminescence
E.coli	Escherichia coli
EPAC	exchange proteins directly activated by cAMP
Epac	Exchange protein directly activated by cAMP
ERK	Extracellular signal regulated kinase

FRET	fluorescence resonance energy transfer
FSK	Forskolin
GDP	guanosine diphosphate
GEF	Guanine nucleotide exchange factor
GFP	Green fluorescent protein
Gi	Inhibitory G protein
GPCR	G protein-coupled receptor
Gs	Stimulatory G protein
GTP	guanosine triphosphate
HEK	Human embryonic kidney
IBMX	3-isobutyl-1-methylxantine
IC50	Half maximal inhibitor concentration
IP3	inositol-triphosphate
ISO	isoproterenol
Makap	Muscle-specific A-kinase anchoring protein
MAPK	Mitogen-activated protein kinase
MEF	Myocyte enhancer factor
mRNA	Messenger RNA
OD	optical density

PDE	phosphodiesterase
PPi	Inorganic Pyrophosphate
PGE1	prostaglandin E1
PIP3	Phosphatidylinositol-trisphosphate
PKA	cAMP-dependent protein kinase
PKG	cGMP-dependent protein kinase
PKC	Protein kinase C
PKD	Protein kinase D
PKI	Protein kinase inhibitor
PP1	proteins phosphatase 1
PP2A	protein phosphatase 2A
PPi	inorganic pyrophosphate
PsA	Psoriatic Arthritis
RA	Ras-association domain
RASF `	Rheumatoid Arthritis Synovial Fibroblasts
RPPA	Reverse Phase Protein Array
SEM	standard error of measurement or mean
TNF	Tumour necrosis factor
UCR	upstream conserved region

YFP	yellow fluorescent protein

1 Introduction

1.1 Cyclic 3' 5'- adenosine monophosphate (cAMP) signalling.

Signal transduction can be defined as the process by which an extracellular ligand binds to and activates a cell surface receptor and this in turn initiates a series of intracellular signalling cascades. Extracellular ligands are thought of as 'first messengers' in this context and are usually neurotransmitters, hormones, chemokines, lipid mediators or drugs which cannot cross the plasma membrane. When they interact with a membrane receptor their signals are transduced which causes a change in the level of an intracellular second messenger. Second messengers are small chemical molecules, gases, ions or lipids which bind to and activate protein kinases, channels or other proteins thereby continuing the signalling cascade and mediating intracellular responses that are specific to the receptor that was activated.

The first second messenger to be discovered was Cyclic nucleotide3'5'-adenosine monophosphate (cAMP) (figure1-1)(Sutherland and Rall 1958). cAMP is a ubiquitous second messenger involved in a variety of cellular responses such as inflammation, apoptosis, lipid metabolism, learning and memory, gene regulation, immune response, insulin secretion, cell growth, proliferation and differentiation(Beavo and Brunton 2002) (Suzuki, J et al. 2002). cAMP was discovered by Dr Earl W. Sutherland during his studies into the mechanisms of hormone action (Sutherland and Rall 1958). Other second messengers include the nucleotide cyclic 3'5'-guanine monophosphate (cGMP), calcium and the phosphatidylinositol derivatives inositol phosphate (IP3) and diacylglycerol (DAG) and Nitric Oxide (NO) (Berridge 1984).

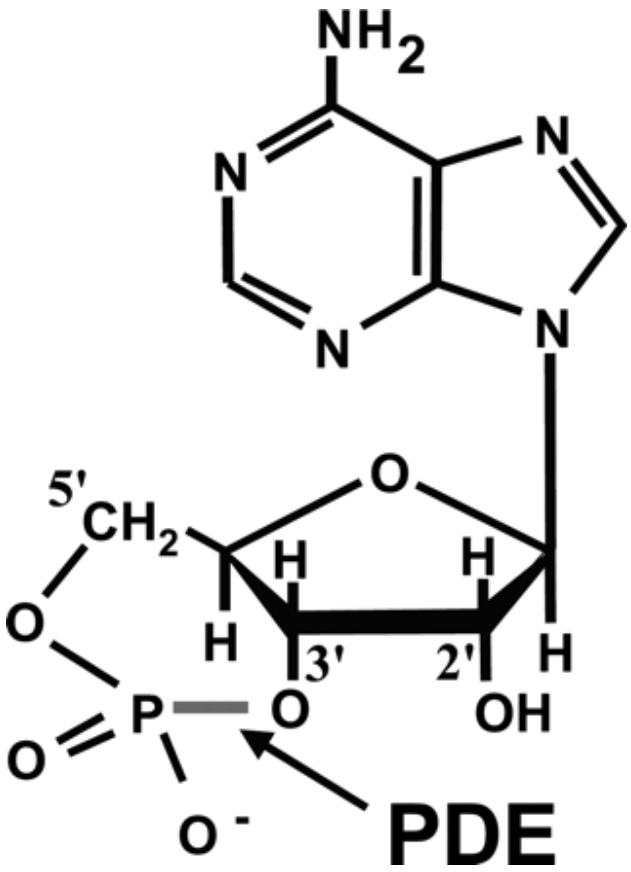

Figure 1-1 Structure of the second messenger cyclic adenosine 3'5'-monophoosphate (cAMP). The 3' bond is hydrolysed by phosphodiesterase (PDE) enzymes indicated by the arrow (Bender and Beavo 2006).

1.1.1 cAMP generation

The level of intracellular cAMP is tightly regulated by the balance of two enzymes: Adenelyl cyclase (AC)(Sutherland and Rall 1958) and the super family of cyclic nucleotide phosphodiesterase (PDEs). The generation of cAMP is initiated following ligand binding to a seven transmembrane –spanning G protein coupled receptor (GPCR) that is coupled to a stimulatory G protein α subunit (Gαs). Ligand binding to the GPCR results in the exchange of GDP for GTP on the Gαs protein, which results in the dissociation from the βγ subunit complex (Landry, Niederhoffer et al. 2006). The free Gαs subunit then activates adenelyl cyclase, the enzyme which catalyses the

cyclisation of adenosine triphosphate (ATP) to generate cAMP and pyrophosphate (Sunahara and Taussig 2002, Kamenetsky, Middelhaufe et al. 2006)(figure 1-3). There are 10 known AC isoforms that are differentially expressed in various tissue types (Sunahara and Taussig 2002) see table 1-1 and 1-2. Some of the best characterised Gαs coupled GPCR ligands include epinephrine and norepinephrine, histamine and serotonin. cAMP exerts its effects by the activation of a limited number of effectors. These are the cAMP dependent protein kinase A (PKA), the exchange proteins directly activated by cAMP (Epac 1 and Epac 2) and the cAMP-gated ion channels (CNG) (figure 1-2).

Termination of the cAMP signal is mediated by the action of phosphodiesterases (PDEs), which hydrolyse 3'5'-cyclic adenosine monophosphate (cAMP) to the inactive 5'-adenosine monophosphate (AMP). This action represents the sole route for termination of cAMP signals. Therefore intracellular levels of cAMP are determined by the balance between generation by adenylyl cyclases (ACs) and degradation by phosphodiesterases (PDEs).

Ac Isoform	G protein regulators		Protein kinases		Calcium
	stimulatory	inhibitory	stimulatory	inhibitory	
Group I					
AC1	Gsα	Gα, i, z, o, Gβγ	PKCα (weak)	CaMK IV	↑CaM
AC8	Gsα	Gβγ			↑CaM
AC3	Gsα	Gβγ	PKCα (weak)	CaMK II	↑CaM
Group II					
AC2	Gsα, Gβγ		PKCα		
AC4	Gsα, Gβγ			PKCa	
AC7	Gsα, Gβγ		PKCα		
Group III					
AC5	Gsα, Gβγ	Gα, i, z	PKC (a, ζ)	PKA	↓Free Ca^{2+}
AC6	Gsα, Gβγ	Gα, i, z		PKA, PKC (δ,ε)	↓Free Ca^{2+}
Group IV					
AC9	Gsα			PKC	↓ via calcineurin

Table 1-1 Regulatory properties of membrane-bound ACs. (Sadana and Dessauer 2009).

AC isoform	Site of expression
AC1	Brain, adrenal medulla
AC2	Brain, lung, skeletalmuscle,h eart
AC3	Olfactory epithelium, pancreas, brain, heart, lung, testis
AC4	Widespread
AC5	Heart, triatum, kidney, liver, lung, testis, skeletal muscle, adrenal
AC6	Heart, kidney, liver, lung, brain, testis, skeletal muscle, adrenal
AC7	Widespread
AC8	Brain, lung, pancreas, testis, adrenal
AC9	Widespread

Table 1-2 Tissue distribution of ACs. Adapted from (Sadana and Dessauer 2009)

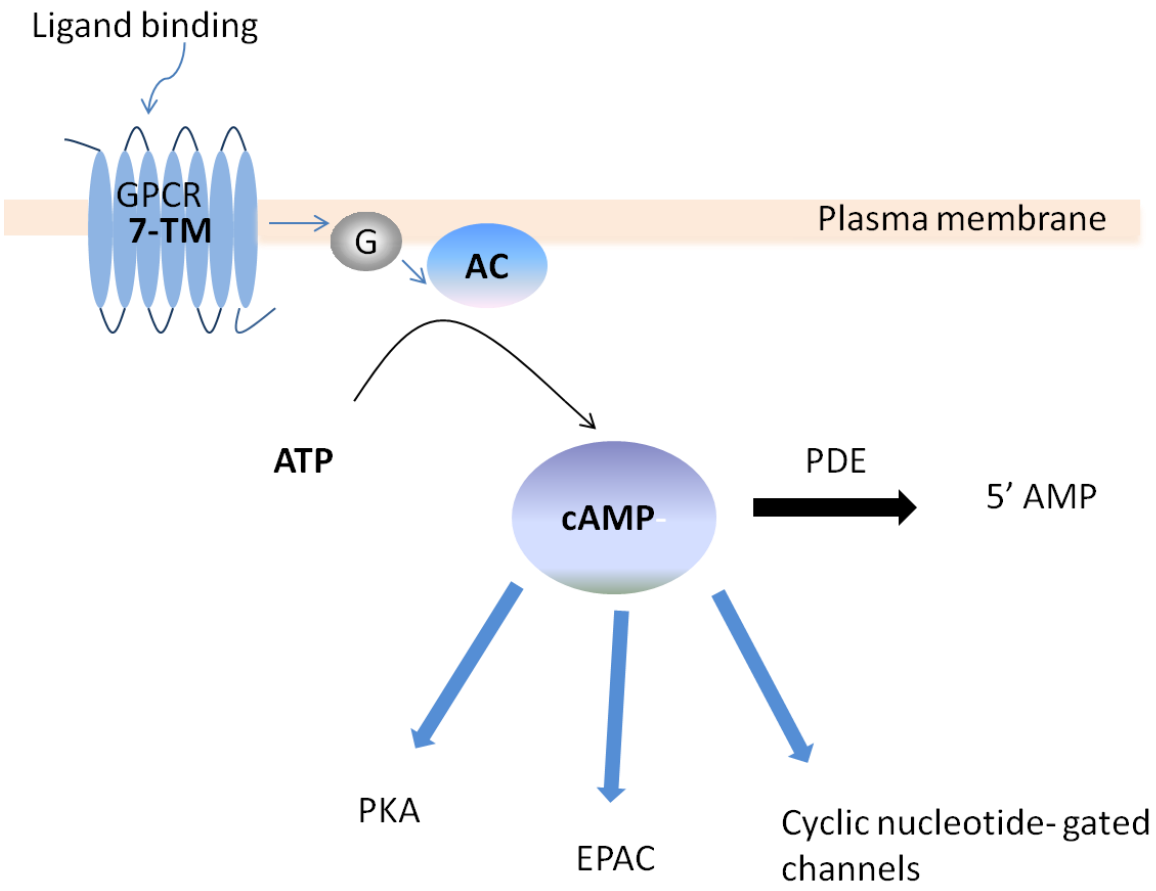

Figure 1-2 Overview of cAMP signalling in cells. cAMP is produced following stimulation of 7-transmembrane domain receptors (GPCRs) at the plasma membrane. These receptors couple to G-proteins, which activate adenylyl cyclases leading to the conversion of ATP into cAMP. The effects of cAMP within the cell are mediated by three distinct effector proteins: PKA, EPAC and Cyclic nucleotide-channels. cAMP is degraded by phosphodiesterase enzymes. 7-TM, 7-transmembrane domain receptor; G, G-protein; AC, adenylyl cyclase; PKA, cAMP dependent protein kinase A; PDE, phosphodiesterase.

.

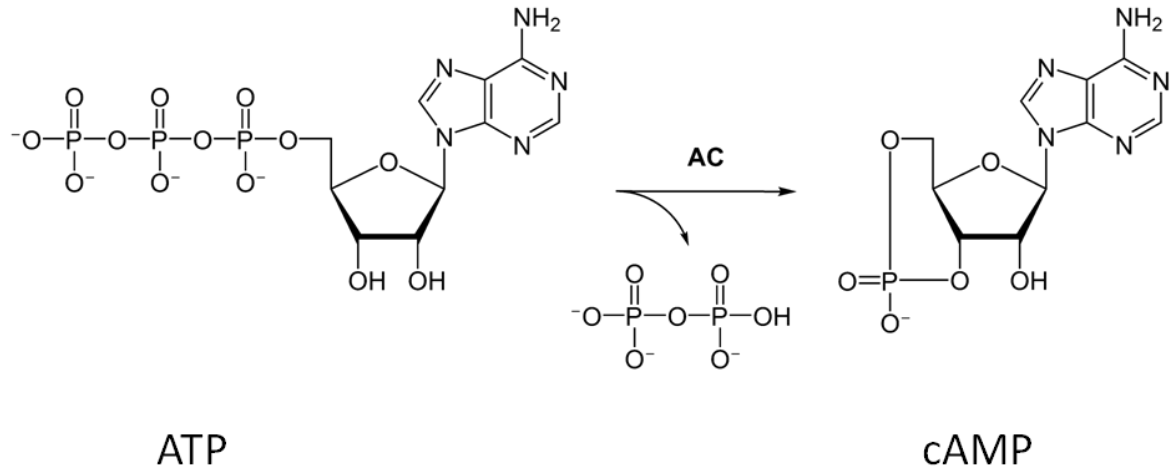

Figure 1-3 Conversion of ATP to cylic adenosine 3'5'-monophosphate (cAMP) by adenylyl cyclase enzymes. Adenylyl cyclases catalyse the conversion of ATP to pyrophosphate (PPi)

and 3'5-cAMP, which acts as a second messenger in cells. PDE hydrolyse the catalytic cleavage of cAMP to 5'AMP, terminating the cAMP signal (Section 1.3, (figure 1-1).

1.1.2 cAMP Compartmentalisation

Levels of cAMP do not rise and fall uniformly in cells and in fact are compartmentalised into microdomains controlled by proximity to the generating adenylyl cyclases and the phosphodiesterases that degrade it to 5'AMP. Such sculpting of cAMP pools underpins the specificity of receptor function. Compartmentalisation is a key feature of cyclic nucleotide signalling with phosphodiesterases playing a pivotal role in achieving spatial control of cAMP, since phosphodiesterases are the only known route of cAMP degradation.

Once cAMP is synthesised it interacts with several spatially restricted effector proteins, primarily the cAMP-dependent serine-threonine protein kinase A (PKA) and exchange protein activated by cAMP (EPAC) (Tasken and Aandahl 2004, Bos 2006).

1.1.2.1 Protein Kinase A (PKA)

The primary target of cAMP is Protein Kinase A (PKA), which is a heterotetramer composed of two cAMP binding regulatory (R) subunits, together with 2 catalytic (C) subunits. There are two major subtypes of the regulatory subunits known as type I and type II R subunits (Lee, Carmichael et al. 1983, Takio, Smith et al. 1984). Depending on whether a type I or type II regulatory subunit is present, PKA holoenzymes are classified as either type I or type II. Each R subunit contains two cAMP binding sites, which when occupied by cAMP, leads to a conformational change in the enzyme releasing the active C subunits which can then phosphorylate their substrate protein (Taylor, Kim et al. 2005). PKA C subunits phosphorylate their target proteins on serine-threonine residues which are typically found in a consensus sequence of R-R-X-S/T-X (Kemp, Graves et al. 1977) (Figure 1-4).

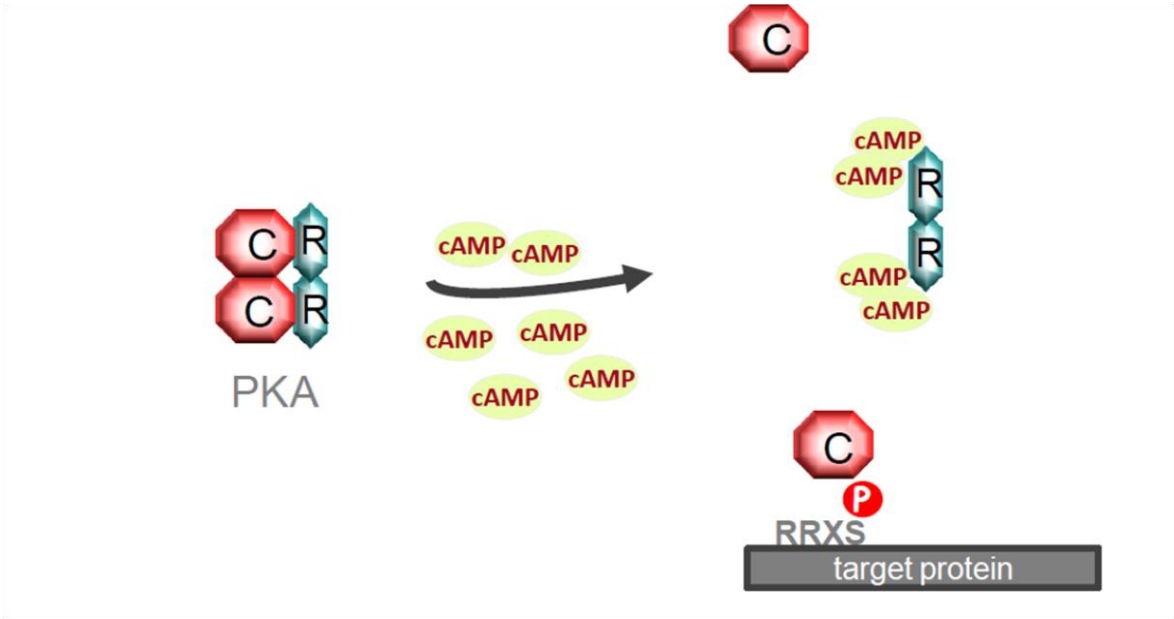

Figure 1-4 Activation of the cAMP-dependent protein kinase (PKA) in response to increased cAMP levels. When cAMP is low, PKA exists as an inactive heterotetramer with and R_2C_2 conformation. The two catalytic subunits are maintained in an inhibited state by the regulatory subunits. When cAMP levels are raised, cAMP binds to the R-subunits with 2:1 stoichometry. Active C-subunits are then released to go on to phosphorylate their downstream targets which are involved in a diverse range of biological processes.

1.1.2.2 Exchange Protein activated by cAMP (EPAC)

Epacs are guanine nucleotide exchange factors (GEFs) for Rap 1 and Rap 2 (de Rooij, Zwartkruis et al. 1998). These Rap GTPases cycle between an inactive GDP-bound state and an active GTP-bound state with GEFs mediating this exchange of GDP for GTP. The N terminus of Epac 1 contains a regulatory domain, which houses a cAMP-binding site, which is similar to those present in the R subunit of PKA. In addition to this site, there is also a Disheveled, Egl-10 and pleckstrin homology (DEP) domain which mediates membrane attachment (de Rooij, Zwartkruis et al. 1998). The C-terminal region consists of a catalytic domain that is characteristic of exchange factors for the Ras family of GTPases. At low levels of cAMP, Epac folds into an inactive state conformation, and steric hindrance prevents the binding of Rap. When cAMP binds to the protein, Epac unfolds, allowing Rap to bind (Rehmann, Prakash et al. 2003).

PKA and Epac are intrinsically soluble proteins and subpopulations of each are present in the cytosol. However, for compartmentalisation to occur, it is critical

that subpopulations of these cAMP effectors are sequestered to specific intracellular complexes, whether located at the membrane or in the cytosol along with their downstream targets. At different locations, the cAMP effectors "sample" the cAMP concentration and drive signalling only when the cAMP concentration breaches the threshold of activation of these proteins.

1.1.2.3 A Kinase Anchoring Proteins (AKAPs)

The discovery of a family of anchor proteins called AKAPs (A kinase anchoring proteins), have been fundamental in establishing the concept of compartmentalised cAMP signalling. AKAPs specifically sequester PKA (Tasken and Aandahl 2004) (Carnegie, Means et al. 2009) via a short α helical structure which interacts with a groove formed by the N-terminal dimerisation domain of PKA R- subunits. PKA RII provides the majority of membrane associated PKA (Wong and Scott 2004) whereas the majority of R I is generally considered to be located in the cytosol (Miki and Eddy 1998, Gronholm, Vossebein et al. 2003). Originally it was thought that only PKA R II was able to bind AKAPs, but recent evidence suggests that AKAPs can interact specifically with PKA RI (Miki and Eddy 1998, Gronholm, Vossebein et al. 2003) or with both PKA type RI and II (Huang, Durick et al. 1997, Huang, Durick et al. 1997).

AKAPs not only act as scaffolds for PKA, but also bind additional proteins of the cAMP signalling pathway. For example, Phosphodiesterases (PDEs), protein phosphatases,a variety of kinases and substrates of PKA (Gronholm, Vossebein et al. 2003).

By hydrolysing cAMP, PDEs act as "sinks" for the otherwise freely diffusible cAMP, and this action creates distinct pools of cAMP in the cytoplasm. Basically cAMP only exists in high concentration in areas that are devoid of PDE activity or following receptor activation where cAMP can "swamp" the PDE pool in one location. So PDEs along with protein phosphatases, which counteract PKA mediated phosphorylation, serve to efficiently terminate cAMP signals.

Some AKAPs can bind both GPCRs and adenylyl cyclases, which therefore directs PKA functionality to targets associated with cAMP production. For example mAKAP, which is muscle specific, can provide dual output of the cAMP signalling

system as it sequesters both Epac and PKA (Dodge-Kafka, Soughayer et al. 2005). Therefore sequestered and spatially constrained PKA and Epac subpopulations provide the machinery to interpret intracellular cAMP gradients formed by PDEs.

In the past however, the idea of cAMP being compartmentalised was hard to envisage as it was generally considered to be freely diffusible in the cytosol with a calculated diffusion constant of – 150-700μm^2 s^{-1} (Bacskai, Hochner et al. 1993, Kasai and Petersen 1994, Nikolaev, Gambaryan et al. 2005). The traditional approach for the measurement of cAMP was by radioimmunoassay (RIA) which utilised anti- cAMP antibodies and radio-labelled cAMP as a tracer, which is displaced by the endogenous cAMP present in the sample (Steiner, Kipnis et al. 1969) resulting in a concentration dependent signal decrease. However, antibody based methods can only detect cAMP accumulation at defined time points and so only determine total steady state cAMP levels in a cell population, not in a single cell which would be desirable in many applications. Therefore RIA failed to provide quantitative information required to visualise cAMP gradients in real time. Recently this has been solved by the development of genetically encoded optical probes that are able to visualise formation of cAMP gradients within living cells in real time.

1.2 Measurement of cAMP gradients using FRET

Fluorescence Resonance Energy Transfer (FRET) is a method for visualising cAMP levels in intact living cells. FRET is a quantum-mechanical event that occurs when two flourophores are placed in close proximity to each other (< 100 Å) provided that the emission spectrum of the flourophore that acts as the “donor” overlaps the excitation spectrum of the acceptor fluorophore. Under these conditions, part of the vibrational energy of the excited state of the “donor” is transferred to the acceptor that emits its own wavelength. This process results in a reduction in the emission of the FRET donor, along with an increase in the emission of the FRET acceptor. The ratio of acceptor/donor emissions can therefore be used as a measure of resonance energy transfer.

The dipole-dipole interactions underlying the FRET phenomenon are highly sensitive to distance and orientation of the flourophores. Generally,

flourophores must be within 1-10nm of each other for FRET to occur, while at the same time maintaining an appropriate spatial orientation.

The efficiency of this process (E) depends on the distance (R) between the donor and acceptor with an inverse sixth power law, as described by Försters equation: $E=1/(1+R/R_{\circ})^{6}$ (Förster 1948) where $R_{\circ}$ is the distance at which half of the energy is transferred. According to the Försters equation, the doubling of the distance between the two flourophores, for example, from $R_{\circ}$ to 2 $R_{\circ}$ decreases the efficiency of transfer from E=50% to E= 1.5%. Therefore FRET can provide a highly sensitive approach to measure intermolecular distance. If the two flourophores are held together by proteins that undergo a conformational change upon binding to cAMP, FRET can be used to measure cAMP concentration.

In general, a FRET-based cAMP probe will comprises of two essential components: 1) a cAMP sensor, which consists of either two separate interacting protein domains or a single protein domain that will undergo a conformational change upon cAMP binding and 2) a donor and acceptor fluorophore fused to the cAMP sensor. A cAMP induced conformational change will affect the distance or the orientation of the two flourophores, and therefore the efficiency of energy transfer. Variations in this energy transfer then correlate with changes in cAMP concentration.

A number of FRET biosensors have been developed (figure1-5) (Nikolaev and Lohse 2006, Berrera, Dodoni et al. 2008, Willoughby and Cooper 2008).These sensors measure relative fluorescence of two fluorescent proteins used as donor and acceptor fluorophores, typically cyan (CFP) and yellow fluorescent proteins (YFP). These fluorophores are genetically fused to the regulatory and catalytic subunits of the cAMP-dependent protein kinase (PKA) (Zaccolo and Pozzan 2002), to full length or partially truncated EPAC (DiPilato, Cheng et al. 2004, Nikolaev, Bunemann et al. 2004, Ponsioen, Zhao et al. 2004), or to a single cAMP binding domain from a cyclic nucleotide-gated channel. The sensors can be expressed in the cytoplasm or targeted to specific sub-cellular locations. With such sensors, changes in cAMP concentration ([cAMP]i) can be estimated by changes in FRET measured as changes in the CFP-to-YFP emissions ratio (480 nm/545 nm), a value that is proportional to ([cAMP]i).

Many studies have been performed utilising the different PKA and EPAC biosensors, which have resulted in data that suggest cAMP has the ability to form discrete and often minute gradients within cells as it diffuses from the membrane after receptor stimulation. Compartmentalised phosphodiesterases play a vital role in this as they control the magnitude and duration of cAMP dependent events.(Houslay, Baillie et al. 2007)

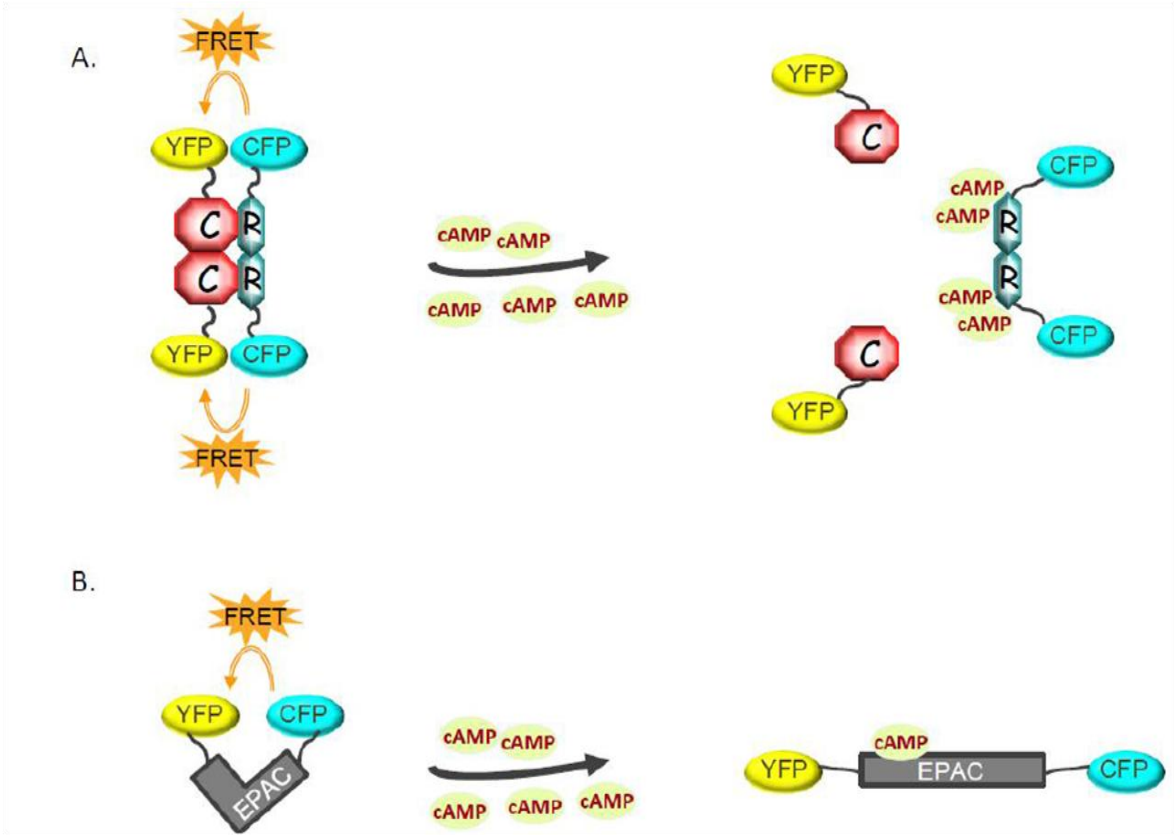

Figure 1-5 Genetic engineering of different FRET sensors to monitor real time changes in cAMP levels within cells.

A. FRET sensor based on PKA, with CFP and YFP linked to the R and C subunits of PKA respectively. In basal conditions, cAMP is low and PKA is in its inactive conformation. Excitation of CFP at 440nm will result in FRET, as CFP and YFP are in close proximity, and YFP emission at 545nm. In stimulated cells, cAMP rises. Two molecules of cAMP bind to each PKA-R subunit, leading to the dissociation of the active catalytic units. CFP and YFP then diffuse further apart and FRET is reduced, leading to detection of CFP emission at 480nm. Changes in FRET ratio (480/545nm) are directly proportional to R/C subunit dissociation, and therefore to cAMP levels (Zaccolo and Pozzan 2002). B. FRET sensor with CFP and YFP linked to the cAMP-binding domain of Epac1. Binding of cAMP leads to a conformational change in the sensor that moves the fluorophores apart, abolishing FRET (Nikolaev, Bunemann et al. 2004).

1.3 cAMP degradation by Phosphodiesterases

cAMP signalling plays a critical role in a variety of biologic responses within cells such as inflammation, apoptosis and lipid metabolism (Tasken and Aandahl 2004). Phosphodiesterases (PDEs) are the only enzymes that degrade cAMP (Conti and Beavo 2007). They belong to a group of 11 families of metallophosphohydralases which hydrolyse the cyclic nucleotides, cyclic adenosine 3'-5' monophosphate (cAMP) and cyclic guanine-3'-5' monophosphate (cGMP) to their inactive 5' monophosphate 5'AMP and 5'GMP respectively (Beavo and Brunton 2002)

Each of family of PDE differ in their selectivity for cAMP and cGMP and are characterised by their regulatory and kinetic properties (Beavo, Hansen et al. 1982) Twenty one genes encoding PDEs have been identified in the human genome, and these have been grouped into 11 PDE families based on their amino acid sequence, structure, enzyme kinetics, modes of regulation and tissue distributions (Conti and Beavo 2007, Houslay 2010) (table1-3).

Each family of PDE differ in their selectivity for cAMP and cGMP. PDEs 3,4,7 and 8 selectively hydrolyse cAMP, while PDEs 5,6 and 9 are selective for cGMP. PDEs 1,2,10 and 11 hydrolyse both cyclic nucleotides with varying efficiencies (Conti and Beavo 2007). Within each family multiple isoforms are expressed and over 50 are known to date. These are generated via alternative mRNA splicing and the use of multiple promoter sites (Houslay, Baillie et al. 2007).

Family	Genes	Substrate (cAMP, cGMP)	Regulation	Tissue distribution	Inhibitors
PDE1	A, B, C	Both; cGMP preferentially	Ca_{2+}/CaM; PKA phosphorylation	Heart, vascular smooth muscle, CNS	Vinpocetine
PDE2	A	Both; equal kMs	cGMP via GAF domains	Adrenal, heart, liver, brain	EHNA, BAY 60-7550
PDE3	A, B	cAMP	Inhibited by cGMP. Activated by PKA/Akt phosphorylation	Cardiovascular system, lung, liver, adipose tissue	Cilostamide, Cilostazol, Milrinone
PDE4	A, B, C, D	cAMP	**UCR1 and UCR2; phosphorylation by PKA and ERK1/2**		**Rolipram, Roflumilast , Apremilast, Cilomilast**
PDE5	A	cGMP	cGMP via GAF domains; PKA and PKG	Lung, heart, smooth muscle, brain, kidney	Sildenafil, Tadalafil, Zaprinast, Dipyridamole
PDE6	A, B, C	cGMP	Rhodopsin, transducin; cGMP via GAFs	Retinal photo-receptors	PDE5 inhibitors
PDE7	A, B	cAMP	Pancreas, brain, heart, immune system		ASB16165
PDE8	A, B	cAMP	PAS domain, Phosphorylation by PKA	Heart, reproductive tissue, bowel, thyroid	Dipyridamole
PDE9	A	cGMP		Brain	Zaprinast, BAY 73-6691
PDE10	A	Both; cAMP preferentially	GAF domains; PKA	Brain	Novel agents (see text), IBMX, Zaprinast
PDE11	A	Both; similar Km and V_{max} values	GAF domains	Skeletal muscle, kidney, liver, prostate, testis	IBMX, Dipyridamole Tadalafil

Table 1-3 Summary of the characteristics of the 11 PDE families.

1.3.1 PDE Catalytic and Regulatory Domains

PDEs have a modular structure consisting of catalytic, regulatory and cell localisation domains. Although they do not share a high sequence identity, structural information shows that the catalytic domain structure is highly conserved across all 11 PDE families (Xu, Hassell et al. 2000, Zhang, Card et al. 2004).

The catalytic domain of PDEs contains 16 α helices which are grouped into 3 subdomains, forming a deep binding pocket for either cAMP, cGMP or inhibitors. Many of the amino acid residues which are conserved across all PDEs are found within this active site pocket (Zhang, Card et al. 2004). The catalytic domain also contains one Zn^{2+} ion and one Mg^{2+} ion (Xu, Hassell et al. 2000), which are essential to catalysis. The position of an invariant glutamine residue that stabilises the purine ring of the cyclic nucleotide in the binding pocket is thought to determine substrate selectivity and depending on the orientation of this residue in the pocket, the enzyme will have specificity for either cAMP, cGMP or both (Zhang, Card et al. 2004). Other amino acids conserved across PDE families are thought to contribute to substrate and inhibitor specificities by altering the shape and size of the binding pocket (Wang, Liu et al. 2005).

PDEs differ markedly at their N and C termini and contain a number of different regulatory domains. These include regions for ligand binding, inhibition of the catalytic domain, kinase phosphorylation sites and domains, which mediate oligomerisation and cell localisation (Conti and Beavo 2007). The characteristics of the 11 PDE families are summarised in table 1-1 and domain structures illustrated in figure 1-6.

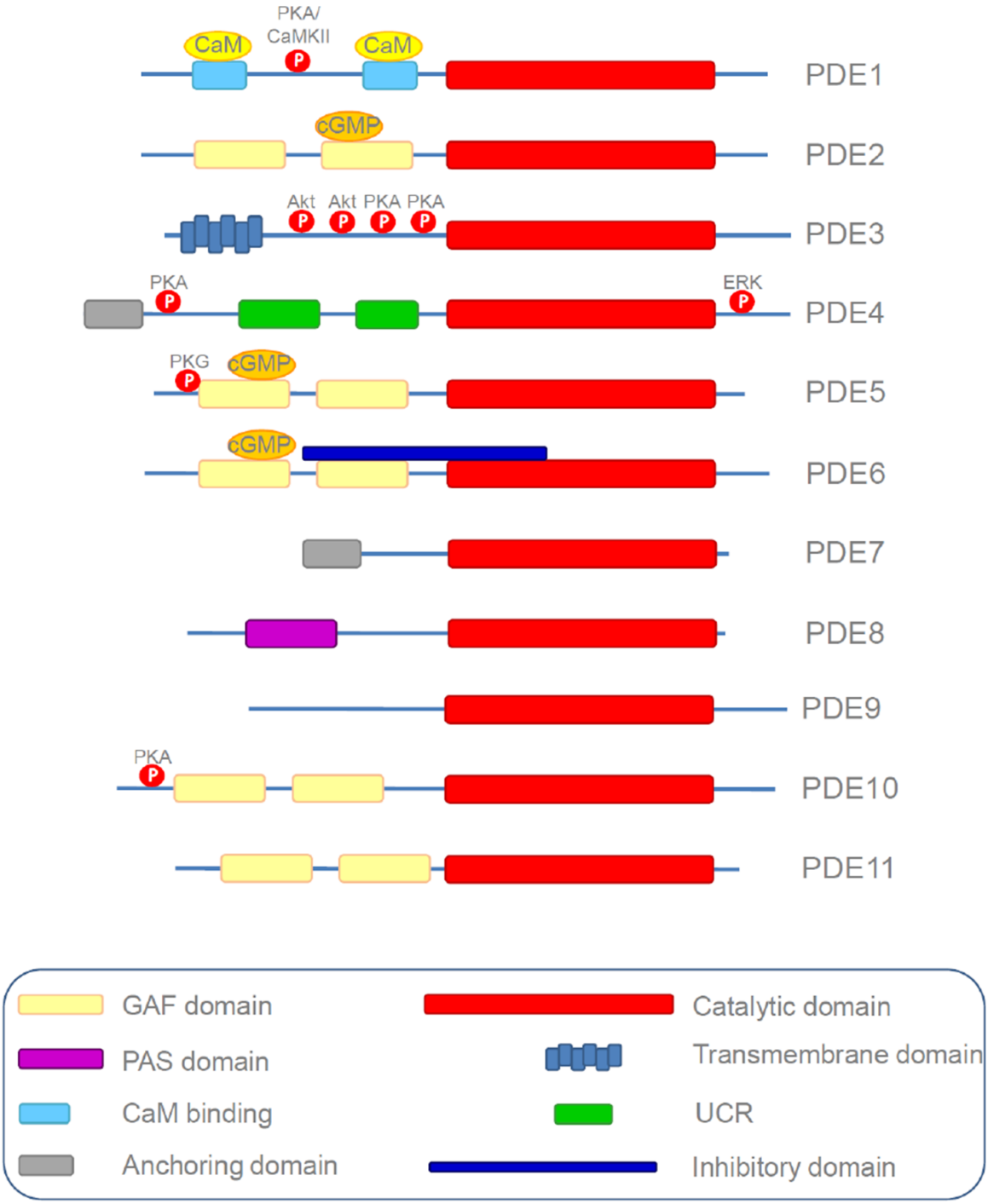

Figure 1-6 Domain structures of PDE families 1-11. Adapted from (Conti and Beavo 2007). The 11 PDE families shown are grouped according to their differing structures, kinetics, tissue distributions and modes of regulation

1.4 Phosphodiesterase 4 (PDE4)

PDE 4 enzymes are cAMP-specific phosphodiesterases. The family of PDE4 enzymes is encoded by four genes (PDE4A, PDE4B, PDE4C, PDE4D) and each exhibit distinct functional and regulatory properties (Torphy 1998). Each of these genes can produce multiple protein products due to mRNA splice variants, which results in approximately 20 different PDE4 isoforms, each of which are characterised by a unique N-terminal region (NTR) encoded by 1 or 2 exons under the control of a specific promoter (Torphy 1998, Conti and Beavo 2007). PDE4 isoforms have a modular structure, consisting of an isoform specific N terminus, regulatory domains known as upstream conserved regions (UCRs), the conserved catalytic domain common to all PDE families, and a subfamily specific C terminal region (Lynch, Baillie et al. 2007).

1.4.1 N-terminal Region

The N terminal region of PDE4 is unique to each isoform, and plays an important role in protein-protein interactions and intracellular targeting of the enzyme (Houslay and Adams 2010). For example, PDE4D5 isoforms are targeted to the signalling scaffold protein ß-arrestin at the plasma membrane to modulate ß - adrenergic signalling (Bolger, McCahill et al. 2003, Bolger, Baillie et al. 2006).

1.4.2 Upstream conserved regions (UCRs)

Different PDE4 isoforms can be classified as long, short, supershort and dead short isoforms see figure 1-7 and table 1-4 below.

PDE4s are classified based on the presence of the two regulatory domains UCR1 and UCR2 (Houslay and Adams 2003).The long isoforms can be differentiated from the short isoforms by an upstream conserved regions or UCRs. Long forms possess both UCR1 and UCR2, as well as two linker regions (LRs) which join them to the catalytic domain. Short forms lack UCR1 and the first linker region, and supershort forms lack UCR1 and LR1, and also have an N terminal truncation of UCR2. Finally, dead short isoforms such as PDE4A7 lack UCR1 and UCR2, and have a truncated catalytic domain which renders them catalytically inactive

(Houslay, Baillie et al. 2007).The UCR sequences play a key role in the regulation of PDE4 via phosphorylation in UCR1 by Protein kinase A (PKA) and in the C-terminal region by the extracellular signal-regulated kinase(ERK) (Houslay and Adams 2003). For example, the catalytic domain of all PDE4 subfamilies with the exception of PDE4A, possess a serine residue that can be phosphorylated by ERK (Baillie, MacKenzie et al. 2000). Phosphorylation of the long form PDE4 enzymes at this site results in its inhibition, whereas phosphorylation of this site in shortform PDE4s such as PDE4B2 isoform results in activation. Inactivation of PDE4 shortforms by ERK leads to the accumulation of cAMP which in turn activates PKA. PKA phosphorylation of PDE4 longforms within UCR1 can activate the enzyme which overrides the effect of ERK phosphorylation-dependent inhibition (Hoffmann, Baillie et al. 1999, Hill, Sheppard et al. 2006). Therefore UCRs can determine the functional outcome of ERK phosphorylation.

Class	**Truncations**	**Isoforms**
Long	None	4A4/5, 8, 10, 11 4B1, 3, 4 4C1, 2, 3 4D3, 4, 5, 7, 8, 9
Short	Lack UCR1	4B2 4D1, 2
Super short	Lack UCR1, LR1, N terminus of UCR2	4A1 4B5 4D6
Dead short	Lack UCR1 and UCR2; truncated catalytic unit	4A7

Table 1-4 Classification of PDE4 isoforms

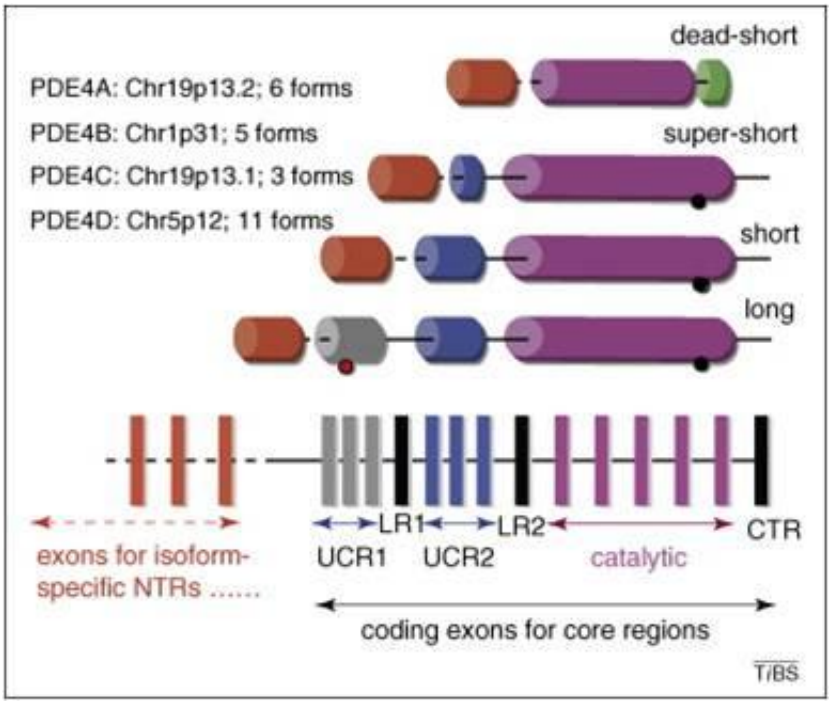

Figure 1-7 Domain structures of PDE4 isoforms (Houslay 2010).

The four genes of PDE4 encode over 20 distinct isoforms which can be classified into categories of long, short, supershort and dead-short as indicated. Different splicing mechanisms endow these isoforms with different combinations of the UCR1 (grey) and UCR2 (blue) regulatory components. Sites for PKA-mediated phosphorylation of UCR1 (red circle) and ERK-mediated phosphorylation of the catalytic unit (black circle) are shown. LR1, Linker Region 1 and LR2, Linker Region 2, are stretches of sequence that differ markedly in all four PDE4 subfamilies. CTR, C-terminal region is a stretch of sequence that differs markedly in all four PDE4 subfamilies. NTR (red), is the N-terminal region encoded by distinct exon(s) and defines each isoform. The chromosome localisation of all four genes is shown, together with the known number of isoforms generated by each gene (Houslay 2010).

1.4.3 Conserved Catalytic Domain

The catalytic domain of PDE4 is common to all PDE families, previously discussed in section 1.3.1.

1.4.4 Unique C terminal Region

The final exon of PDE4 genes encodes a sub-family specific C terminal region. The significance of this region is not yet fully understood, but may involve a regulatory function, as recent structural studies of PDE4 isoforms bound to inhibitors have revealed.

1.5 PDE4 and the Inflammatory Response

PDE4 plays a particularly important role in inflammatory and immunomodulatory cells and is ubiquitously found in inflammatory cells including mast cells, eosinophils, neutrophils, T cells, macrophages as well as structural cells such as sensory nerves, epithelial , smooth muscle cells and keratinocytes (Torphy 1998). Three PDE4 subtypes, PDE4A, PDE4B and PDE4D are expressed in these cells, while PDE4C is minimal or absent (Press and Banner 2009, Page and Spina 2011). PDE4 promotes production of proinflammatory mediators and decreases production of anti-inflammatory mediators (Schafer, Parton et al. 2010). PDE4 promotes inflammation by degrading cAMP that normally helps maintain immune homeostasis. PDE4 degradation of cAMP can cause immune cell activation and release of proinflammatory mediators such as TNFα, IL-17 and IFN-γ (Liu, Chen et al. 2000, Jimenez, Punzon et al. 2001, Sheibanie, Tadmori et al. 2004). By degrading cAMP PDE4 indirectly decreases the production of anti-inflammatory mediators such as IL-10. PDE4 has been implicated in a number of inflammatory diseases, including Psoriasis, psoriatic arthritis, Ankylosing spondylitis, Chronic Obstructive Pulmonary disease (COPD) and Rheumatoid Arthritis (Lipworth 2005) (Pathan E , McCann, Palfreeman et al. 2010)

1.5.1 The PDE4/PKA signalling Pathway

Non Clinical studies show that cAMP/PKA pathway plays an important regulatory role in several cell types involved in the pathophysiology of inflammatory diseases (Tasken and Aandahl 2004).Tumour Necrosis Factor – α (TNFα) is a pro-inflammatory cytokine produced mainly by monocytes and macrophages. Its levels were found to be decreased upon inhibition of PDE4 (Houslay, Schafer et al. 2005). Elevation of cAMP via inhibition of PDE4, triggers the Protein Kinase A pathway, inhibits TNFα production and suppresses the immune response. Therefore a number of PDE4 inhibitors are currently under development for the treatment of inflammatory diseases such as asthma, chronic obstructive pulmonary disease (COPD), rheumatoid arthritis, psoriasis and cancer (Calverley, Rabe et al. 2009, Sengupta, Sun et al. 2011, Schett G and Stevens R 2012, Papp, Kaufmann et al. 2013).

An increase in cAMP signalling via a PDE4 inhibitor results in the activation of the downstream effecter PKA, which directly phosphorylates and enhances gene transcription driven by CREB (cAMP response element binding protein). Figure 1-8 below shows the effect of PDE4 inhibition on signal transduction and cytokine gene transcription in monocytes and macrophages.

Activation of PKA results in extensive regulation of gene transcription in the cell, including a primary group of CRE-containing genes (Zambon, Zhang et al. 2005). The major transcription factor directly responsible for these primary changes in gene transcription is CREB. However, transcription driven primarily by NFκB tends to be inhibited by cAMP elevation due to the competition between CREB and the NFκB p65 subunit for binding the co-activator CREB binding protein (CBP), which directly binds to the TATA box and initiates transcription (Ollivier, Parry et al. 1996).

In human peripheral blood mononuclear cells, TNFα production induced by the lipopolysaccharide (LPS), a bacterial endotoxin, is inhibited by a variety of agents that activate the PKA pathway. These include $ß_2$-adrenoceptor agonists, 8-bromo-camp, cholera toxin, prostaglandin E_2 as well as various PDE4 inhibitors such as Rolipram (Seldon, Barnes et al. 1995). This inhibition is accompanied by the elevation of intracellular cAMP and the activation of PKA in both monocytes and macrophages. Treatment with the adenylate cyclase activator forskolin or with the PKA activator dibutyryl cAMP inhibits transactivation of p65 NFκB subunit, which is required for TNFα transcription (Parry and Mackman 1997). Conversely, in monocytes, PKA directly phosphorylates and activates CREB leading to production of IL-10 an anti-inflammatory cytokine (Platzer, Fritsch et al. 1999, Brenner, Prosch et al. 2003). Ultimately there is a positive effect on CREB and negative effects on NFκB upon cAMP elevation.

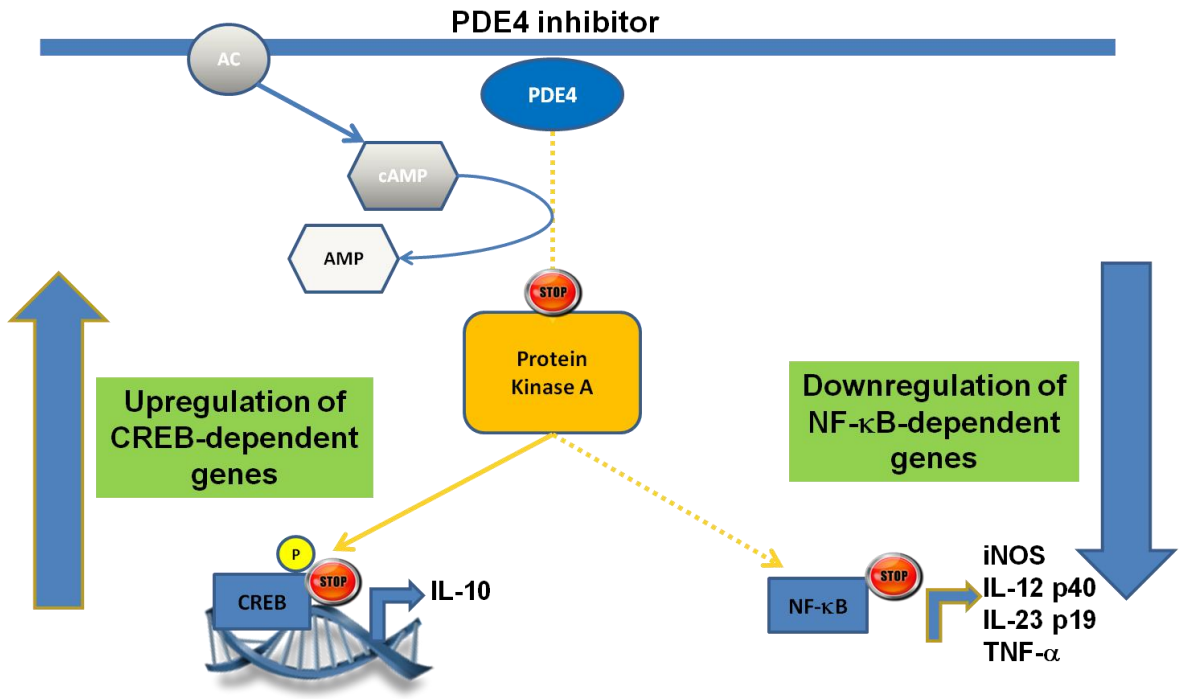

Figure 1-8 The PDE4/PKA signalling pathway. Adapted from (Schafer, Parton et al. 2010).

1.5.2 Role of PDE4 in Psoriasis and Psoriatic Arthritis

Psoriasis is a chronic inflammatory disease of the skin and affects more than 125 million people worldwide. Inflammation is normally tightly regulated and is part of the body's protective response to injury or infection. It prevents damage to surrounding tissue and in response to inflammation, several mechanisms work to regulate this immune response and establish homeostasis (Van Parijs and Abbas 1998).

The most common type of Psoriasis is plaque psoriasis and it manifests as raised, scaly, erythematous skin lesions (Mason, Mason et al. 2013). These lesions can be found anywhere on the body but are most commonly found to be on the scalp, elbows, nails, lower back and knees (Mason, Mason et al. 2013).

The formation of Psoriasis plaques is thought to be caused by dysregulated immune activity within the skin (Lowes, Bowcock et al. 2007, Mason, Mason et

al. 2013). This leads to an imbalance and overproduction of proinflammatory cytokines such as TNFα, IL-17 and IL-23 from immune cells (Nestle, Kaplan et al. 2009, Mason, Mason et al. 2013). The increase in production of these cytokines promotes chronic inflammation of the epidermis which leads to keratinocyte hyperproliferation (Perera, Di Meglio et al. 2012). These changes then cause the redness, itching, epidermal thickening and scaly plaques found in psoriasis (Menter, Gottlieb et al. 2008, Nestle, Kaplan et al. 2009). Since PDE4 is the predominant phosphodiesterase in a variety of inflammatory cells, its degradation of cAMP allows immune cells to produce elevated levels of the pro-inflammatory cytokines and decreased levels of anti-inflammatory cytokines (Souness, Griffin et al. 1996, Baumer, Hoppmann et al. 2007). Therefore this overproduction of pro-inflammatory cytokines is thought to drive the hyper proliferation and altered differentiation of keratinocytes.

Psoriatic arthritis (PsA) is an inflammatory arthritis associated with psoriasis and is characterised by stiffness, pain, swelling and tenderness of the joints and surrounding ligaments and tissue tendons (Gottlieb, Korman et al. 2008). Studies have confirmed that increased levels of proinflammatory mediators are found in psoriatic lesions and synovium of patients with PsA (van Kuijk, Reinders-Blankert et al. 2006, Boniface, Guignouard et al. 2007). In psoriatic arthritis, abnormal levels of multiple pro-inflammatory and anti inflammatory mediators have been observed in B cells, chondrocytes and synovial cells (Ritchlin, Haas-Smith et al. 1998).

It is known that PDE4 plays an important role in the regulation of pro and anti-inflammatory mediators involved in both psoriasis and psoriatic arthritis.

1.6 PDE4 inhibitors and their use in Inflammatory Disease

Inhibition of PDE4 has been shown to suppress a diverse range of inflammatory responses in vitro and in vivo (Torphy 1998, Press and Banner 2009, Page and Spina 2011). A significant number of PDE4 inhibitors have been developed and are currently being investigated for their use in inflammatory disorders such as

asthma, chronic obstructive pulmonary disease (COPD), psoriasis, inflammatory bowel disease and rheumatoid arthritis (Souness, Aldous et al. 2000, Page and Spina 2011).

The multiple isoforms of PDE4 and their widespread expression pattern has made PDE4 a good target for therapeutic intervention. A major challenge in the development of these inhibitors however, is their propensity to promote nausea and emesis. The recent development of PDE4 inhibitors with low emotogenic potential has proved successful, for example the recent approval of Roflumilast for COPD and the ongoing studies involving Apremilast for the treatment of Psoriasis and other inflammatory diseases(Gottlieb A, open-label et al. 2008) (Pathan E , Schett G 2009, McCann, Palfreeman et al. 2010, Baughman, Judson et al. 2012).

1.6.1 Structural basis of Inhibitor binding to PDE4

Each PDE4 sub-family contains a highly conserved catalytic unit containing 17 α helices, which are organised into 3 sub-domains: a bivalent metal binding pocket (Zn^{2+}, Mg^{2+}) which is thought to form a complex with the phosphate moiety of cAMP, a pocket containing an invariant glutamine (Q pocket), which forms hydrogen bonds with the nucleotide moiety of cAMP, and a solvent pocket. PDE4 inhibitors occupy this active site via a number of key interactions and prevent degradation of cAMP (Zhang, Card et al. 2004).

Co-crystal structures of many inhibitors in complex with various PDEs have identified two common features of inhibitors binding to PDEs (Figure1-9) (Card, England et al. 2004). 1) Direct binding to the metal ions by hydrogen bonds to water, while hydrophobic interactions between the planar ring structure of inhibitors and hydrophobic amino acid residues such as phenylalanine and isoleucine act to “clamp” the inhibitor within their active site. 2) Hydrogen bonding interactions between the aromatic structure of inhibitors and the Q pocket, which is normally occupied by the nucleotide moiety of cAMP (Xu, Hassell et al. 2000, Card, England et al. 2004, Wang, Peng et al. 2007).

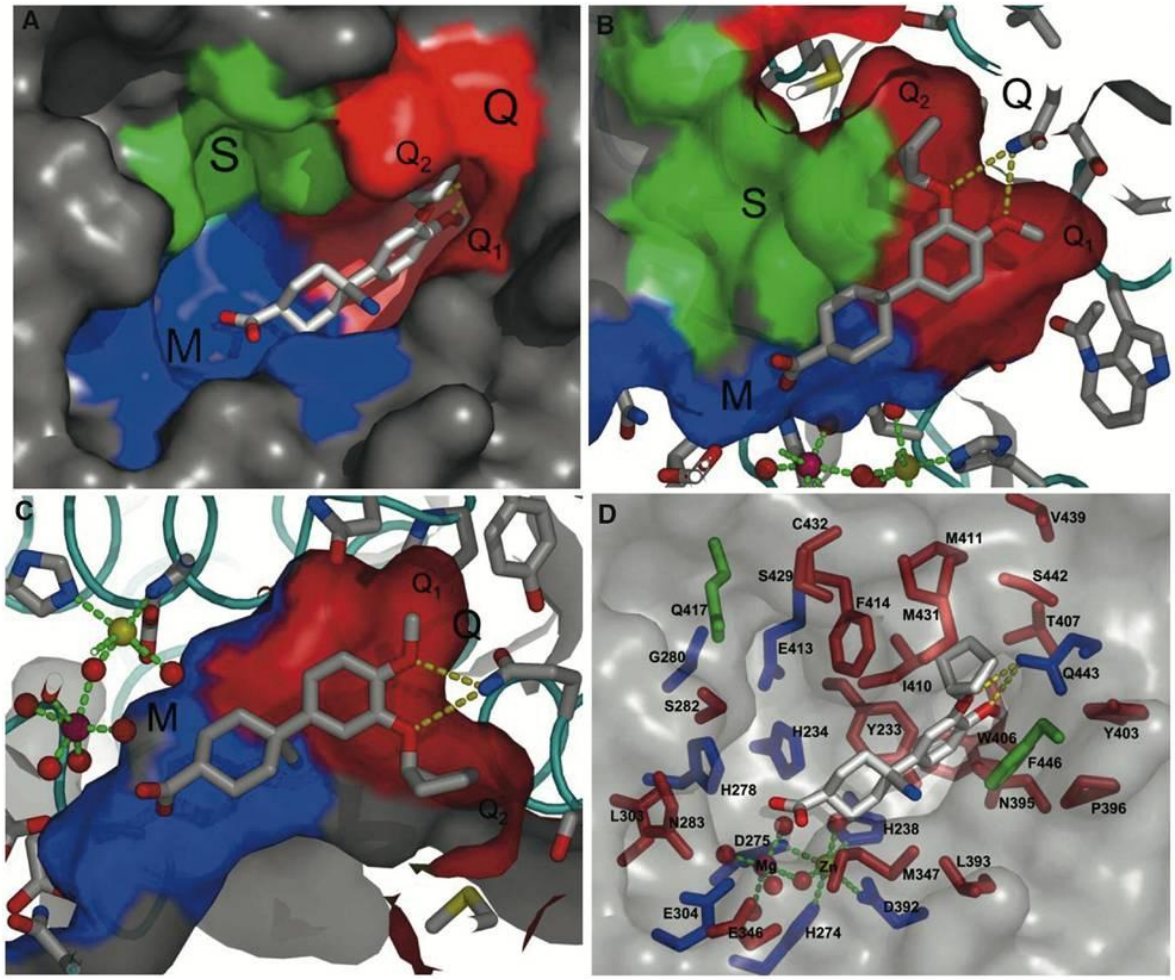

Figure 1-9 Classification of the Active Site of PDEs

(A) The active site of PDEs is divided into three pockets: the metal binding pocket (M) shown in blue, the purine-selective glutamine and hydrophobic clamp pocket (Q) shown in red (which is further divided into Q1 and Q2 subpockets), and the solvent-filled side pocket (S) shown in green. This colour coding of the active site pocket is mapped on the surface of PDE4B in complex with cilomilast, which is shown as a stick model bound at the active site. The cocrystal structure of PDE4B in complex with cilomilast has also been used to display the surfaces in (B)–(D). (B) Same as (A), but a view of the PDE active site looking toward the S pocket. This view is a clockwise rotation of about 90 along the length of cilomilast from the view in Figure 1A. The subpockets that subdivide the Q pocket are also labelled: Q1 is the small subpocket, and Q2 is the large subpocket. (C) Same as (A), but a view of the PDE active site looking away from the S pocket. This view is a counter clockwise rotation of about 90 along the length of cilomilast from the view in Figure 1-9A. All the subpockets are labelled. (D) Residues lining the three active site pockets. The active site surface is semitransparent to reveal residues that make up the active site. The absolutely conserved residues in all PDEs are coloured blue. Residues conserved in both cAMP- and cGMP-specific PDEs are coloured green. The other variable residues are coloured red. (Card, England et al. 2004)

1.6.2 The main chemical classes of PDE 4 inhibitors

All the reported inhibitors that bind PDE4 can be divided into four scaffold classes based on the structural motifs present: catechol, xanthine, pyrazole and purine analogs. These can then be further divided into three main chemical

classes: 1. Catechol ethers belong to the most widely represented class of inhibitors and are structurally related to Rolipram. Many examples of catechol diether- containing compounds are reported as PDE4 inhibitors for example, Mesopram (daxalipram was discovered as an improved rolipram analogue by Schering as a potential treatment for MS. However, Schering discontinued any further development of Mesopram. Other examples would be Zardaverine, a dual PDE3 and PDE4 inhibitor (Schudt, Winder et al. 1991) and Piclamilast which was developed as a treatment for arthritis and was a very potent inhibitor of PDE4 (0.7Nm) (Souness, Maslen et al. 1995). However, its development was discontinued due to toxic side effects. Cilomilast, Roflumilast and Apremilast discussed in sections 1.6.4, 5, and 6 are also Catechol diether containing compounds. These agents are characterised by the presence of the substructure (A) (figure 1-10) in which R1 is generally a methyl and R2 a cyclopentyl group; alternatively highly lipophilic groups are present at R2. 2. Quinazolinediones, in which are classified the PDE 4 inhibitors structurally related to Nitraquazone, which was developed by Syntex as a PDE4 inhibitor for the treatment of inflammatory diseases in the 1980s (Glaser and Traber 1984) (B) (figure 1-10). 3. Xanthines, which are generally non selective for PDE4 and have clear structural similarities to cAMP. Examples of Xanthines would be Theophyline which represents the natural product class of xanthines and 3-isobutyl-1-methylxanthine (IBMX) which was discovered through medicinal chemistry and developed specifically as a PDE inhibitor structure (C) (figure1-10). IBMX binds at the common core of the active- site pocket shared by all the PDEs and interacts with highly conserved residues. IBMX will flip its orientation when bound to cAMP-specific PDEs versus cGMP-specific PDEs so it can adapt to the H-bond characteristics of the nucleotide recognition glutamine (Huai, Liu et al. 2004). These features contribute to IBMX being a relatively weak and non selective PDE inhibitor compared to newer generation inhibitors. However, according to the pharmacophoric model proposed by Polimeropoulous et al (Polymeropoulos 1997) for PDE4 inhibitors, Classes 2 and 3 could be referred to the unique general structure in (D) (figure1-10) in which X= N, CO,CH, Y = bulky akyl or aryl Z = N,C, and W = N, CH. Inside this class, two subclasses can be distinguished, namely quinazolindiones and xanthines (Figure 1-10).

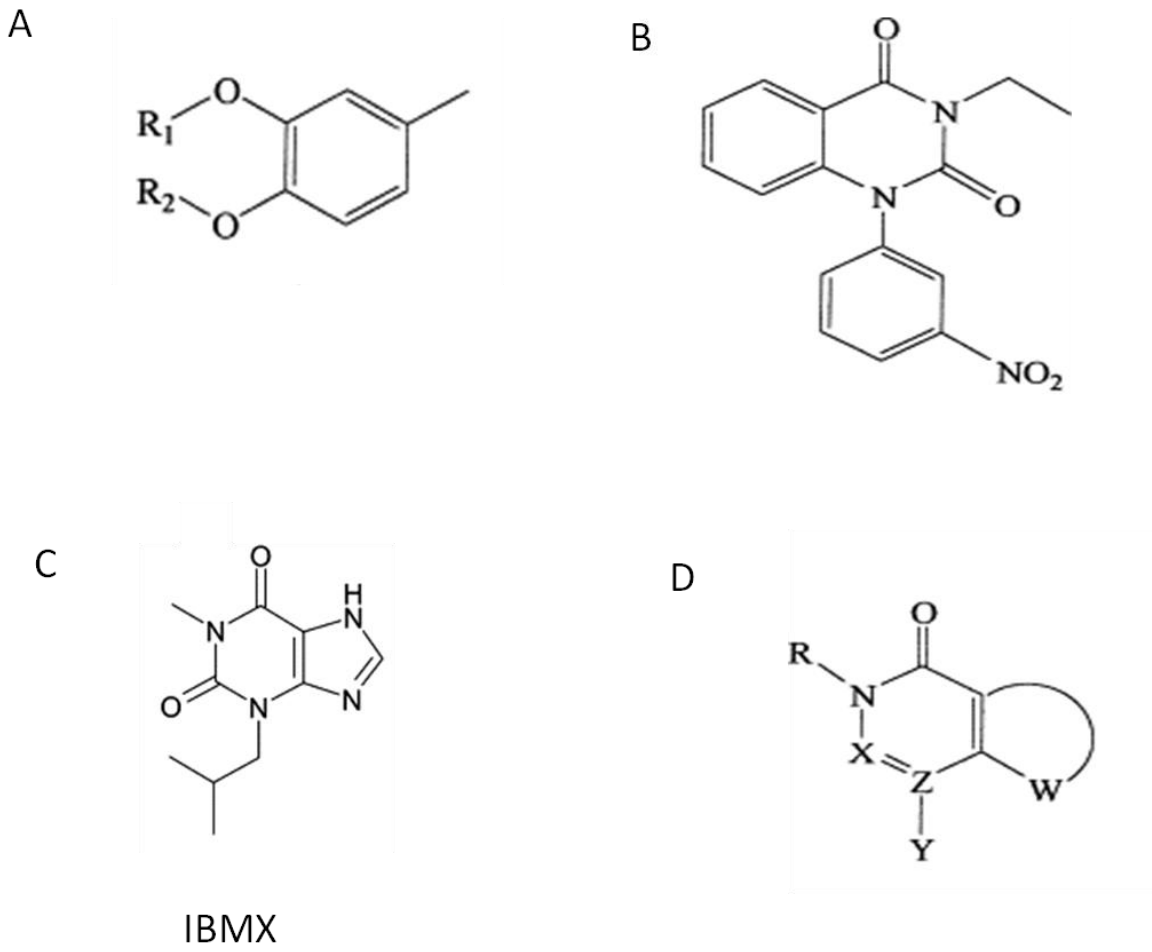

Figure 1-10 Structures of A) General structure of Catechol diethers, B) Nitraquazone, C) IBMX and D) general structure of quinazolindiones and xanthines (modified from (Dal Piaz and Giovannoni 2000).

1.6.3 Rolipram

Among the first generation of selective PDE4 inhibitors was Rolipram (4-[3-(cyclopentyloxy)-4 methophenyl]- 2-pyrrolidinone)(figure 1-9), which was originally developed as a putative antidepressant agent (Wachtel 1982). This compound exhibits at least 100-fold selectivity for PDE4 relative to the other 10 PDE families. It is directed against the active site of the PDE, binding competitively with cAMP, and therefore inhibits all PDE4 family members with

similar efficacy (Spina 2008). However, its clinical use was hindered by dose limiting gastrointestinal effects (Zeller, Stief et al. 1984). Nausea and emesis are also common problems associated with PDE4 inhibition and often limit their therapeutic window. It is thought that most of these effects are mediated by the central nervous system (CNS) and so it has been difficult to separate the effects of emesis from the more desirable effects. Studies in knockout mice have suggested that PDE4D is the main isoform that is associated with emesis (Robichaud, Stamatiou et al. 2002). While PDE4B appears to be the main isoform responsible for mediating release of TNFα (Jin and Conti 2002). Investigations found that nearly all PDE4 isoforms exist in two confirmations: a high- affinity rolipram binding site and a low-affinity rolipram binding site (Souness, Aldous et al. 2000). The adverse effects of rolipram and other compounds were found to occur when rolipram inhibited high affinity rolipram binding sites (Souness, Aldous et al. 2000). High affinity binding predominates in the central nervous system, while low predominates in inflammatory cells.

In light of this, development of PDE4B specific inhibitors that act on PDE4s in the low affinity Rolipram binding sites would be a possible means of maintaining anti-inflammatory activity without retention of the emetic side effects of PDE4 inhibition. Indeed, the development of several, newer generation PDE4 inhibitors are thought to have decreased emetic side effects. These include Cilomilast, Roflumilast and Apremilast.

1.6.4 Cilomilast

Cilomilast (figure1-9) was the first PDE4 inhibitor to go through extensive clinical testing (Rennard, Schachter et al. 2006). It was in phase 1 and 11 studies that cilomilast significantly improved lung function and reduced exacerbation rates in chronic obstructive pulmomary disease (COPD) (Giembycz 2006). However, its development was suspended in phase 111 trials due to its greater selectivity for PDE4D and its unfavourable side effects (Lipworth 2005).

1.6.5 Roflumilast

Roflumilast (DAXAS®, Bristol-Myers-Squibb) (3-cyclopropylmethoxy-4-diflouromethoxy-N- (3,5-dichloropynol-4-yl)-benzamide) (figure1-9) is an oral PDE4 inhibitor for the treatment of severe Chronic obstructive pulmonary disease (COPD). COPD is a very common, poorly reversible inflammatory disease of the airways and is thought to be mainly caused by smoking. It is the fourth most common cause of death in the US and is also a major cause of morbidity (Mannino 1971). COPD is characterised by lung parenchymal destruction i.e emphysema and obstructive bronchitis and is characterised functionally by progressive airway obstruction. Roflumilast and its primary metabolite, Roflumilast N-oxide are potent and competitive inhibitors of PDE4. It has been licensed in the UK for treatment of severe exacerbations of COPD and it is thought to act by increasing cAMP in the lung.

In COPD, blood levels of the pro-inflammatory cytokines (IL-1, IL-6 and tumour necrosis factor α (TNFα) are increased. Using PDE4 isolated from human neutrophils, which contains a mixture of different PDE4s, Roflumilast and Roflumilast N-oxide have IC50 values of 800pM and 2nM respectively (Hatzelmann and Schudt 2001). However, there is no discrimination between PDE4 gene variants in these compounds; they inhibit all 4 sub-families equally. This lack of subtype selectively contributes to its improved therapeutic ratio compared with its predecessors. For example Roflumilast has proportionately less effect on PDE4D than Cilomilast, is less likely to cause nausea and emesis than Cilomilast and is also a more potent anti-inflammatory (Field 2008). Roflumilast and Roflumilast N-oxide potently inhibit PDE4B activity. Roflumilast is well tolerated in patients with COPD and inhibits mediator release from immune and pro-inflammatory cells as well as in structural cells in the lung (Rennard, Schachter et al. 2006). It has been found to improve lung function in patients with moderate and severe COPD (Lipworth 2005). In phase III clinical trials Roflumilast was found to reduce the requirement for steroid and antibiotic treatments, and reduce hospitalisations resulting from exacerbations of COPD (Calverley, Rabe et al. 2009, Fabbri, Calverley et al. 2009). Therefore Roflumilast has become the first in class PDE4 inhibitor for COPD therapy and provides physicians with another treatment option for patients with severe COPD.

1.6.6 Apremilast

In addition to COPD, PDE4 inhibitors are also being developed for asthma, arthritis and psoriasis. Apremilast (Otezla ®) is a novel PDE4 inhibitor with TNFα inhibitory activity (Spina 2003) and has recently (January 2015) been approved by the European Commission for the treatment of patients with both Psoriasis and Psoriatic Arthritis. In Phase III studies Apremilast resulted in significant and clinically meaningful improvements in plaque psoriasis as well as having a consistent safety and tolerability profile across clinical trials (Papp, Kaufmann et al. 2013) (Gottlieb, Strober et al. 2008). The approval of Apremilast was based primarily on safety and efficacy results from two multi-centre, randomized, double-blind, placebo-controlled studies - ESTEEM 1 and ESTEEM 2 - conducted in adult patients with moderate to severe plaque psoriasis: body surface area (BSA) involvement of ≥10%, static Physician Global Assessment (sPGA) of ≥3 (moderate or severe disease), Psoriasis Area and Severity Index (PASI) score ≥12, and candidates for phototherapy or systemic therapy(Papp, Kaufmann et al. 2013).

Apremilast (figure1-9) (S)-N-[2-[1-(3-ethoxy-4-methoxyphenyl)-2-methanesulfonylethyl]-1,3-dioxo-2,3-dihy dro-1H-isoindol-4-yl] also known as CC-10004 has a molecular weight of 460.5. It binds to the catalytic site of PDE4, competitively blocking cAMP degradation. When it was initially screened for PDE4 inhibition, Apremilast was found to have an IC50 of approximately 0.074μM (Man, Schafer et al. 2009). The Ki value (affinity constant) of Apremilast for PDE4 is 68nM. Apremilast is a partial competitive inhibitor of PDE4 based on Lineweaver-Burk Analysis (Schafer, Parton et al. 2010). Apremilast is non selective within the PDE4 subfamily as demonstrated by cAMP-degradation assays for PDE4 A4,B2, C2 and D3 with similar potencies at IC50s ranging from 20 to 50nM, therefore is not a PDE4 subtype selective inhibitor (Schafer, Parton et al. 2010).

Apremilast has pharmacodynamic properties with potential therapeutic benefit for treating inflammatory disorders that involve elevated serum cytokine levels. Recent work (Schafer, Parton et al. 2010) has demonstrated the broad anti-inflammatory effects of Apremilast *in vitro* and in human cellular models (See figure 1-12). This included the inhibition of production of multiple mediators

including TNFα, IFN-γ, IL-2, IL-12, IL-13,IL23, macrophage inflammatory protein (MIP), monocyte chemoattract protein (MCP-1) and granulocyte macrophage colony stimulating factors (GM-CSF) from Peripheral blood monocytes. TNFα production by NK cells and keratinocytes was inhibited by Apremilast *in vitro*, which demonstrated that these two cell types, which are involved in the pathophysiology of psoriasis, are directly affected by a PDE4 inhibitor. Therefore these *in vitro* anti- inflammatory activities, and in particular the inhibition of production of TNFα, IL-12 and IL-23 and the ability of Apremilast to suppress psoriasis lesions *in vitro* suggested that it may be useful in the treatment of psoriasis via a multi-faceted mechanism (Schafer, Parton et al. 2010). Additionally, apremilast is known to augment IL-10 production, which is a known suppressor of other pro-inflammatory chemokines.

When comparing Apremilast to for example Cilomilast, Cilomilast is 10 fold more selective for PDE4D than Apremilast (Giembycz 2006). This lack of PDE4D selectivity in Apremilast may explain its better therapeutic index compared with other inhibitors. It has also been shown to have low binding to HARBS and so does not induce central nervous system effects such as lethargy, fatigue and nausea (McCann, Palfreeman et al. 2010).

Therefore Apremilast seems to elicit less emetic side effects while also having a wider therapeutic window. However, the underlying mechanism for this increased tolerability is unknown, although only 10% of the compound passes over the blood brain barrier.

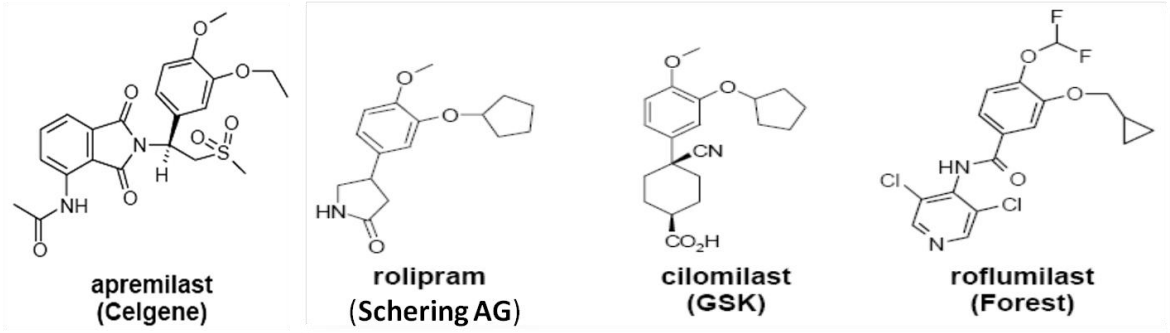

Figure 1-11 Chemical structures of the PDE4 inhibitors Apremilast, Rolipram, Cilomilast and Roflumilast

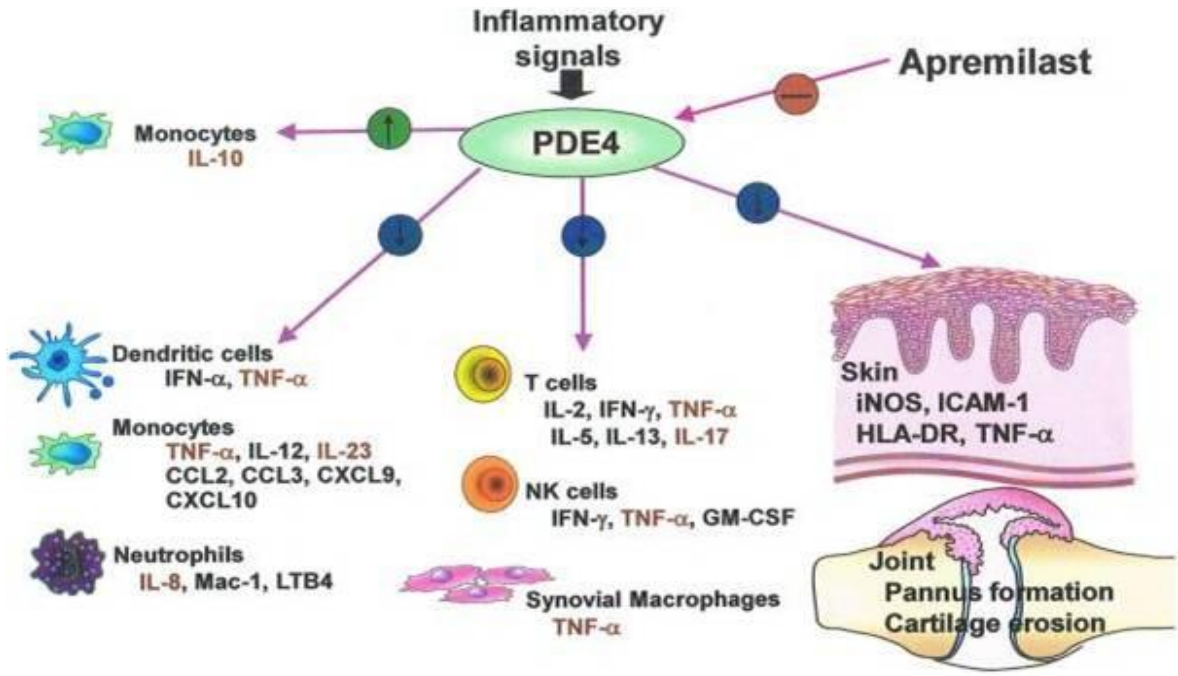

Figure 1-12 An overview of proposed mechanism of action of Apremilast in various cell types derived from *in vitro* studies. By blocking PDE4 activity, apremilast affects several cell types in the immune system including monocytes, dendritic cells , neutrophils, T cells, natural killer cells and macrophages (Samrao, Berry et al. 2012).

1.6.7 Comparing Apremilast and Roflumilast

The latest generation of selective PDE4 inhibitors such as Apremilast and Roflumilast seem to have an improved therapeutic index. While Roflumilast has been approved for treatment of COPD in 2010, Apremilast was more recently approved for Psoriasis and Psoriatic Arthritis. Apremilast may also prove useful in the future for other dermatological and Rheumatological conditions for example Rheumatoid arthritis and ankylosing spondyltis. Studies by Celgene in Psoriasis and Psoriatic Arthritis have demonstrated clinical activity of Apremilast (Papp, Kaufmann et al. 2013).

A number of similarities and differences were found in studies performed by PH Schafer et al between Apremilast and Roflumilast (Schafer, Parton et al. 2010). For example a direct comparison of cAMP elevation within prostaglandin E2 (PGE_2)-stimulated peripheral blood monocytes was made between Apremilast and Roflumilast (figure1-8). Other PDE4 inhibitors Rolipram and Cilomilast were also included. Results indicated that while Apremilast elevated cAMP in a

manner similar to Cilomilast and Rolipram, Roflumilast elevated cAMP levels approximately twice as high as Apremilast, Cilomilast and Rolipram.

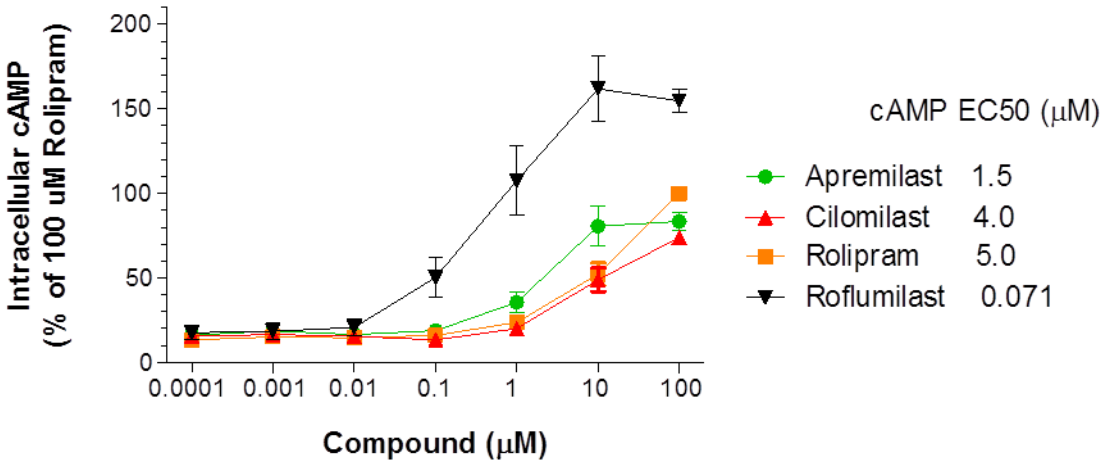

Figure 1-13 Intracellular cAMP levels in PGE2-stimulated PBMC treated with various PDE4 inhibitors (n=3) (data courtesy of Celgene)

The data in figure 1-13 suggested that roflumilast might inhibit a cAMP-hydrolyzing enzyme other than PDE4. Possibilities included PDE1, 2, 3, 7, 8, 10, or 11. Therefore roflumilast and apremilast were tested for inhibition of both cAMP- and cGMP-hydrolyzing PDE enzymes in recombinant human enzyme assays (figure 1-14).

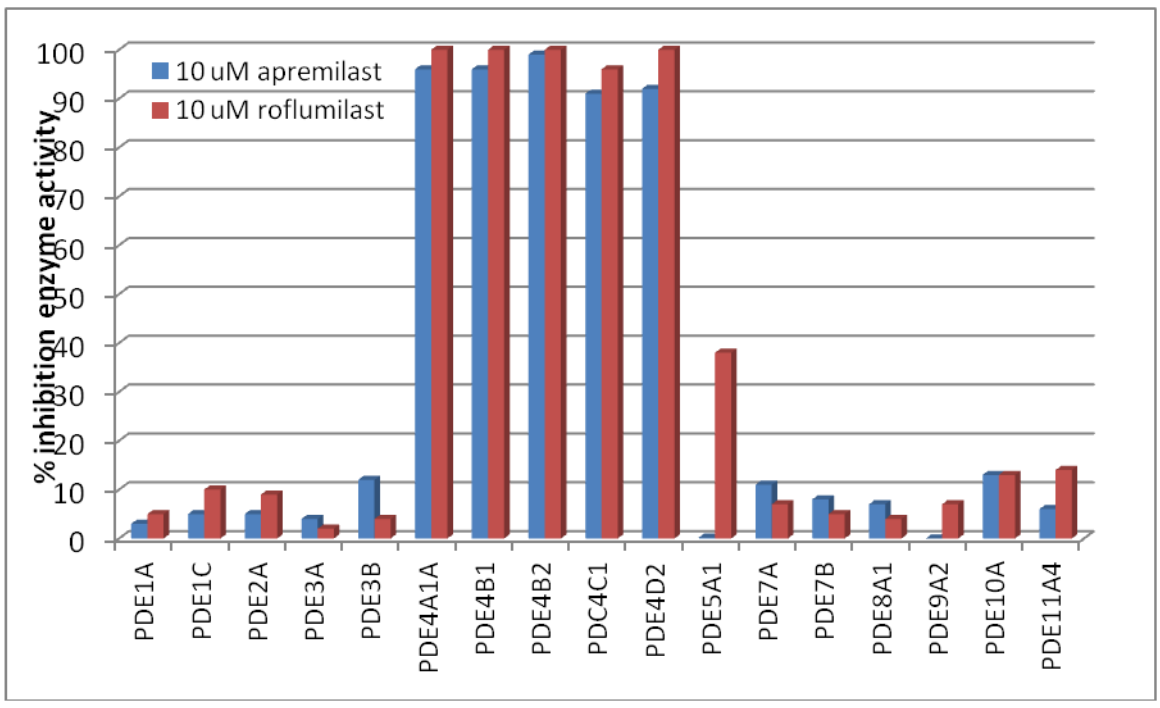

Figure 1-14 . Selectivity of apremilast and roflumilast against recombinant human PDE enzymes (data courtesy of Celgene)

Based on the data in Figure 1-14, both apremilast and roflumilast are highly selective for PDE4 over other PDEs. Roflumilast does exhibit some PDE5A1 inhibition, but this is a cGMP-selective phosphodiesterase. The other cAMP-hydrolyzing phosphodiesterases (PDE1, 2 3, 7, 8, 10, 11) are not significantly inhibited at 10 µM roflumilast. Therefore, lack of PDE selectivity cannot explain the very high cAMP levels attained by roflumilast treatment in PGE2-stimulated PBMC. Apremilast and roflumilast were then tested against several PDE4 isozymes to determine if PDE4 subtype selectivity might explain the differences in cAMP elevation. Results are shown in Table 1-5.

Compound	IC_{50} (nM) for specific PDE4 isoforms						
	A1A	***B1***	***B2***	***C1***	***D2***	***D3***	***D7***
apremilast	14	43	27	118	33	28	30
roflumilast	0.5	0.8	0.3	5.9	0.5	0.5	0.7
rolipram*	188	418	135	847	858	825	913

*** Rolipram was used as a positive control**

Table 1-5 IC_{50} values of the compounds against example PDE4 isoforms from each of the four PDE4 sub-families, A1A,B1,B2,C1,D2,D3,D7 (Study BPS Bioscience Celgene_PDE4_1001).

The data in Table 1-3 indicate that roflumilast is 20- to 90-fold more potent in inhibiting PDE4 isoforms *in vitro* than apremilast. However, it is extermely unlikely that potency alone can explain the different maximal cAMP elevation shown in Figure 1-9 as, for example, a concentration of 100 µM rolipram can be expected to inhibit completely all PDE4 isoforms. With the exception of PDE4C1, which is poorly expressed in the majority of cell types, apremilast and roflumilast are largely non-selective among these isozymes. So it appears that there are no major differences in selectivity which could explain the excessive cAMP elevation induced by roflumilast.

Since PDE4 enzymes have the ability to assume conformations that bind certain compounds (such as rolipram) with high affinity, it is possible that any conformational switch may be triggered by the compound itself, or by the association of the enzyme with other proteins. The long isoform PDE4A4 (aka PDE4A4B, PDE46, or PDE4A isoform1, Bolger 1993), for example, can assume a

high affinity conformation when associated with SH3 domain-containing proteins such as the Src-family kinase Lyn. This enzyme has been found to co-localize with Lyn when the two proteins are co-expressed in COS7 cells (Figure 1-15) (McPhee, Yarwood et al. 1999).

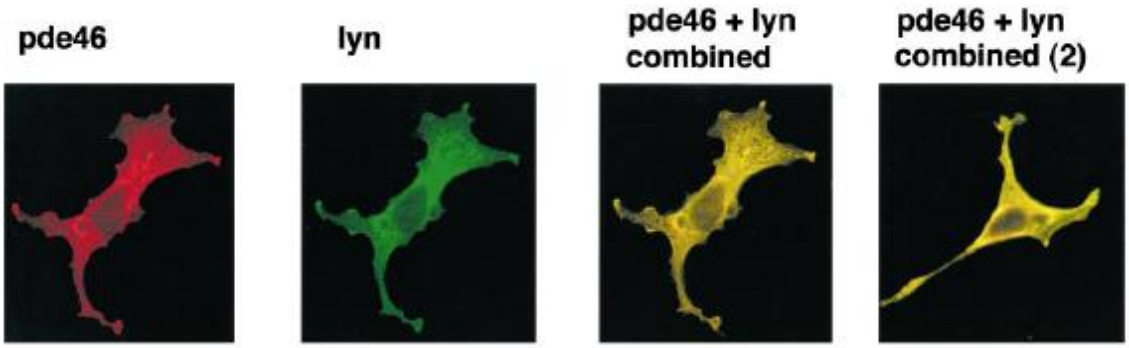

Figure 1-15 Colocalization of PDE4A4B (PDE46) with the kinase Lyn (McPhee, Yarwood et al. 1999).

The binding of apremilast and roflumilast was tested using the low affinity (cytosolic, isolated from cell lysate supernatant) and high affinity (membrane-associated, isolated from cell lysate pellet) forms of PDE4A4. Results indicated that while roflumilast bound to the membrane-associated fraction of PDE4A4 with 12-fold greater affinity than the cytosolic fraction, apremilast behaved in the opposite manner. Apremilast actually exhibited a 7-fold lower affinity for the so called high affinity form of PDE4A4 (Table 1-6). This indicates that apremilast, unlike roflumilast and rolipram, does not readily bind to the membrane-associated fraction of PDE4A4.

IC_{50} (μM)	*PDE4A4 low affinity (supe 2)*	*PDE4A4 high affinity (pellet 2)*	*PDE4A4 low/high ratio*
apremilast	0.02	0.136	0.15
roflumilast	0.0005	0.00004	12.5
rolipram	0.568	0.156	3.64

Table 1-6 . Inhibition of the low affinity and high affinity forms of PDE4A4 expressed in COS7 cells.

Due to the differential binding of these inhibitors to the 'high' and 'low' affinity forms of PDE4A4, one would expect there to be a commensurate differential effect in cAMP elevation within microdomains, which should be detectable using the appropriate cAMP probes, discussed in section 1.2.

Therefore in comparing Apremilast and Roflumilast, Celgene found no major differences in PDE selectivity or PDE4 isoform selectivity pattern. However, they found different cAMP elevation and PDE4A4 conformer inhibition pattern.

1.7 Thesis aims

Apremilast is a novel, orally available small molecule that specifically inhibits phosphodiesterase 4 (PDE4) and thus modulates multiple pro- and anti-inflammatory mediators and has recently (January 2015) been approved by the European Commission for the treatment of patients with both Psoriasis and Psoriatic Arthritis. Apremilast may be useful in the future for use in other diseases such as Rheumatoid arthritis and Ankylosing Spondylitis for example, Apremilast has undergone phase 2 clinical studies in Rheumatoid Arthritis (RA-002) and a Phase III study (AS-001) (Celgene) is also underway for Ankylosing Spondylitis. In the phase III trials in psoriasis and psoriatic arthritis, the clinical efficacy of apremilast was within the range of efficacy of low dose etanercept. With this biologic-like efficacy, oral route of administration, favourable safety and acceptable tolerability profile, apremilast is expected to fill a market niche as a new safe oral medication in dermatology and rheumatology that is suitable for use prior to the biologics.

Within the inflammatory disease therapeutic landscape, there are now several approved biologics targeting pro-inflammatory cytokines, namely TNF-α, IL-1ß, IL-6, and IL-12/IL-23 (Gottlieb, Chamian et al. 2005, Krueger, Langley et al. 2007, Cantarini, Vitale et al. 2015). Novel biologics targeting IL-17, IL-22, and oral small molecules targeting JAK3, Syk, and other intracellular targets others are in late stage clinical development (Jiang, Ghoreschi et al. 2008) (Chao, Chen et al. 2011). Therefore the dermatology and rheumatology space will become increasingly crowded with new therapies over the next decade. Furthermore, the presence of another PDE4 inhibitor (Roflumilast) on the market for the treatment of respiratory disease will further complicate the therapeutic landscape. Roflumilast is approved in the EU for the treatment of COPD and was recently approved in the US for treatment to reduce the risk of COPD exacerbations. Roflumilast is a selective PDE4 inhibitor, administered as an oral

tablet once daily, and is thought to act by increasing cAMP within lung cells. Therefore, there is a need for a clear understanding of Apremilast's mechanism of action (MOA), and how it compares to that of biologic and other small molecule drugs, for the purposes of labelling, for communication to the scientific community, physicians, and patients, and for an extension of utility to other diseases and therapeutic areas. In order to obtain a complete picture of the apremilast MOA, additional molecular and cellular biology studies are required to more fully elucidate the signalling mediators downstream of PDE4 inhibition which result in alterations in pro- and anti-inflammatory gene expression. My studies were conducted to directly compare Apremilast with Roflumilast, in order to substantiate the differences observed in the molecular and cellular effects of these compounds, and to search for other possible differentiating effects. Therefore the main aim of this thesis is to utilise biochemical techniques to discover whether Apremilast and Roflumilast work with different modes of action ie:

Clarify the Apremilast mechanism of action in comparison to Roflumilast:

1. Measure differences in cAMP elevation within cellular microdomains of cells treated with apremilast and roflumilast, to determine where within the cell the cAMP elevation differs between the two compounds.

2. Identify potential differences in PKA substrate phosphorylation patterns elicited by the two PDE4 inhibitors.

2 Materials and Methods

All materials and chemicals were from Sigma-Aldrich (Gillingham, Dorset, UK), unless otherwise stated.

2.1 Mammalian Cell Culture

All cell culture was performed in a class II tissue culture hood unless otherwise stated using an aseptic technique. All reagents were filter-sterilised or autoclaved prior to use.

2.1.1 HEK293 cells

The HEK293 cell line is derived from transformed human embryonic kidney cells (Graham, Smiley et al. 1977). HEK293 cells were cultured in Dulbecco's modified Eagle's medium (DMEM) supplemented with10% fetal bovine serum (FBS), 1% penicillin (10 000 U/ml)/streptomycin (10mg/ml) and 2mM L-glutamine. Cells were maintained in an atmosphere of 37°C and 5% CO_2, and passaged at 70-90% confluence. To passage, the growth media was removed and 2ml of1x trypsin-EDTA added per 10cm_2 of growth area. Cells were incubated at 37°C until they were seen to detach when viewed under a light microscope. 8ml of growth media was then added to inactivate trypsin. Cells were collected by centrifugation at 150g for 3minutes, and the cell pellet resuspended in 5-10ml fresh growth medium to remove the trypsin, then 1ml of suspended cells and 9ml of complete growth medium was added per10cm dish. Cells were then re-incubated at 37°C and 5% CO_2 until required. Media was changed every 48 hours.

2.1.2 Jurkat T and U937 cells

Jurkat Clone E6-1 is a human T lymphoblastoid cell line derived from an acute T cell leukemia (Gillis and Watson 1980). The cells are suspension lymphoblasts. Cells were maintained in RPMI1640 media supplemented with 5% foetal bovine serum, 0.1% Penicillin and Streptomycin (10000U/ml), 2mM Glutamine. Cells were generally sub-cultured at 80% confluence and re-seeded at a density of 10% confluence. Cultures can be maintained by the addition of fresh medium or replacement of medium.

Alternatively, cultures can be established by centrifugation with subsequent resuspension at 1 to 2 X 10^5 viable cells/mL.

The U-937 cell line was derived by (Nilsson and Sundstrom 1974) from malignant cells obtained from the pleural effusion of a patient with histiocytic lymphoma. The cells are suspension monocytes. Cells were maintained in RPMI1640 media supplemented with 5% foetal bovine serum, 0.1% Penicillin and Streptomycin (10000U/ml), 2mM Glutamine. Subculture in the same way as Jurkat T cells.

2.1.3 Rheumatoid Arthritis Synovial Fibroblasts

Primary Human Rheumatoid Arthritis Synovial Fibroblasts Rheumatoid arthritis synovial fibroblasts (RASFs) were purchased from Asterand Bioscience and culture was performed according to the manufacturer's instructions. Cells were grown in DMEM containing 5% FBS supplemented with 2 mM L-glutamine, 100 µg/ml penicillin, and 100 µg/ml streptomycin in a humidified atmosphere containing 5% CO_2.

2.1.4 Transfection of cells for FRET analysis

HEK 293 cells were transfected using TransIT-LT1 transfection reagent (Mirus Bio, Madison, USA). Cells were passaged 24 hours before transfection to ensure 40-60% confluence on the day of transfection, and maintained as described above (Section 2.2.1.) Cells were seeded onto sterilsed 24-mm diameter round glass coverslips mounted onto 6-well plates, transfections were performed at 50-70% confluence with Mirus transfection reagent according to the manufacturer's instructions using 1–2 µg DNA (sensor) per coverslip. 36µl of Mirus transfection reagent was added to 1.5ml Opti-MEM (Invitrogen), and the solution pippetted briefly to mix, then incubated at room temperature for 5 minutes. 12µg of sensor was then added, the solution pipetted once more to mix, and incubated at room temperature for a further 15 minutes. Meanwhile, the cell media was replaced with 750µl/well of complete growth medium. The transfection solution was then added drop-wise to the coverslips and swirled to mix. Cells were incubated at 37°C and 5% CO_2 for 24-48 hours to allow protein expression, prior to FRET experiments.

Transfection of RASFS and Jurkat T cells was performed using Nucleofector™ Technology (Lonza). Electroporation is a transfection technology based on the momentary creation of small pores in cell membranes by applying an electrical pulse. For nucleofection the required numbers of cells were centrifuged at 90xg for 10 minutes at room temperature. Supernatant was removed and the cell pellet was resuspended in 100µl room temperature Nucleofector® solution per sample and then combined with required amount of DNA. The Cell/DNA suspension was transferred into a certified cuvette (sample must cover bottom of cuvette without air bubbles). Sample was then inserted into nucleofector device and appropriate Nucleofector® programme X-001 was selected. Immediately after programme was finished the cells were resuspended in 500µl of media and gently transferred to a 6 well plate with 24-mm diameter round glass coverslips. Fret imaging experiments were performed after 24–48 h.

2.1.5 PDE4 inhibitor treatments for western blotting analysis

1 x 10^7 Jurkat T Cell Leukemia or U937 cells were plated in tissue culture dishes (10 x 10 cm) in 10 ml Complete Media (RPMI-1640 + 10% FBS, 2 mM L-glutamine, 100 units/ml Penicillin and 100 µg/ml Streptomycin) and incubated overnight at 37^{o}C, 5% CO_2. The next day, the cells were treated with 0.1% DMSO (vehicle), 0.1, 1 and 10 µM Apremilast (CC-10004), 10 µM Forskolin (Sigma, Cat# 89156-988) with and without 10 µM Apremilast, 1, 0.1 and 0.01 µM Roflumilast (CC-14064) for 30 minutes at 37^{o}C. All compounds were prepared in DMSO as a 10 mM stock. After 30 minutes, the cells were collected and centrifuged at 1200 RPM for 10 minutes. The supernatant was discarded and the cells were washed twice with cold 1X PBS and then PBS removed completely. The cells were then lysed with 100 µl 3T3 lysis buffer (25mM HEPES, 10% w/v glycerol, 50mM NaCl, 1% w/v Triton x100, 50mM NaF, 30mM NaPP, 5mM EDTA pH7.4) supplemented with complete EDTA-free Protease Inhibitor Cocktail Tablets (Roche®) . The same treatments were used for HEK 293 cells however; lysate preparation was performed as described below in section 2.1.6 for adherent cells.

2.1.6 Preparation of whole cell lysates

Lysates for Western blotting were prepared using 3T3 lysis buffer (25mM HEPES, 10% w/v glycerol, 50mM NaCl, 1% w/v Triton x100, 50mM NaF, 30mM NaPP, 5mM EDTA pH7.4). Complete, EDTA-free Protease Inhibitor Cocktail Tablets (Roche®) were also added to the lysis buffer prior to use. Adherent cells were detached from the tissue culture vessel by vigorous scraping with a scraper. Lysates were pipetted up and down to homogeneity and immediately transferred to a 1.5ml tube and kept on ice. Lysates were then centrifuged at 14000 x g for 5 minutes to remove insoluble material. Suspension cells were lysed as described above in (section 2.1.5). Concentration was immediately assessed and cleared lysates were either used the same day, or snap frozen on dry ice and stored at -80oC for future use.

2.1.7 Protein Assay

The concentration of protein in cell lysates was determined using the Bradford method (Bradford 1976). Protein assays were performed in clear 96 well plates. All samples were prepared in a final volume of 50µl 3T3 lysis buffer, and were tested in triplicate. A standard curve of known BSA concentrations between 0 and 5 µg was prepared. Each protein sample of unknown concentration was then diluted 1:50 – 1:200 in 3T3 lysis buffer. Bradford reagent (Bio-Rad) was diluted 1:5 in sterile dH_20, and 200µl of diluted reagent added per well. Samples and standards were analysed with a 595nm filter on an Anthos 2010 plate reader using ADAP software. Protein concentrations were calculated using a curve derived from the BSA standard values, and adjusted for sample dilution.

2.2 Western Blot

2.2.1 SDS- PAGE

Sodium dodecylsulphate polyacrylamide gel electrophoresis (SDS-PAGE) was used to separate proteins by molecular weight. Proteins were separated using the

Invitrogen NuPage Novex gel system. Protein samples were denatured and reduced for gel electrophoresis by diluting in 5x Laemmli protein sample buffer (Bio-Rad) and boiling for 5 minutes, then 1-100µg of protein per well was loaded directly onto 4-12% Bis-Tris NuPage gels. Gels were immersed in NuPage MES (for <50kDa proteins) or MOPS (for >50kDa proteins) running buffer. 3µl of Bio-Rad Precision Plus Dual Colour Protein Standard was added to the first well of each gel. This is a pre-stained standard protein ladder used to aid analysis of the molecular weight of the protein samples. Protein samples were subjected to gel electrophoresis at 180V for approximately 1.5 hours, or until protein separation was achieved.

2.2.2 Western Immunoblotting

Western immunoblotting allows the detection of individual SDS-PAGE separated proteins with specific anti-sera. The proteins separated by SDS-PAGE were transferred to nitrocellulose membrane using the XCell® blotting apparatus and NuPAGE® transfer buffer containing 20% methanol. The proteins were transferred with an applied voltage of 30V for 1 hour.

Following the transfer of the sample proteins, as indicated by successful transfer of the pre-stained molecular weight markers, the nitrocellulose membrane was washed 3 time with 1xTBST (20mM Tris-Cl pH 7.6, 150mM, NaCl and 0.1% Tween20). Nitrocellulose membranes were then incubated with Odyssey blocking buffer (LI-COR Biosystems) for 1hour at room temperature on an orbital shaker. Primary antibodies were diluted 1:1000 in odyssey block plus 0.1% Tween 20 (see table 2-1 for details of primary antibodies used). The blocked nitrocellulose membrane was then heat-sealed in an airtight bag containing the primary antibody solution. This was incubated overnight at 4°C on an orbital shaker. The membrane was then washed 3 times with TBST. LI-COR Biosystems® fluorophore conjugated secondary antibodies raised against the appropriate primary immunoglobulin species were diluted 1:10000 in odyssey block plus 0.1% Tween 20 (see table 2-2 for details of secondary antibodies used). The secondary antisera were incubated with primary immunoglobulin bound membranes within heat sealed bags for 1hour at room temperature on an orbital shaker (in the dark). The blots were washed 4 times for 5 minutes each with 1X TBST and once with 1X TBS to remove Tween 20. LI-COR Biosystems® fluorophore conjugated

secondary antibodies were visualised using the LI-COR Biosystems® Odyssey infrared western blot scanning visualisation system. Membranes were placed face down on the scanner and visualised at medium sensitivity at a resolution of 100µm at either 680 or 800nm wavelengths according to the secondary fluorophore. The resulting Tif files were analysed using LI-COR Biosystems® proprietary Odyssey® software.

Primary Antibody	Type	Dilution	Supplier
Anti-β-Actin	Mouse Monoclonal	1:20,000	Sigma Aldrich
Phospho-CREB (Ser133)	Rabbit Polyclonal	1:1000	Cell Signalling
Phospho-VASP (Ser157)	Rabbit Polyclonal	1:1000	Cell signalling
Phospho-PKA Substrate (RRXS*/T*)	Rabbit Polyclonal	1:1000	Cell Signalling
Phospho- Fyn (Y530)	Rabbit Polyclonal	1:1000	Abcam
Phospho-Src (Y416)	Rabbit Polyclonal	1:1000	Cell Signalling
Phospho-Akt (Thr 308)	Rabbit Polyclonal	1:1000	Cell Signalling
Phospho-Akt (Ser 473)	Rabbit Polyclonal	1:1000	Cell Signalling
S6 Ribosomal Protein	Rabbit Monoclonal	1:1000	Cell Signalling
Phospho-S6 Ribosomal Protein (Ser240/244)	Rabbit Polyclonal	1:1000	Cell Signalling
Phospho-S6 Ribosomal Protein (Ser235/236)	Rabbit Polyclonal	1:1000	Cell Signalling
PI3 Kinase p85	Rabbit Polyclonal	1:1000	Cell Signalling
p70 S6 Kinase	Rabbit Polyclonal	1:1000	Cell Signalling
Phospho-p70 S6 Kinase (Thr421/Ser424)	Rabbit Polyclonal	1:1000	Cell Signalling
p44/42 MAPK (Erk1/2)	Rabbit Monoclonal	1:1000	Cell Signalling
Phospho-p90RSK (Thr359/Ser363)	Rabbit Polyclonal	1:1000	Cell Signalling
p90RSK	Rabbit Polyclonal	1:1000	Cell Signalling
Anti-phosphotyrsoine	Rabbit monoclonal	1:1000	Abcam
Anti- MBP	Rabbit polyclonal	1:1000	Abcam

Table 2-1 List of Primary antibodies, their source and working dilutions.

Secondary Antibody	Type	Dilution	Supplier
Donkey anti Rabbit IRDye 800CW	Donkey Polyclonal	1:10,000	LICOR
Goat anti- Mouse IRDye 680LT	Goat Polyclonal	1:10,000	LICOR
Goat anti-Rabbit HRP	Rabbit	1:5000	Sigma

Table 2-2 List of Secondary antibodies, their source and working dilutions.

2.3 Fluorescence Resonance Energy Transfer (FRET) imaging

2.3.1 FRET based imaging

Fluorescence Resonance Energy Transfer (FRET) is a non-radiative process of energy transfer from an excited donor fluorophore to an acceptor fluorophore. This phenomenon can only occur when the two fluorophores are in close proximity to one another. This technique has been exploited to generate genetically-encoded sensors to visualise cyclic adenosine monophosphate (cAMP) dynamics in intact living cells (Zaccolo, De Giorgi et al. 2000). A FRET-based indicator of cAMP is usually composed of a cAMP-binding domain and the cyan and yellow variants of the green fluorescent protein, CFP and YFP respectively. Excitation of CFP (430 nm) results in the transfer of the excited state energy to YFP (emitting a signal at 545 nm). Both emissions are collected for analysis. Binding of cAMP to the sensor induces a conformational change which alters the distance between the two fluorophores thereby affecting the energy transfer between them. When this occurs only the CFP emission (480nm) is detected. FRET changes can be expressed as changes in the ratio between CFP emission (480 nm)/ YFP emission (545 nm) upon illumination at a wavelength that excites selectively the donor CFP (430 nm). Changes in FRET can be used in real-time imaging experiments as variations in FRET efficiency correlates with changes in cyclic nucleotide intracellular concentration.

2.3.2 Fret Sensors

The FRET sensors employed in this study were based on the Epac1-camps sensor (Nikolaev et al 2004), which consists of the cAMP-binding domain of Epac1 sandwiched between CFP and YFP (Figure 3-1) and PKA-RI and PKA-RII localizing probes based on the AKAP-binding domain of PKA-RIα or PKA-RIIß, fused to the cAMP-binding domain of EPAC (Di Benedetto, Zoccarato et al. 2008). Binding of cAMP to EPAC, results in a conformational change which increases the distance between the two fluorophores, reducing the FRET signal. These were kindly donated by Manuela Zaccolo.

2.3.3 FRET Imaging Set up

The set up utilised to perform FRET experiments is generally composed of an epiflouresence microscope, a light source that can excite the donor flouorophore, a beam splitter, a charge coupled device (CCD) camera and a computer. The FRET set up I have used for this thesis is described below:

Microscope: Olympus 1x71 inverted microscope

Objective: Olympus PlanApoN, 60X, NA 1.42 oil, 0.17/FN 26.5

Immersion oil: IMMERSOL 518f Zeiss®

Illumination Source: Xenon Mercury mixed gas arc burner (MT-ARC/HG LG2076, Ushio).

Excitation Filters: CFP: excitation filter ET436/20x, dichroic mirror T455LP, (Chroma Technology). YFP: excitation filter ET500/30x, dichroic mirror T515LP (Chroma Technology).

Emission Filters: CFP: emission filter ET480/40m; YFP: emission filter ET535/30m (Chroma Technology).

Beam Splitter: Dichroic mirror 505DCLP, YFP emission 545 nm, CFP emission 480 nm (Chroma Technology). Light emitted by the sample comprises both CFP and YFP emission wavelengths. The dichroic mirror splits the emitted light in two beams. Wavelengths below 505 nm, which include CFP emission at 480 nm, are reflected and directed through a series of mirrors towards to the CFP emission filter. Wavelengths over 505 nm, which include YFP emission at 545 nm, pass through the dichoric and are directed to the YFP filter.

Objective: Olympus PlanApoN, 60X, NA 1.42 oil, 0.17/FN 26.5

Immersion Oil: Immersion oil "IMMERSOL" 518F , Carl Zeiss

Camera: ORCA AG (model C4742-80-12AG, Hamamatsu Photonics K.K., Japan) and HAMAMATSU camera controller.

Computer: Dell DE6700, 2.66 GHz Intel Core 2 Duo CPU, 3.50 GB RAM, 400 GB hard drive, Windows XP Professional version 2002

Image acquisition and analysis: All devices of this imaging system, such as the shutter, the motorised filter wheel and digital camera are controlled by Cell^R software (Olympus BioSystems). Offline image analysis was performed using ImageJ free software.

2.3.4 Fret imaging acquisition

Cells to be investigated were grown on 24mm glass cover-slips. When using Jurkat T cells cover slips were coated with Fibronectin (Sigma Aldrich). Targeted FRET sensors were transiently transfected 24 hours after seeding. FRET imaging experiments were performed 18 h after transfection. The coverslip was firstly placed into a metal slide holder which, when sealed, creates a bath where stimuli can be directly added. The bath is filled with 900 µl of Hepes-buffered Ringer-modified saline solution containing 125 mM NaCl, 5 mM KCl, 1 mM Na_3PO_4, 1 mM $MgS0_4$, 5.5 mM glucose, 1mM $CaCl_2$, and 20 mM Hepes, pH 7.5 and maintained at room temperature. Cells were stimulated in real time with 10µM Apremilast, 10µM Roflumilast, 100µM IBMX (Sigma Aldrich) and 25µM Forskolin

(Sigma Aldrich) which were diluted to 10x final concentration in saline before addition.

Before starting the experiment a standard protocol for all experiments was designed (detailed explanation of this protocol can be found in (Gesellchen et al. 2011). Briefly, the following parameters must be set and remain the same throughout each set of experiments:

Binning: Most of the camera detection systems used for FRET have the ability to combine the information in adjacent pixel and make them into one effective superpixel. The benefit of binning is that there is a reduced noise in the signal. A binning of 1x1 means that each individual pixel is used as such; a binning of 2x2 means that an area of 4 adjacent pixels is combined into one larger pixel, and so on. The drawback of binning is the loss of resolution. In the case of 2x2 binning; there is a fourfold increase in signal (the four single pixel contributions), a twofold loss in resolution but a twofold improvement in signal-tonoise. All experiments in this thesis have been acquired with binning 2x2.

Exposure Time: The exposure time determines the period of time cells are illuminated and photons are collected and converted into charges for each channel. Optimal exposure time depends on the expression levels of fluorophores as well as the characteristics of the lamp, the optics and the camera. Generally an exposure time of 50 – 300 ms should be used, depending on the brightness of the sample. Increasing the exposure time allows the photons coming from the sample to accumulate and enhance the intensity of the image. At the same time this will increase the photobleaching of the fluorophores. There is also the risk of saturation of pixel charges and any further change in the signal cannot be detected. Experiments in this thesis have been acquired at an exposure time of 200 ms.

Time course and Number of Acquisitions: The frequency of acquisition defines the interval between each data recording. This time between acquisitions depends on the characteristics of the sensor and the kinetics being investigated, but the normal range is 2 – 60 seconds. A short interval between illuminations may again result in photo-damaging of the cells and photo-bleaching of the signal. All experiments have been acquired with a frequency of 5 seconds. After

these parameters have been set, the experiment can be started. A small drop of oil is added to the objective lens before mounting the coverslip. A bright (well tranfected) cell, which is well attached and not contracting, is selected to perform the experiment. Cell^R software allows for a live display of the ratio between the mean fluorescence intensity of each channel, so it is possible to estimate when the signal has stabilised before adding the stimulus (usually after 25 acquisitions). Further stimuli can be carefully added after each plateau phase. Only once the signal has stabilised after the final stimulus should the experiment be concluded.

The first step in analysing the experiment is to split and align the images taken by the CFP and YFP channels (this and the following steps is conducted offline using ImageJ) resulting in a perfectly superimposed image. Alignment, drift of the focus or change in the position of the cell is checked. A region of interest (ROI) is drawn on the background area and another around the cell of interest. Mean intensities for each acquisition is calculated and both CFP and YFP are subtracted from the background intensities, reducing any artefacts. cAMP changes are expressed as $\Delta R / R0$ %, Where $\Delta R = Rt2 - Rt1$. Rt1 is the average of at least 5 ratio (ICFP/IYFP) values calculated before the addition of the stimulus; Rt2 is the average of at least 5 ratio values at the plateau phase of reached after the addition of the correspondent stimulus. R0 corresponds to ICFP/IYFP at basal FRET level.

Ratiometric measurements correct for unequal probe distribution and, within certain limits, for bleaching occurring during the experiment and changes in focus. Ratio drift is corrected and calculated on the basis of the baseline drift before stimulus is added. However, care must be taken when aligning the two channels (to avoid artefacts) and when interpreting ratio values. To assess whether the increases in ratio correspond to actual increases in cAMP, CFP and YFP intensities are plotted over time and accurately analysed on how fluorescence intensity changes in the two channels over time. Ratio changes can reliably be considered as FRET changes only when determined by a change in donor emission which is paralleled by an opposite change in acceptor emission (e.g. an increase in CFP emission must be paralleled by a decrease in YFP emission).

Compound	Mode of Action	Company
Apremilast (CC-10004)	PDE4 inhibitor	Celgene
Roflumliast (Daxas)	PDE4 inhibitor	Selleckchem
IBMX	Non specific PDE inhibitor	Sigma-Aldrich
Forskolin	Adenylyl Cyclase Activator	Sigma-Aldrich

Table 2-3 Table of agonist and inhibitor treatments used in experiments.

2.4 CelluSpots™ tyrosine kinase substrate arrays

CelluSpots™ tyrosine kinase substrate arrays were purchased from Intavis (described in detail in Chapter 4). RASFs were seeded on $10cm_3$ plates and after 24hrs cells were treated with 10μM Apremilast, 10μM Roflumilast, as well as one plate with no treatment, for 30 mins at 37°C. After 30 minutes media was removed and cells were washed twice in ice cold PBS. The cells were lysed with 100μl lysis buffer [20mM Tris-Hcl (pH7.5), 150mM NaCl, 1mM Na_2 EDTA, 1mM EGTA, 1% Triton X-100, 2.5mM sodium pyrophosphate, 1mM beta-glycerophosphate,1mM Na_3V0_4, 1Mm NaF, (2μg/ml leupeptin and 1mM PMSF added fresh before use). Protein concentrations of the cell lysates were quantified using the Bradford assay (described in section 2.1.7). The cell lysates were then stored in -80°C until use. Slides were blocked in 5% BSA, 50mM Hepes pH7.4, 150mM NaCl and 0.05% TX 100. The arrays were then overlaid with 200μg/ml protein from each lysate in (1%BSA, 1x tyrosine kinase buffer (cell signalling) supplemented with 10μM final ATP) for two hours. Slides were washed briefly in TBST. Slides were then incubated with phospho-tyrosine antibody in 1% BSA/TBST at 1:2000 dilution overnight at 4°C. Slides were washed 5 times in TBST. Slides were then incubated with anti-rabbit HRP secondary antibody in 1%BSA/TBST for one hour and then washed 5 times in TBST. The arrays were then subjected to analysis using the enhanced chemi-luminescence (ECL) method (Amersham BioSciences, Little Chalfont, UK) to detect antibody complexes bound to proteins of interest. Arrays were covered with ECL solution for 5 minutes and then exposed to light-sensitive autoradiography film, which was developed on a Kodak X-Omat Model 2000 processor. Densitometric analysis was performed using Quantity One software (Biorad).

2.5 Reverse Phase Protein Array preparation of cells

Cells were prepared for RPPA by seeding RASFs on $10cm^3$ plates and after 24 hours either incubating with no treatment, 10μM Apremilast, or 10μM Roflumilast for 30 mins at 37°C. After the 30 minutes all media was removed and cells were washed twice in ice cold PBS and stored in -80°C. RPPA procedure was performed at Edinburgh Cancer Research Unit. Described in more detail in Chapter 4. Table 2-4 shows the antibodies tested in RPPA.

FAK1	Cell Signalling Technologies	3285	rabbit
FAK1 P Y397	Cell Signalling Technologies	3283	rabbit
ATM	Merck (Calbiochem)	PC116	rabbit
ATM/ATR Substrate P Ser/Thr	Cell Signalling Technologies	2851	rabbit
Aurora A/B/C P Thr288/Thr232/Thr198	Cell Signalling Technologies	2914	rabbit
Bad P Ser136	Cell Signalling Technologies	9295	rabbit
Bad P Ser112	Cell Signalling Technologies	9291	rabbit
Bak	Epitomics	1542-1	rabbit
Met P Tyr1234	Signal way	11227-1	rabbit
CamKII P Thr286	Cell Signalling Technologies	3361	rabbit
CrkL P Tyr207	Cell Signalling	3181	rabbit

	Technologies		
FLT3 P Tyr591 P Tyr591	Cell Signalling Technologies	3461	rabbit
HSP27 (HSPB1) P Ser78	Cell Signalling Technologies	2405	rabbit
IkB-alpha	Cell Signalling Technologies	4812	rabbit
IKK alpha/beta P Ser176/Ser177	Cell Signalling Technologies	2078	rabbit
JAK1	Cell Signalling Technologies	3332	rabbit
MEK1/2	Cell Signalling Technologies	9122	rabbit
MEK1/2 P Ser217/221	Cell Signalling Technologies	9154	rabbit
MNK1 (MKNK) P Thr197,Thr202	Cell Signalling Technologies	2111	rabbit
MSK1 P Ser376	Cell Signalling Technologies	9591	rabbit
PARP	Cell Signalling Technologies	9542	rabbit
PI3 Kinase p110-alpha	Cell Signalling Technologies	4249	rabbit
PKA RII P Ser96	Epitomics	1151-1	rabbit
PKC (pan) P Ser660 (beta-2)	Cell Signalling	9371	rabbit

	Technologies		
PKC substrate P (R/K)X(S*)(Hyd)(R/k)	Cell Signalling Technologies	2261	rabbit
PKC-zeta	Cell Signalling Technologies	9372	rabbit
PKC-zeta/lambda P Thr410/403	Cell Signalling Technologies	9378	rabbit
Bim	Epitomics	1036	rabbit
GSK-3-beta	Cell Signalling Technologies	9315	rabbit
Met P		11238	
Rap1	Cell Signalling Technologies	4938	rabbit
IGF-1R beta P Tyr1162,Tyr1163	Invitrogen (Biosource)	44-804G	rabbit
ErbB-1/EGFR	Cell Signalling Technologies	2232	rabbit
ErbB-2/Her2/EGFR P Tyr1248/Tyr1173	Cell Signalling Technologies	2244	rabbit
ErbB-3/Her3/EGFR	Cell Signalling Technologies	4754	rabbit
ErbB-3/Her3/EGFR P Tyr1289	Cell Signalling Technologies	4791	rabbit
Stat5	Invitrogen (Biosource)	44-368G	rabbit

Stat5	Cell Signalling Technologies	9351	rabbit
EGFR P Tyr1173	Cell Signalling Technologies	4407	rabbit
Akt P Thr308	Cell Signalling Technologies	2965	rabbit
Met	Cell Signalling Technologies	4560	rabbit
Stat3 P Tyr705	Cell Signalling Technologies	9131	
IkB-alpha P Ser32	Cell Signalling Technologies	2859	rabbit
mTOR P Ser2448	Cell Signalling Technologies	2971	rabbit
S6 Ribosomal Protein	Cell Signalling Technologies	2217	rabbit
S6 Ribosomal protein P Ser235,Ser236	Cell Signalling Technologies	2211	rabbit
p44/42 MAPK (ERK1/2)	Cell Signalling Technologies	9102	rabbit
p44/42 MAPK (ERK1/2) P Thr202/Thr185,Tyr204/Tyr187	Cell Signalling Technologies	4370	rabbit
Src	Cell Signalling Technologies	2109	rabbit
Akt	Cell Signalling Technologies	9272	rabbit

Akt P Ser473	Cell Signalling Technologies	4060	rabbit
Akt P Ser473	Cell Signalling Technologies	9271	rabbit
PARP cleaved Asp214	Cell Signalling Technologies	9541	rabbit
beta-actin	Cell Signalling Technologies	4970	rabbit
NFkB p65 Ser536	Cell Signalling Technologies	3033	rabbit
cdc25c P Ser216	Cell Signalling Technologies	4901	rabbit
Chk1 P Ser345	Cell Signalling Technologies	2348	rabbit
Chk2 P Thr68	Cell Signalling Technologies	2661	rabbit
c-Jun P Ser73	Cell Signalling Technologies	9164	rabbit
c-Myc	Cell Signalling Technologies	5605	rabbit
E-Cadherin	Cell Signalling Technologies	3195	rabbit
Rb	Epitomics	2655-1	rabbit
M-CSF P Tyr723	Cell Signalling Technologies	3155	rabbit

4E-BP1 P Ser65	Cell Signalling Technologies	9451	rabbit
4E-BP1 P Thr37,Thr46	Cell Signalling Technologies	2855	rabbit
beta-Catenin	Cell Signalling Technologies	9562	rabbit
beta-Catenin P Ser33,Ser37,Thr41	Cell Signalling Technologies	9561	rabbit
beta-Catenin P Thr41,Ser45	Cell Signalling Technologies	9565	rabbit
cdc25A	Cell Signalling Technologies	3652	rabbit
VEGFR P Tyr1175	Cell Signalling Technologies	3770	rabbit
PTEN	Cell Signalling Technologies	9552	rabbit
Tyk2 P Tyr1054,Tyr1055	Cell Signalling Technologies	9321	rabbit
Tsc-2 (Tuberin) P Thr1462	Cell Signalling Technologies	3617	rabbit
Tsc-2 (Tuberin)	Cell Signalling Technologies	3612	rabbit
Survivin	Cell Signalling Technologies	2808	rabbit
p70 S6 Kinase P Thr389	Epitomics	1175-1	rabbit

PTEN P Ser380,Thr382,Thr383	Cell Signalling Technologies	9554	rabbit
SAPK/JNK	Cell Signalling Technologies	9258	rabbit
p70 S6 Kinase P Thr421,Ser424	Cell Signalling Technologies	9204	rabbit
LKB1	Cell Signalling Technologies	3047	rabbit
GSK-3-alpha/beta P Ser21/Ser9	Cell Signalling Technologies	9331	rabbit
Stat6 P Tyr641	Cell Signalling Technologies	9361	rabbit
SAPK/JNK P Thr182,Tyr185	Cell Signalling Technologies	4668	rabbit
p53 P Ser15	Cell Signalling Technologies	9284	rabbit
p53	Cell Signalling Technologies	9282	rabbit
p38 MAPK PThr180,Tyr182	Cell Signalling Technologies	9211	rabbit
p38 MAPK	Cell Signalling Technologies	9212	rabbit
mTOR P Ser2448	Cell Signalling Technologies	2971	rabbit
mTOR	Cell Signalling Technologies	2972	rabbit

Stat1 P Ser727	Invitrogen (Biosource)	44-382G	rabbit
Raf P Ser259	Cell Signalling Technologies	9421	rabbit
PLC-gamma1 P Tyr783	Cell Signalling Technologies	2821	rabbit
PDK-1 P Ser241	Cell Signalling Technologies	3061	rabbit
p90 S6 kinase (Rsk1-3) P Thr359,Ser363	Cell Signalling Technologies	9344	rabbit
PDK-1	Cell Signalling Technologies	3062	rabbit
p70 S6 Kinase	Cell Signalling Technologies	9202	rabbit
JAK1 P Tyr1022,Thr1023	Invitrogen (Biosource)	44-422G	rabbit
c-Myc P Thr58,Ser62	Epitomics	1203-1	rabbit
SAPK/JNK P Thr183,Tyr185	Cell Signalling Technologies	9251	rabbit
S6 Ribosomal protein p Ser240,Ser244	Cell Signalling Technologies	2215	rabbit
S6 Ribosomal Protein	Cell Signalling Technologies	2217	rabbit
Rb P Ser807,Ser811	Cell Signalling Technologies	9308	rabbit

Rb P Ser780	Cell Signalling Technologies	9307	rabbit
Raf P Ser338	Cell Signalling Technologies	9427	rabbit
MAPKAPK-2 P Thr334	Cell Signalling Technologies	3041	rabbit
Bax		1063.1	rabbit
Stat6	Cell Signalling Technologies	9362	rabbit
Stat1 P Tyr701	Cell Signalling Technologies	9171	rabbit
Src (family) P Tyr416	Cell Signalling Technologies	2101	rabbit
Smad2/3 P Ser465/Ser423,Ser467/Ser425	Cell Signalling Technologies	9510	rabbit
Smad1/5 P Ser463/Ser465	Cell Signalling Technologies	9516	rabbit
Cyclin D1 P Thr286	Cell Signalling Technologies	3300	rabbit
AMPK alpha	Cell Signalling Technologies	2532	rabbit
AMPK alpha P Thr172	Cell Signalling Technologies	2535	rabbit
Bax	Epitomics	1063	rabbit
Bcl-2	Epitomics	1017-1	rabbit

Bcl-x	Epitomics	1018	rabbit
Bid	Epitomics	1008	rabbit
Bim P Ser69	Cell Signalling Technologies	4585	rabbit
c-Jun N-term	Epitomics	1254-1	rabbit
Caspase 3	Cell Signaling Technologies	9662	rabbit
Caspase 3 cleaved	Cell Signaling Technologies	9664	rabbit
CDK1 (p34cdc2) P Tyr15	Cell Signaling Technologies	9111	rabbit
CREB P Ser133	Millipore (Upstate)	06-519	rabbit
CREB	Cell Signalling Technologies	9197	rabbit
EGFR P Tyr1068	Invitrogen (Biosource)	44-788G	rabbit
GSK-3-beta P Ser9	Cell Signalling Technologies	9336	rabbit
IRS-1	Cell Signalling Technologies	2382	rabbit
Hexokinase	Cell Signalling Technologies	2867	rabbit
eEF2	Cell Signalling Technologies	2332	rabbit

P Myosin light chain	Cell Signalling Technologies	3761	rabbit
Tuberin P S1387	Cell Signalling Technologies	5584	rabbit
IRS-1 P S636/639	Cell Signalling Technologies	2388	rabbit
PKM2 XP(R)	Cell Signalling Technologies	4053	rabbit
YB1	Cell Signalling Technologies	4202	rabbit
PABP1	Cell Signalling Technologies	4992	rabbit
SQSTM1	Cell Signalling Technologies	8205	rabbit
PLC-gamma1	Cell Signalling Technologies	2822	rabbit
Puma	Cell Signalling Technologies	4976	rabbit
SHP2 P Tyr542	Cell Signalling Technologies	3751	rabbit
Smad2 P Ser465,Ser467	Cell Signalling Technologies	3108	rabbit
Tau P Ser396	Epitomics	1178-1	rabbit
VEGFRP Tyr1175	Cell Signalling Technologies	2478	rabbit

VEGFR P Tyr951	Cell Signalling Technologies	4991	rabbit
Smad3 P Ser423,Ser425	Cell Signalling Technologies	9520	rabbit
BRCA1	Cell Signalling Technologies	9010	rabbit
CDK2	Epitomics	1134-1	rabbit
MAPKAPK-2	Epitomics	1497-1	rabbit
Stat3	Cell Signalling Technologies	9132	rabbit
Tau	Epitomics	2368-1	rabbit
VEGFR P Tyr1059	Cell Signalling Technologies	3817	rabbit
XIAP	Cell Signalling Technologies	2045	rabbit
Zap70	Cell Signalling Technologies	2705	rabbit
S6 Ribosomal Protein	Cell Signalling Technologies	2211	rabbit
Rsk2 Pser 227	Cell Signalling Technologies	3556	rabbit
NFkB p105/p50	GeneTex	GTX110 585	rabbit
Calmodulin	Calbiochem		

Calpain2	Cell Signalling Technologies	2539	rabbit
Calpastatin	Cell Signalling Technologies	4146	rabbit
PDGFR P Tyr1021	Cell Signalling Technologies	2227	rabbit
PDGFR P Tyr751	Cell Signalling Technologies	4549	rabbit
ErbB-2/Her2/EGFR	Dako	A0485	rabbit
PKA	Abcam	ab26322	rabbit
GFAP	Abcam	ab7260	rabbit
beta-Tubulin	Abcam	ab6046	rabbit
PKC-alpha P Thr638	Abcam	ab32502	rabbit
Raf1 (C-12)	Santa Cruz	sc-133	rabbit
Prohibitin	Santa Cruz	sc-28259	rabbit
p21 CIP/WAF1 p Thr145	Santa Cruz	20220-R	rabbit
FRA1 (R20)	Santa Cruz	sc-605	rabbit
p90 S6 kinase (Rsk1-3)	Santa Cruz	sc-231	rabbit
PKC-gamma P Thr514	GeneTex	GTX25778	rabbit
mTOR P Ser2481	Millipore (Upstate)	09-343SP	rabbit

Ubiquitin (P4D1)	Cell Signalling Technologies	3936	mouseIg G1
Stat3 P Tyr705	Cell Signalling Technologies	9138	mouseIg G1
Cyclin D1	Cell Signalling Technologies	2926	mouseIg G2a
p21 CIP/WAF1	Cell Signalling Technologies	2946	mouseIg G2a
CrkL	Cell Signalling Technologies	3182	mouseIg G1
HSP27 (HSPB1)	Cell Signalling Technologies	2402	mouseIg G1
Ki-67 (Annexin II, p36)	Beckton Dickinson	610968	mouseIg G1
PKC-alpha	Beckton Dickinson	610108	mouseIg G2b
Ras	Beckton Dickinson	8100001	mouseIg G1
Stat1	Cell Signalling Technologies	9176	mouseIg G1
SirT1 (IF3)	Cell Signalling Technologies	8469	mouse
Histone H2A.X P Ser139	Millipore (Upstate)	05-636	mouseIg G1
CamKII alpha (22B1) P Thr286	Abcam	ab2724	mouseIg G1

GAPDH	Abcam	ab9484	mouseIg G2b

Table 2-4 Table of Antibodies used in RPPA

2.6 Phage Display

Purified Protein PDE4A4 was provided by Frank Christian (Baillie Lab member) along with 10mM stock solutions of Apremilast and Roflumilast to Tedd Hupp (Edinburgh Cancer Research Institute) where Phage display technology was performed using their in house generated 12mer peptide library.

2.7 Solid Phase Peptide Array and overlay experiments

Peptide arrays are generated by direct synthesis of peptides onto Whatman cellulose membranes. Arrays were synthesised in-house, using an AutoSpot-Robot ASS 222 (Intavis Bioanalyical Instruments, Köhn, Germany). Arrays were stored dry at 4°C prior to use. To investigate possible protein-protein interactions, peptide arrays were first activated by rinsing for 1 minute in 100% ethanol, then washed in 1x TBST for 10 minutes. Non-specific binding was blocked by incubating with 5% milk solution for 2 hours at room temperature with gentle agitation. The array was then incubated with 10µg/ml of the purified protein of interest in 1% milk solution at 4°C overnight. After 16 hours, the array was washed 3 times for 10 minutes in TBST and incubated with primary antibody to the purified protein of interest at the appropriate dilution for 2 hours at room temperature. After a further 3 washes in TBST, the appropriate HRP-conjugated secondary antibody was added for 1 hour at room temperature. Finally, the array was washed 3 times in TBST. The arrays were then subjected to analysis using the enhanced chemi-luminescence (ECL) method (Amersham BioSciences, Little Chalfont, UK) to detect antibody complexes bound to proteins of interest. Arrays were covered with ECL solution for 5 minutes and then exposed to light-sensitive autoradiography film, which was developed on a Kodak X-Omat Model 2000 processor.

2.8 Basic Local Alignment Search Tool (BLAST)

The BLAST algorithms used within this study to search protein databases can be found on the NCBI website (blast.ncbi.nlm.nih.gov) (Johnson, Zaretskaya et al. 2008).

2.9 Multiple Em for Motif Elicitation (MEME)

MEME is an online consensus motif tool that discovers novel, ungapped motifs (recurring, fixed-length patterns) in nucleotide or protein sequences.
MEME splits variable-length patterns into two or more separate motifs which can be found here: (http://meme.nbcr.net/meme/cgi-bin/meme.cgi

2.10 Statistical analysis

In this thesis, all experiments were performed an n of 3 times, unless otherwise specified in the figure legend. Statistical significance was calculated using either an unpaired two tailed *t*-test in Microsoft Excel or by one way analysis of variance (ANOVA) using Graph Pad Prism software, as stated in the figure legend. A P value > 0.05 was considered not significant (ns), P < 0.05 was considered significant (*), P < 0.01 was considered very significant (**), and P < 0.001 was considered extremely significant (***).

3 FRET imaging for real time cAMP dynamics in cells

3.1 Introduction

Within the cell, cAMP levels do not rise and fall uniformly throughout the cytosol following the activation and desensitization of cell surface receptors. Rather, cAMP levels are compartmentalized into microdomains influenced by proximity to the adenylyl cyclase enzymes located within the plasma membrane that produce cAMP, and by the phosphodiesterases which are associated with receptors such as the ß1-adrenoceptor or the p75 neurotrophin receptor that hydrolyse cAMP (Houslay 2010). When cAMP is elevated, it binds to and activates the downstream effectors protein kinase A (PKA) or exchange protein directly activated by cAMP (EPAC), a cAMP effector protein that acts as a GTP exchange factor to activate the mini G-proteins RAP1 and RAP2. FRET probes based upon the structures of both these cAMP-binding proteins have proven to be useful tools in real time monitoring of cAMP microdomains. For example, the AKAP-binding domains from the cytosolic PKA-RIα and the membrane-associated PKA-RIIß have been fused to the soluble EPAC cAMP-binding domain to generate two probes that reveal spatially distinct activation of PKA-RI and PKA-RII within cardiac myocytes (Di Benedetto, Zoccarato et al. 2008) (Figure 3-1).

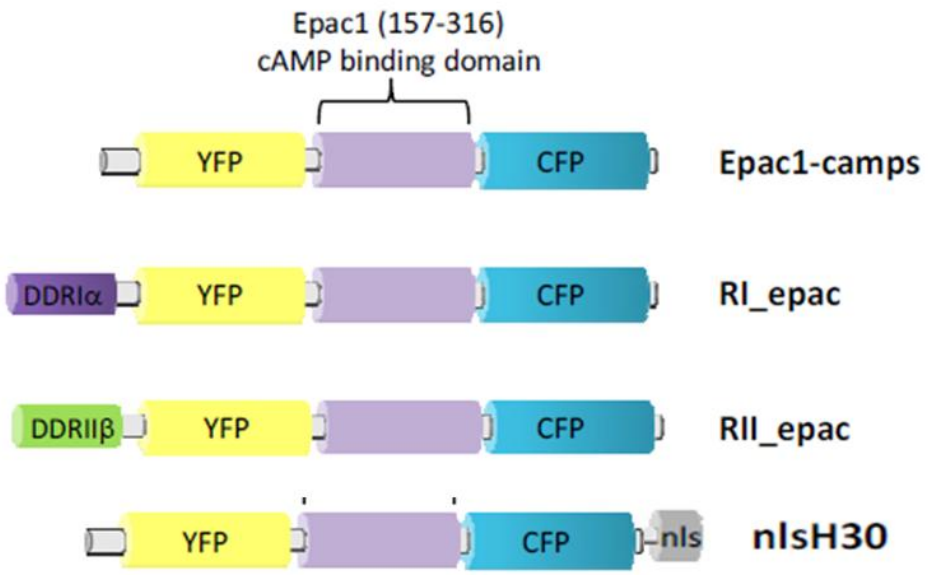

Figure 3-1 PKA-RI and PKA-RII localizing probes based on the AKAP-binding domain of PKA-RIα or PKA-RIIβ, fused to the cAMP-binding domain of EPAC. (Di Benedetto, Zoccarato et al. 2008) Epac1 camps cytosolic localizing probe and Epac 1-nls nuclear localizing probe (Nikolaev, Bunemann et al. 2004).

Using such probes, it is possible to monitor cAMP levels within specific microdomains of the cell that depend upon specific cellular activation signals for Gs-coupled receptors and PDE4 isoform targeting. My studies employed the use of these FRET probes to measure cAMP increases resulting from PDE4 inhibition with Apremilast and Roflumilast. The experiments in this chapter are unique as it has never been determined whether two different PDE4 inhibitors, which show no apparent isoform selectivity, alter cAMP dynamics differently.

Fluorescence resonance energy transfer (FRET), which occurs when two compatible fluorophores are brought into molecular proximity, can be exploited to measure cAMP dynamics in real time and in intact cells, thus allowing detection of signalling events within the complexity of a three-dimensional cell with extremely high resolution in space and time. In my experiments, I used FRET reporters of cAMP that are genetically encoded and exploit FRET between a donor (CFP) and an acceptor fluorophore (YFP) fused to the amino- and carboxy- termini of a cAMP binding domain from Epac, respectively. In the absence of cAMP the donor and acceptor fluorophores are close enough for FRET

to occur. Upon binding of cAMP the cAMP-binding domain undergoes a conformational change that moves CFP and YFP apart, thereby diminishing FRET. With such sensors, changes in cAMP concentration ([cAMP]i) can be estimated by changes in FRET measured as changes in the CFP-to-YFP emissions ratio (480 nm/545 nm), a value that is proportional to ([cAMP]i).

3.2 Specific Aims

The aim of this chapter was to determine whether Apremilast and Roflumilast triggered similar cAMP changes at multiple cellular locations. The experiments were performed using genetically encoded, FRET-based cAMP sensors to assess dynamic changes in cAMP levels in living cells as a consequence of challenge with Apremilast and Roflumilast. In doing this, I employed the use of not only (i) a cytosolic sensor but also those targeted to, (ii) the nucleus and (iii) to the RI and RII sub-populations of protein kinase A, to determine functionally distinct phenotypic outputs in cells. Experiments were conducted in the model cell line HEK 293 cells and then in more physiologically relevant cell lines, Jurkat T Leukemia cells and Rheumatoid arthritis synovial fibroblasts (RASFs). The data provided here affords a unique opportunity of determining whether there is any selectivity of action between Apremilast and Roflumilast in regulating specific cAMP pools in cells. This may provide a means of linking changes in particular cAMP sub-compartments to specific functional effects and determining the relative efficacy of Apremilast and Roflumilast in regulating these.

3.3 Experimental Procedure

Changes in intracellular [cAMP] can be estimated from changes in FRET. FRET can be expressed as the ratio (R) of CFP emission intensity over YFP emission intensity following excitation of the cell at 440nm (R = CFP480/YFP545). Changes in FRET ratio were expressed as the increase in CFP/YFP ratio over the CFP/YFP ratio at time zero (R0), as described in the Materials and Methods Section (Mongillo, McSorley et al. 2004). As [cAMP] rises in the vicinity of the FRET sensor, the two fluorophores move further apart, and FRET is diminished,

resulting in predominantly CFP emission. The CFP/YFP ratio therefore increases in proportion to the rise in [cAMP]i (Mongillo, McSorley et al. 2004).

Cells were transfected with appropriate probes and FRET experiments were performed in resting cells as described in materials and methods section. cAMP was generated by real time stimulus of the transfected cells with either Apremilast or Roflumilast at a concentration of 10μM. The cells expressing the probes were then treated with saturating concentrations of isobutylmethylxanthine (IBMX) 100μM followed by forskolin (FSK) 25μM to obtain a maximal/saturating response. FSK is an adenylyl cyclase activator and stimulates cAMP production by Adenylate cyclases, whereas IBMX is a non-specific PDE inhibitor that blocks cAMP degradation.

3.4 Results

Initial FRET experiments were performed in HEK293 cells using the cytosolic FRET based sensor for cAMP Epac1-camps (Nikolaev, Bunemann et al. 2004). As shown in figure 3-2 the results obtained show that Apremilast induces significantly higher concentrations of cAMP in the cytosol compared to Roflumilast in HEK 293 cells. There is no evidence of the "super cAMP" elevation caused by Roflumilast, which was shown by Schafer and collegues (Schafer, Parton et al. 2014) where Roflumilast elevated cAMP more potently in prostaglandin E2 stimulated human peripheral blood monocytes with an IC_{50} OF 68nM and to a level approximately 50% higher than that of Apremilast , Rolipram and Cilomilast. Apremilast has an effective half maximal concentration (EC50) of 1.4μM. It is possible that HEK cells may need to be stimulated to induce cAMP before addition of the inhibitors in order to see this super cAMP by Roflumilast.

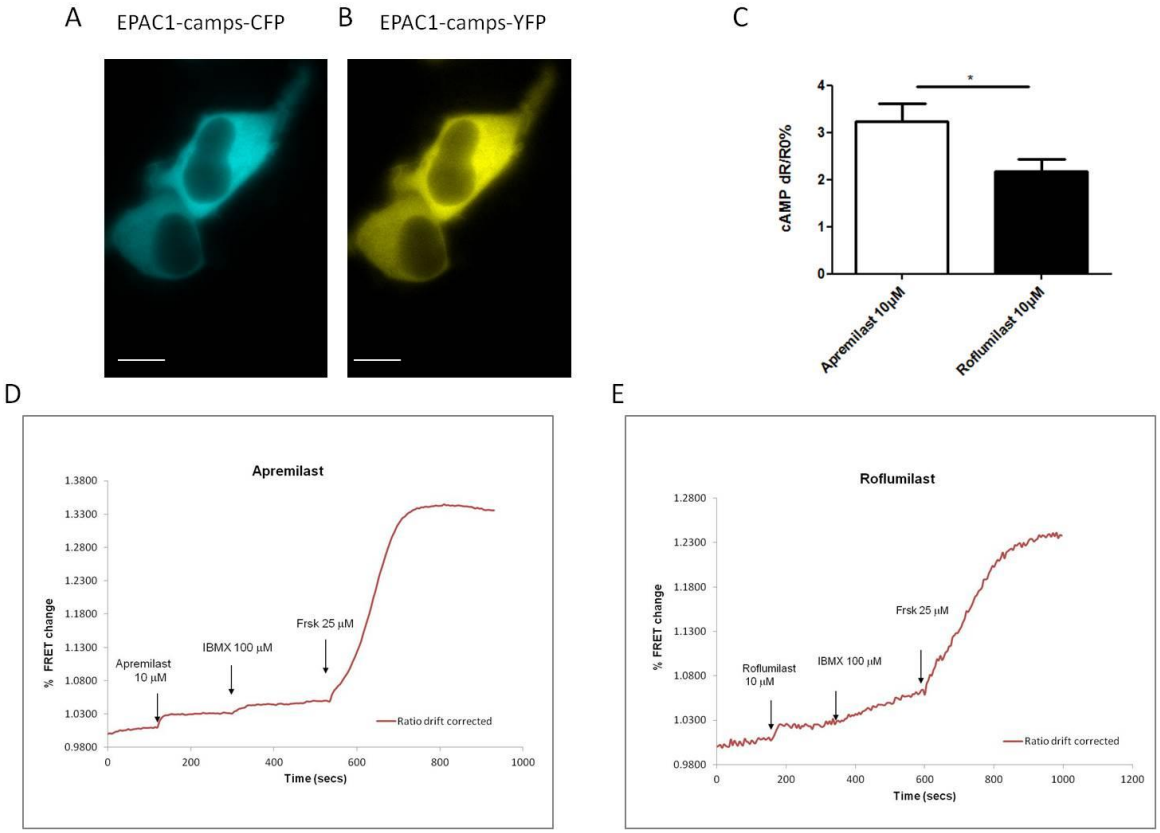

Figure 3-2 Apremilast stimulation of HEK 293 cells induces higher concentrations of cAMP in the cytosol compared to Roflumilast. (A-B) are representative images of HEK cells tranfected with the cytosolic EPAC1-camps sensor. (C) Summary of experiments performed n=18. Error bars represent SEM * P <0.05. (D-E) Representative kinetics of % FRET changes generated in the cytosol upon stimulation of either 10 µM Apremilast or 10 µM Roflumilast followed by 100µM IBMX and 25µM forskolin. Values are normalised to the ratio value at time t=0 (R_o) (scale bar 10µm). Data are corrected for bleaching effect as calculated on the basis of the baseline drift before the stimulus.

I subsequently tested cAMP elevation differences in HEK 293 cells using both the cytosolic PKA-RIα and the membrane-associated PKA-RIIß sensors. These experiments showed differences in cAMP elevation between Apremilast and Roflumilast in the cytosolic and membrane associated compartments. Figure 3-3 below shows Apremilast elevates higher levels of cAMP in the cytosolic associated PKAR1 compartment whereas figure 3-4 showed the opposite where Roflumilast elevates higher levels of cAMP in the membrane associated PKAR11 compartment. This is consistent with information Celgene provided (discussed in Chapter 1) where binding of Apremilast and Roflumilast was tested using the low affinity (cytosolic, isolated from cell lysate supernatant) and high affinity (membrane-associated, isolated from cell lysate pellet) forms of PDE4A4. Results indicated that while Roflumilast bound to the membrane-associated fraction of

PDE4A4 with 12-fold greater affinity than the cytosolic fraction, Apremilast was just the opposite. Apremilast actually exhibited 7-fold lower affinity for the so called high affinity form of PDE4A4. This indicated that Apremilast, unlike Roflumilast and Rolipram, didn't readily bind to the membrane-associated fraction of PDE4A4. So it was expected that there would be a difference in cAMP elevation within micro domains due to this differential binding of these inhibitors to the 'high' and 'low' affinity forms of PDE4A4 (discussed in Chapter 1).

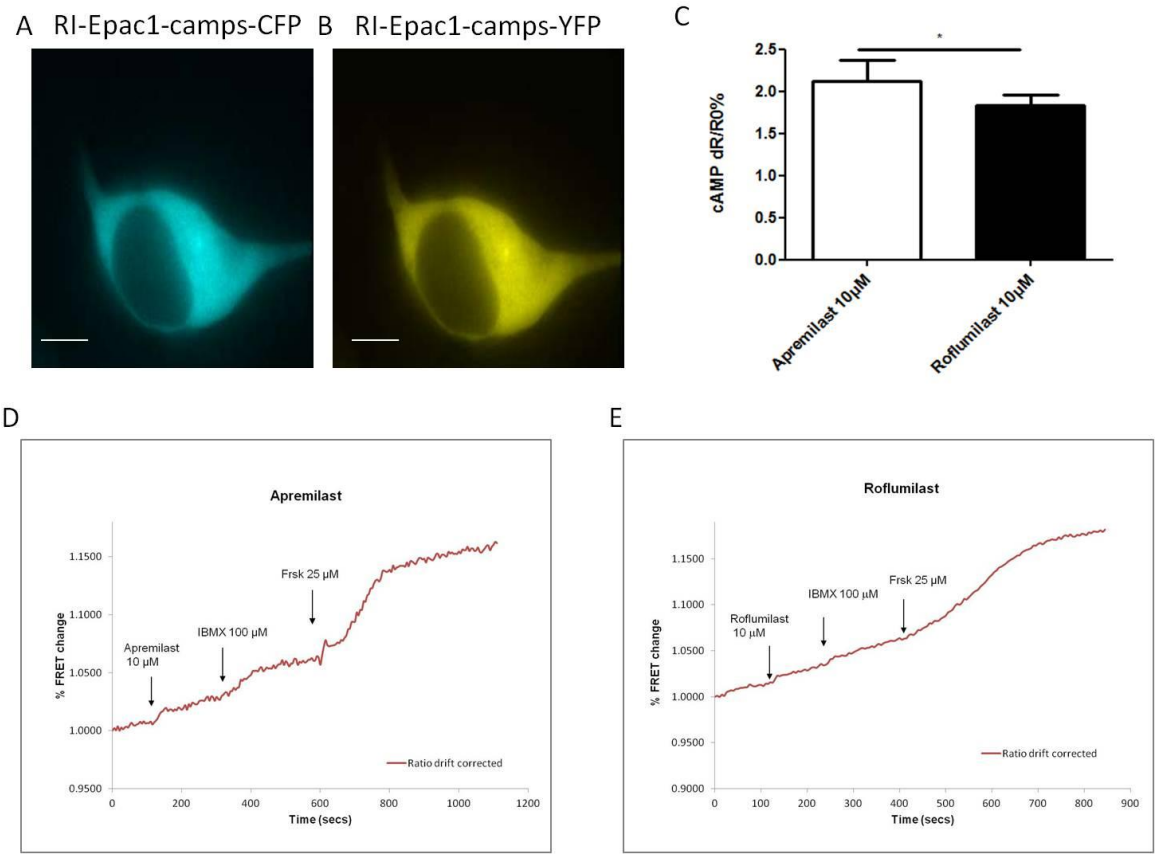

Figure 3-3 Apremilast stimulation of HEK 293 cells induces higher concentrations of cAMP in the PKA-R1 compartment (cytosolic) compared to Roflumilast. (A-B) are representative images of HEK cells tranfected with the cytosolic associated R1-Epac sensor. (C) Summary of experiments performed n=12. Error bars represent SEM * P <0.05. (D-E) Representative kinetics of % FRET changes generated in the cytosol upon stimulation of either 10 µM Apremilast or 10 µM Roflumilast followed by 100µM IBMX and 25µM forskolin. Values are normalised to the ratio value at time t=0 (R_o). (scale bar 10µm). Data are corrected for bleaching effect as calculated on the basis of the baseline drift before the stimulus.

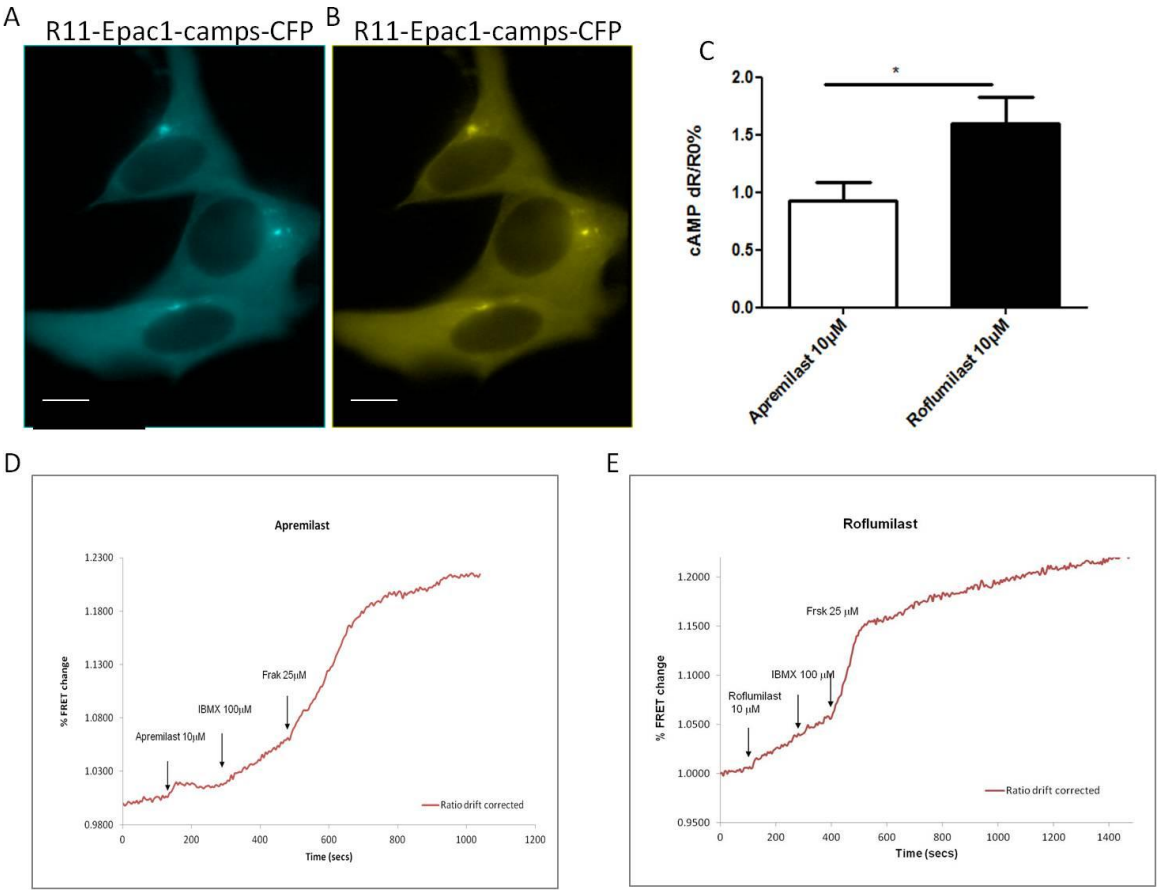

Figure 3-4 Roflllumilast stimulation of HEK 293 cells induces higher concentrations cAMP in the PKA-R11 compartment (membrane associated) compared to Apremilast. (A-B) are representative images of HEK cells tranfected with the membrane associated R11-Epac sensor. (C) Summary of experiments performed n=14. Error bars represent SEM * P <0.05. (D-E) Representative kinetics of % FRET changes generated in the cytosol upon stimulation of either 10 μM Apremilast or 10 μM Roflumilast followed by 100μM IBMX and 25μM forskolin. Values are normalised to the ratio value at time t=0 (R_o). (scale bar 10μm). Data are corrected for bleaching effect as calculated on the basis of the baseline drift before the stimulus.

In a bid to use a more relevant cell line and to perhaps unveil the "super cAMP" elevation shown by Celgene, Jurkat T cells were tranfected with the EPAC1-camps cytosolic sensor. The cells were treated with both Apremilast and Roflumilast as before and results are shown below in figure 3-5. The oppossite effect was found in these cells (compared with HEK293), Roflumilast induced higher levels of cAMP compared to Apremilast. It could perhaps be said the super

cAMP elevation shown in peripheral blood monocytes (Schafer, Parton et al. 2014) is observed in these cells as the levels of cAMP elevation caused by Roflumilast appear to be double that of Apremilast in the cytosol. However, Jurkat cells proved too difficult to continue with their use in FRET experiments as they are suspension cells and so had to be attached to coverslips coated with fibronectin. This was very time consuming as several coverslips had to be discarded when cells that were not fully attached moved when stimulus was added. Therefore it was decided to move onto a primary cell line, Rheumatoid Arthrtis synovial fibroblasts (RASFs). These are cells harvested from the synovial joints of patients with Rheumatoid arthritis. These were particularly relevant and interesting cells to use as Apremilast may prove useful for the treatment of this disease in the future (Schett, Sloan et al. 2010). Experiments were performed in these cells with both the cytosolic Epac-camps sensor in conjunction with a nuclear localised Epac sensor. Results of FRET experiments in these cells (figures 3-6 and 3-7) revealed that there appears to be cell type specific differences in cAMP elevation between Apremilast and Roflumilast, as Apremilast elevates higher levels of cAMP in the cytosol in RASFs compared to Roflumilast, whereas it was the opposite in Jurkat T cells (figure 3-5). Interestingly, however when cAMP elevation was measured in the nucleus of RASFs (figure 3-7) it revealed Roflumilast significantly elevates cAMP levels whereas Apremilast seems to have little or no effect in the nucleus. This major difference could perhaps lead to signficant physiological differences in the effects produced by these two inhibitors.

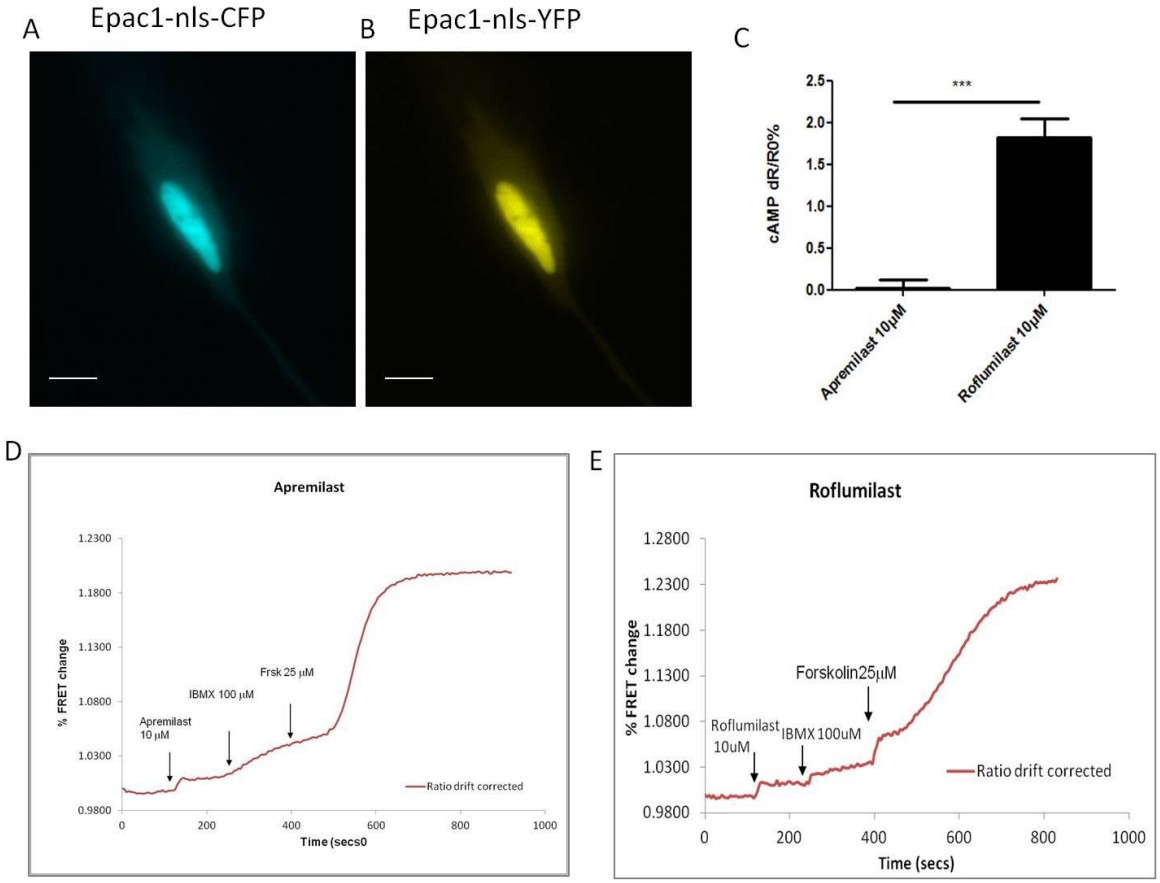

Figure 3-5 Roflumilast stimulation of Jurkat T cells induces higher concentrations of cAMP in the cytosol compared to Apremilast. (A-B) are representative images of Jurkat T cells tranfected with the cytosolic EPAC1-camps sensor. (C) Summary of experiments performed n=14. Error bars represent SEM * P <0.05. (D-E) Representative kinetics of % FRET changes generated in the cytosol upon stimulation of either 10 µM Apremilast or 10 µM Roflumilast followed by 100µM IBMX and 25µM forskolin. Values are normalised to the ratio value at time t=0 (R_o). (scale bar 10µm). Data are corrected for bleaching effect as calculated on the basis of the baseline drift before the stimulus.

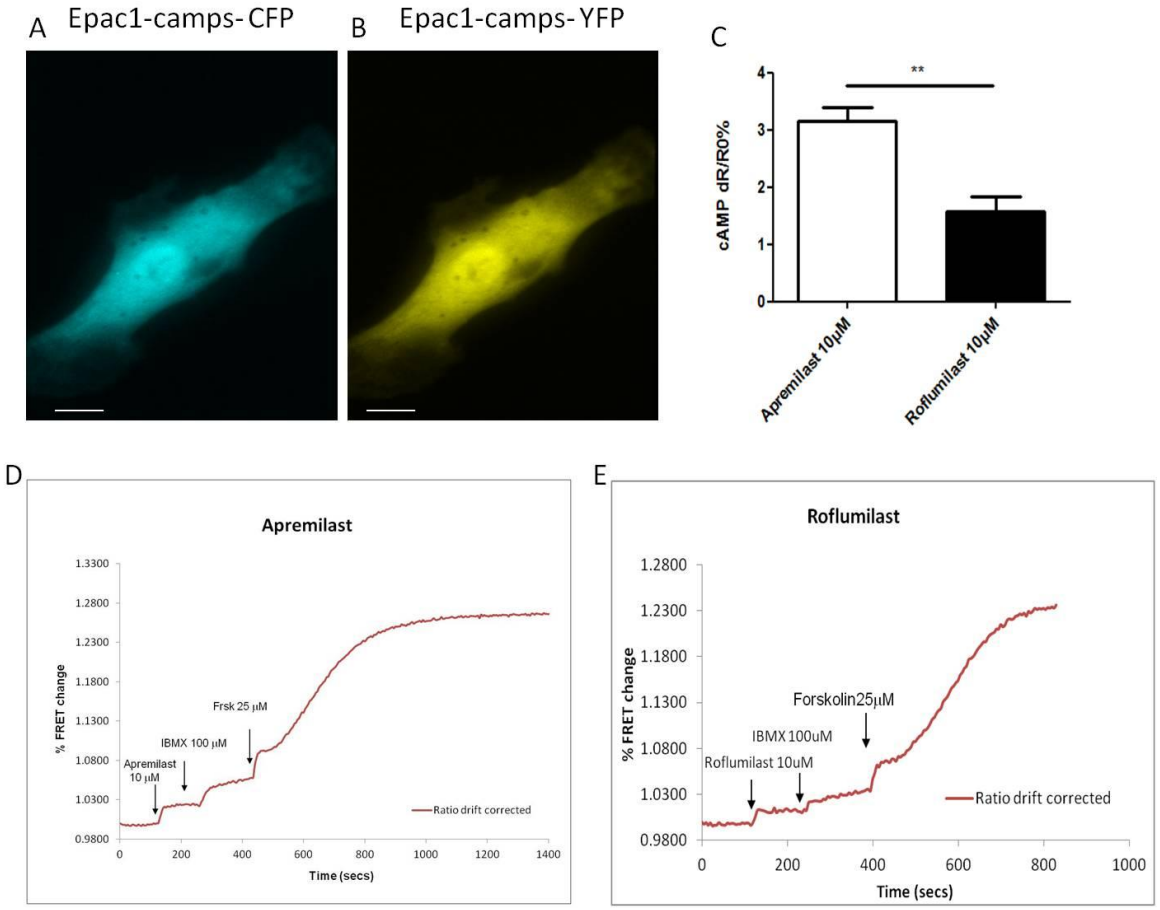

Figure 3-6 Apremilast stimulation of Rheumatoid Arthritis Synovial fibroblast cells induces higher concentrations of cAMP in the cytosol compared to Roflumilast. (A-B) are representative images of HEK cells tranfected with the cytosolic EPAC1-camps sensor. (C) Summary of experiments performed n=18. Error bars represent SEM ** P <0.005. (D-E) Representative kinetics of % FRET changes generated in the cytosol upon stimulation of either 10 µM Apremilast or 10 µM Roflumilast followed by 100µM IBMX and 25µM forskolin. Values are normalised to the ratio value at time t=0 (R_o). (scale bar 10µm). Data are corrected for bleaching effect as calculated on the basis of the baseline drift before the stimulus.

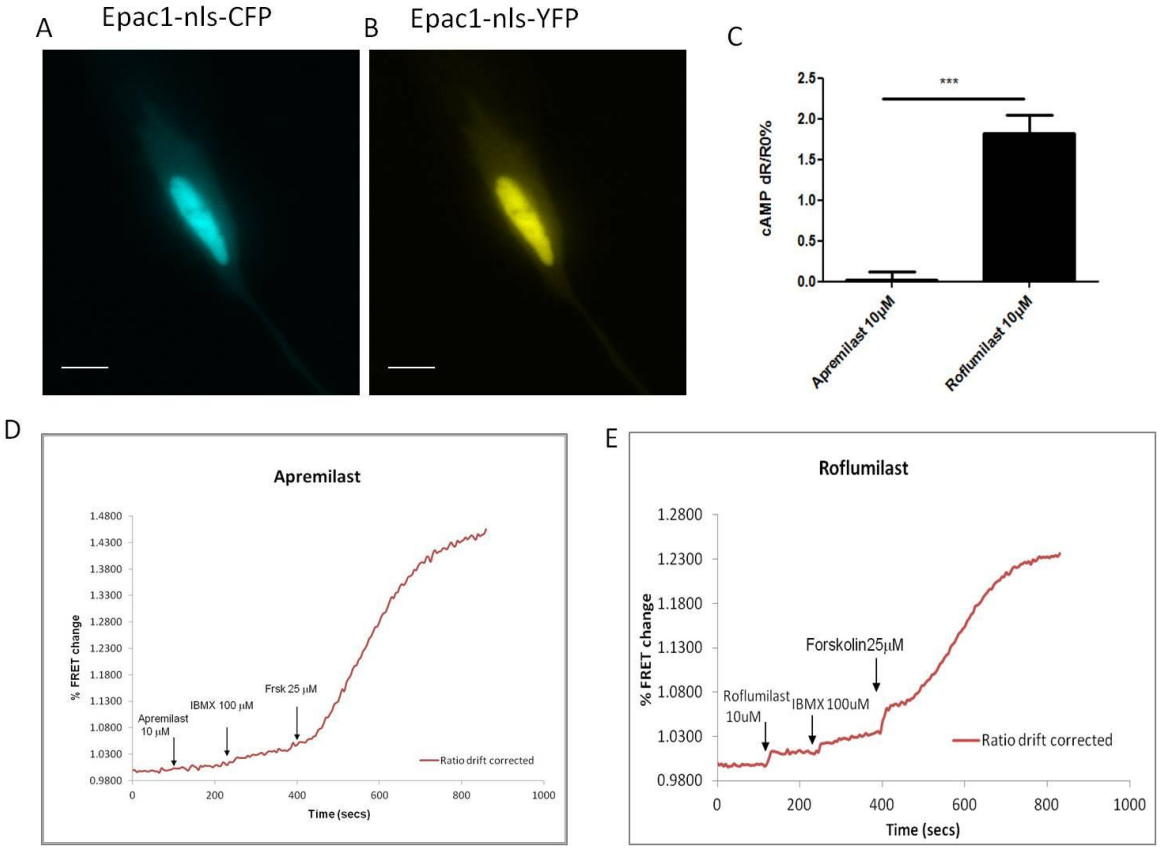

Figure 3-7 Apremilast stimulation of Rheumatoid Arthritis Synovial fibroblast (RASF) cells has no effect on cAMP production in the nucleus whereas Roflumilast does stimulate cAMP production in the nucleus. (A-B) are representative images of RASF cells transfected with the nuclear localised EPAC1-nls camps sensor. (C) Summary of experiments performed n=12. Error bars represent SEM *** P <0.0005. (D-E) Representative kinetics of % FRET changes generated in the cytosol upon stimulation of either 10 µM Apremilast or 10 µM Roflumilast followed by 100µM IBMX and 25µM forskolin. Values are normalised to the ratio value at time t=0 (R_o). (scale bar 10µm). Data are corrected for bleaching effect as calculated on the basis of the baseline drift before the stimulus.

3.5 Discussion

The FRET experiments performed in this chapter have shown for the first time that Apremilast and Roflumilast do appear to regulate different pools of cAMP within the cell which may be cell type specific. For example in HEK 293 and RASFs, Apremilast seems to induce significantly higher levels of cAMP compared to Roflumilast in the cytoplasm. The opposite was found in Jurkat T cells where Roflumilast elevated higher levels of cAMP compared to Apremilast . Apremilast and Roflumilast also exert differential effects in the PKAR1 and PKAR11 which are associated with the cytoplasm and membrane compartments respectively. The most interesting difference revealed from these FRET experiments however, was that in the nucleus of RASFs, Roflumilast significantly elevates cAMP levels whereas Apremilast seems to have little or no effect. This could perhaps lead to Roflumilast having a distinct biological effect from that of Apremilast, as it is able to enter the nucleus in these cells and elevate cAMP which could perhaps elicit different downstream PKA signalling effects from that of Apremilast, which is seemingly unable to affect cAMP in the nucleus in these cells at least. Perhaps Roflumilast has nuclear penetrating ability and gets into nucleus to increase cAMP and activate PKA to produce different signals from Apremilast in the cytosol or membrane compartment, as it has been shown that some nuclear localised GPCRs produce different cell signals from that localised in the cell membrane (Yu, Zhong et al. 2013)

The “super cAMP” elevation that (Schafer, Parton et al. 2014) found could perhaps be explained then by the possibilty that there may be more cAMP specific PDEs in the nucleus of that cell type (PBMCs) leading to this larger increase in cAMP elevation compared to Apremilast, Rolipram and Cilomilast . The “super cAMP elevation” caused by roflumilast may also be caused by off-target effects, such as agonism or antagonism of a G-protein coupled receptor (adenosine, adrenergic, histamine, etc.), direct activation of adenylyl cyclase, or other non-PDE4 effects. Data recenlty published by (Schafer, Parton et al. 2014) has shown that Apremilast doesn’t significantly inhibit any other PDEs, kinases, enzymes or receptors and mediates it’s effects in monocytes and T cells via PKA and NF-κB pathways. Therefore the only known molecular targets at this point for Apremilast are the PDE4 family of enzymes.

It is known that Roflumilast inhibits Lipopolysaccharide (LPS)-induced inflammatory mediators via the suppression of Nuclear Factor-κB, p38 Mitogen-activated protein kinase, and C jun NH_2-terminal kinase activation (Kwak, Song et al. 2005).Roflumilast inhibits production of of several inflammatory mediators such as NO, TNF-α and IL-1ß in RAW264.7 cells via the inhibition of NF-κB activation and SAPK/JNK and p38 MAP kinase pathways . Kwak and collegues (Kwak, Song et al. 2005) found that besides Roflumilast inhibiting NF-κB, Roflumilast may inhibit proinflammatory gene expression via an additional mechanism of JNK and p38 MAP kinase inactivation in RAW 264.7 macrophages.

Gene chip analysis has also recently been published by (Schafer, Parton et al. 2014) where clear differences in gene expression were noted between Apremilast, Roflumilast and Cilomilast. It identified the top gene sets regulated by all three PDE4 inhibitors as belonging to the immune response, inflammatory response and, cytokine activity, chemokine signalling and stress response biogroups. See table 3-1 and 3-2. However there were numerous gene sets that were regulated by Roflumilast and Cilomilast but not by Apremilast. The main gene set differences found between the three PDE inhibitors belonged to the cytoplasmic ribosome, peptide chain elongation, ribosome, protein complex disasembly and viral infectious cycle biogroups. Therefore it was noted that while Apremilast gene regulation was focused on the inflammatory and immune response, cytokine and chemokine pathways and stress response genes, cilomilast and Roflumilast exhibited a wider pattern of gene regulation that included ribosomal genes, protein translation and disassembly, and the viral response genes. Specific targets of gene regulation by Apremilast identified in this paper by (Schafer, Parton et al. 2014) included the inhibition of many chemokines, chemokine receptors and Th1 cytokine genes, as well as the enhancement of the genes encoding the anti-inflammatory factor SOCS-3, which is an inhibitor of the cytokine receptor/JAK-STAT pathway and was previously reported to be induced by cAMP elevation via the activation of Epac1 (Williams and Palmer 2012). So, Apremilast may be able to suppress cytokine signalling through IL-6 and other class 1 cytokine receptors via the activation of Epac 1, expression of SOCs-3 and by the inhibition of JAK-STAT signalling.

Top-scoring gene transcript biogroups regulated concordantly by PDE4 inhibitors in LPS-stimulated monocytes.				
Compound	Common genes	Direction	p-Value	Score
Immune response (GO)	118.14			
Apremilast	45	↓	5.20E − 16	35.2
Cilomilast	97	↓	5.60E − 23	51.25
Roflumilast	36	↓	1.70E − 14	31.7
Inflammatory response (GO)	82.73			
Apremilast	27	↓	7.80E − 15	32.49
Cilomilast	34	↓	9.80E − 12	25.35
Roflumilast	26	↓	1.60E − 11	24.89
Cytokine activity (GO)	67.7			
Apremilast	20	↓	7.00E − 14	30.3
Cilomilast	17	↓	3.90E − 06	12.46
Roflumilast	15	↓	1.50E − 11	24.94
Chemokine signaling (Broad MSigDB — canonical pathway	64.62			
Apremilast	13	↓	2.80E − 11	24.31
Cilomilast	22	↓	6.20E − 10	21.2
Roflumilast	14	↓	5.00E − 09	19.1
Response to stress (GO)	64.52			
Apremilast	72	↓	5.60E − 09	19
Cilomilast	196	↓	1.70E − 20	45.52
Roflumilast	71	↓	1.60E − 07	15.64

Table 3-1 Top scoring gene transcript biogroups regulated concordantly by PDE4 inhibitors in LPS-stimulated monocytes (Schafer, Parton et al. 2014).

Top-scoring gene transcript biogroups regulated discordantly by apremilast versus other PDE4 inhibitors in LPS-stimulated monocytes.				
Compound	Common genes	Direction	p-Value	Score
Ribosome<comma> cytoplasmic (Broad MSigDB—canonica	96.05			
Apremilast	0		ns	0
Cilomilast	30	↑	1.30E − 28	64.21
Roflumilast	22	↑	1.50E − 14	31.84
Peptide chain elongation (Broad MSigDB—canonical pathw	92.19			
Apremilast	0		ns	0
Cilomilast	30	↑	1.30E − 27	61.94
Roflumilast	22	↑	7.30E − 14	30.25
Ribosome (Broad MSigDB—canonical pathways)	90.71			
Apremilast	0		ns	0
Cilomilast	29	↑	1.00E − 26	59.84
Roflumilast	22	↑	3.90E − 14	30.87
Protein complex disassembly (GO)	86.74			
Apremilast	0		ns	0
Cilomilast	30	↑	3.10E − 25	56.43
Roflumilast	24	↑	6.90E − 14	30.31
Viral infectious cycle (GO)	85.49			
Apremilast	1	↓	ns	1.69
Cilomilast	30	↑	1.40E − 23	52.6
Roflumilast	25	↑	2.80E − 14	31.21

Table 3-2 Top-scoring transcript biogroups regulated discordantly by Apremilast versus other PDE4 inhbitors in LPS-stimulated monocytes (Schafer, Parton et al. 2014).

cAMP signalling in the nucleus remains largely unresearched, however several papers have noted PKA and AKAP signalling routes to the nucleus (Okamoto, Takemori et al. 2004, Haj Slimane, Bedioune et al. 2014).
While most PKA substrates are phosphorylated by PKA anchored by an AKAP in close vicinity to the substrate, PKA signalling to the nucleus involves nuclear entry of the free C subunit, due to size exclusion preventing the entry of the PKA holoenzyme. The classical view of nuclear PKA signalling is where cAMP binds to PKA outside the nucleus where the C subunits dissociate from the R subunits and then cross the nuclear envelope by passive diffusion, a slow process (Harootunian, Adams et al. 1993). However, recent evidence revealed that in HEK293 cells, a nuclear resident pool of PKA exists which is isolated from cAMP that is generated in the plasma membrane by AKAP anchored PDE4 (Sample, DiPilato et al. 2012). This research revealed that PDE4D played an important role in controlling nuclear PKA activity in HEK293 cells as PDE4 inhibition dramatically accelerated the nuclear PKA response to a chronic Forskolin treatment, (Sample, DiPilato et al. 2012) However, another group(Haj Slimane, Bedioune et al. 2014) revealed a different arrangement in cardiac myocytes, when they found that there was no acceleration of nuclear PKA activation upon inhibtion of PDE4 and suggested that perhaps in cardiac myocytes a different arrangement of components may exist with PDE4 being located at the nuclear envelope (Lugnier, Keravis et al. 1999, Dodge, Khouangsathiene et al. 2001). Here the PDE4 pool would control the extent of C subunits released upon ß-adrenergic stimulation and gate the transfer of C subunits into the nucleus from an extra-nuclear pool of PKA holoenzyme.

In cardiac myocytes, it has been reported that muscle AKAP (mAKAP) targets PKA to multiple locations including the nucleus (Yang, Drazba et al. 1998) and the nuclear membrane (Kapiloff, Jackson et al. 2001). mAKAP is known to bind PDE4D3, a cAMP specific PDE isoform that may control cAMP levels in this compartment and therefore modulate the release of PKA C subunits into the nucleus or the nuclear membrane. The pool of PKA that delivers the C subunit for diffusion into the nucleus is thought to be located in the cytoplasm. Interestingly, disruption of anchored PKA complexes by overexpression of soluble AKAP fragments affects cAMP signalling to the nucleus and gene regulation measured for example CREB phosphorylation (Feliciello, Giuliano et al. 1996)

Furthermore, targetting of PKA via AKAP75/79/150 associated with the cytoskeleton enhances signalling to the nucleus by delivering the C subunit to the nucleus (Feliciello, Li et al. 1997). Anchoring of PKA11 in actin cortical cytoskelaton increases the rate, magnitude and sensitivity of cAMP signalling in the nucleus also (Feliciello, Li et al. 1997).

A study by (Haj Slimane, Bedioune et al. 2014) used FRET probes targeted to the cytoplasm and nucleus to study spatiotemporal dynamics of nuclear cAMP and PKA activity in adult cardiac myocytes and revealed a differential integration of cytoplasmic and nuclear PKA responses to ß-AR stimulation. ß-AR stimulation activates a GTP-binding protein (Gs), which stimulates adenylyl cyclase to produce cAMP, which in turn activates PKA. PKA is well characterised in various subcellular compartments of adult cardiac myocytes, its regulation in the nucleus, however, is unknown. PKA regulates many effetors in cardiac myocytes including CREB and class 11 histone diacetylase (HDAC 4 and 5) in the nucleus (Muller, Neumann et al. 2000, Ha, Kim et al. 2010, Backs, Worst et al. 2011, Chang, Lee et al. 2013).
Hence, it is possible that distinct PDEs and AKAPs are tethered to nuclear compartments and Roflumilast is able to inhibit these PDEs and activate PKA in the nucleus, which could lead to different physiological outputs for Roflumilast compared to Apremilast. PDE4D3 is known to bind mAKAP at the nuclear membrane, mAKAP is expressed in myocytes,skeletal muscle and the brain. In COPD, in addition to pulmonary manifestations, patients develop systemic problems, including skeletal muscle and other organ specific dysfunctions. Could Roflumilast be targetting PDEs tethered to this mAKAP in skeletal muscle, increasing cAMP and increasing anti inflammatory mediators in this vicinity, helping to alleviate symptoms?

Another interesting study, (Yang, Polanowska-Grabowska et al. 2014) found that nuclear PKA activity in myocytes is not regulated by nuclear cAMP compartmentation but rather by direct compartmentation of the PKA catalytic subunit and that the nucleus may constitute a PKA signalling domain distinct from the cytosol.They observed that cytosolic and nuclear PKA exhibit different sensitivities to ß-adrenergic stimulation which suggested that the nucleus contains an independant PKA signalling microdomain. This PKA

compartmentation drove differential activation of PKA substrates associated with contractility and hypertrophy. This data suggests that Roflumilast induced cAMP increases in the nucleus of RASF could result in different physiological responses from those driven by Apremilast. Perhaps an increase in nuclear cAMP by Roflumilast will cause a differential phosphorylation of PKA substrates compared to those in the cytosol. It has also been suggested that some nuclear localised GPCRs produce different cell signals from that localised on the cell membrane (Yu, Zhong et al. 2013). Perhaps nuclear PKA signalling could lead to different physiological outcomes in different cell types and this could unveil PKA signalling differences between Apremilast and Roflumilast with Apremilast seemingly unable to affect cAMP in the nucleus in these cells at least.

In light of the information discussed above and the data revealing that there is selectivity of action between Apremilast and Roflumilast in regulating specific cAMP pools in cells, which therefore will be likely to then result in a unique set of phentotypic outputs. The following chapters of this thesis therefore will try to elucidate any differential signalling events triggered by each of these PDE4 inhibitors.

4 Profiling Signalling differences between Apremilast and Roflumilast.

4.1 Comparing effects of Apremilast and Roflumilast on PKA phosphorylation states in cells

4.1.1 Introduction

In the presence of inflammatory extracellular signals, G-protein coupled receptors bind with a number of ligands such as leukotrienes, prostaglandins, chemokines and histamines which activate adenylyl cyclase and promote increased production of cAMP (Serezani, Ballinger et al. 2008). cAMP mediates a myriad of cellular responses and biological functions via the activation of a limited number of effectors including the cAMP-dependent protein kinase A (PKA), the exchange proteins directly activated by cAMP (Epac 1 and 2) and the cAMP-gated ion channels (CNG). cAMP interacts with PKA and Epac to elicit changes in protein expression (Zambon, Zhang et al. 2005).The phosphodiesterase 4 inhibitors Apremilast and Roflumilast are known to mediate their effects in monocytes and T cells via PKA and NF-κB pathways (Kwak, Song et al. 2005, Schafer, Parton et al. 2014). PKA is anchored to specific sub cellular targets by its interaction with AKAPs, therefore only particular pools of PKA are exposed to activating concentrations of cAMP at any one time (Baillie 2009). Therefore, because of the discrete compartmentalisation of signalling proteins, signals from one second messenger (in this case cAMP) can result in the activation of distinct signal transduction pathways, and diverse physiological responses (Buxton and Brunton 1983). Hundreds of cytosolic and nuclear proteins have been identified as substrates for PKA (Tasken, Skalhegg et al. 1997). Regulation of transcription by PKA is mainly achieved by direct phosphorylation of the cAMP-responsive binding element family of transcription factors, including cAMP response (CRE)-binding protein (CREB) and activating transcription factor - 1 (ATF-1), while inhibiting the activity of other promoters such as the nuclear factor kappa B (NF-κB) (Ollivier, Parry et al. 1996, Schafer 2012). CREB is involved in numerous physiological processes and regulates gene expression in a phosphorylation dependent fashion (Brindle, Linke et al. 1993, Mayr and

Montminy 2001). Ser 133 is the major phosphorylation site of CREB that is phosphorylated by PKA (Gonzalez, Yamamoto et al. 1989). The phosphorylation of Serine residues alters the affinity of CREB to CREB-binding protein and p300, and results in a change in transcription efficiency (Chrivia, Kwok et al. 1993, Lundblad, Kwok et al. 1995, Mayr and Montminy 2001). Effects of phosphorylation of PKA on CREB , ATF-1 and NF-κB cause decreased mRNA expression of cytokines and other inflammatory mediators as well as increased expression of anti-inflammatory signals (Jimenez, Punzon et al. 2001, Serezani, Ballinger et al. 2008). In this chapter I will employ a number of different techniques to try and elucidate signalling differences between Apremilast and Roflumilast.

4.1.2 Specific aims

Spatially distinct pools of cAMP control particular PKA sub-populations able to phosphorylate distinct substrate cohorts (Baillie 2009). Insight into this can be gained by the use of phospho-antibodies to proteins that are phosphorylated by PKA and also by antisera raised to the PKA target motif 'RRxS' that are able to detect a variety of PKA substrates. I exploited this powerful technology to complement the FRET studies in chapter 3 in order to assess whether Apremilast and Roflumilast cause differential effects on the PKA phosphorylation state of proteins in cells. I have specifically evaluated (i) selectivity of phosphorylation of a defined set of proteins; (ii) differences in the magnitude of phosphorylation of particular proteins (iii) differential temporal phosphorylation of a defined set of proteins and (iv) the effect of both drugs under basal conditions or at high cAMP following activation of adenylate cyclase. I studied the effects of Apremilast and Roflumilast in a range of cell types, HEK 293, Jurkat T cell leukemia and U937 monocytic cells. Cells were treated with 0.1, 1 and 10 μM Apremilast and 0.01, 0.1 and 1 μM Roflumilast with and without forskolin at 10 μM for 30 mins and then western blot analysis was performed using specific antibodies for known PKA substrates.

4.1.3 Results

The effects of Apremilast and Roflumilast on CREB phosphorylation at Ser 133 was studied in HEK293, Jurkat T and U937 cells. The results in (figure 4-1) show that there were little differences between Apremilast and Roflumilast on CREB phosphorylation in any of the cell lines. Apremilast 10μM with and without forskolin 10μM, significantly induced CREB phosphorylation at Ser133 in Jurkat T cells (C) whereas Roflumilast application alone did not have a significant increase in CREB phosphorylation, but did when co-treated with Forskolin 10μM. In HEK 293 cells (B) Apremilast shows a trend in increased CREB phosphorylation but this increase is not statistically significant, however when treated with Forskolin 10μM, Apremilast does show a statistically significant increase in CREB Ser133 phosphorylation. In U937 cells (A) however, both Apremilast (10μM) and Roflumilast (1μM) significantly increase CREB phosphorylation at Ser133 when they are added along with 10μM forskolin. Neither induce a statistically significant increase when applied alone, however there does look to be a trend in increased phosphorylation with both inhibitors, which is indicative of PKA activation.

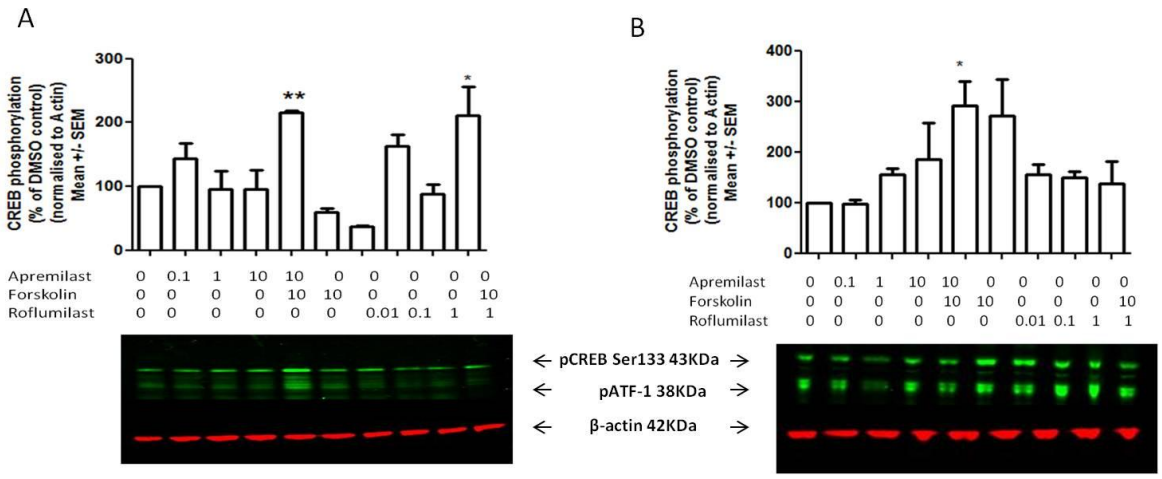

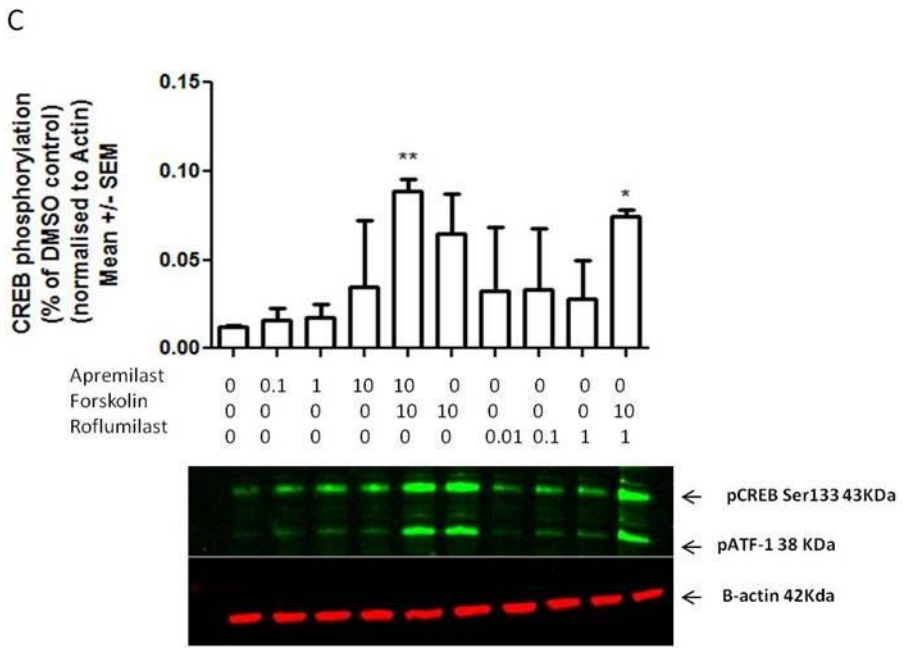

Figure 4-1 Effect of Apremilast and Roflumilast on CREB phosphorylation. A-C Western blot analysis of CREB protein Ser133 phosphorylation in A) U937 cells B) HEK 293 cells and C) Jurkat T cells. A representative Western blot is presented with each graph. All treatment groups were compared with DMSO by one-way ANOVA followed by Dunn's Multiple Comparison Post- Test (n=3. No statistically significant differences were observed between Apremilast and Roflumilast. *p<0.05 versus DMSO, **p<0.01 versus DMSO, 30-minute stimulation with drug.

Detection of 'pan' PKA phosphorylated proteins (PKA phospho-proteome) using a PKA substrate antiserum raised against a phosphorylated PKA target motif (R-X-X-pS/T) that is able to detect a variety of PKA substrates was then used to evaluate the effects of Apremilast and Roflumilast. Jurkat T cells were treated as before which is described in the materials and methods section. The results showed (figure 4-2) that although there was not a statistically different increase in the phosphorylation of PKA substrates in Jurkat T cells with either inhibitor there does look to be a trend in increased phosphorylation of PKA substrates with the consensus motif R-X-X-pS/T when treated together with Forskolin (10µM).

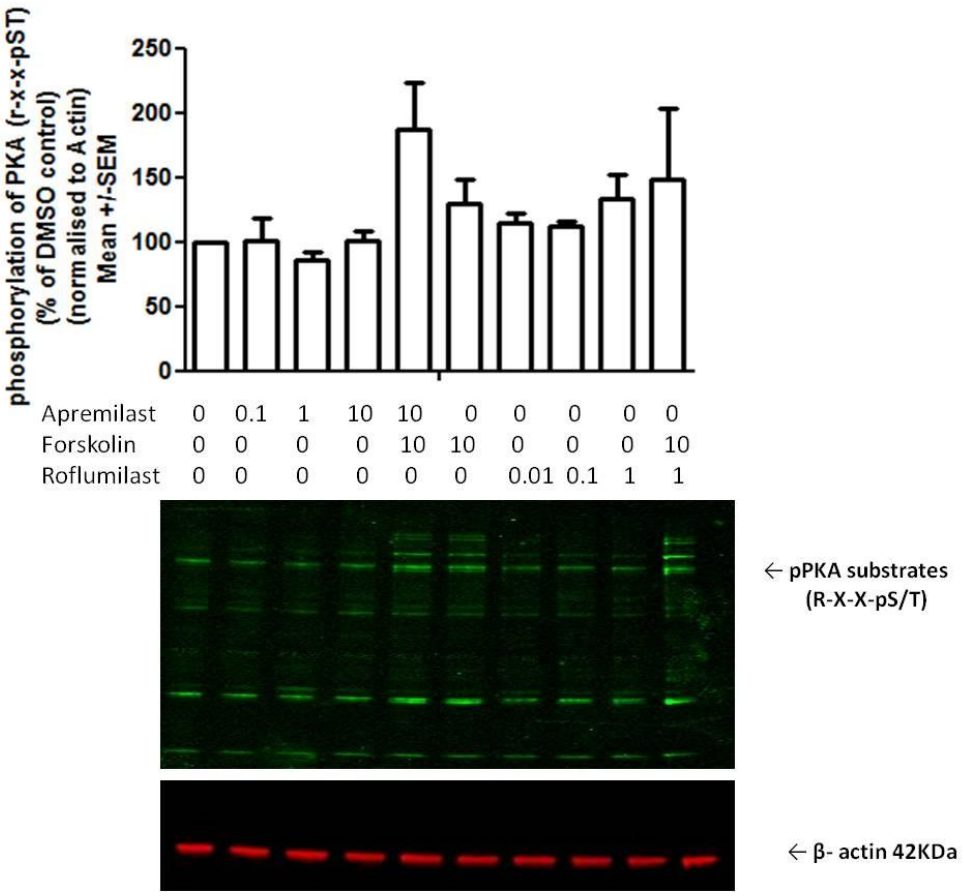

Figure 4-2 Effect of Apremilast and Roflumilast on PKA phosphorylation. Western blot analysis of PKA substrate phosphorylation (R-X-X-p S/T) in Jurkat T cells. A representative Western blot is presented with graph. All treatment groups were compared with DMSO by one-way ANOVA followed by Dunn's Multiple Comparison Post- Test (n=3). No statistically significant differences were observed between Apremilast and Roflumilast. 30-minute stimulation with drug.

Members of the vasodilator-stimulated phosphoprotein (VASP) family are important regulators of actin cytoskeletal dynamics whose functions and protein-protein interactions are regulated by (PKA) at serine 157 (Butt, Abel et al. 1994). Therefore, the effects of Apremilast and Roflumilast on the phosphorylation of this well defined PKA substrate was studied (figure 4-3) in both HEK 293 and U937 cells. The results show that in U937 cells neither Apremilast or Roflumilast increase the phosphorylation of VASP at ser 157 on their own however they both significantly increase VASP phosphorylation at (10μM) Apremilast and (1μM) Roflumilast when added with Forskolin (10μM). The opposite is seen in HEK 293 cells however, where only Apremilast (10μM) with Forskolin (10μM) significantly increases the phosphorylation of VASP at Ser133 whereas Roflumilast has no effect on VASP phosphorylation in these cells.

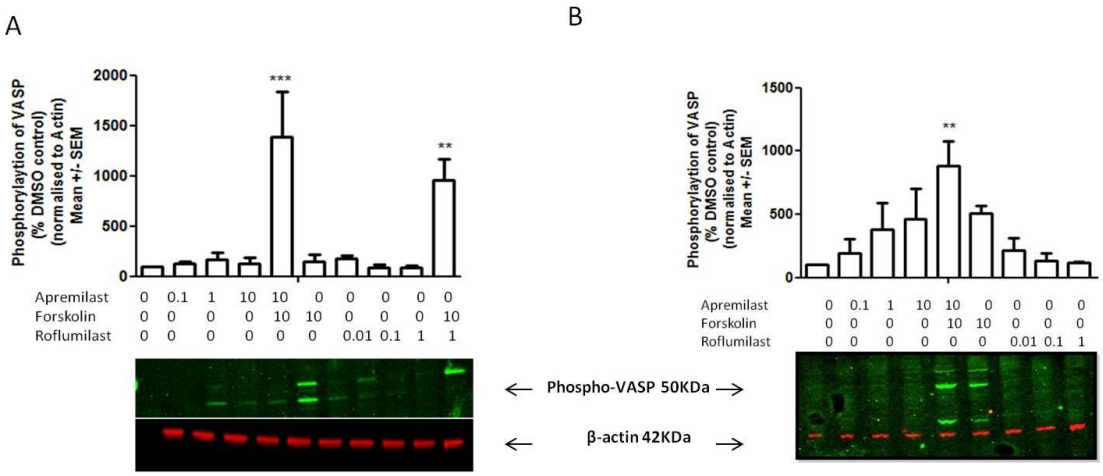

Figure 4-3 Effect of Apremilast and Roflumilast on the phosphorylation of VASP at Ser157. A-B Western blot analysis of VASP phosphorylation in A) U937 cells and B) HEK 293 cells. A representative Western blot is presented with each graph. All treatment groups were compared with DMSO by one-way ANOVA followed by Dunn's Multiple Comparison Post-Test (n=3). No statistically significant differences were observed between Apremilast and Roflumilast in U937 cells. *p<0.05 versus DMSO, **p<0.01 versus DMSO ***p<0.001 versus DMSO, 30-minute stimulation with drug.

4.1.4 Discussion

The data presented shows that Apremilast and Roflumilast both significantly increase CREB phosphorylation in Jurkat T cells and U937 cells in the presence of Forskolin which is consistent with reports that Apremilast and Roflumilast activate the PKA pathway as it is known that PDE4 inhibitors increase intracellular cAMP which leads to the phosphorylation and activation of PKA (Schafer, Parton et al. 2010), which results in the up regulation of CREB and down regulation of NFκB-dependent genes (Houslay, Schafer et al. 2005, Schafer, Parton et al. 2010). Apremilast along with forskolin treatment in HEK cells increases the phosphorylation of CREB but not Roflumilast in these cells. There does seem to be cell type differences in whether the inhibitors induce CREB phosphorylation or not.

U937 and Jurkat T cell data in figure 4-1 is consistent with a recent paper by (Schafer, Parton et al. 2014) that showed Apremilast activates the PKA-CREB/ATF-1 pathway in Jurkat T and THP-1 monocytic cells, which results in enhancement of CRE-driven gene transcription and inhibition of NFκB- driven gene transcription. In addition to this it has been shown that Apremilast inhibits NF-Kb transcriptional activity, which normally drives expression of genes such as TNFα (Schafer, Parton et al. 2010).

In human peripheral blood mononuclear cells, cAMP elevation caused by forskolin or treatment with the PKA activator dibutyryl cAMP inhibits NF-κB-dependent gene transcription (Ollivier, Parry et al. 1996). This effect is not dependent on nuclear translocation or phosphorylation of the NF-κB subunits p65, p50, or c-Rel, but rather by direct inhibition of NF-κB transcriptional activity (Ollivier, Parry et al. 1996) . In TNF-α-stimulated Jurkat T cells, forskolin or db-cAMP inhibit NF-κB luciferase activity, but interestingly, not IκBα degradation or NF-κB DNA binding activity (Takahashi, Tetsuka et al. 2002). Rolipram has been shown to inhibit NF-κB and NFAT activation in Jurkat and primary T cells (Navarro, Punzon et al. 1998) and to inhibit LPS-induced NF-κB luciferase activity in alcohol-exposed RAW264.7 cells (Gobejishvili, Barve et al. 2008). These studies suggest that the inhibition of NF-κB is only at the level of transcriptional activity. However, it has also been shown that roflumilast inhibits LPS-induced NF-κB DNA binding, IκBα phosphorylation, and IκBα degradation in RAW264.7 cells (Kwak, Song et al. 2005). Therefore the mechanism action of roflumilast may be somewhat different from that of rolipram.

The positive effects on CREB induced by PDE4 inhibitors and the negative effects on NF-κB are manifested in modulation of gene expression. Hence, CREB-dependent gene expression tends to be augmented, with two examples being IL-10 and IL-6, which bear CRE sites within their promoters. Expression of the anti-inflammatory cytokine IL-10 is enhanced by PDE4 inhibitors in a PKA-dependent manner (Eigler, Siegmund et al. 1998). The mechanism of this enhancement involves multiple CRE elements within the IL-10 promoter and enhancer, which recruit the CRE binding proteins CREB and ATF-1, both of which are substrates of PKA (Platzer, Fritsch et al. 1999). A thorough analysis of the CREB regulation has revealed many genes; including SOCS, SOCS1, and TGF-β2 are regulated in this way (Impey, McCorkle et al. 2004). Conversely, NF-κB-dependent gene

transcription tends to be inhibited by cAMP-elevating agents. A review by (Barnes and Adcock 1998) discussed in detail the relative roles for NF-κB, CREB, and other transcription factors in the regulation of pro-inflammatory mediator expression. The interplay between CREB-dependent and non-CREB-dependent gene transcription thus defines the relative sensitivity of individual promoters to the effects of PDE4 inhibition. Inhibition of TNF-α, IFN-γ, IL-12A, and IL-23A by Apremilast was found to occur through suppression of mRNA expression (Schafer, Parton et al. 2010), which is consistent with the evidence in the literature described above that cAMP-elevating agents regulate expression of genes at the transcriptional level. Expression of the common IL-12 and IL-23 p40 subunit, encoded by the IL-12B gene, is known to be NF-κB-dependent (Ma, Zhang et al. 2004) and inhibited by the cAMP analog 8-Br-cAMP(Feng, Wang et al. 2002). However, suppression of the IL-12A (p35) and IL-23A (p19) subunits by a PDE4 inhibitor was previously unreported. The inhibition of IL-12 gene expression is reflected in the decreased IL-12 p70 protein levels (Schafer, Parton et al. 2010). Inhibition of IL-12 and IL-23 could be an important aspect of psoriasis therapy, supported by the significant efficacy of ustekinumab, an anti-IL-12/IL-23 p40 monoclonal antibody which is in development for the treatment of patients with chronic moderate to severe plaque psoriasis (Chien, Elder et al. 2009). In contrast to inhibition of IP-10, IFN-γ, MIG, TNF-α, IL-12p70, MIP-1α, MCP-1, and GM-CSF, Apremilast enhanced LPS-stimulated IL-10 production (with significant elevation at 1 μM), and to a lesser extent, IL-6 production (with significant elevation only at 10 μM) (Schafer, Parton et al. 2010).

My data is consistent with the above findings as it confirms that the Apremilast and Roflumilast act via the PKA pathway to increase the phosphorylation of CREB and thereby should inhibit NFκB activation and increase the production of anti inflammatory cytokines. Further downstream effects and whether Apremilast and Roflumilast will cause differential phosphorylation of other proteins will be investigated further in this chapter.

In addition to data in figure 4-1 showing that Apremilast and Roflumilast increase the phosphorylation of CREB at Ser 133 in U937 and Jurkat T cells, and Apremilast only in HEK 293 cells, Figure 4-2 shows that although not significant, there does look to be an increase in the phosphorylation of PKA substrates. Figure 4-3 revealed that both inhibitors increase the phosphorylation of VASP at

Ser157 in the presence of forskolin in U937 cells, however in HEK cells only Apremilast in the presence of forskolin increases VASP phosphorylation significantly at Ser157. This could be interesting as VASP phosphorylation has been implicated in a number of diseases such as Asthma and colon cancer (Hastie, Wu et al. 2006, Kohler, Birk et al. 2011, Ali, Rogers et al. 2015). Vasodilator-stimulated phosphoprotein (VASP) phosphorylation occurs on two serine and one threonine (Ser 157, Ser 239 and Thr 278) through cAMP and cGMP dependent protein kinases A and G (Butt, Abel et al. 1994). Phosphorylation by cAMP protein kinase preferentially occurs at Ser 157 (Butt, Abel et al. 1994). Attachment and migration of airway epithelial cells is an important aspect of repair of injury induced by allergens and other agents in asthma. VASP mediates focal adhesion, actin filament binding and polymerization in a variety of cells, thereby inhibiting cell movement (Krause, Dent et al. 2003). Phosphorylation of VASP via cAMP and cGMP dependent protein kinases releases this "brake" on cell motility and it is thought that phosphorylation of VASP may be necessary for epithelial cell repair of damage from allergen-induced inflammation (Hastie, Wu et al. 2006). Hastie et al found that decreased VASP phosphorylation was observed in epithelial cells of asthmatics compared to non-asthmatic individuals, despite response to ß-agonist. The observed decrease in VASP phosphorylation suggested greater inhibition of actin reorganization which is necessary for altering attachment and migration required during epithelial repair.

Phosphorylation of VASP has also been found to be involved in inflammatory tissue injury repair by (Kohler, Birk et al. 2011) who found it to dampen Hepatic Ischemia-Reperfusion Injury. This study examined the role of differential VASP Ser phosphorylation in regulating cell survival and apoptosis in human colon carcinoma cells. It found that in human colon carcinoma cells suppression of VASP Ser157 phosphorylation reduced F-actin content and survival and increased apoptosis, while inhibition of VASP Ser239 phosphorylation increased F-actin content and survival and reduced cell death. Also, while 8Br-cAMP induced VASP Ser157 phosphorylation and reduced cell death, treatments with 8CPT-cGMP elevated VASP Ser239 phosphorylation and promoted apoptosis.

Therefore, since both Apremilast and Roflumilast increase the phosphorylation of VASP at Ser157 in U937 cells and Apremilast only in HEK 293 cells, perhaps pharmacological manipulation of VASP Ser phosphorylation could be exploited to

affect the malignant actin cytoskeleton and induce apoptosis in colorectal cancer cells. This could perhaps present a use for PDE4 inhibitors as a therapeutic target of controlling cell survival and death behaviour in colon cancer via VASP phosphorylation. Further studies would have to be done to assess the effects of PDE4 inhibition on VASP phosphorylation in more detail and in appropriate cells. Some of the results in this chapter could be limited by low n numbers which could be addressed in the future.

4.2 CelluSpots™ - Kinase Substrate Arrays to potentially identify signalling differences

Most signalling networks are regulated by reversible protein phosphorylation. The specificity of this regulation depends on the capacity of protein kinases to recognize and efficiently phosphorylate particular sequence motifs in their substrates. Therefore, in a bid to further attempt to profile signalling differences between Apremilast and Roflumilast, I employed the use of peptide substrate arrays to try and identify whether Apremilast and Roflumilast have differentiating effects on any kinase substrates which will perhaps unveil PKA signalling differences. For this I used CelluSpots™ Y-kinase substrate arrays (figure 4-4). The arrays consist of a series of peptides derived from sequences of tyrosine kinase substrates as well as consensus sequences of some other kinases, generated as peptide-cellulose conjugates, and spotted on glass slides. Each spot is a known 15-mer peptide bound to cellulose via the C-terminus and with an acetylated N-terminus with Tyr found at the 7^{th} position of the peptides. Rheumatoid arthritis synovial fibroblast (RASF) cells were used in these experiments.

Slides were incubated with protein lysates from RASFs, untreated and treated with either inhibitor at 10μM as described in materials and methods section. They were then probed with an anti phospho-tyrosine antibody which was detected by ECL. Each black spot on the array corresponds to a known peptide sequence that has been phosphorylated by kinases present in the lysate. Non phosphorylated sequences appear as negative (no visible spot). Densitometry analysis was then performed and the results did reveal some interesting hits although no significant differences between inhibitors were found.

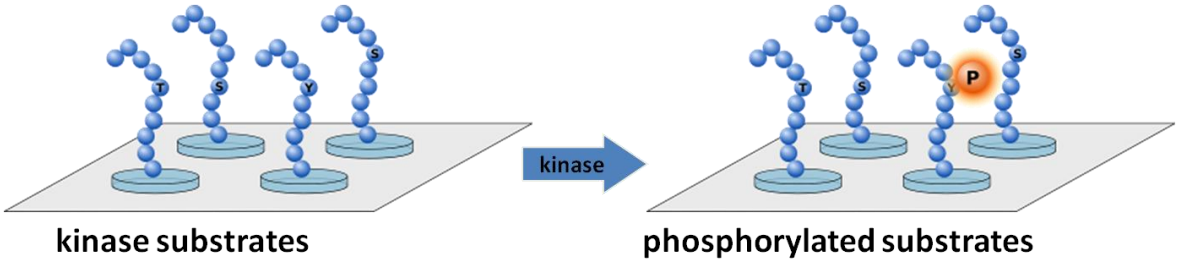

Figure 4-4 CelluSpots™ - Kinase Substrate Arrays illustration. Ready to screen kinase arrays with tyrosine- and serine/threonine-kinase substrates from annotated phosphorylation sites. (Intavis Bioanalytical Instruments)

4.2.1 Results

CelluSpots™ Y-kinase substrate array experiments (figure 4-5) revealed that treatment of RASFs with both Apremilast and Roflumilast led to some significant increases in several different kinase substrates. Densitometry analysis of the arrays show a few significant differences between untreated RASFs and RASFs treated with either of the inhibitors, table 4-1 shows the phosphorylated peptide sequences following treatment with the inhibitors. Interestingly, Apremilast and Roflumilast treatment significantly increased the phosphorylation of a member of Src family kinases, Src, when compared with control lysate. Analysis also showed that only Apremilast significantly induced the phosphorylation of Fyn, a tyrosine specific phosphotransferase that also belongs to the Src family of tyrosine kinases.

This increase in phosphorylation of Src by Apremilast and Roflumilast and Fyn by Apremilast is interesting as it has previously been shown that PDE 4 binds to both of these tyrosine specific phosphotransferases and inhibits PKA phosphorylation (McPhee, Yarwood et al. 1999). They found that PDE4A4 selectively binds SH3 domains of SRC family tyrosyl kinases. Fyn is primarily located in the cytoplasmic leaflet of the plasma membrane and it is known to play a role in the immune response and in the control of cell growth. Several aspects of Fyn function are of clinical interest. Fyn is involved in keratinocyte development, and it is thought alteration of Fyn levels may aid in treatment of skin disorders (Resh 1998).

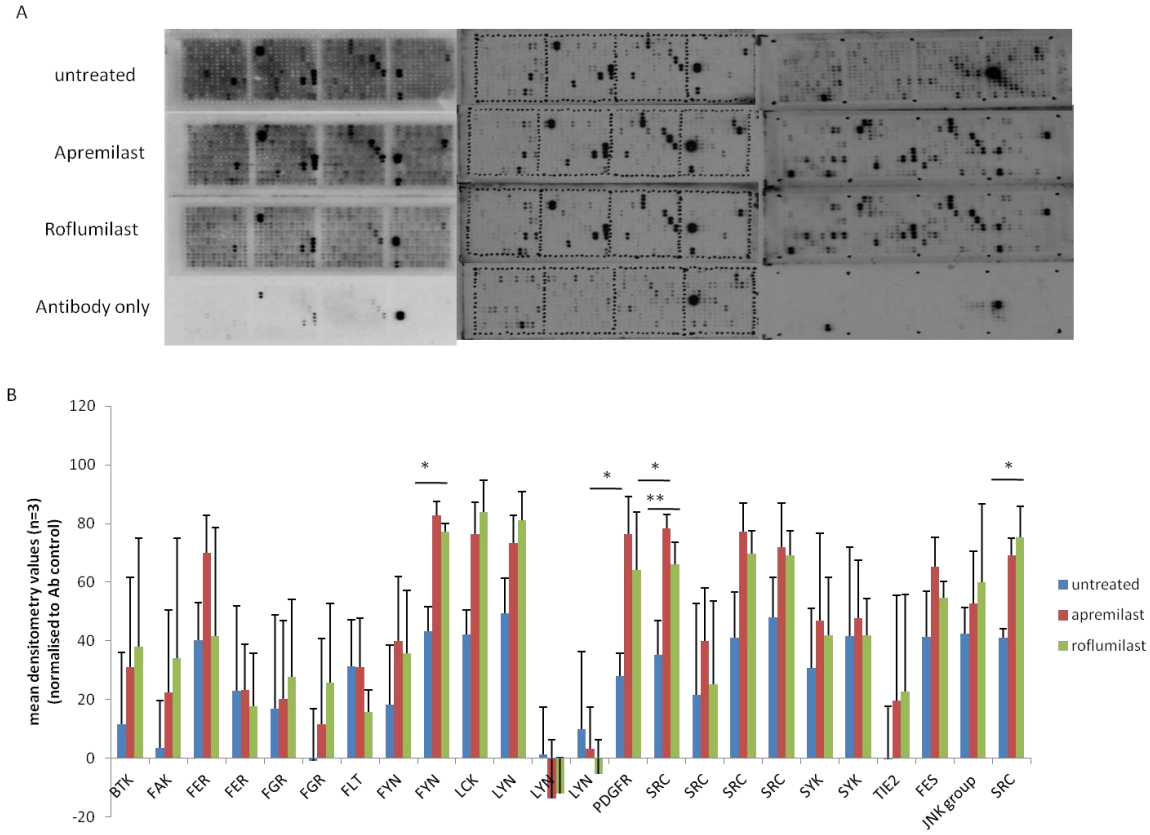

Figure 4-5 CelluSpots™ Tyrosine Kinase Substrate Arrays. A) N=1-3 tyrosine kinase substrate arrays overlaid with lysates from RASF cells either untreated or treated with Apremilast 10μM or Roflumilast 10μM includes an antibody only control. Each black spot corresponds to a known peptide sequence that has been phosphorylated by kinases in the lysate. Non-phosphorylated sequences appear as negative (no spot) B) Densitometry analysis of the arrays normalised to antibody only control. Data is shown as SEM for three experiments * P <0.05 and ** p<0.01.

Spot number	Kinase	Sequence	Substrate	Description
22	BTK	A-E-T-S-K-L-I-Y-D-F-I-E-D-Q-G	WASP	Downstream effector molecule
65	FAK	A-S-E-E-E-H-V-Y-S-F-P-N-K-Q-K	paxillin	Cytoskeletal protein; component of focal adhesion.
70	Fer	R-P-P-S-S-P-I-Y-E-D-A-A-P-F-K	Src substrate cortactin	Involved in the organization of cell structure
72	Fer	R-P-A-S-D-P-I-Y-E-D-A-E-A-D-G		cons.seq_1L
86	Fgr	E-D-E-P-E-G-D-Y-E-E-V-L-E-P-E		
87	Fgr	R-L-I-K-D-D-E-Y-N-P-C-Q-G-S-K	FGR	Tyrosine kinase
93	FLT3	F-D-D-D-E-Y-E-Y-D-Y-D-D-E-F-E		cons.seq_1L
99	Fyn	L-E-E-T-N-N-D-Y-E-T-A-D-G-G-Y	CD32	CD antigen. Binds to the Fc region of immunoglobulins gamma.
110	Fyn	E-E-D-D-D-N-L-Y-E-T-V-S-N-P-D		cons.seq_1L
166	Lck	E-E-E-E-D-D-I-Y-E-S-L-E-K-H-E		cons.seq_1L
156	Lck	E-A-E-G-D-E-I-Y-E-D-L-M-R-S-E	Vay	Adaptor molecule. GDP/GTP exchange factor in Rho/Rac molecule
168	Lyn	E-Y-E-D-E-N-L-Y-E-G-L-N-L-D-D	CD79A	B cell antigen receptor
172	Lyn	I-E-R-R-C-K-H-Y-V-E-L-L-V-A-Q	Vanilloid receptor like channel 2	Membrane transport protein
176	Lyn	T-S-L-G-S-Q-S-Y-E-D-M-R-G-I-L	CD19	Antigen of human B-lymphocytes
198	PDGFR_group	R-E-D-S-A-R-V-Y-E-N-V-G-L-M-Q		
210	Src	S-G-A-S-T-G-I-Y-E-A-L-E-L-R-D	Alpha enolase	alpha enolase (from PhosphoBase)
223	Src	L-E-E-E-E-E-A-Y-G-W-M-D-F-G-R	GAST	gastrin precursor (from PhosphoBase)
226	Src	R-N-E-E-E-N-I-Y-S-V-P-H-D-S-T	Glucocorticoid receptoe DNA	Nuclear receptor
239	Src	R-D-A-D-E-G-I-Y-D-V-P-L-L-G-P	SRC-interacting protein	Adapter protein. Member of the p130Cas and CasL family plays a role in cell mobility. Other name: embryonal-Fyn associated substrate
252	Syk	S-E-S-S-D-D-D-Y-D-D-V-D-I-P-T	MAP4K1	Hematopoietic progenitor kinase
255	Syk	C-S-I-E-S-D-I-Y-A-E-I-P-D-E-T	PYK2	Focal adhesion kinase 2
265	Tie2	T-L-E-E-A-E-L-Y-E-K-F-T-L-G-A		cons.seq_1L
338	JNK_group	X-X-X-X-X-X-T-P-pY-X-X-X-X		consensus sequence
374	Src	X-X-D-ED-ED-MVLI-Y-E-E-I-F-X-X		consensus sequence
323	Fes	X-X-ED-EA-EA-IEV-Y-ED-ED-IEV-IEV-X-X		consensus sequence

Table 4-1 Peptide sequence information of phosphorylated peptides on Tyrosine Kinase Substrate Arrays followed by treatment of Apremilast and Roflumilast in Rheumatoid arthritis synovial fibroblasts.

Western blot analysis was performed (Figure 4-6) in RASFs treated with Apremilast and Roflumilast at 10μM to verify the data from the substrate arrays. Apremilast and Roflumilast both appear to significantly increase the phosphorylation of SRC substrates indicating a possible increase in Src phosphorylation. Results showed that Apremilast only, increases the phosphorylation of Fyn at Y530. It also appears that both inhibitors increase the phosphorylation of Src although this was not found to be statistically significant,

an increase in n numbers might unveil this which would again suggest an agreement with the kinase array data.

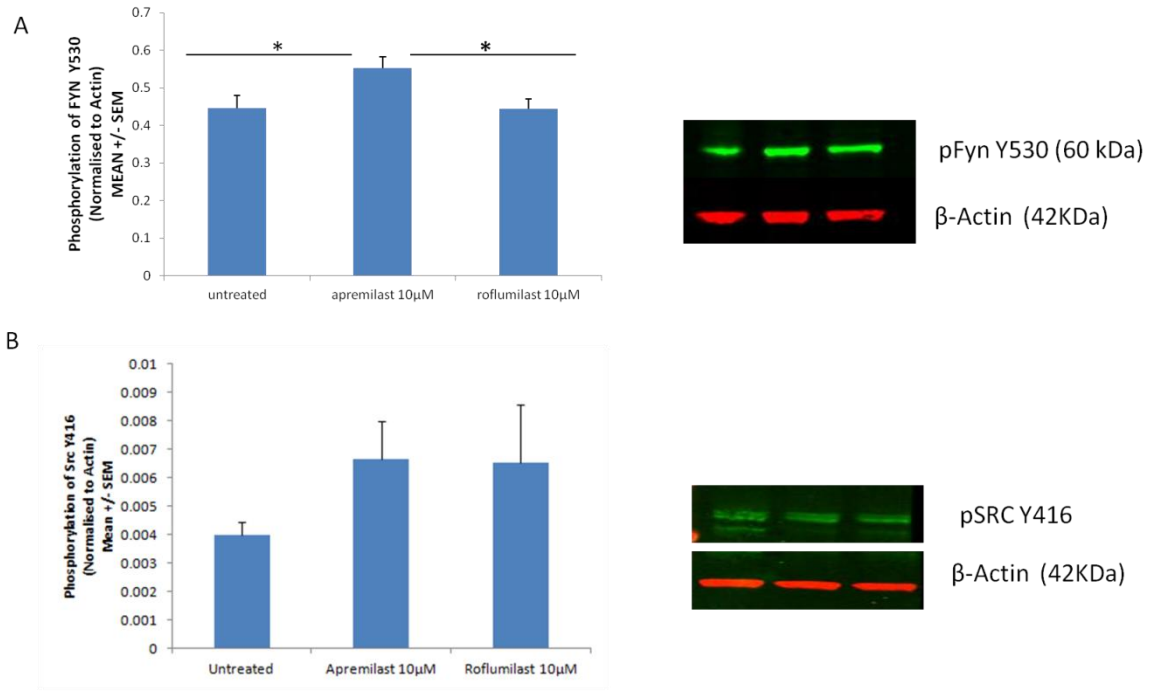

Figure 4-6 Effect of Apremilast and Roflumilast on the phosphorylation of Fyn at Y530 (A) and Src Y416 (B) in Rheumatoid Arthritis Synovial Fibroblasts (RASFs). A) Western blot analysis of Phosphorylation of Fyn (Y530) in RASF cells (n=4) and representative blot for graph. B) Western blot analysis of Phosphorylation of Src (Y416) (n=3) along with representative blot. Student's t- test was used to compare treatments with the untreated cells. No statistically significant differences were observed between Untreated, Apremilast and Roflumilast on phosphorylation of Src (Y416) in RASFs. Statistical significant differences were found between untreated and Apremilast treated cells as well as a significant difference between Apremilast and Roflumilast in the phosphorylation of Fyn (Y530) *p<0.05. 30 minutes stimulation with 10 μM Apremilast or Roflumilast.

4.2.2 Discussion

The results from Kinase substrate arrays are interesting as it has shown that both Apremilast and Roflumilast significantly increase the phosphorylation of a number of tyrosine kinase substrates. For example, both inhibitors significantly increased the phosphorylation of a few Src substrates as well as a PKA consensus site motif in Src kinase itself. Only Apremilast significantly increased the phoshorylation of a Fyn kinase consensus sequence. This information was then

used to confirm via western blot that Apremilast does significantly increase the phosphorylation of Fyn at Tyr506 which would explain the increase in phosphorylation of the Fyn in the celluspot arrays. Western blot analysis was also used to test the affect of the inhibitors on the phosphorylation of Src, however an increase in phosphorylation of Src was not found to be significant by either of the inhibitors in these cells.

Fyn is a member of the Src family of non receptor tyrosine kinases with diverse biological functions including the regulation of mitogenic signalling and cell cycle entry, proliferation, integrin-mediated interactions, reproduction and fertilization, axonal guidance, and differentiation of oligodendrocytes and keratinocytes (Saito, Jensen et al. 2010). Fyn is primarily localized to the cytoplasmic leaflet of the plasma membrane, where it phosphorylates tyrosine residues on key targets involved in a variety of different signalling pathways. Importantly, though Fyn has extensively been described for its role in immune function. Fyn positively regulates mast cell responsiveness (Parravicini, Gadina et al. 2002) and is involved in the differentiation of natural killer cells (Gadue, Morton et al. 1999).). It is also known that functionally, the loss of Fyn in mast cells impairs mast cell degranulation and cytokine production (Parravicini, Gadina et al. 2002, Gomez, Gonzalez-Espinosa et al. 2005). Fyn primarily functions to positively regulate mast cell responsiveness (Gilfillan and Rivera 2009). The fact then, that Fyn positively regulates mast cell responses could be interesting as increasing evidence indicates that mast cells are critical for the pathogenesis of inflammatory diseases (Theoharides 1996, Theoharides and Cochrane 2004), such as arthritis (Woolley 2003), atopic dermatitis, psoriasis (Harvima, Viinamaki et al. 1993, Ozdamar, Seckin et al. 1996),and multiple sclerosis (Theoharides 1990). Mast cell-related atopic dermatitis (AD) and psoriasis are triggered or exacerbated by stress through mast cell activation (Church and Clough 1999, Katsarou-Katsari, Filippou et al. 1999). Psoriasis is characterized by keratinocyte proliferation and inflammation, as well as mast cell accumulation and activation (Harvima, Viinamaki et al. 1993, Harvima, Nilsson et al. 2008). Mast cells have also been found to be increased in lesional psoriatic skin (Harvima, Viinamaki et al. 1993, Ozdamar, Seckin et al. 1996). Since Apremilast increases the phosphorylation of Fyn in RASFs, could this perhaps be a reason for its success in the treatment of psoriasis?

Multiple signalling pathways have been identified to modulate Fyn activity (yaka etal 2003, Maksumova et al 2005) of which PKA plays a critical and special role in inflammatory pain (Malmberg, Brandon et al. 1997). Fyn is involved in inflammatory responses and in this context, it is interesting that PKA specifically activated Fyn Kinase in spinal dorsal horn to evoke pain hypersensitivity (Yang, Yang et al. 2011). Evidence indicated that PKA appears to play a unique role in inflammatory pain, as genetic knockout of PKA regulatory subunit R1ß selectively inhibits pain hypersensitivity induced by peripheral inflammation rather than nerve injury (Malmberg, Brandon et al. 1997). This could be quite interesting to follow up as in our lab it has been previously been shown that PDE4 binds directly to Fyn and inhibits PKA (McPhee, Yarwood et al. 1999). Fyn has multiple phosphorylation sites which can affect its kinase activity, and it has been reported that S21 phosphorylation of Fyn by PKA can enhance its activity (Yeo, Oh et al. 2011). Therefore it is possible to say that perhaps Apremilast while inhibiting PDE4 is activating Fyn via the phosphorylation of PKA and influencing the inflammatory response.

4.3 Reverse Phase Protein Array

Reverse phase protein array (RPPA) is a high-throughput antibody-based technique with the procedures similar to that of Western blots. Proteins are extracted from cultured cells and denatured by SDS. The Protein lysates are then arrayed as micro spots on nitrocellulose- coated glass slides and probed with highly specific antibodies that have been validated for RPPA. At least 200 antibodies are currently validated to monitor protein levels and post translational modifications. Each micro spot contains the whole proteome repertoire of the cell. Therefore the protein array allows measurement of protein expression levels and their modification by phosphorylation in a large number of biological samples simultaneously in a quantitative manner using high-quality validated antibodies. Reverse Phase Protein Arrays have emerged over the last 10 years as a powerful functional proteomics tool for high throughput signalling pathway analysis. Therefore I decided to employ RPPA analysis of lysates from Rheumatoid arthritis synovial fibroblasts treated with 10μM Apremilast and Roflumilast, which was performed at the Edinburgh Cancer

Research Centre by Dr Bryan Serrels, to do some further pathway analysis of Apremilast and Roflumilast. Figure 4-5 shows the RPPA set up used for these experiments.

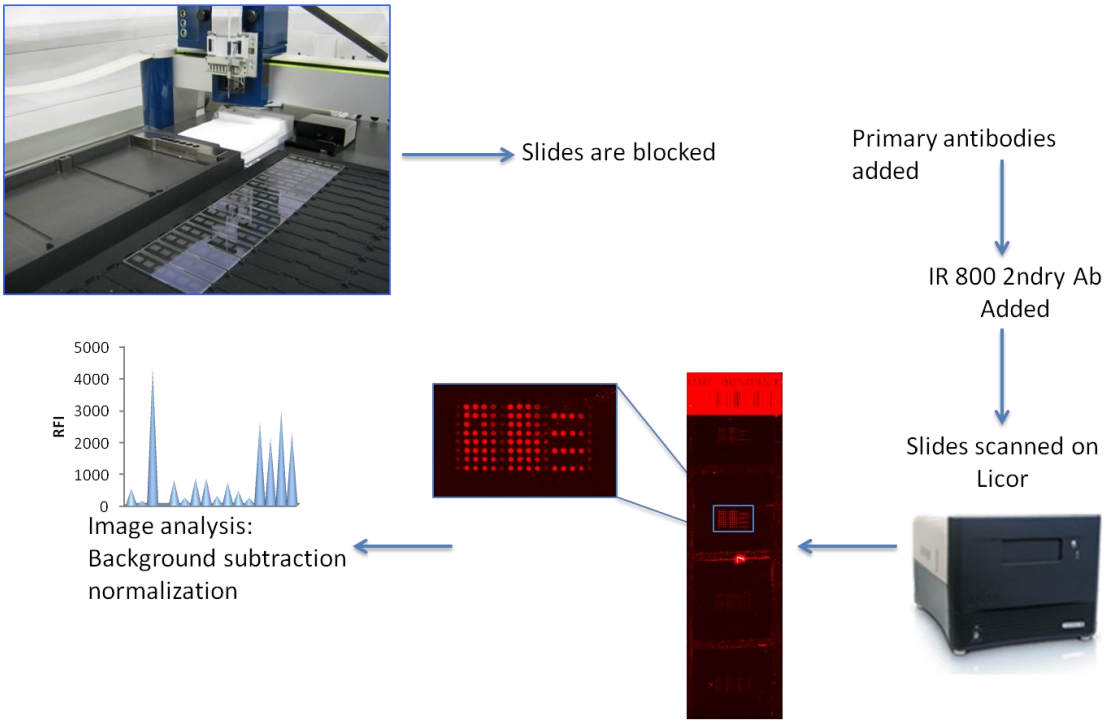

Figure 4-7 Schematic representation of Reverse Phase Protein Array platform. Cell lysates are arrayed onto nitrocellulose-coated slides and subsequently incubated with primary and secondary validated antibodies. The slides are then scanned and analysed on a Licor Oddyssey Scanner.

4.3.1 Results

The results from RPPA analysis showed a number of interesting hits, where Apremilast and Roflumilast seem to increase the phosphorylation or expression of different proteins, shown in figure 4-8. Among these hits are several proteins that are involved in the inflammatory response for example Src which showed up in the kinase arrays, the protein kinase Akt at threonine 308, mTor pSER 248, S6

ribosomal protein and several others. CREB Ser133 was used as a control for these experiments since we know that both Apremilast and Roflumilast increase the phosphorylation of this protein. Accompanying images (figure 4-9) from the arrays are presented along with the graphs (formed from the analysis of the images). One of the more interesting images with most striking difference between untreated cells as well as between Apremilast and Roflumilast was the total and phospho S6 ribosomal protein at Ser240/244 (figure 4-9) as well as phospho Akt at Thr308 and Ser473, although there doesn't look to be a difference between the inhibitors here.

A

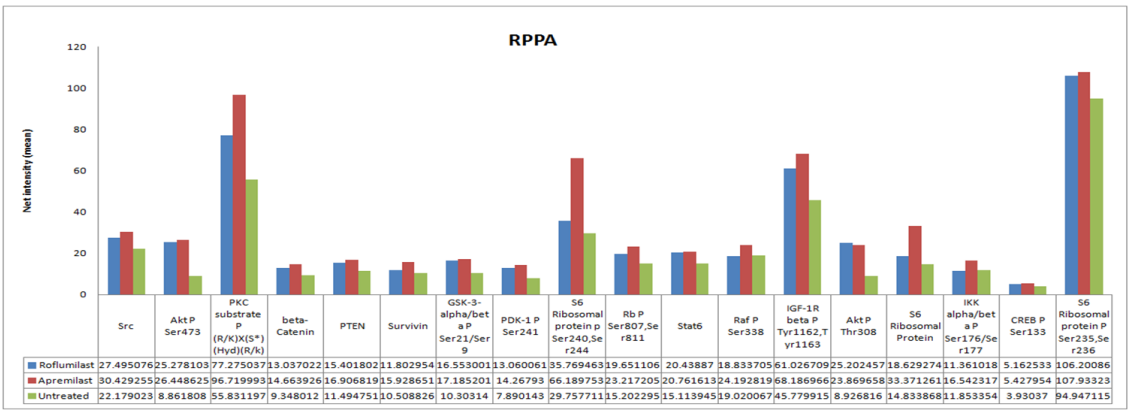

	Src	Akt P Ser473	PKC substrate P (R/K)X(S*)(Hyd)(R/k)	beta-Catenin	PTEN	Survivin	GSK-3-alpha/beta P Ser21/Ser9	PDK-1 P Ser241	S6 Ribosomal protein p Ser240,Ser244	Rb P Ser807,Ser811	Stat6	Raf P Ser338	IGF-1R beta P Tyr1162,Tyr1163	Akt P Thr308	S6 Ribosomal Protein	IKK alpha/beta P Ser176/Ser177	CREB P Ser133	S6 Ribosomal protein P Ser235,Ser236
Roflumilast	27.495076	25.278103	77.275037	13.037022	15.401802	11.802954	16.553001	13.060061	35.769463	19.651106	20.43887	18.833705	61.026709	25.202457	18.629274	11.361018	5.162533	106.20086
Apremilast	30.429255	26.448625	96.719993	14.663926	16.906819	15.928651	17.185201	14.26793	66.189753	23.217205	20.761613	24.192819	68.186966	23.869658	33.371261	16.542317	5.427954	107.93323
Untreated	22.179023	8.861808	55.831197	9.348012	11.494751	10.508826	10.30314	7.890143	29.757711	15.202295	15.113945	19.020067	45.779915	8.926816	14.833868	11.853354	3.93037	94.947115

B

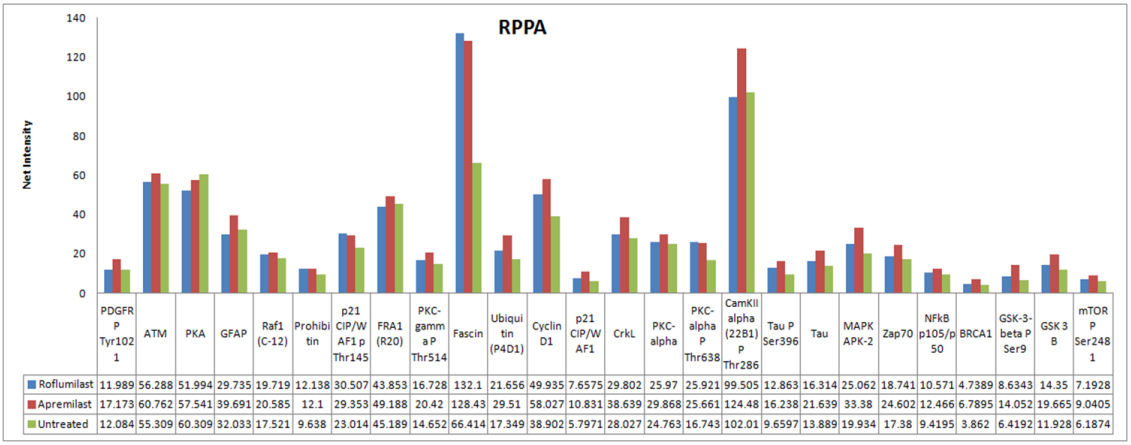

	PDGFR P Tyr1021	ATM	PKA	GFAP	Raf1 (C-12)	Prohibitin	p21 CIP/WAF1 p Thr145	FRA1 (R20)	PKC-gamma P Thr514	Fascin	Ubiquitin (P4D1)	Cyclin D1	p21 CIP/WAF1	CrkL	PKC-alpha	PKC-alpha P Thr638	CamKII alpha (22B1) P Thr286	Tau P Ser396	Tau	MAPK APK-2	Zap70	NFkB p105/p50	BRCA1	GSK-3-beta P Ser9	GSK 3 B	mTOR P Ser2481
Roflumilast	11.989	56.288	51.994	29.735	19.719	12.138	30.507	43.853	16.728	132.1	21.656	49.935	7.6575	29.802	25.97	25.921	99.505	12.863	16.314	25.062	18.741	10.571	4.7389	8.6343	14.35	7.1928
Apremilast	17.173	60.762	57.541	39.691	20.585	12.1	29.353	49.188	20.42	128.43	29.51	58.027	10.831	38.639	29.868	25.661	124.48	16.238	21.639	33.38	24.602	12.466	6.7895	14.052	19.665	9.0405
Untreated	12.084	55.309	60.309	32.033	17.521	9.638	23.014	45.189	14.652	66.414	17.349	38.902	5.7971	28.027	24.763	16.743	102.01	9.6597	13.889	19.934	17.38	9.4195	3.862	6.4192	11.928	6.1874

Figure 4-8 Reverse Phase Protein Array. A-B show all hits from RPPA, Over 150 antibodies were tested (See materials and method section). Arrays were scanned on Licor Oddyssey scanner and intensities of spots were quantified (Bryan Serrels Edinburgh Cancer Research Centre).

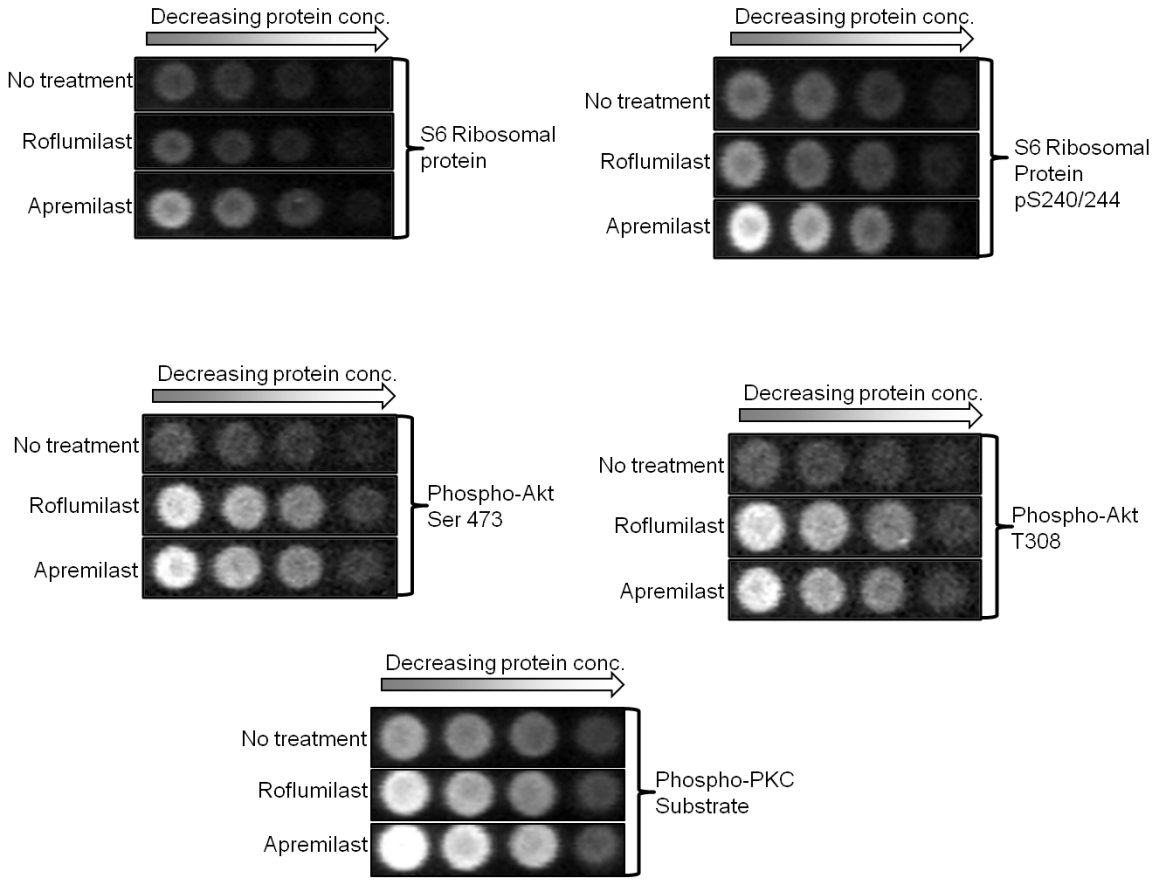

Figure 4-9 Reverse Phase Protein Array Images. Selection of images of interesting RPPA hits including, S6 Ribosomal protein, S6 Ribosomal protein pS240/244, Phospho-Akt Ser473, Phospho-Akt T308 and Phospho-PKC. Images obtained from Oddyssey® scanning system.

To evaluate the observations made by RPPA, selected antibodies were used to test RASF lysates treated with 10μM Apremilast or Roflumilast and analysed by Western blot. Total S6 ribosomal protein and S6 ribosomal pSer240/244 as well as Akt Thr 308 and Ser 473 antibodies were selected (figure 4-10 and 4-11).

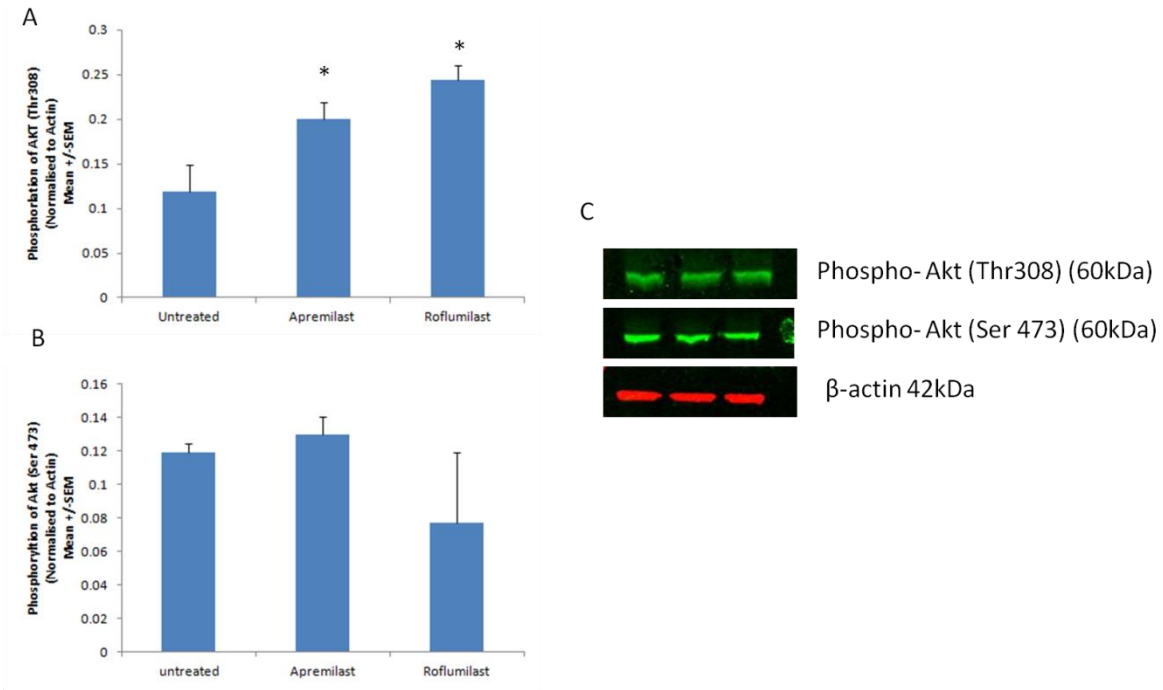

Figure 4-10 Effect of Apremilast and Roflumilast on the phosphorylation of Akt at Thr 308 and Ser 473 in Rheumatoid Arthritis Synovial Fibroblasts (RASF). A-B Western blot analysis of Akt phosphorylation in RASF cells A) pAkt (Thr308) B)pAkt (ser473). C) Representative Western blots for each graph. Student's t- test was used to compare treatments with the untreated cells. No statistically significant differences were observed between Apremilast and Roflumilast on phosphorylation of Akt (Ser473) in RASFcells. *p<0.05. 30 minutes stimulation with 10 µM Apremilast or Roflumilast.

Results from figure 4-10 show that both Apremilast and Roflumilast increased the phosphorylation of Akt at Thr308 in RASFs, which confirms the findings from RPPA however there were no significant differences between PDE4 inhibitors. There was, however, no significant increase in the phosphorylation of Akt at Ser 473, which is in disagreement with the RPPA data. Interestingly, the PI3K/Akt/mTOR pathway is thought to be involved in positively regulating the immune response (Weichhart and Saemann 2008) as well as the phosphorylation of Akt being known to mediate anti inflammatory activity (Vo, Lee et al. 2014).

I then probed (by western blot) for Ribosomal S6 (rpS6) phosphorylation as the RPPA data looked positive. rpS6 has been found to be hyper activated and differentially phosphorylated in epidermal lesions of patients with psoriasis and atopic dermatitis (Ruf, Andreoli et al. 2014) as well as rpS6 pSer 240/244 said to be expressed in lesional skin from patients with autoimmune skin blistering

diseases (Abreu-Velez, Googe et al. 2013). The western blot data in figure 4-11 below backs up the RPPA data for this protein as it appears that Apremilast significantly increases the phosphorylation of the rpS6 at Ser240/244 in RASFs whereas Roflumilast does not show a significant increase in these cells. Total rpS6 expression does also look to be enhanced by Apremilast, again agreeing with the RPPA data although this was not shown to be significant.

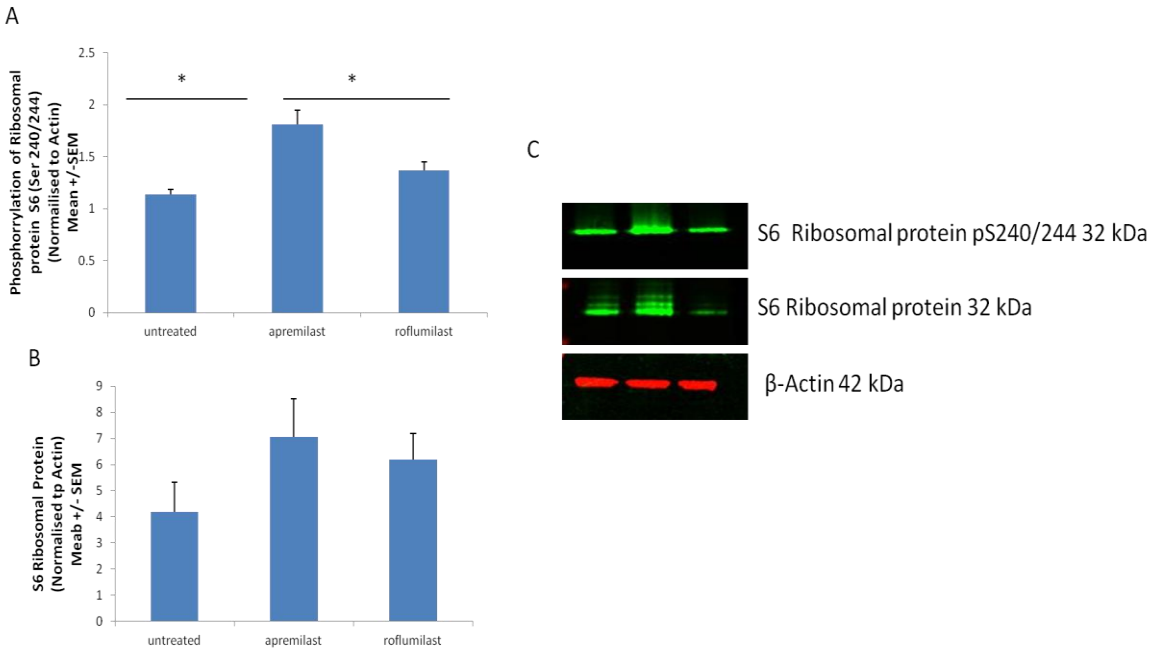

Figure 4-11 Effect of Apremilast and Roflumilast on rpS6 in RASF cells. A-B Western blot analysis of A) phosphorylation of S6 ribosomal protein at Ser 240/244 B) Total rpS6. C) Representative western blots for each graph. Student's t-test was used to compare treatments with untreated cells (n=3) Significant differences were found between Apremilast and Roflumilast on the phosphorylation of rpS6 Ser240/244. * p<0.05

Therefore the kinase substrate array, RPPA and western blot data prompted me to investigate the S6 ribosomal protein (rpS6) pathway as it appears clear that treatment of RASFs with Apremilast leads to an increased phosphorylation of the S6 Ribosomal protein at Ser 240/244 as well as leading to increased phosphorylation of Fyn protein in these cells, whereas Roflumilast doesn't seem to significantly increase the phosphorylation of either of these proteins in these cells. A paper by (Salmond, Emery et al. 2009) has described a signalling event

where T cell receptor pathways lead to ribosomal protein rpS6 phosphorylation and this acts as a point of convergence for multiple TCR-induced signalling pathways. The paper also showed that Fyn contributes to the induction of rpS6 phosphorylation via the activation of mTOR – and MAPK-dependent pathways. Figure 4-12 explains this pathway. I wanted to try and investigate where in this pathway PKA may contribute and what effect the inhibitors have on each point since it is known that Apremilast and Roflumilast increase the activation of PKA. It is possible that an increase in PKA phosphorylation of Fyn following Apremilast treatment is activating Fyn directly. It is also possible that an increase in PKA activity triggered by the inhibitors results in a phosphorylation of rpS6, as there is evidence that suggests that PKA may be a third in vivo Ribosomal S6 kinase in pancreatic ß-cells (Moore, Xie et al. 2009).

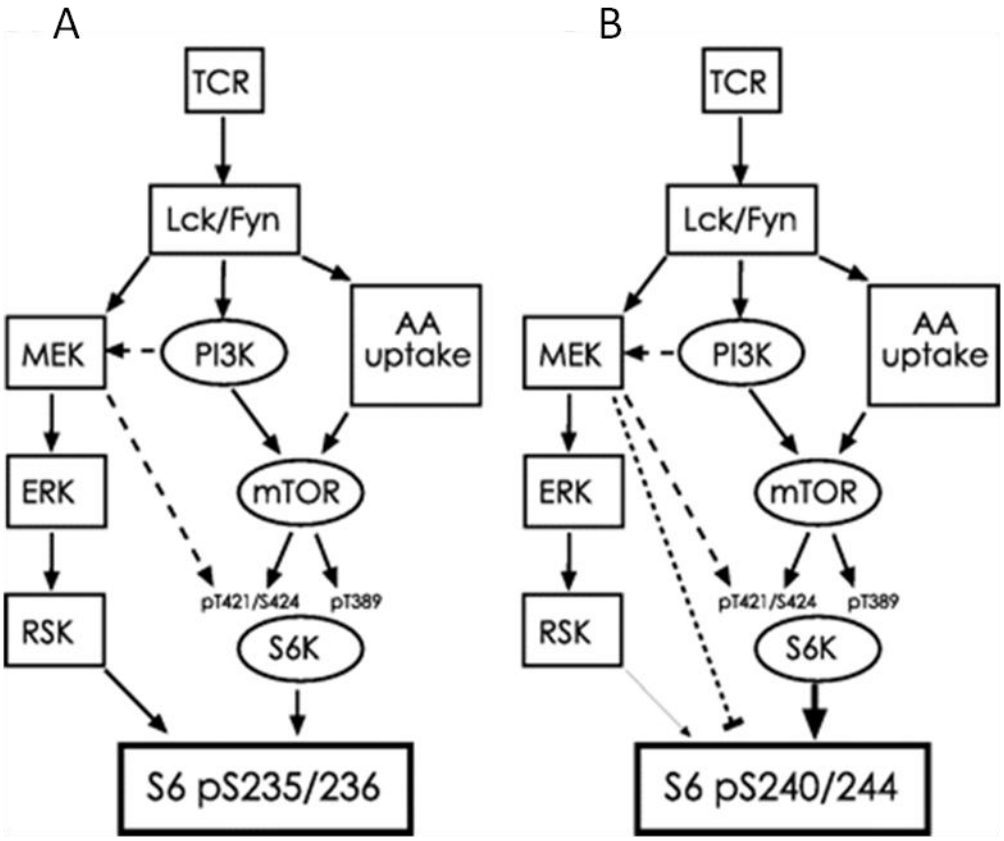

Figure 4-12 TCR signalling pathways leading to ribosomal rpS6 phosphorylation (Salmond, Emery et al. 2009). A) TCR induced activation of Lck and Fyn results in downstream activation of MEK and PI3K, and uptake of amino acids (AA) from the extracellular environment. MEK activates its downstream effector ERK that in turn activates RSK. PI3K and AA signalling facilitates activation of mTOR. mTOR is critical for phophorylation of S6K at residue T389, whereas both Mtor and MEK – dependent signals are required for phosphorylation of S6K T421/S424. RSK and S6K both contribute to maximal phosphorylation of rpS6 at residues Ser235/236. B) Upstream signals required for rpS6 Ser 240/244 phosphorylation are similar for rpS6 Ser 235/236 as described in A. However RSK plays a minor role in Ser240/244 and mTOR-dependent S6K activity is dominant for rpS6240/244 phoshorylation. Furthermore, MEK may also be an inhibitory pathway, decreasing rpS6 phosphorylation.

Below is a model which I based my pathway analysis on and shows the pharmacological inhibitors available for each point in the pathway, some of which I have used in my experiments (figures 4-14-16). Unfortunately due to time constraints, all of the inhibitors were unable to be tested and so a complete analysis of this pathway was not performed.

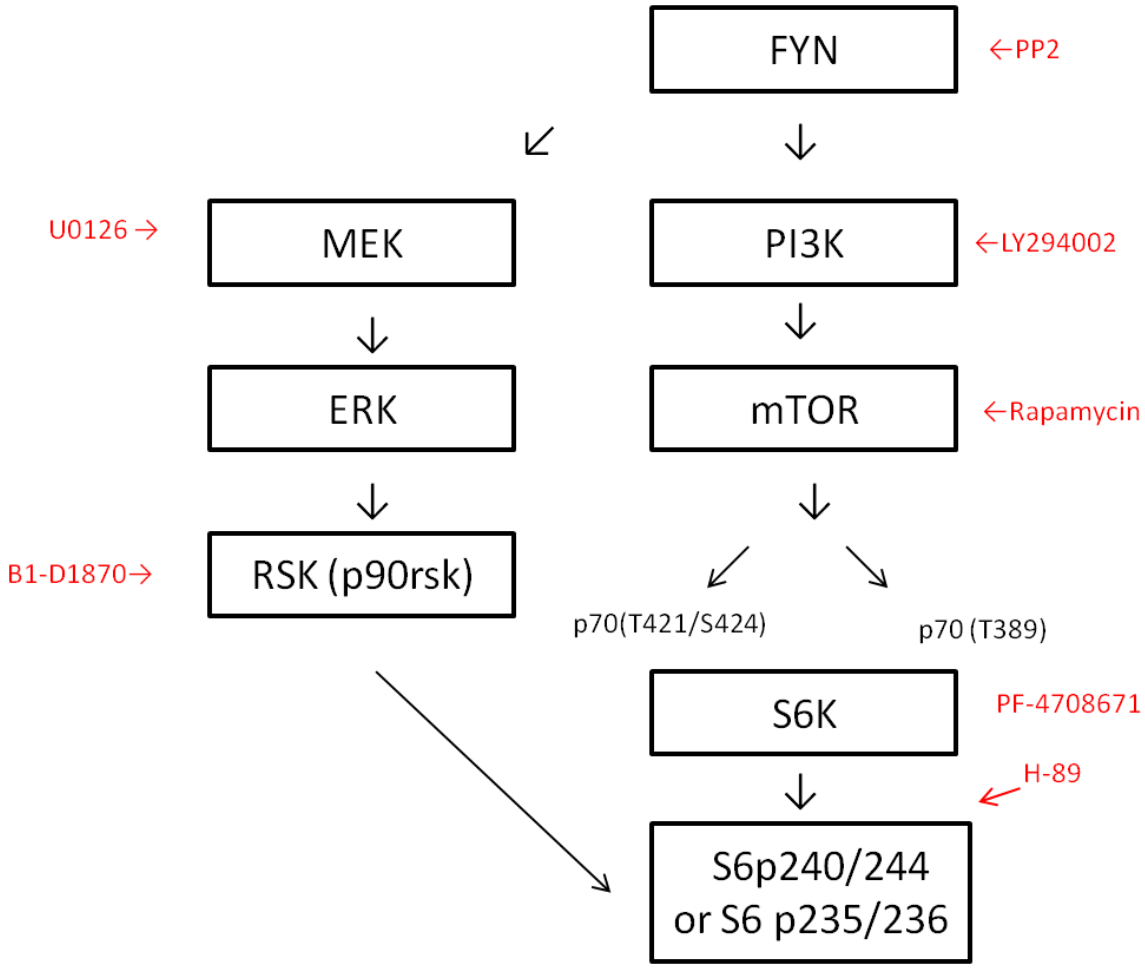

Figure 4-13 TCR signalling pathway leading to rpS6 phosphorylation. Indicated points of inhibition shown on the pathway by available pharmacological inhibitors. Adapted from (Salmond, Emery et al. 2009).

Hek 293 cells were used for these experiments due to ease of cell culture and the ability to produce lots of protein for western blot analysis quickly and easily, compared to the more difficult propagation and time consuming nature of primary RASFs. Ideally RASFs would have been used but due to lack of available time this was not possible. Figure 4-14 below shows the results for western blot analysis using the PKA inhibitor H-89 +/- Apremilast or Roflumilast. The phosphorylation of rpS6 was then assessed using phospho-specific antibodies for rpS6 at Ser240/244 and Ser235/236. The phosphorylation of rpS6 at ser 235/236 was a hit in the RPPA analysis although there appeared to be no differences between the inhibitors here. In addition the following kinases and proteins upstream of rpS6 were monitored: S6 kinase p70 (T421/S424), PI3K p85 and at

Fyn Y506. The data showed that rpS6 phosphorylation at Ser 240/244 and 235/236 was significantly reduced with H-89 treatment which suggests that PKA is involved here; however treatment with either of the inhibitors after H-89 treatment had no effect. Similarly in RASFs, rpS6 phosphorylation was significantly increased in HEK 293 cells, whereas Roflumilast was not. There was no significant difference between Apremilast and Roflumilast treatments in HEK cells though. Interestingly, Apremilast and Roflumilast both significantly increased the phosphorylation of P70 S6 kinase T421, however Apremilast seems to significantly increase the phosphorylation of this protein above that of Roflumilast as there is a significant difference between the two inhibitors here. Again, H-89 significantly reduces the phosphorylation of this protein. Total rpS6 expression appears to be mainly unchanged by H-89 treatment although it looks to be decreased slightly this is not significant. Phosphorylation of PI3K is unchanged by H-89 treatment, although it is not significant, Apremilast appears to increase the phosphorylation of PI3K. Mirroring the situation in RASFs, Apremilast increases the phosphorylation of Fyn in HEK cells. H-89 treatment does significantly reduce Fyn phosphorylation although this reduction is not significant when either Apremilast or Roflumilast is added; suggesting perhaps that Fyn phosphorylation induced by Apremilast is via PKA.

A

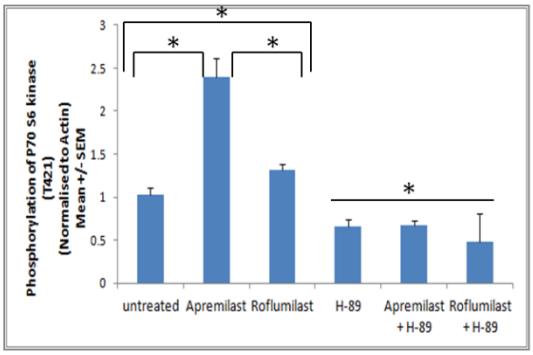
Phosphorylation of P70 S6 kinase (T421) (Normalised to Actin) Mean +/- SEM
untreated
Apremilast
Roflumilast
H-89
Apremilast + H-89
Roflumilast + H-89

B

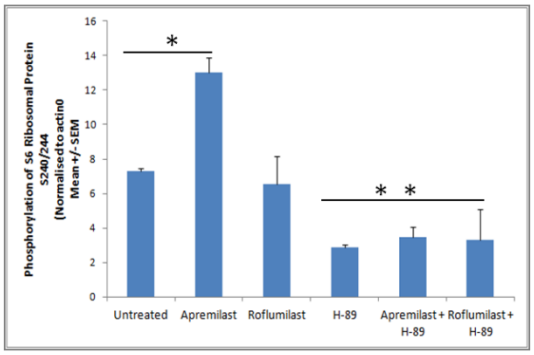
Phosphorylation of S6 Ribosomal Protein S240/244 (Normalised to actin0 Mean +/- SEM
Untreated
Apremilast
Roflumilast
H-89
Apremilast + H-89
Roflumilast + H-89

C

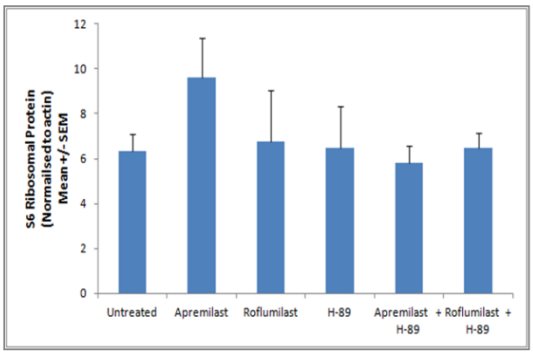
S6 Ribosomal Protein (Normalised to actin) Mean +/- SEM
Untreated
Apremilast
Roflumilast
H-89
Apremilast + H-89
Roflumilast + H-89

D

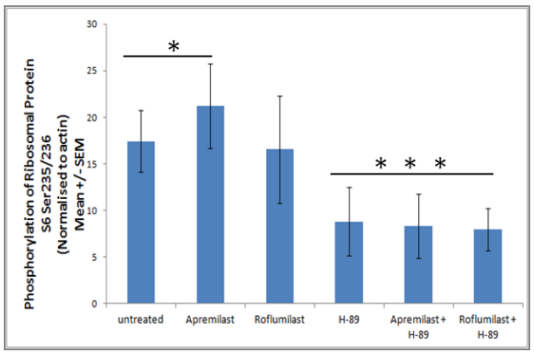
Phosphorylation of Ribosomal Protein S6 Ser235/236 (Normalised to actin) Mean +/- SEM
untreated
Apremilast
Roflumilast
H-89
Apremilast + H-89
Roflumilast + H-89

E

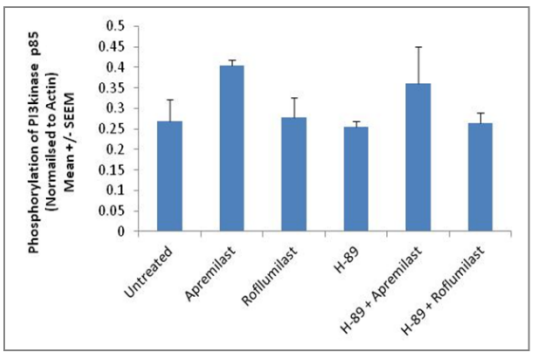
Phosphorylation of PI3kinase p85 (Normalised to Actin) Mean +/- SEEM
Untreated
Apremilast
Roflumilast
H-89
H-89 + Apremilast
H-89 + Roflumilast

F

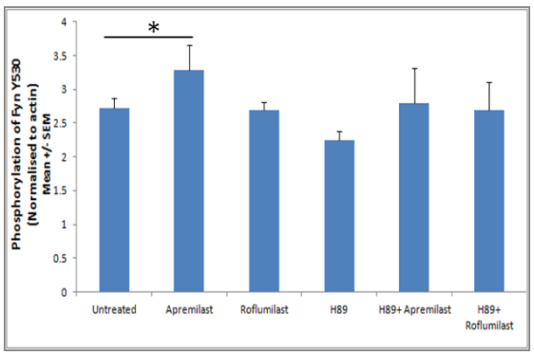
Phosphorylation of Fyn Y530 (Normalised to actin) Mean +/- SEM
Untreated
Apremilast
Roflumilast
H89
H89+ Apremilast
H89+ Roflumilast

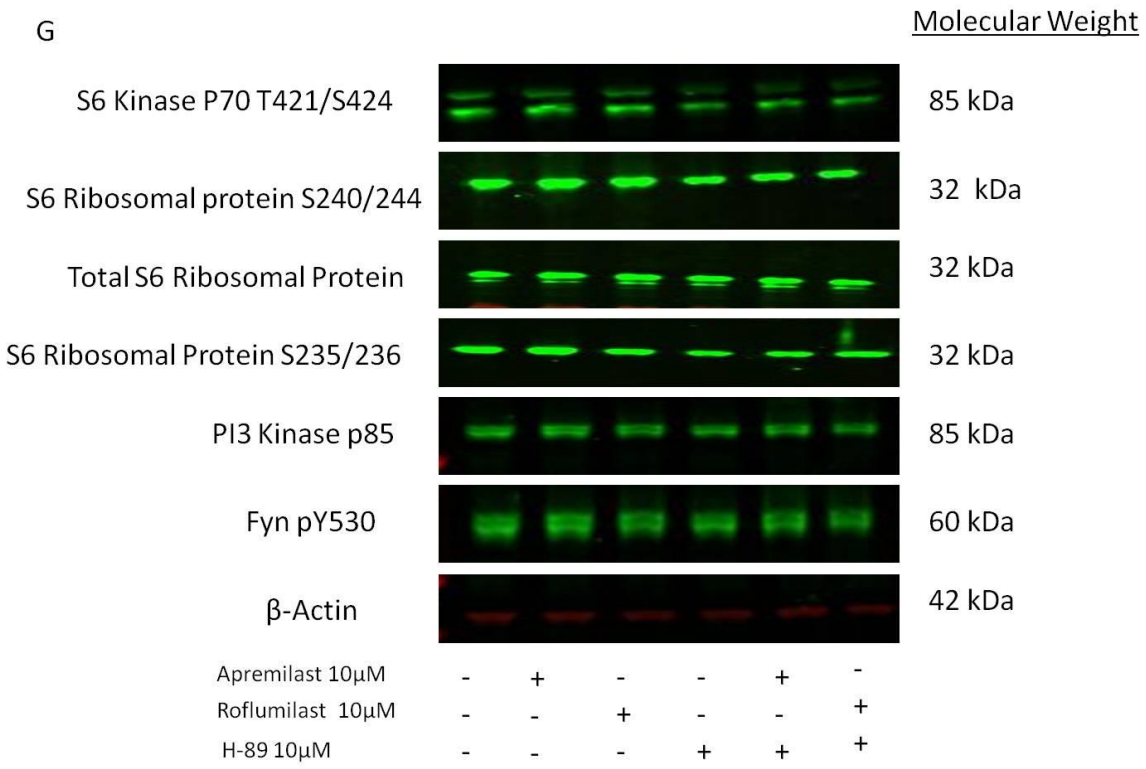

Figure 4-14 Effect of inhibition of PKA before stimulation with Apremilast and Roflumilast on the S6 ribosomal pathway. Hek 293 cells were pretreated with +/- H-89 for 30 mins before stimulation with Apremilast and Roflumilast 10μM for 30 mins. A-F) Western blot analysis of phosphorylation of rpS6 Ser240/244, Ser235/236, total rpS6, S6 kinase p70 (T421/S424), PI3K p85 and Fyn Y506. G) Representative blots and loading control. Values represent the mean of 3 experiments, error bars represent SE. *p<0.05,*p<0.001.**

The next inhibitor in the pathway studied was the mTOR inhibitor Rapamycin (figure 4-15). Data showed that phosphorylation of P70 S6 Kinase was significantly blocked by rapamycin as was the phosphorylation of rpS6 240/244. Total rpS6 and total P70 S6 kinase were largely unchanged by mTOR inhibition.

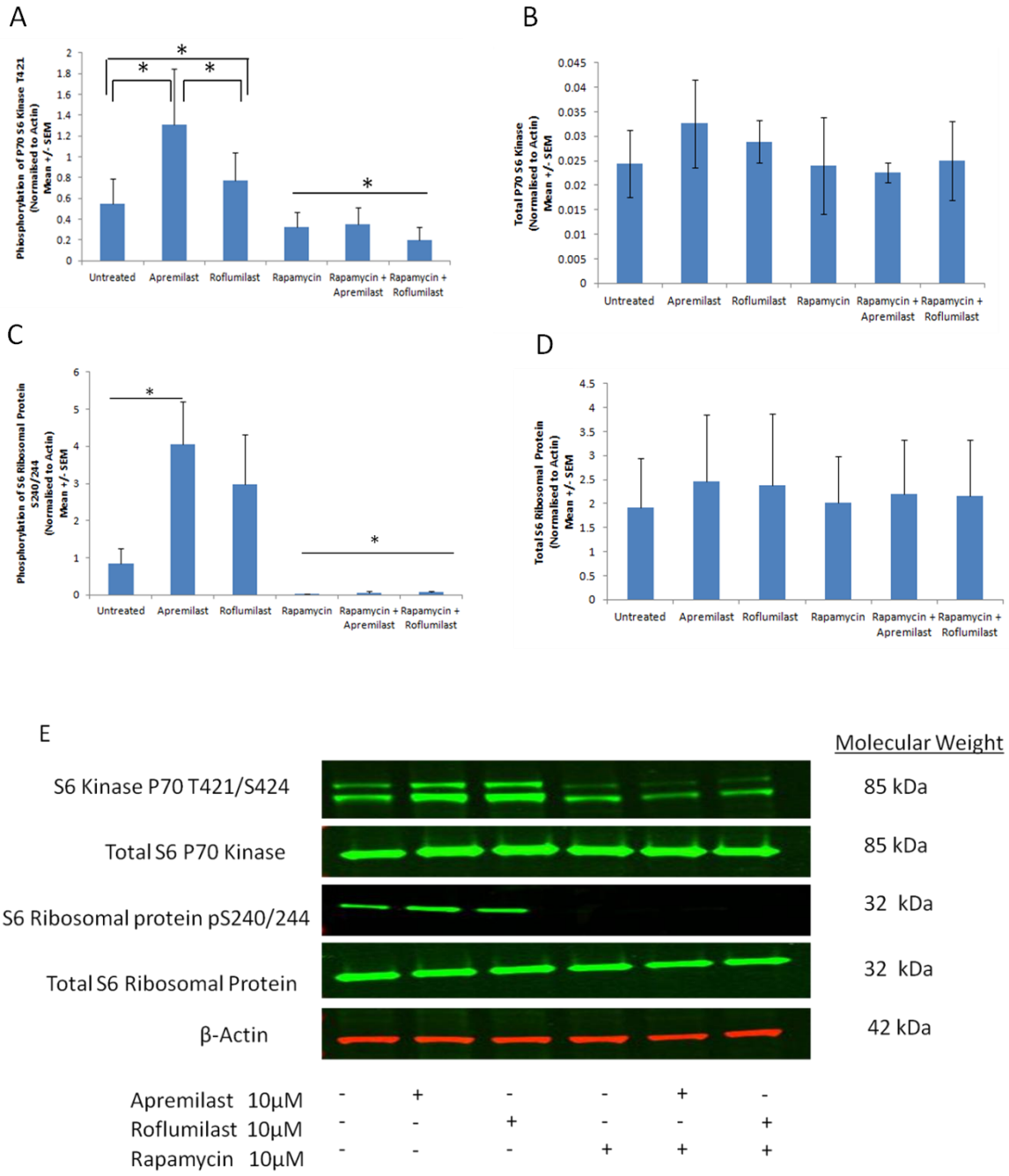

Figure 4-15 Effect of inhibition of mTOR before stimulation with Apremilast and Roflumilast on the S6 ribosomal pathway. Hek 293 cells were pre-treated with +/- H-89 for 30 mins before stimulation with Apremilast and Roflumilast 10μM for 30 mins. A-D) Western blot analysis of phosphorylation of rpS6 Ser240/244, S6 kinase p70 T421/S424, Total rpS6 and Total S6 Kinase p70. E) Representative blots and loading control. Values represent the mean of 3 experiments, error bars represent SE. *p<0.05.

The MEK inhibitor U0126 was the next pharmacological inhibitor to be tested (figure 4-16). This inhibitor appeared to have a small inhibitory effect on the phosphorylation of rpS6 240/244. Interestingly, I observed that both Apremilast and Roflumilast significantly induce the phosphorylation of rpS6 at Ser235/236. Could the inhibitors differentially phosphorylate different residues on rpS6 by

acting on different PKA pools that affect this pathway? Since Apremilast only appears to increase the phosphorylation of rpS6 at Ser240/244 whereas both inhibitors increase the phosphorylation of rpS6 at Ser235/236. Perhaps Apremilast increases the phosphorylation of Fyn upstream of rpS6 resulting in rpS6 phosphorylation at ser240/244. Could they be regulating different pools of PKA, as PKA is thought to exclusively phosphorylate rpS6 at Ser235/236 in pancreatic ß-cells (Moore, Xie et al. 2009). Apremilast-induced phosphorylation of rpS6 at Ser240/244 may lead to different physiological outcomes from that of Ser235/236 phosphorylation for example, and therefore might produce different biological effects than Roflumilast. For example, an up-regulation of human ribosomal protein S6-p240 has been documented in psoriasis and it has also been found to be expressed in lesional skin areas of skin biopsies from patients with autoimmune skin blistering diseases (Abreu-Velez, Googe et al. 2013). If rpS6 is activated for protein synthesis needed to repair lesional skin in these disorders, this could then explain the success of Apremilast in the treatment of psoriasis patients (Papp, Kaufmann et al. 2013).

Both Apremilast and Roflumilast significantly increase the phosphorylation of p44/42 MAPK or ERK1/2 in this pathway (figure 4-16). Expectedly, this increase was completely inhibited by the MEK inhibitor U0126. Apremilast and Roflumilast had no effect on total or phospho p90 RSK, which is interesting as this suggests they are exerting their affects on rpS6 phosphorylation via both MEK and mTOR.

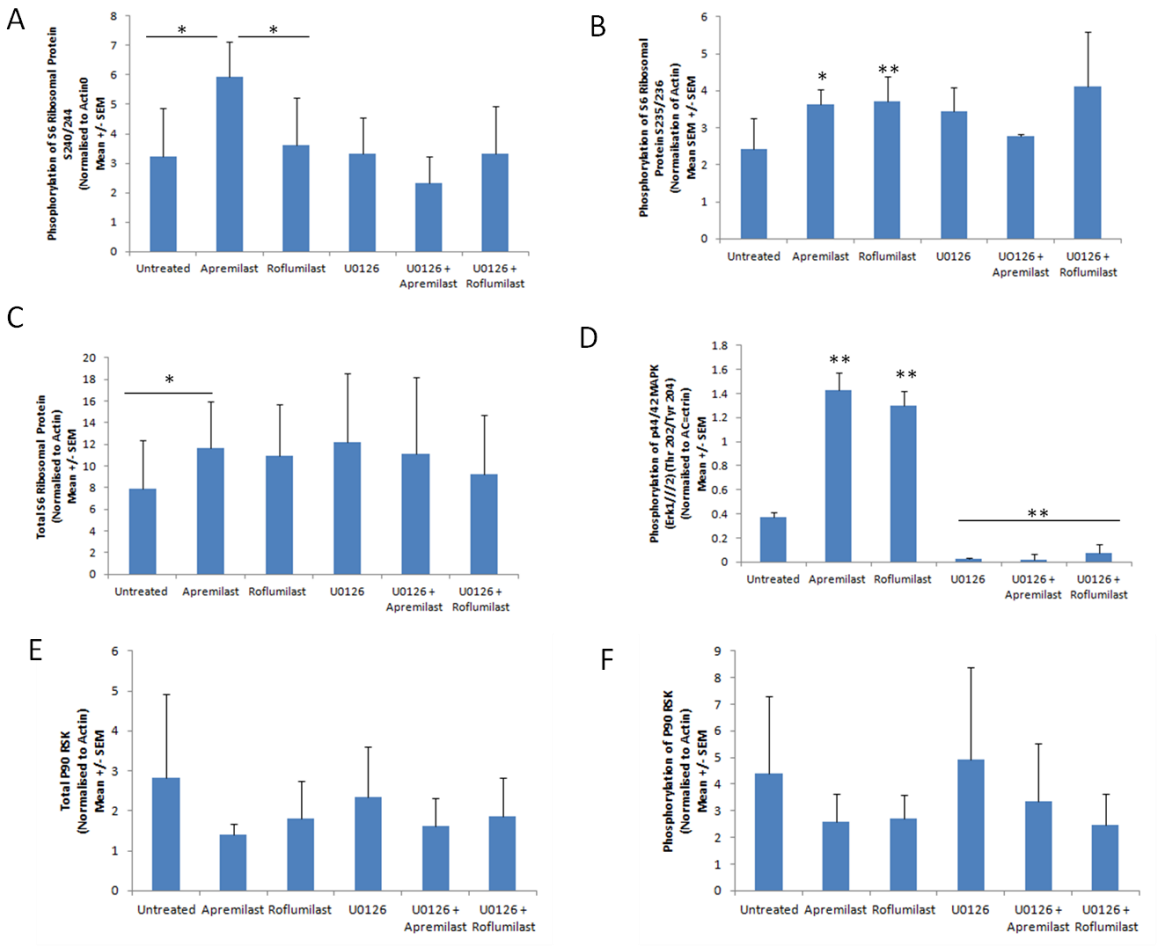

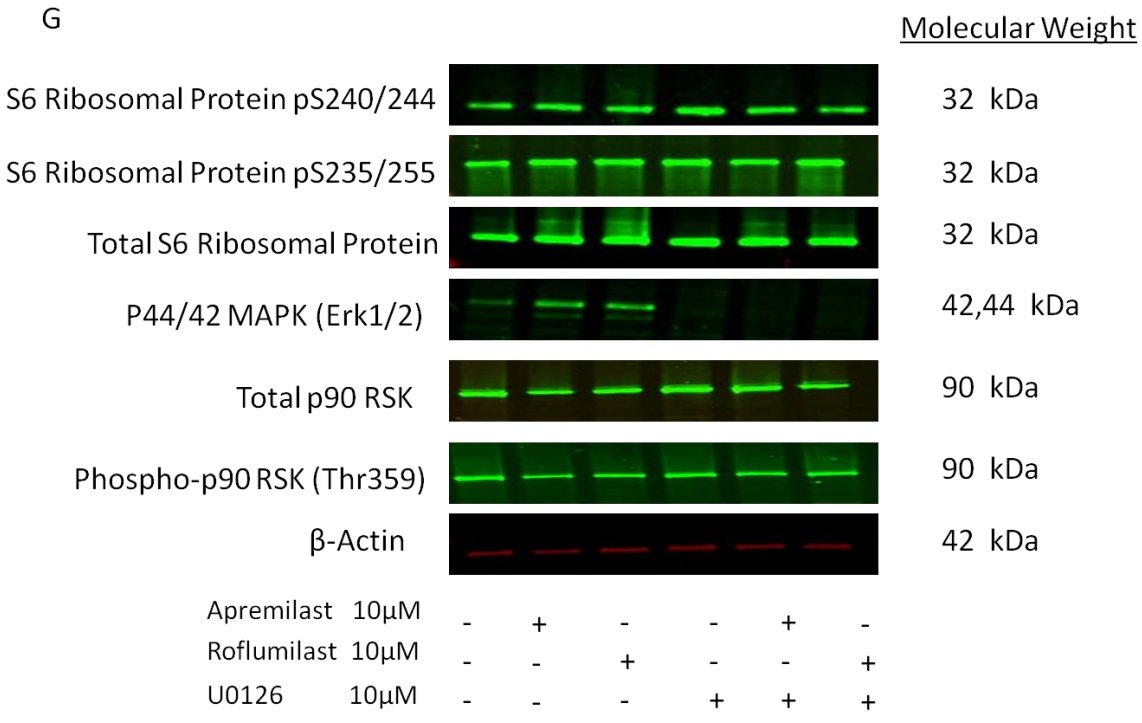

Figure 4-16 Effect of inhibition of MEK1/2 before stimulation of Apremilast and Roflumilast on the S6 ribosomal pathway. Hek 293 cells were pretreated with +/- H-89 for 30 mins before

stimulation with Apremilast and Roflumilast 10μM for 30 mins. A-F) Western blot analysis of phosphorylation of rpS6 Ser240/244, Ser235/236, p90 RSK, total rpS6 and total p90 RSK. G) Representative blots and loading control. Values represent the mean of 3 experiments, error bars represent SE. *p<0.05.

4.3.2 Discussion

Collectively the results from RPPA and western blot analysis of the rpS6 pathway have shown that Apremilast alone increases the phosphorylation of rpS6 at Ser240/244 whereas Roflumilast does not significantly increase the phosphorylation of this site in RASFs or HEK cells. Analysis of the rpS6 pathway has shown that both inhibitors do increase the phosphorylation of S6 Kinase p70 and MAPK both which lead to phosphorylation of rpS6 and that rapamycin treatment blocked the phosphorylation of both of these proteins. However, there was little effect when stimulated with Apremilast or Roflumilast following pre-treatment with rapamycin.

Apremilast also increases the phosphorylation of Fyn Y506, which is upstream of both MAPK and S6 kinase in this pathway. It was shown by (Salmond, Emery et al. 2009) that Fyn can transduce TCR signals via the MAPK and PI3K pathway (Lovatt, Filby et al. 2006, Salmond, Filby et al. 2009), both of which likely contribute to Fyn dependent rpS6 phosphorylation. So it is likely that Apremilast-induced increases in the phosphorylation of Fyn, is contributing to the phosphorylation of rpS6 at Ser240/244 as this is found downstream of Fyn in this pathway. Perhaps Apremilast is affecting a different pool of PKA from that of Roflumilast as both Apremilast and Roflumilast increase the phosphorylation of rpS6 at Ser235/236, which is known to be phosphorylated by PKA directly at this residue (Moore, Xie et al. 2009).

It is important to note that cAMP can activate PKB (Filippa, Sable et al. 1999, Brennesvik, Ktori et al. 2005), which can in turn stimulate S6K1/2 via the activation of Tsc1/Tsc2 and a subsequent increase in mTORC1 activity (Manning, Tee et al. 2002). In addition, cAMP can also activate the Erk signalling pathway (Stork and Schmitt 2002) which via RSK can directly phosphorylate rpS6 at 235/236 (Roux, Shahbazian et al. 2007). In addition, the ERK pathway can

stimulate the activity of S6K1/2 via the activation of mTORC1. Therefore rps6 phosphorylation is likely mediated via S6K, however rpS6 phosphorylation was inhibited by H89 so we know PKA is involved here. It is possible that rpS6 phosphorylation by Apremilast is mediated by PKA and could this lead to a distinct biological role of rpS6 Sr240/244 compared to ser 235/236, as a number of ribosomal proteins have been known to have extra ribosomal functions (Wool 1996).

Unfortunately experiments were not completed with the use of PI3K inhibitor LY294002, PP2 (inhibits Fyn) or B1-D870 (RSK inhibitor) to assess their affects and subsequent treatment with Apremilast or Roflumilast. It has been shown (Salmond, Emery et al. 2009) that rpS6 phosphorylation at Ser240/244 is blocked by this inhibitor since it is downstream in the pathway. However, western blot data didn't show an increase in phosphorylation of PI3k with either inhibitor in my experiments. This could possibly be a cell specific effect as different cells were used in each study.

Ribosomal protein S6 is a component of the 40S ribosomal subunit. The regulated phosphorylation of ribosomal protein rpS6, which occurs in response to a wide variety of stimuli, takes place on five conserved serine residues — Ser235, Ser236, Ser240, Ser244, and Ser247 (Krieg, Olivier et al. 1988). This signalling event has attracted much attention since its discovery in 1974, yet its physiological role has remained obscure. Studies have shown that it is involved in the regulation of cell size, cell proliferation, and glucose homeostasis (Ruvinsky, Sharon et al. 2005). It is thought the protein may contribute to the control of cell growth and proliferation through the selective translation of particular classes of mRNA. rpS6 phosphorylation is tightly controlled by the pathway of mammalian target of rapamycin complex 1 (mTORC1)/p70 ribosomal protein S6 kinases 1 and 2 (p70S6K1/2) (Meyuhas 2008), as well as by ERK (Sturgill, Ray et al. 1988, Roux, Shahbazian et al. 2007), casein kinase 1(Hutchinson, Shanware et al. 2011), PKC (House, Wettenhall et al. 1987, Ohtsubo, Yamada et al. 2014), and cAMP-dependent protein kinase (PKA) (Moore, Xie et al. 2009, Valjent, Bertran-Gonzalez et al. 2011, Ohtsubo, Yamada et al. 2014) signalling cascades. This is confirmed in my experiments as Rapamycin an mTOR inhibitor ablates the phosphorylation of rpS6 at Ser240/244. Upstream mechanisms of regulation of rpS6 are poorly studied and its role in protein synthesis remains largely debated

and the exact molecular mechanisms regulating rpS6 and the function of phosphorylated rpS6 remain poorly understood.

One study has shown (Ruvinsky, Sharon et al. 2005) that ribosomal protein S6 phosphorylation is a determinant of cell size and glucose homeostasis as the rates of global protein synthesis and accumulation are increased in $rpS6^{P-/-}$ MEFs. This observation implies that protein synthesis, at least in this cell type, is down-regulated by rpS6 phosphorylation. Conversely rpS6-pS240 is found to be expressed in lesional areas of skin biopsies from patients (Abreu-Velez, Googe et al. 2013). It is thought that perhaps that rpS6-pS240 may be influencing protein synthesis and/or with the inflammatory/anti-inflammatory immune response in patients affects by skin diseases. The phosphorylation of ribosomal protein S6 correlates with an increase in mRNAs that encode for proteins involved in cell cycle progression and therefore controlling mammalian cell growth and proliferation. This protein could then be activated for protein synthesis needed to repair lesional skin in these disorders. Perhaps the combination of Apremilast triggered increases in phosphorylation of rpS6 Ser240 along with the known increase in anti-inflammatory mediators is the reason that Apremilast has been so successful in psoriasis trials (Papp, Kaufmann et al. 2013).

Recent data has suggested a surprising new function for rpS6 phosphorylation in cancer biology (Khalaileh, Dreazen et al. 2013). rpS6 phosphorylation protects against DNA damage induced by mutant Kras, a gene mutated in many cancers. Work suggests that phosphorylated rpS6 could in principle act to reduce the formation of reactive oxygen species (ROS), a known inducer of DNA damage(Tanaka, Halicka et al. 2006), or alternatively to reduce oncogene-induced replication stress and consequent DNA damage (Halazonetis, Gorgoulis et al. 2008). This opens up a possible repositioning space for Apremilast in the future.

5 Phage Display

5.1 Introduction

In the final part of my studies Phage display technology was employed to discover new linear motifs as binding partners for PDE4. Phage display is a versatile in vitro technology that allows expression of exogenous (poly) peptides on the surface of phage particles. It can be used as a tool for mapping novel protein-protein interactions. Using randomly generated DNA sequences and molecular biology techniques, large diverse peptide libraries can be displayed on the phage surface. The phage library can be incubated with a target of interest and the phage which binds can be isolated and sequenced to reveal the displayed peptides' primary structure. The filamentous phage M13 is the most commonly used vector to create random peptide display libraries (Hamzeh-Mivehroud, Alizadeh et al. 2013). The rapid isolation of specific ligands by phage display is advantageous for many applications including selection of inhibitors for the active and allosteric sites of enzymes, receptor agonists and antagonists, and G-protein binding modulatory peptides. Consequently, the phage display technique has been extensively employed for the identification of novel *in vitro* and *in vivo* ligands in different areas such as cancer, vaccine development, and epitope mapping. From increasing number of phage display collections, numerous new applications have also emerged. For example , selections from a variety of different libraries have been used to identify peptide agonists and antagonists for receptors (Sidhu 2000), determine binding specificity of domains (Sparks, Rider et al. 1996) (Linn, Ermekova et al. 1997), map carbohydrates and protein functional epitopes (Sidhu 2000), select antibodies that recognise post-translational modifications (Kehoe, Velappan et al. 2006), identifying targets for the inhibition of tumour-specific angiogenesis (Zurita, Arap et al. 2003) as well as vaccine development (Lidqvist, Nilsson et al. 2008). Most recently however, there has been a move towards the use of phage display for the production of humanised antibodies and development of new therapeutics, and recently phage display has been a driver for the development of clinically useful peptides and peptidomimetics (Brissette, Prendergast et al. 2006). A few selected peptides and proteins are in clinical or preclinical stages of development and some are reaching the market (Rothe, Hosse et al. 2006).

The most common screening method for identifying and isolating ligands that bind to the target of interest is based on enriching the phage clones with binding affinity for the target by a process called bio panning (Smith and Petrenko 1997, Christensen, Gottlin et al. 2001, Pande, Szewczyk et al. 2010). Bio panning involves the following steps: i) Target immobilisation: the purified target of interest is immobilised on plates. ii) Phage binding: the phage library is added and allowed to bind to the target in conditions suitable for binding. iii) Washing: the unbound phages are removed. (iv) Phage elution: due to the high stability of filamentous phage, a wide variety of methods can be applied to elute the bound phage. Common methods for recovering bound phage are disruption of the interaction between the displayed ligand and the target by changing the pH or adding a competing ligand, denaturant or protease (e.g. because a protease-cleavage site has been engineered between the displayed protein/peptide at the N-terminus and the coat protein itself). (v) Increasing stringency: the eluted phage is then amplified in bacterial cells and bio panning repeated for several rounds (usually 3–5). This tends to select against phage with low affinity/ non-specific binding to the target of interest. (vi) Identification of selectants using DNA sequencing. See figure 5-1 below.

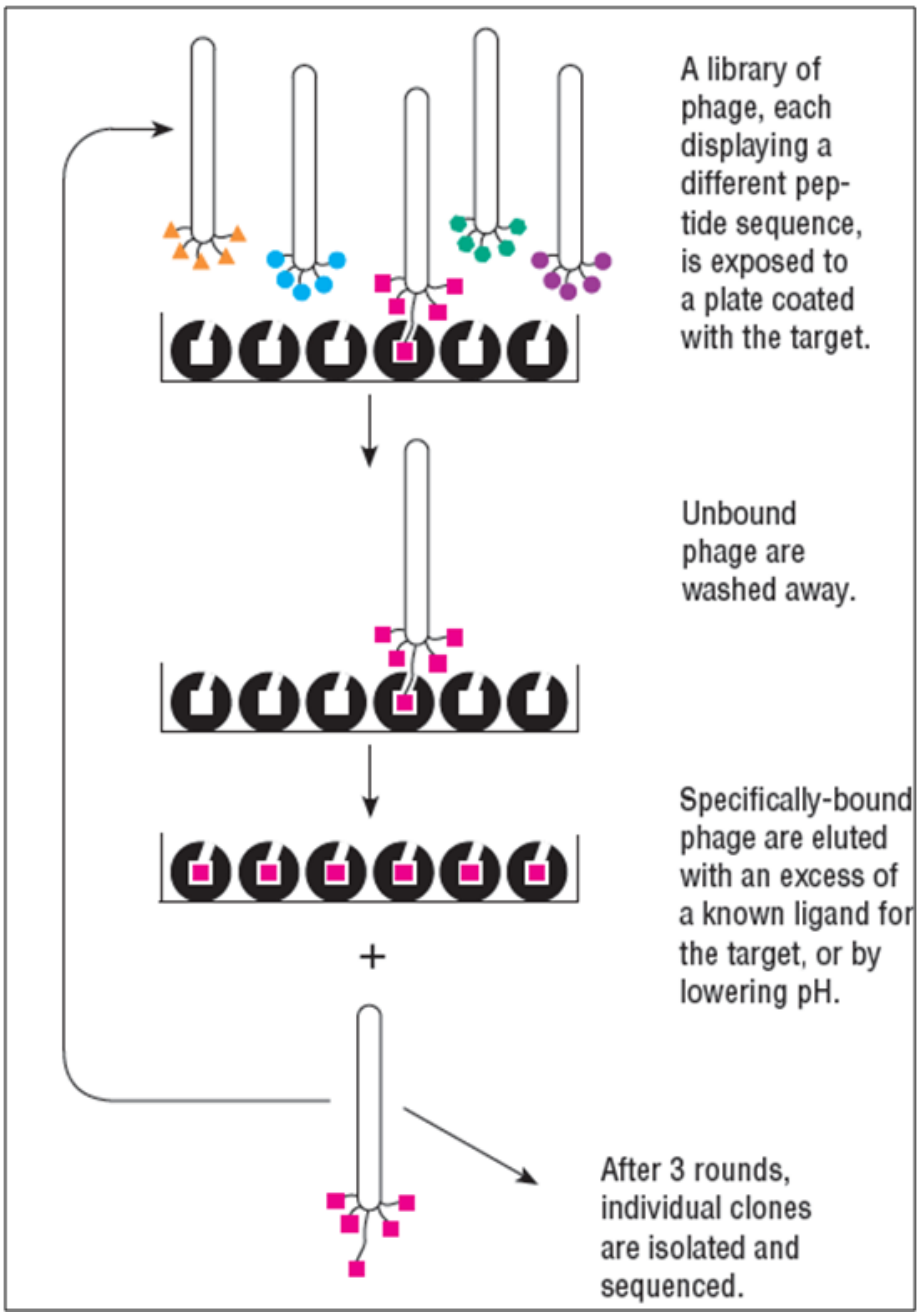

Figure 5-1 Biopanning. The process for affinity selection of phage-displayed peptide or protein: Step 1, target is immobilized and phage library is added.Step 2,washing to remove unbound phage. Step 3, elution of bound phage as the result of conformational changes to the binding site caused by pH change or other means which disrupts the interaction between displayed ligand and the target. Step 4, amplification of eluted phage for next round of biopanning.

Random peptide libraries can be constructed using degenerate oligonucleotides introduced into the phage genome. Peptide libraries can be generated with lengths of the displayed peptides varying from 6 to 30 residues. It is usually difficult to predict the optimum length required for the randomized displayed peptides as this depends on a number of factors including the folding properties

of the displayed peptide, the characteristics of the target, and the purpose of investigation (Noren and Noren 2001). The construction of the library is a key step because the probability of being able to select ligands that bind the target is highly dependent on library diversity and sequence length.

In this chapter Phage display technology was employed in order to identify any novel binding motifs that associate with PDE4. Specifically, we were interested in the binding cohort of peptides that were changed by the association of Apremilast or Roflumilast to the active site of full length, purified PDE4. Our aim was to identify sequences that were differentially regulated by the inhibitors in an attempt to find binding motifs that may exist in previously characterised signalling proteins. Such information may explain the differences in signalling and cAMP generation induced by the different inhibitors.

Phage display experiments presented in this chapter were kindly performed by Tedd Hupp at Edinburgh Cancer research centre. Peptide phage display was carried out through three rounds on captured PDE4A4 alone and PDE4A4 with either Apremilast or Roflumilast bound using an in-house generated 12-mer peptide library. Results were analysed initially by the Tedd Hup group. Over 5000 peptides bound to PDE4A4 alone and the number of times a peptide sequence bound was either increased or decreased when Apremilast or Roflumilast was bound to PDE4a4. I analysed the results of the 1st 1000 hits and looked for any differences between the inhibitors and whether they increased or decreased the number of times each peptide bound to PDE4A4. Figure 5-1 below shows an example of some of the peptide sequences identified to either increase or decrease binding with inhibitors bound. Peptide arrays were then produced (Ruth Macleod, Baillie Lab) using the sequences I identified to validate these binding peptides. The peptides were synthesised on continuous cellulose membrane supports on Whatman 50 cellulose membranes by Ruth Macleod (Baillie lab) using Fmoc (9- fluorenylmethyloxycarbonyl) chemistry with the AutoSpot-Robot ASS222 (Intavis Bioanalytical Instruments, Berlin).This technique has been used extensively by the Baillie lab in the past to map the interfaces between interacting proteins such as PDE4D5-barrestin (Sachs, Baillie et al. 2007), Epac-barrestin(Berthouze-Duquesnes, Lucas et al. 2013) , RACK1-PDE4D530, PDE8A-RAF131,PDE4-Hsp2032, JNK-barrestin(Li, MacLeod et al. 2009).

PDE4 binding decreased with inhibitors			
sequence	PDE4a4	Apremilast	Roflumilast
SGVYKVAYDWQH	8742	2097	2205
TGAPPRLDARPA	627	445	398
NTEQVTANHSLH	226	202	211
SHRWNSEPFLLS	877	433	459
LAVTESKISPMR	236	173	126
DLFGSRHNPGNI	253	153	140
ADQTHTRNLLRQ	197	149	155
NLHDASSFPYHW	150	136	127
ELNTRFVEAVPD	220	101	158
FSGTVTTAGLLF	147	98	88
SALKGLFPADHH	858	167	178
DGSSSLYALHAR	572	243	287
FSSSFVSLPELV	232	144	140
HQLLWVDRLPQK	100	89	89
NIVCPNEHPRCS	146	62	91
RMDSDMVLIARG	104	76	54
ADWYHWRSHSSS	167	86	101
EVMAWQNQMLFK	121	80	78
DVRIYPWMTTAF	369	170	173
NANASHRTFNLI	131	106	121
VPSWPRALQVPS	103	46	44
YLNNDHFGQALT	64	49	41
RTPEMTSLMAWG	1330	148	153
IRGGTSYDLITV	44	40	33

Differences between inhibitors			
sequence	PDE4a4	Apremilast	Roflumilast
GLHTSATNLYLH	1369	7936	14823
KASGSPSGFWPS	333	311	450
EITHPGWSTVTH	1047	7654	14053
FIPFDPMSMRWE	712	4693	10424
GDGNSVLKPGNW	312	213	338
SQDIRTWNGTRS	205	361	485
RGTDAYLMPNRW	386	2441	4460
RGTDAYLMPNRW	386	2441	4460
GTGLVTLPRLTV	281	2027	2242
TTSIKINKYAFH	63	52	68
HDDVLWTPRLYK	336	1135	116
VVSPDMNLLLTN	259	869	1518
TSIQISNAHPKS	148	295	107
LDLHDWSEDTTG	54	45	52
LPAWSGWGYRVL	65	41	55
DDFRVWWPNFPR	93	106	187
VSSRVPIAAAHS	127	92	133
SSYYNSRWAFYP	155	1249	3504
SNSIDKVNRPIN	106	1444	2558
HTGLIGQDCWTC	161	989	2194
TTKFPPFVSVLS	55	48	56
SMRASYPMPTFI	73	60	97
DSQFNKYSIATV	72	81	62
STPIFAEATARS	167	308	539

Figure 5-2 Identification of 12mer peptide sequences that bound PDE 4A4 alone or in its ligand bound state with either Apremilast or Roflumilast. Selection of some of the sequences identified, where binding affinity was either increased or decreased when Apremilast or Roflumilast was bound to PDE4A4 and any differences noted between the inihibitors.

478 sequences were identified where there appeared to be differences in binding when Apremilast or Roflumilast is bound to PDE4a4. Peptide arrays were produced containing these peptide sequences (described in materials and methods section) to validate PDE4a4 binding to these sequences. Purified PDE4a4 tagged with MBP (Maltose binding Protein) was overlaid on the array (described in materials and methods section) as well as an MBP only control and then probed using an anti- MBP antibody. The results of the peptide array and subsequent densitometry analysis in figure 5-3 confirm the binding of many of these peptide sequences to PDE4a4.

A

PDE4a4-MBP

MBP only

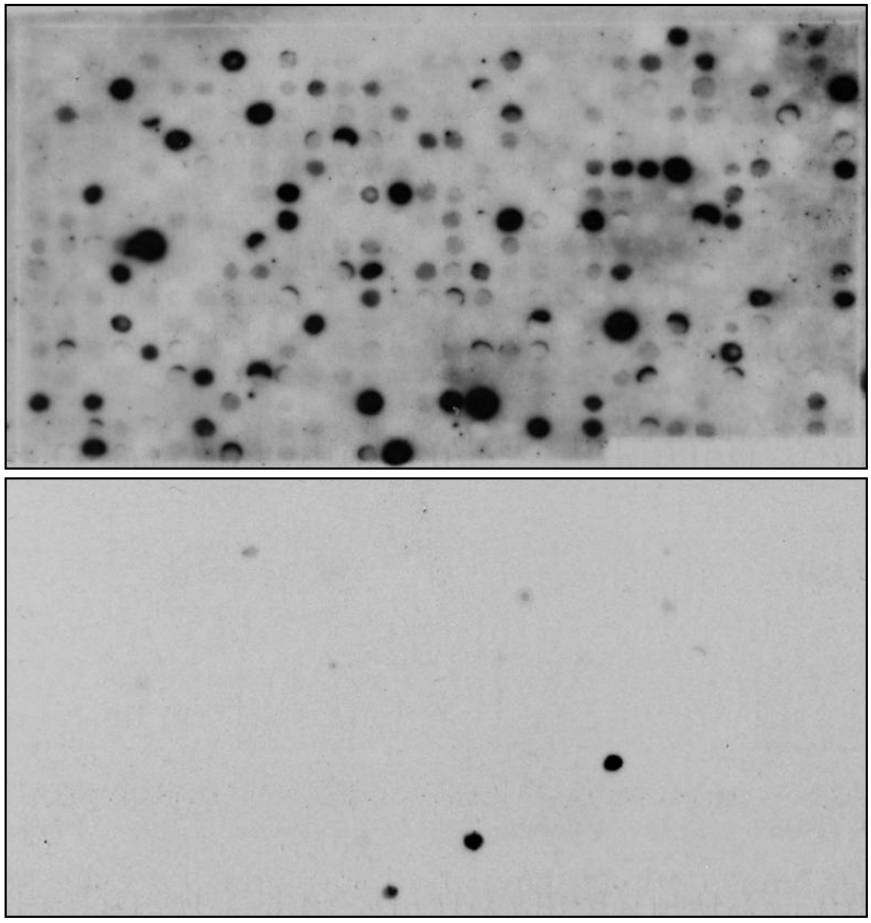

B

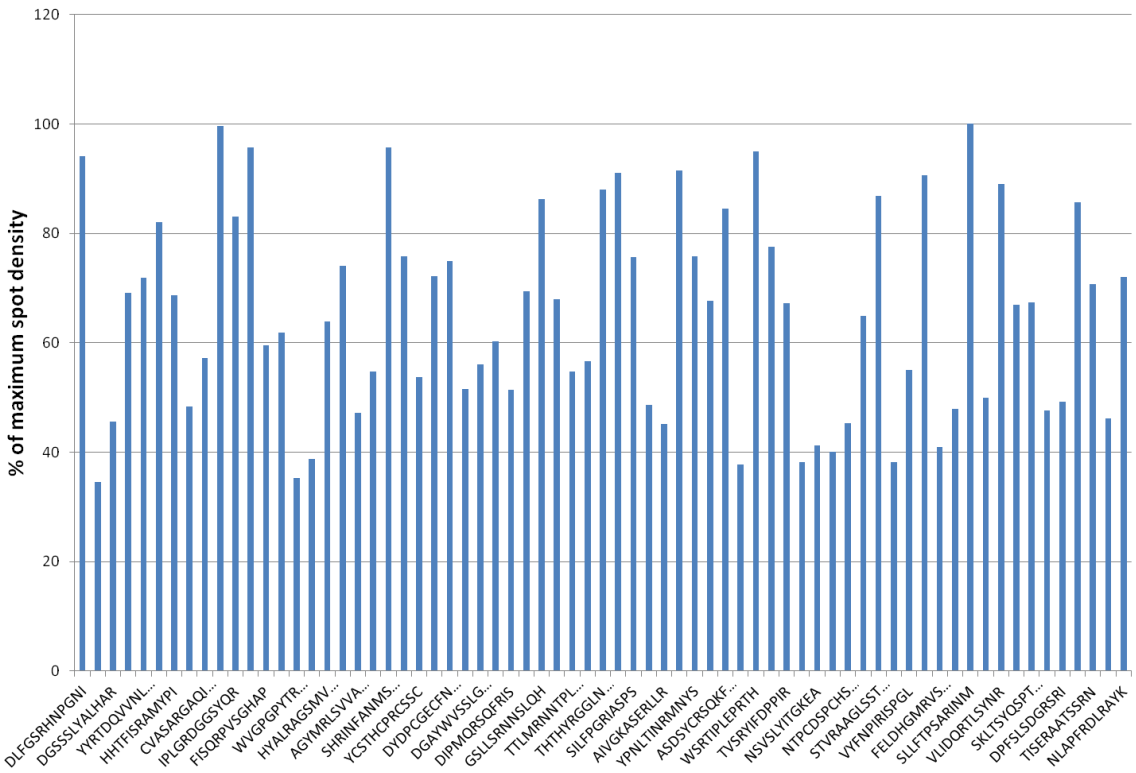

Figure 5-3 Peptide array containing phage display sequences identified from analysis. A) Peptide array was overlaid with either purified PDE4a4-MBP protein or as a control MBP only and probed using anti-MBP antibody. Positively interacting peptides generate dark spots on the array. B) Bar chart represents densitometry analysis of array shown as % of the maximum spot density.

Densitometry analysis was performed on the arrays and spots that were identified as over 80% of the maximum spot density were chosen and processed using Protein Blast search programme to identify targets in the human proteome that may match to these sequences (Altschul, Madden et al. 1997). The results for this are in table 5-1 below and show a number of interesting hits where Apremilast and Roflumilast may increase or decrease the binding of PDE4a4 to certain sequences that are present in proteins.

Sequence	PDE4	Apremilast	Roflumilast	Blast results of binding spots on array
DLFGSRHNPGNI	253	153	140	Retinol binding protein, deleted breast cancer protein 1,zincfinger protein 569, A kinase anchor protein 11,Cohesin subunit SA-1 (STAG1)
TANGVYRNLINP	56	42	35	SAS10(something about silencing protein 10, ATP binding cassette protein(MABC2),Fbox protein 695,DOCK8(dedicator of cytokinesis 8)
IRLPGRIPPEFS	462	73	116	PB1(Androgen regulated protein 3),ribonuclease H1,E3 ubiquitn ligase,
IPLGRDGGSYQR	39	9	22	SPRY domain-containing SOCS box protein 1,ATP binding cassette protein c13,Neurexin-3-alpha
VSFYSTTDKPIR	30	18	12	TRIM 1(e3 ubiquitin ligase), ALMS1 (Alstrom syndrome 1)
SHRINFANMSQL	12	5	5	P13Kinase, Protein kinase C binding protein, Ribosomal Protein L27, lung canecr oncogene 3, Toll like receptor protein 1,myosin 111A
GSLLSRNNSLQH	26	366	749	FOXO4 transcription factor AFX1 containing 1 fork-head domain,fbox protein 34, motor neuron receptor 1, syntaxin,olfactory receptor family 8
THTHYRGGLNAG	14	278	520	NOTCH1, PHD finger protein 13,Rapamycin-insensitive companion of mammalian target of rapamycin (RICTOR)
DYANRLSGRGQV	15	15	2	Heat shock protein 60 (HSP60), ankyrin repeat domain containing protein, small membrane A kinase anchor protein,
YDAIGRYTRMFG	14	85	217	Ribosomal protein L6,Ankyrin repeat domain 28 (ANKRD28)
ASDSYCRSQKFM	10	69	3	G protein coupled receptor, Defective in cullin neddylation protein 1-like protein 1
WSRTIPLEPRTH	6	111	312	Dystrophin, Neural proliferation differentiation and control protein 1
STVRAAGLSSTM	6	31	54	Ubiquitin specific protease 42(USP42),Rapamycin-insensitive companion of mammalian target of rapamycin (RICTOR),zinc finger protein 609
NGYTNSLRTSPQ	13	28	2	transcriptional regulator (ATRX1),mu opiod receptor
SLLFTPSARINM	5	36	2	Mucin, WD repeat containng protein 90 (wdr90),nuclear distribution protein (nudE),URP1,Bruton's tyrosine kinase (Btk),zinc finger protein 609
VLIDQRTLSYNR	5	22	0	Na/H exchanger (NHE2),Furin, ASB-2 (ankyrin repeat and SOCS box containing protein 2, Toll like receptor 9
DAACSSLGCDLG	0	19	0	Keratin associated protein, leucocyte interferon protein, zing finger protein s13, Eph family protein

Table 5-1 Blast search results from selected binding spots from Phage array data. The number of times each particular sequence is bound to PDE4a4 alone or PDE4a4 bound to Apremilast or Roflumilast is shown in the left hand columns.

There are a number of interesting results from the blast searches, one example being that sequence DAACSSLGCDLG only appears to bind to PDE4a4 in the presence of Apremilast. One of the blast hits from this for example is a Keratin

associated protein. Keratin belongs to a family of fibrous structural proteins and is the protein that protects epithelial cells from damage or stress. Studies have shown that it is expressed aberrantly in the suprabasal keratinocytes of psoriatic lesions, compared to in normal epidermis (Fu and Wang 2012).

More interestingly however, some of the blast hits were proteins found in the Ubiquitin protease system, for example TRIM1 (an U3 Ubiquitin ligase) and USP42 (Ubiquitin specific protease 42) as well as some F box proteins which form part of the SCF ubiquitin ligase complex. This is interesting as some F-box proteins are known to be up regulated in some cancers.

As an additional screen, based on a second set of analysis of phage peptide hits binding to PDE4a4 was screened for evidence of the top 10 consensus site motifs using an online consensus motif tool known as MEME or Multiple Em for Motif Elicitation (Bailey, Boden et al. 2009) MEME discovers novel, ungapped motifs (recurring, fixed-length patterns) in nucleotide or protein sequences.
MEME splits variable-length patterns into two or more separate motifs. The first 1000 peptides were sorted and entered into the online tool (figure5-4). Once identified each motif sequence was then synthesised on peptide array as before courtesy of Ruth Macleod (Baillie lab) (figure5-5). Subsequently, any hits from the peptide arrays were then entered into protein Blast search tool to identify any targets in the human proteome (Altschul, Madden et al. 1997). An example of some of the blast results are shown in table 5-2. The motifs found were again associated with some Ubiquitin proteins. For example being HERC2 which is an E3 Ubiquitin protein ligase and Cul7, a component of an E3 ubiquitin ligase complex. This is interesting as peptide array has been used by the Baillie lab to successfully identify ubiquitination sites on PDE4D5 (Li, Baillie et al. 2009).

A

Name	Start	*p*-value	Sites
1	1	3.81E-15	GYMPVVSVVAPG
398	1	1.22E-14	GYMPVVSVVVPG
664	1	2.16E-14	GYMPVVSVVATG
459	1	2.16E-14	GYMPVVSVVGPG
200	1	2.16E-14	GYMPVVSVFAPG
563	1	3.19E-14	GYMPVVSAVAPG
166	1	3.19E-14	GYMPVVSVVSPG
301	1	4.21E-14	GYMPVVSVVASG
572	1	4.46E-14	GYMPVVSDVAPG
825	1	5.61E-14	GYMPVVSVGAPG
178	1	6.55E-14	GYMPVVSGVAP

B

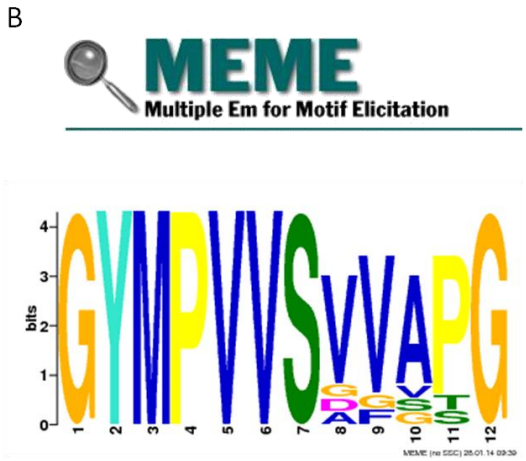

Figure 5-4 Identification of consensus site motifs (a) 1000 peptides that were identified as binding to PDE4a4 were processed using MEME (B) to identify consensus motifs (http://meme.nbcr.net/meme/cgi-bin/meme.cgi). The panel in A) represents data from the one of the core motifs identified from the 12mer peptide library as GYMPVVS which is also shown in B). Example of a consensus site motif that can be developed from the deep Sequencing using MEME.

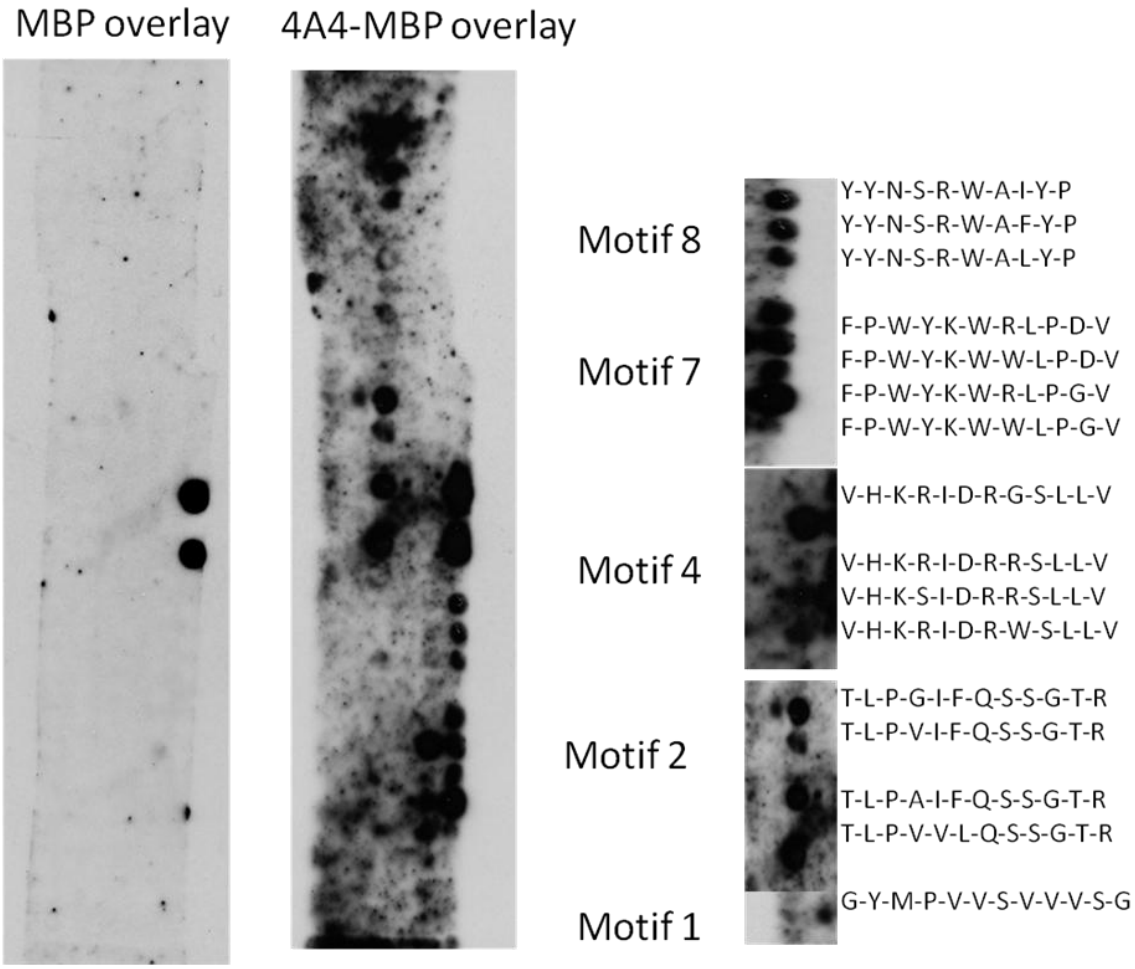

Figure 5-5 PDE4a4 binding to peptide arrays consisting of peptide spots containing identified motifs. Positively interacting peptides generate dark spots, while those that do

not interact leave blank spots. Positive interactions were identified on motifs 1,2,4,7 and 8 on the array.

Motif	Sequence	Blast Results	Description
1	G-Y-M-P-V-V-S-V-V-V-S-G	HERC2	E3 ubiquitin-protein ligase that regulates ubiquitin-dependent retention of repair proteins on damaged chromosomes.
2	T-L-P-V-V-L-Q-S-S-G-T-R	NOC2L	Nucleolar Complex Associated 2 Homolog.Involved in the regulation of p53/TP53-dependent apoptosis.
4	V-H-K-R-I-D-R-W-S-L-L-V	CUL7	Cullin 7. component of an E3 ubiquitin-protein ligase complex.
7	F-P-W-Y-K-W-W-L-P-G-V	ATM	Ataxia telangiectasia mutated (ATM) is a serine/threonine protein kinase that is recruited and activated by DNA double-strand breaks.It initiates activation of the DNA damage checkpoint, leading to cell cycle arrest, DNA repair or apoptosis
8	Y-Y-N-S-R-W-A-L-Y-P	PGRA	Platelet-Derived Growth Factor Receptor, Alpha Polypeptide.Tyrosine-protein kinase that acts as a cell-surface receptor for PDGFA, PDGFB and PDGFC and plays an essential role in the regulation of embryonic development, cell proliferation, survival and chemotaxis. Depending on the context, promotes or inhibits cell proliferation and cell migration.

Table 5-2 Blast results from identified binding motifs.

5.2 Discussion

The data in this chapter has led to the discovery of novel binding motifs that associate with PDE4A4, some of which seem to differentially regulated by Apremilast and Roflumilast (Table 5-1). The most interesting discovery was that many of the motifs are found in proteins that are known to participate in the Ubiquitin Proteosome System (UPS).

The Ubiquitin Proteasome System (UPS) is the main route for targeted destruction of cellular proteins by the proteasome (Hershko 2005) (Ciechanover 2005). It plays a role in protein synthesis and turnover, cell cycle progression, protein localisation, trafficking, DNA repair, sodium channel function, regulating immune and inflammatory responses as well as cellular response to stress (Ciechanover 1998, Ciechanover 2006) (Malik, Price et al. 2006). Ubiquitination marks proteins for ATP-dependent degradation by the 26S proteasome. Aberration of this system can lead to the dysregulation of cellular homeostasis and the development of multiple diseases such as cancer (Adams, Palombella et al. 2000, Hideshima, Bradner et al. 2005, Spano, Bay et al. 2005), neurodegenerative diseases (Ciechanover and Brundin 2003), cardiovascular

disease (Herrmann, Ciechanover et al. 2004, Versari, Herrmann et al. 2006, Zolk, Schenke et al. 2006) as well as inflammatory and autoimmune diseases (Mountz 2002, Colmegna, Sainz et al. 2005). Therefore the UPS provides a rich source of targets for intervention for disease.

The UPS is thought to be involved in the development of inflammatory and autoimmune diseases through multiple pathways, including MHC-mediated antigen presentation, cytokine and cell cycle regulation, and apoptosis (Colmegna, Sainz et al. 2005) and is thought to play a role in inflammatory arthritis, psoriasis, asthma, inflammatory bowel disease and autoimmune thyroiditis (Elliott, Zollner et al. 2003). Therefore the UPS has the potential to be an exciting novel therapeutic target for the treatment of inflammatory and autoimmune diseases and perhaps PDE4 inhibitors such as Apremilast might be useful in this sphere as PDE4s are known to be ubiquitinated. (Li, Baillie et al. 2009) found that PDE4D5 is ubiquitinated, via the discovery of a Ubiquitin interacting motif (UIF) present in the C- terminal portion of PDE4D5. It was also found that the ß-arrestin-sequestered E3 ligase, Mdm2 was critical for this ubiquitination. These UIMs have an important role in directing the ubiquitination of many substrate proteins (Hoeller, Hecker et al. 2007) (Li, Vadrevu et al. 2010).

It is interesting that the ubiquitin/proteasome pathway can be regulated via cAMP-signaling. For example, studies have shown that *in vitro* and *in vivo* elevation of cAMP in rodent skeletal muscle decreased proteasome activity, ubiquitin-protein conjugates, and the levels of atrogin-1, an E3 ubiquitin-ligase that plays a role in muscle atrophy (Goncalves, Lira et al. 2009). Furthermore, inhibition of PDE4 with rolipram, down regulated proteasome activity and suppressed up-regulation of the E3 ubiquitin-ligases atrogin-1 and MuRF-1, induced in rat skeletal muscle by fasting (Lira, Goncalves et al. 2011) . The use of cAMP-PKA signalling to reduce proteasome activity as well as the levels of the two a forementioned E3 ubiquitin-ligases may constitute a novel potential therapeutic approach to treat skeletal muscle atrophy (Lira, Goncalves et al. 2011).

Apremilast and Roflumilast treatments reduce binding of PDE4A4 to a TRIM1 peptide (figure 5-1). TRIM1is an E3 ubiquitin ligase. The link between PDE4 is

exciting because the E3-ligase TRIM family of proteins are known to regulate signalling pathways triggered by innate immune pattern-recognition receptors. (Versteeg, Rajsbaum et al. 2013) demonstrated that many TRIM proteins are important regulators of the innate immune response and that regulatory TRIMs are likely to act at different steps during the induction of IFN and pro-inflammatory cytokines.

One of the other motifs found via the MEME programme that interacts with PDE4A4 belongs to HERC2, another E3 Ligase. This is interesting as it has been shown that HERC2 targets BRCA1, a breast cancer suppressor, for ubiquitination and degradation. HERC2 expression has also been found in breast epithelial cells and breast carcinomas which suggests that it may play a role in breast carcinogenesis (Versteeg, Rajsbaum et al. 2013) . Perhaps, there is a yet to be discovered input from the cAMP signalling system in the function of HERC2 in cancer and if so, Apremilast and Roflumilast may also be useful in the future for treatment for certain cancers via this signalling axis.

A rising theory in the protein science field has been the concept that the majority of amino acid sequences in higher eukaryotes are intrinsically disordered and this allows for specific and rapid adaptation to signalling change required for complex multi-cellular metazoan life (Tompa 2012). It is now recognized that a large proportion of protein-protein interactions are not driven necessarily just through globular domains. There is increasing understanding that protein-protein interaction can be driven through small peptide motifs that form critical interfaces in signalling proteins and that these high affinity protein-protein interactions can be disrupted by small molecules or peptide mimetics (Jubb, Higueruelo et al. 2012). Low throughput peptide phage libraries have in fact given rise to novel peptides that bind with a high affinity to a target protein (Stevens, Lin et al. 2009, Phan, Li et al. 2010).

The data presented in this chapter has provided evidence that Apremilast and Roflumilast can either enhance or decrease the binding of PDE4A4 to specific peptide sequences or motifs that are found in a variety of proteins in the human proteome, most interestingly Ubiquitin-related proteins. The information presented here is preliminary but may be used in the discovery of a novel binding partners for PDE4 or a new role for PDE inhibition in disease. The Baillie

lab has optimized an assay workflow to discover disruptor peptides and have two patents on such agents. Firstly N and C truncations are used to define the “minimum” core binding motif. Each residue in the “core motif” is sequentially substituted with each of the twenty naturally occurring amino acids or a range of apt synthetic non-native replacements. Iterative rounds of substitution of amino acids in key positions that demonstrate enhanced binding, eventually results in a disruptor peptide that has a higher affinity for the protein of interest than does its protein partner in the complex. The final stage is to chemically “cap” the disruptor peptide to further enhance affinity and stability. The peptides can be rendered cell permeable (for experiments involving cell, tissue or animals) by addition of a stearate group at the N-terminal site. Amino acid substitution scan and truncation mutagenesis can be used to optimize the binding of aptamers to each protein of interest.

Phage display therefore, represents an important approach in the development of peptides and peptidomimetics for therapeutics in the future. The information gathered in this chapter therefore will be useful for further study and could lead to the possible development of a new peptidomimetic for use in disease treatment and perhaps further information that could lead to the repositioning of Apremilast to other diseases such as cancer.

6 Final Discussion and Future Perspectives

cAMP signalling plays a critical role in a variety of biologic responses within cells such as inflammation, apoptosis and lipid metabolism (Tasken and Aandahl 2004). In the presence of extracellular inflammatory signals, G protein coupled receptors bind to a variety of ligands and activate adenlyl cyclase, which promotes the production of cAMP (Serezani, Ballinger et al. 2008). CAMP interacts with effector proteins such as PKA and Epac to induce changes in gene expression (Zambon, Zhang et al. 2005) and promote downstream physiological events. Activation of PKA results in the phosphorylation of CREB and ATF-1, with concomitant inhibition of the activity of other promoters such as NFκB (Schafer 2012). Effects on CREB, ATF-1 and NFκB lead to decreased expression of cytokines and other inflammatory mediators as well as the increased expression of anti-inflammatory mediators (Jimenez, Punzon et al. 2001, Serezani, Ballinger et al. 2008). Therefore, cAMP helps to maintain immune homeostasis by modulating the production of pro and anti- inflammatory mediators. On balance, increased cAMP levels leads to a reduction in inflammatory signalling.

Intracellular levels of cAMP are controlled partly by production via adenylyl cyclase, and partly by degradation via cyclic nucleotide phosphodiesterases (PDEs), which are the only enzymes that degrade cAMP (Conti and Beavo 2007). Twenty one genes encoding PDEs have been identified in the human genome, and these have been grouped into 11 PDE families based on their amino acid sequence, structure, enzyme kinetics, modes of regulation and tissue distribution (Conti and Beavo 2007, Houslay 2010). Thus, as central regulators of the intracellular levels of cAMP, several PDEs have been targeted for therapeutic intervention in diseases such as congenital heart failure (Uretsky, Generalovich et al. 1983), erectile dysfunction (Boolell, Gepi-Attee et al. 1996), depression and schizophrenia (Siuciak 2008, Zhang 2009) and in particular, PDE4, for its role in inflammatory disease.

PDE4 plays a particularly important role in inflammatory and immunomodulatory cells and is ubiquitously found in inflammatory cells including mast cells, eosinophils, neutrophils, T cells, macrophages as well as structural cells such as sensory nerves, epithelial , smooth muscle cells and keratinocytes (Torphy 1998) PDE4 has been implicated in a number of inflammatory diseases, including

Psoriasis, psoriatic arthritis, Ankylosing spondylitis, Chronic Obstructive Pulmonary disease (COPD) and Rheumatoid Arthritis (Lipworth 2005, McCann, Palfreeman et al. 2010). PDE4 inhibition elevates intracellular levels of cAMP which then results in the down regulation of inflammatory responses by reducing the expression of TNFα, IL-23 and other pro inflammatory cytokines, whilst increasing anti-inflammatory cytokines such as IL-10 (Houslay, Schafer et al. 2005, Schafer 2012). Therefore PDE4 is of interest as a therapeutic target and a significant number of PDE4 inhibitors have been developed and are currently being investigated for their use in inflammatory disorders such as asthma, chronic obstructive pulmonary disease (COPD), psoriasis, inflammatory bowel disease and rheumatoid arthritis (Souness, Aldous et al. 2000, Page and Spina 2011). Currently marketed PDE4 inhibitors include Apremilast (Otezla®, Celgene corporation)(2014) approved in the United States for treatment of patients with Psoriatic Arthritis (PsA) and Roflumilast (Daliresp®, Forest Pharmaceuticals) for the treatment of Chronic obstructive pulmonary disease (COPD).

The studies in this thesis were conducted to directly compare Apremilast with Roflumilast, in order to substantiate the differences observed in the molecular and cellular effects of these compounds, and to search for mechanisms that underpin differentiating effects.

cAMP is a freely diffusible molecule, and could potentially flood the interior of the cell, leading to the indiscriminate activation of multiple downstream effectors (Houslay, Baillie et al. 2007). It is now accepted that this situation is avoided by the compartmentalisation of cAMP signals. Discrete micro domains of cAMP, created by the actions of phosphodiesterases, have been directly visualised in live cells using genetically encoded cAMP sensors (Zaccolo and Pozzan 2002). PKA is anchored to specific sub cellular targets by its interaction with AKAPs, therefore only particular pools of PKA are exposed to activating concentrations of cAMP at any one time (Baillie 2009). Therefore, signals from a single second messenger can result in the activation of distinct signal transduction pathways, and diverse physiological responses (Buxton and Brunton 1983).

FRET-based cAMP sensors have given considerable insight into the compartmentalisation of cAMP and proteins involved in cAMP signalling (Smith,Langeberg et al. 2006; Baillie 2009; Houslay 2010).

In the first part of my thesis (Chapter 3) I used genetically encoded, FRET-based cAMP sensors to assess dynamic changes in cAMP levels in living cells as a consequence of challenge with Apremilast and Roflumilast to determine whether Apremilast and Roflumilast triggered similar cAMP changes at multiple cellular locations. The data provided a unique opportunity of determining whether there is any selectivity of action between Apremilast and Roflumilast in regulating specific cAMP pools in cells. The data showed for the first time that Apremilast and Roflumilast do appear to regulate different pools of cAMP within the cell, which may cell type specific. For example, my data showed that in HEK 293 and RASFs, Apremilast seems to induce significantly higher levels of cAMP compared to Roflumilast in the cytoplasm. The opposite was found in Jurkat T cells where Roflumilast elevated higher levels of cAMP compared to Apremilast. Apremilast and Roflumilast also exert differential effects in the PKAR1 and PKAR11 which are associated with the cytoplasm and membrane compartments respectively. The most interesting difference revealed from the FRET experiments however, was that in the nucleus of RASFs, Roflumilast significantly elevates cAMP levels whereas Apremilast seems to have little or no effect.

It is clear that cAMP signalling in the nucleus is largely under researched. However, PKA signalling in the nucleus is known to produce distinct biological effects from that of other cellular compartments, for example a study by (Haj Slimane, Bedioune et al. 2014) used FRET probes targeted to the cytoplasm and nucleus to study spatiotemporal dynamics of nuclear cAMP and PKA activity in adult cardiac myocytes and revealed a differential integration of cytoplasmic and nuclear PKA responses to ß-AR stimulation. Therefore, the specific elevation of cAMP by Apremilast and Roflumilast in different cell types may lead to different biological outcomes. An illustratioin of this was shown recently when clear differences in gene expression were noted following treatment with Apremilast and Roflumilast (Schafer, Parton et al. 2014). Gene chip analysis identified that numerous gene sets were regulated by Roflumilast but not Apremilast. It was noted that while Apremilast gene regulation was focused on the inflammatory and immune response, cytokine and chemokine pathways and

stress response genes, Roflumilast exhibited a wider pattern of gene regulation that included ribosomal genes, protein translation and disassembly, and the viral response gene.

Data also showed that Apremilast and Roflumilast exerted differential effects in the PKAR1 (cytoplasm) and PKAR11 (membrane) compartments of RASFs. This was expected due to the differential binding of these inhibitors to the 'high' and 'low' affinity forms of PDE4A4. However other insights into this phenomenon will be provided in the future from molecular modeling of PD4A4 with each inhibitor bound in the active site (PH Schafer, personal communication). It appears Apremilast occupies a different space within the binding pocket to Roflumilast. Apremilast influences the position of Y274, T278, and F279 of the UCR domain of PDE4A4 whereas Roflumilast does not. This could explain why Roflumilast binds more tightly to the high affinity conformer of PDE4A4, but Apremilast binds more tightly to the low affinity conformer. The membrane vs cytosolic distribution could then explain these cAMP compartmentalisation differences. This discrepancy in ligand binding may also contribute to mechanistic differences. During my studies I made PDE4A4 constructs with residues Y274, T278 and F279 mutated to alanine. However, I was unable to do further studies with these mutants due to lack of time. The next step for these studies then, would be to use these mutants along with wild type PDE4A4 to perform phosphodiesterase activity assays, which is a two step radioactive assay of cAMP hydrolysis, previously described by (Marchmont and Houslay 1980). These assays could be used to test the wild type and mutant PDE4A4s in both the membrane and cytosolic fractions of cells to see if this selectivity difference in the high and low affinity conformers would disappear, and perhaps then explain compartmentalisation differences.

Apremilast and Roflumilast are known to mediate their effects in monocytes and T cells via PKA and NF-κB pathways (Kwak, Song et al. 2005, Schafer, Parton et al. 2014). In the second part of the thesis (Chapter 4), I focused on study of the signalling differences caused by Apremilast and Roflumilast by using a number of different biochemical techniques. I found that Apremilast increases the phosphorylation of a number of distinct PKA substrates suggesting possible signalling differences compared to Roflumilast.

In the first part of this chapter I found that Apremilast and Roflumilast both significantly increase CREB phosphorylation in a cell type specific manner. For example, Apremilast and Roflumilast both significantly increase CREB phosphorylation in Jurkat T cells and U937 cells in the presence of forskolin. Whereas, Apremilast along with forskolin treatment in HEK cells increases the phosphorylation of CREB but not Roflumilast in these cells suggesting CREB phosphorylation induced by these inhibitors is cell type specific. I also found that both inhibitors increase the phosphorylation of VASP at Ser157 (a known PKA substrate) in U937 cells in the presence of forskolin. However, in HEK cells only Apremilast in the presence of forskolin increases VASP phosphorylation significantly at Ser157.

This data is consistent with reports that Apremilast and Roflumilast activate the PKA pathway as it is known that PDE4 inhibitors increase intracellular cAMP which leads to the phosphorylation and activation of PKA (Schafer, Parton et al. 2010), which results in the up regulation of CREB and down regulation of NFκB-dependent genes (Houslay, Schafer et al. 2005, Schafer, Parton et al. 2010).

Collectively data from Kinase substrate and Reverse Phase protein arrays showed that only Apremilast increases the phosphorylation of Fyn Y530 and rpS6 Ser240/244 in RASFs and HEK 293 cells, whereas Roflumilast does not significantly increase the phosphorylation of either of these proteins. Analysis performed on the S6 Ribosomal Pathway in HEK 293 cells confirmed this finding by showing that both inhibitors increase the phosphorylation of S6 Kinase p70 and MAPK both which lead to phosphorylation of rpS6.

Further analysis of the rpS6 pathway using pharmacological inhibitors led to the hypothesis that Apremilast and Roflumilast may be regulating different pools of PKA as Apremilast only increases the phosphorylation of rpS6 Ser240/244 significantly, which was found to be mediated via PKA. While both Apremilast and Roflumilast increase the phosphorylation of rpS6 at Ser235/236, which is known to be phosphorylated by PKA directly at this site (Moore, Xie et al. 2009). It is likely that Apremilast-induced increases in the phosphorylation of Fyn, is contributing to the phosphorylation of rpS6 at Ser240/244 as this is found downstream of Fyn in this pathway.

This finding could be significant as rpS6-pS240 is found to be expressed in lesional areas of skin biopsies from patients (Abreu-Velez, Googe et al. 2013) and rpS6-pS240 is thought to influence protein synthesis and/or with the inflammatory/anti-inflammatory immune response in patients affects by skin diseases (Abreu-Velez, Googe et al. 2013).

The combination of Apremilast triggered increases in phosphorylation of rpS6 Ser240 along with the known increases in anti-inflammatory mediators is perhaps the reason that Apremilast has been so successful in psoriasis trials (Papp, Kaufmann et al. 2013). This information along with recent data suggesting a new function for rpS6 phosphorylation in cancer biology (Khalaileh, Dreazen et al. 2013) opens up a possible repositioning space for Apremilast in the future.

A paper recently published by PH Schafer et al (Schafer, Parton et al. 2014) studied the pharmacodynamic properties of Apremilast and it showed that Apremilast had no other identified binding targets other than PDE4. The paper also confirmed that Apremilast mediates its effect in monocytes and T cells via PKA and NF-κB pathways. It modulates gene expression in monocytes, reduces interferon-α production induced by TLR9 signalling in dendritic cells and inhibits cytokine production in T cells.

In the final chapter in my thesis I employed the use Phage Display and the data presented provided evidence that Apremilast and Roflumilast can either enhance or decrease the binding of PDE4A4 to specific peptide sequences or motifs that are found in a variety of proteins in the human proteome, most interestingly Ubiquitin-related proteins. The data is preliminary but may be used in the discovery of a novel binding partner for PDE4 or a new role for PDE inhibition in disease.

6.1 Final Conclusion

Apremilast and Roflumilast are both PDE inhibitors with a high specificity and similar affinity for PDE4 (vs the other 10 PDE families). Work has shown that both drugs do not show a preference for any of the 25 or so isoforms of PDE4, and hence should work in a similar fashion. Studies looking at cAMP production following treatment of both compounds highlighted the fact that there is a

differential cAMP response that may impinge on downstream signalling events. Using cutting-edge biochemical techniques, I set out to investigate the molecular nature of this difference, and my thesis supports the notion that there are not only differences in cAMP dynamics but this also leads to differential PKA substrate phosphorylation and a possible change in PDE4-binding partner profile. These variances are likely due to small but specific differences in binding mode between the two isoforms. My work has provided a unique snapshot of the complexity of the cAMP signalling system and is the first to directly compare action of the two approved PDE4 inhibitors in a detailed way. The work contained in this thesis should act as a stepping-stone for other work that seeks to better investigate the link to PDE4s and the UPS and to better define the significance of rpS6 Ser240/244 phosphorylation induced specifically by Apremilast

7 List of References

(2014). "Apremilast (otezla) for psoriatic arthritis." Med Lett Drugs Ther **56**(1443): 41-42.

Abreu-Velez, A. M., P. B. Googe, Jr. and M. S. Howard (2013). "Ribosomal protein s6-ps240 is expressed in lesional skin from patients with autoimmune skin blistering diseases." N Am J Med Sci **5**(10): 604-608.

Adams, J., V. J. Palombella and P. J. Elliott (2000). "Proteasome inhibition: a new strategy in cancer treatment." Invest New Drugs **18**(2): 109-121.

Ali, M., L. K. Rogers and G. M. Pitari (2015). "Serine phosphorylation of vasodilator-stimulated phosphoprotein (VASP) regulates colon cancer cell survival and apoptosis." Life Sci **123**: 1-8.

Altschul, S. F., T. L. Madden, A. A. Schaffer, J. Zhang, Z. Zhang, W. Miller and D. J. Lipman (1997). "Gapped BLAST and PSI-BLAST: a new generation of protein database search programs." Nucleic Acids Res **25**(17): 3389-3402.

Backs, J., B. C. Worst, L. H. Lehmann, D. M. Patrick, Z. Jebessa, M. M. Kreusser, Q. Sun, L. Chen, C. Heft, H. A. Katus and E. N. Olson (2011). "Selective repression of MEF2 activity by PKA-dependent proteolysis of HDAC4." J Cell Biol **195**(3): 403-415.

Bacskai, B. J., B. Hochner, M. Mahaut-Smith, S. R. Adams, B. K. Kaang, E. R. Kandel and R. Y. Tsien (1993). "Spatially resolved dynamics of cAMP and protein kinase A subunits in Aplysia sensory neurons." Science **260**(5105): 222-226.

Bailey, T. L., M. Boden, F. A. Buske, M. Frith, C. E. Grant, L. Clementi, J. Ren, W. W. Li and W. S. Noble (2009). "MEME SUITE: tools for motif discovery and searching." Nucleic Acids Res **37**(Web Server issue): W202-208.

Baillie, G. S. (2009). "Compartmentalized signalling: spatial regulation of cAMP by the action of compartmentalized phosphodiesterases." FEBS J **276**(7): 1790-1799.

Baillie, G. S., S. J. MacKenzie, I. McPhee and M. D. Houslay (2000). "Sub-family selective actions in the ability of Erk2 MAP kinase to phosphorylate and regulate the activity of PDE4 cyclic AMP-specific phosphodiesterases." Br J Pharmacol **131**(4): 811-819.

Barnes, P. J. and I. M. Adcock (1998). "Transcription factors and asthma." Eur Respir J **12**(1): 221-234.

Baughman, R. P., M. A. Judson, R. Ingledue, N. L. Craft and E. E. Lower (2012). "Efficacy and safety of apremilast in chronic cutaneous sarcoidosis." Arch Dermatol **148**(2): 262-264.

Baumer, W., J. Hoppmann, C. Rundfeldt and M. Kietzmann (2007). "Highly selective phosphodiesterase 4 inhibitors for the treatment of allergic skin diseases and psoriasis." Inflamm Allergy Drug Targets **6**(1): 17-26.

Beavo, J. A. and L. L. Brunton (2002). "Cyclic nucleotide research -- still expanding after half a century." Nat Rev Mol Cell Biol **3**(9): 710-718.

Beavo, J. A., R. S. Hansen, S. A. Harrison, R. L. Hurwitz, T. J. Martins and M. C. Mumby (1982). "Identification and properties of cyclic nucleotide phosphodiesterases." Mol Cell Endocrinol **28**(3): 387-410.

Bender, A. T. and J. A. Beavo (2006). "Cyclic nucleotide phosphodiesterases: molecular regulation to clinical use." Pharmacol Rev **58**(3): 488-520.

Berrera, M., G. Dodoni, S. Monterisi, V. Pertegato, I. Zamparo and M. Zaccolo (2008). "A toolkit for real-time detection of cAMP: insights into compartmentalized signaling." Handb Exp Pharmacol(186): 285-298.

Berridge, M. J. (1984). "Inositol trisphosphate and diacylglycerol as second messengers." Biochem J **220**(2): 345-360.

Berthouze-Duquesnes, M., A. Lucas, A. Sauliere, Y. Y. Sin, A. C. Laurent, C. Gales, G. Baillie and F. Lezoualc'h (2013). "Specific interactions between Epac1, beta-arrestin2 and PDE4D5 regulate beta-adrenergic receptor subtype differential effects on cardiac hypertrophic signaling." Cell Signal **25**(4): 970-980.

Bolger, G. B., G. S. Baillie, X. Li, M. J. Lynch, P. Herzyk, A. Mohamed, L. H. Mitchell, A. McCahill, C. Hundsrucker, E. Klussmann, D. R. Adams and M. D. Houslay (2006). "Scanning peptide array analyses identify overlapping binding sites for the signalling scaffold proteins, beta-arrestin and RACK1, in cAMP-specific phosphodiesterase PDE4D5." Biochem J **398**(1): 23-36.

Bolger, G. B., A. McCahill, E. Huston, Y. F. Cheung, T. McSorley, G. S. Baillie and M. D. Houslay (2003). "The unique amino-terminal region of the PDE4D5 cAMP phosphodiesterase isoform confers preferential interaction with beta-arrestins." J Biol Chem **278**(49): 49230-49238.

Boniface, K., E. Guignouard, N. Pedretti, M. Garcia, A. Delwail, F. X. Bernard, F. Nau, G. Guillet, G. Dagregorio, H. Yssel, J. C. Lecron and F. Morel (2007). "A role

for T cell-derived interleukin 22 in psoriatic skin inflammation." Clin Exp Immunol **150**(3): 407-415.

Boolell, M., S. Gepi-Attee, J. C. Gingell and M. J. Allen (1996). "Sildenafil, a novel effective oral therapy for male erectile dysfunction." Br J Urol **78**(2): 257-261.

Bos, J. L. (2006). "Epac proteins: multi-purpose cAMP targets." Trends Biochem Sci **31**(12): 680-686.

Bradford, M. M. (1976). "A rapid and sensitive method for the quantitation of microgram quantities of protein utilizing the principle of protein-dye binding." Anal Biochem **72**: 248-254.

Brenner, S., S. Prosch, K. Schenke-Layland, U. Riese, U. Gausmann and C. Platzer (2003). "cAMP-induced Interleukin-10 promoter activation depends on CCAAT/enhancer-binding protein expression and monocytic differentiation." J Biol Chem **278**(8): 5597-5604.

Brennesvik, E. O., C. Ktori, J. Ruzzin, E. Jebens, P. R. Shepherd and J. Jensen (2005). "Adrenaline potentiates insulin-stimulated PKB activation via cAMP and Epac: implications for cross talk between insulin and adrenaline." Cell Signal **17**(12): 1551-1559.

Brindle, P., S. Linke and M. Montminy (1993). "Protein-kinase-A-dependent activator in transcription factor CREB reveals new role for CREM repressors." Nature **364**(6440): 821-824.

Brissette, R., J. K. Prendergast and N. I. Goldstein (2006). "Identification of cancer targets and therapeutics using phage display." Curr Opin Drug Discov Devel **9**(3): 363-369.

Butt, E., K. Abel, M. Krieger, D. Palm, V. Hoppe, J. Hoppe and U. Walter (1994). "cAMP- and cGMP-dependent protein kinase phosphorylation sites of the focal adhesion vasodilator-stimulated phosphoprotein (VASP) in vitro and in intact human platelets." J Biol Chem **269**(20): 14509-14517.

Buxton, I. L. and L. L. Brunton (1983). "Compartments of cyclic AMP and protein kinase in mammalian cardiomyocytes." J Biol Chem **258**(17): 10233-10239.

Calverley, P. M., K. F. Rabe, U. M. Goehring, S. Kristiansen, L. M. Fabbri, F. J. Martinez, M and M. s. groups (2009). "Roflumilast in symptomatic chronic obstructive pulmonary disease: two randomised clinical trials." Lancet **374**(9691): 685-694.

Cantarini, L., A. Vitale, P. Scalini, C. A. Dinarello, D. Rigante, R. Franceschini, G. Simonini, G. Borsari, F. Caso, O. M. Lucherini, B. Frediani, I. Bertoldi, L. Punzi, M. Galeazzi and R. Cimaz (2015). "Anakinra treatment in drug-resistant Behcet's disease: a case series." Clin Rheumatol **34**(7): 1293-1301.

Card, G. L., B. P. England, Y. Suzuki, D. Fong, B. Powell, B. Lee, C. Luu, M. Tabrizizad, S. Gillette, P. N. Ibrahim, D. R. Artis, G. Bollag, M. V. Milburn, S. H. Kim, J. Schlessinger and K. Y. Zhang (2004). "Structural basis for the activity of drugs that inhibit phosphodiesterases." Structure **12**(12): 2233-2247.

Carnegie, G. K., C. K. Means and J. D. Scott (2009). "A-kinase anchoring proteins: from protein complexes to physiology and disease." IUBMB Life **61**(4): 394-406.

Chang, C. W., L. Lee, D. Yu, K. Dao, J. Bossuyt and D. M. Bers (2013). "Acute beta-adrenergic activation triggers nuclear import of histone deacetylase 5 and delays G(q)-induced transcriptional activation." J Biol Chem **288**(1): 192-204.

Chao, C. C., S. J. Chen, I. E. Adamopoulos, N. Davis, K. Hong, A. Vu, S. Kwan, L. Fayadat-Dilman, A. Asio and E. P. Bowman (2011). "Anti-IL-17A therapy protects against bone erosion in experimental models of rheumatoid arthritis." Autoimmunity **44**(3): 243-252.

Chien, A. L., J. T. Elder and C. N. Ellis (2009). "Ustekinumab: a new option in psoriasis therapy." Drugs **69**(9): 1141-1152.

Christensen, D. J., E. B. Gottlin, R. E. Benson and P. T. Hamilton (2001). "Phage display for target-based antibacterial drug discovery." Drug Discov Today **6**(14): 721-727.

Chrivia, J. C., R. P. Kwok, N. Lamb, M. Hagiwara, M. R. Montminy and R. H. Goodman (1993). "Phosphorylated CREB binds specifically to the nuclear protein CBP." Nature **365**(6449): 855-859.

Church, M. K. and G. F. Clough (1999). "Human skin mast cells: in vitro and in vivo studies." Ann Allergy Asthma Immunol **83**(5): 471-475.

Ciechanover, A. (1998). "The ubiquitin-proteasome pathway: on protein death and cell life." EMBO J **17**(24): 7151-7160.

Ciechanover, A. (2005). "Intracellular protein degradation: from a vague idea thru the lysosome and the ubiquitin-proteasome system and onto human diseases and drug targeting." Cell Death Differ **12**(9): 1178-1190.

Ciechanover, A. (2006). "The ubiquitin proteolytic system: from a vague idea, through basic mechanisms, and onto human diseases and drug targeting." Neurology **66**(2 Suppl 1): S7-19.

Ciechanover, A. and P. Brundin (2003). "The ubiquitin proteasome system in neurodegenerative diseases: sometimes the chicken, sometimes the egg." Neuron **40**(2): 427-446.

Colmegna, I., B. Sainz, Jr., R. F. Garry and L. R. Espinoza (2005). "The proteasome and its implications in rheumatology." J Rheumatol **32**(7): 1192-1198.

Conti, M. and J. Beavo (2007). "Biochemistry and physiology of cyclic nucleotide phosphodiesterases: essential components in cyclic nucleotide signaling." Annu Rev Biochem **76**: 481-511.

Dal Piaz, V. and M. P. Giovannoni (2000). "Phosphodiesterase 4 inhibitors, structurally unrelated to rolipram, as promising agents for the treatment of asthma and other pathologies." Eur J Med Chem **35**(5): 463-480.

de Rooij, J., F. J. Zwartkruis, M. H. Verheijen, R. H. Cool, S. M. Nijman, A. Wittinghofer and J. L. Bos (1998). "Epac is a Rap1 guanine-nucleotide-exchange factor directly activated by cyclic AMP." Nature **396**(6710): 474-477.

Di Benedetto, G., A. Zoccarato, V. Lissandron, A. Terrin, X. Li, M. D. Houslay, G. S. Baillie and M. Zaccolo (2008). "Protein kinase A type I and type II define distinct intracellular signaling compartments." Circ Res **103**(8): 836-844.

DiPilato, L. M., X. Cheng and J. Zhang (2004). "Fluorescent indicators of cAMP and Epac activation reveal differential dynamics of cAMP signaling within discrete subcellular compartments." Proc Natl Acad Sci U S A **101**(47): 16513-16518.

Dodge-Kafka, K. L., J. Soughayer, G. C. Pare, J. J. Carlisle Michel, L. K. Langeberg, M. S. Kapiloff and J. D. Scott (2005). "The protein kinase A anchoring protein mAKAP coordinates two integrated cAMP effector pathways." Nature **437**(7058): 574-578.

Dodge, K. L., S. Khouangsathiene, M. S. Kapiloff, R. Mouton, E. V. Hill, M. D. Houslay, L. K. Langeberg and J. D. Scott (2001). "mAKAP assembles a protein kinase A/PDE4 phosphodiesterase cAMP signaling module." EMBO J **20**(8): 1921-1930.

Eigler, A., B. Siegmund, U. Emmerich, K. H. Baumann, G. Hartmann and S. Endres (1998). "Anti-inflammatory activities of cAMP-elevating agents:

enhancement of IL-10 synthesis and concurrent suppression of TNF production." J Leukoc Biol **63**(1): 101-107.

Elliott, P. J., T. M. Zollner and W. H. Boehncke (2003). "Proteasome inhibition: a new anti-inflammatory strategy." J Mol Med (Berl) **81**(4): 235-245.

Fabbri, L. M., P. M. Calverley, J. L. Izquierdo-Alonso, D. S. Bundschuh, M. Brose, F. J. Martinez, K. F. Rabe, M and M. s. groups (2009). "Roflumilast in moderate-to-severe chronic obstructive pulmonary disease treated with longacting bronchodilators: two randomised clinical trials." Lancet **374**(9691): 695-703.

Feliciello, A., P. Giuliano, A. Porcellini, C. Garbi, S. Obici, E. Mele, E. Angotti, D. Grieco, G. Amabile, S. Cassano, Y. Li, A. M. Musti, C. S. Rubin, M. E. Gottesman and E. V. Avvedimento (1996). "The v-Ki-Ras oncogene alters cAMP nuclear signaling by regulating the location and the expression of cAMP-dependent protein kinase IIbeta." J Biol Chem **271**(41): 25350-25359.

Feliciello, A., Y. Li, E. V. Avvedimento, M. E. Gottesman and C. S. Rubin (1997). "A-kinase anchor protein 75 increases the rate and magnitude of cAMP signaling to the nucleus." Curr Biol **7**(12): 1011-1014.

Feng, W. G., Y. B. Wang, J. S. Zhang, X. Y. Wang, C. L. Li and Z. L. Chang (2002). "cAMP elevators inhibit LPS-induced IL-12 p40 expression by interfering with phosphorylation of p38 MAPK in murine peritoneal macrophages." Cell Res **12**(5-6): 331-337.

Field, S. K. (2008). "Roflumilast: an oral, once-daily selective PDE-4 inhibitor for the management of COPD and asthma." Expert Opin Investig Drugs **17**(5): 811-818.

Filippa, N., C. L. Sable, C. Filloux, B. Hemmings and E. Van Obberghen (1999). "Mechanism of protein kinase B activation by cyclic AMP-dependent protein kinase." Mol Cell Biol **19**(7): 4989-5000.

Flinn IW, P. M., Wagner-Johnston N, Pandey A, Coffey G, Leeds J, Hollenbach SJ, Levy G and Curnutte J and . (2014). "Pharmacokinetics and pharmacodynamics of the dual Syk/Jak inhibitor PRT062070
(Cerdulatinib) in patients with advanced B cell malignancies." J Clin Oncol, Chicago IL.

Förster, T. (1948). "Intermolecular energy migration and flourescence." Ann Phys **2**: 55-75.

Fu, M. and G. Wang (2012). "Keratin 17 as a therapeutic target for the treatment of psoriasis." J Dermatol Sci **67**(3): 161-165.

Gadue, P., N. Morton and P. L. Stein (1999). "The Src family tyrosine kinase Fyn regulates natural killer T cell development." J Exp Med **190**(8): 1189-1196.
Giembycz, M. A. (2006). "An update and appraisal of the cilomilast Phase III clinical development programme for chronic obstructive pulmonary disease." Br J Clin Pharmacol **62**(2): 138-152.
Gilfillan, A. M. and J. Rivera (2009). "The tyrosine kinase network regulating mast cell activation." Immunol Rev **228**(1): 149-169.
Gillis, S. and J. Watson (1980). "Biochemical and biological characterization of lymphocyte regulatory molecules. V. Identification of an interleukin 2-producing human leukemia T cell line." J Exp Med **152**(6): 1709-1719.
Glaser, T. and J. Traber (1984). "TVX 2706--a new phosphodiesterase inhibitor with antiinflammatory action. Biochemical characterization." Agents Actions **15**(3-4): 341-348.
Gobejishvili, L., S. Barve, S. Joshi-Barve and C. McClain (2008). "Enhanced PDE4B expression augments LPS-inducible TNF expression in ethanol-primed monocytes: relevance to alcoholic liver disease." Am J Physiol Gastrointest Liver Physiol **295**(4): G718-724.
Gomez, G., C. Gonzalez-Espinosa, S. Odom, G. Baez, M. E. Cid, J. J. Ryan and J. Rivera (2005). "Impaired FcepsilonRI-dependent gene expression and defective eicosanoid and cytokine production as a consequence of Fyn deficiency in mast cells." J Immunol **175**(11): 7602-7610.
Goncalves, D. A., E. C. Lira, A. M. Baviera, P. Cao, N. M. Zanon, Z. Arany, N. Bedard, P. Tanksale, S. S. Wing, S. H. Lecker, I. C. Kettelhut and L. C. Navegantes (2009). "Mechanisms involved in 3',5'-cyclic adenosine monophosphate-mediated inhibition of the ubiquitin-proteasome system in skeletal muscle." Endocrinology **150**(12): 5395-5404.
Gonzalez, G. A., K. K. Yamamoto, W. H. Fischer, D. Karr, P. Menzel, W. Biggs, 3rd, W. W. Vale and M. R. Montminy (1989). "A cluster of phosphorylation sites on the cyclic AMP-regulated nuclear factor CREB predicted by its sequence." Nature **337**(6209): 749-752.
Gottlieb, A., N. J. Korman, K. B. Gordon, S. R. Feldman, M. Lebwohl, J. Y. Koo, A. S. Van Voorhees, C. A. Elmets, C. L. Leonardi, K. R. Beutner, R. Bhushan and A. Menter (2008). "Guidelines of care for the management of psoriasis and psoriatic arthritis: Section 2. Psoriatic arthritis: overview and guidelines of care

for treatment with an emphasis on the biologics." J Am Acad Dermatol **58**(5): 851-864.
Gottlieb A, S. B., Krueger J, Rohane P, Zeldis JB, Hu CC, Kipnis C: An, s.-a. p. s. i. p. w. s. p.-t. open-label and a. psoriasis treated with an oral anti-inflammatory agent (2008). "An open-label, single-arm pilot study in patients with severe plaque-type
psoriasis treated with an oral anti-inflammatory agent, apremilast*.
." Curr Med Res Opin 2008, 24:1529–1538 **24**: 1529–1153

Gottlieb, A. B., F. Chamian, S. Masud, I. Cardinale, M. V. Abello, M. A. Lowes, F. Chen, M. Magliocco and J. G. Krueger (2005). "TNF inhibition rapidly down-regulates multiple proinflammatory pathways in psoriasis plaques." J Immunol **175**(4): 2721-2729.
Gottlieb, A. B., B. Strober, J. G. Krueger, P. Rohane, J. B. Zeldis, C. C. Hu and C. Kipnis (2008). "An open-label, single-arm pilot study in patients with severe plaque-type psoriasis treated with an oral anti-inflammatory agent, apremilast." Curr Med Res Opin **24**(5): 1529-1538.
Graham, F. L., J. Smiley, W. C. Russell and R. Nairn (1977). "Characteristics of a human cell line transformed by DNA from human adenovirus type 5." J Gen Virol **36**(1): 59-74.
Gronholm, M., L. Vossebein, C. R. Carlson, J. Kuja-Panula, T. Teesalu, K. Alfthan, A. Vaheri, H. Rauvala, F. W. Herberg, K. Tasken and O. Carpen (2003). "Merlin links to the cAMP neuronal signaling pathway by anchoring the RIbeta subunit of protein kinase A." J Biol Chem **278**(42): 41167-41172.
Ha, C. H., J. Y. Kim, J. Zhao, W. Wang, B. S. Jhun, C. Wong and Z. G. Jin (2010). "PKA phosphorylates histone deacetylase 5 and prevents its nuclear export, leading to the inhibition of gene transcription and cardiomyocyte hypertrophy." Proc Natl Acad Sci U S A **107**(35): 15467-15472.
Haj Slimane, Z., I. Bedioune, P. Lechene, A. Varin, F. Lefebvre, P. Mateo, V. Domergue-Dupont, M. Dewenter, W. Richter, M. Conti, A. El-Armouche, J. Zhang, R. Fischmeister and G. Vandecasteele (2014). "Control of cytoplasmic and nuclear protein kinase A by phosphodiesterases and phosphatases in cardiac myocytes." Cardiovasc Res **102**(1): 97-106.
Halazonetis, T. D., V. G. Gorgoulis and J. Bartek (2008). "An oncogene-induced DNA damage model for cancer development." Science **319**(5868): 1352-1355.

Hamzeh-Mivehroud, M., A. A. Alizadeh, M. B. Morris, W. B. Church and S. Dastmalchi (2013). "Phage display as a technology delivering on the promise of peptide drug discovery." Drug Discov Today **18**(23-24): 1144-1157.

Harootunian, A. T., S. R. Adams, W. Wen, J. L. Meinkoth, S. S. Taylor and R. Y. Tsien (1993). "Movement of the free catalytic subunit of cAMP-dependent protein kinase into and out of the nucleus can be explained by diffusion." Mol Biol Cell **4**(10): 993-1002.

Harvima, I. T., G. Nilsson, M. M. Suttle and A. Naukkarinen (2008). "Is there a role for mast cells in psoriasis?" Arch Dermatol Res **300**(9): 461-478.

Harvima, I. T., H. Viinamaki, A. Naukkarinen, K. Paukkonen, H. Neittaanmaki, R. J. Harvima and M. Horsmanheimo (1993). "Association of cutaneous mast cells and sensory nerves with psychic stress in psoriasis." Psychother Psychosom **60**(3-4): 168-176.

Hastie, A. T., M. Wu, G. C. Foster, G. A. Hawkins, V. Batra, K. A. Rybinski, R. Cirelli, J. G. Zangrilli and S. P. Peters (2006). "Alterations in vasodilator-stimulated phosphoprotein (VASP) phosphorylation: associations with asthmatic phenotype, airway inflammation and beta2-agonist use." Respir Res **7**: 25.

Hatzelmann, A. and C. Schudt (2001). "Anti-inflammatory and immunomodulatory potential of the novel PDE4 inhibitor roflumilast in vitro." J Pharmacol Exp Ther **297**(1): 267-279.

Herrmann, J., A. Ciechanover, L. O. Lerman and A. Lerman (2004). "The ubiquitin-proteasome system in cardiovascular diseases-a hypothesis extended." Cardiovasc Res **61**(1): 11-21.

Hershko, A. (2005). "The ubiquitin system for protein degradation and some of its roles in the control of the cell division cycle." Cell Death Differ **12**(9): 1191-1197.

Hideshima, T., J. E. Bradner, D. Chauhan and K. C. Anderson (2005). "Intracellular protein degradation and its therapeutic implications." Clin Cancer Res **11**(24 Pt 1): 8530-8533.

Hill, E. V., C. L. Sheppard, Y. F. Cheung, I. Gall, E. Krause and M. D. Houslay (2006). "Oxidative stress employs phosphatidyl inositol 3-kinase and ERK signalling pathways to activate cAMP phosphodiesterase-4D3 (PDE4D3) through multi-site phosphorylation at Ser239 and Ser579." Cell Signal **18**(11): 2056-2069.

Hoeller, D., C. M. Hecker, S. Wagner, V. Rogov, V. Dotsch and I. Dikic (2007). "E3-independent monoubiquitination of ubiquitin-binding proteins." Mol Cell **26**(6): 891-898.

Hoffmann, R., G. S. Baillie, S. J. MacKenzie, S. J. Yarwood and M. D. Houslay (1999). "The MAP kinase ERK2 inhibits the cyclic AMP-specific phosphodiesterase HSPDE4D3 by phosphorylating it at Ser579." EMBO J **18**(4): 893-903.

House, C., R. E. Wettenhall and B. E. Kemp (1987). "The influence of basic residues on the substrate specificity of protein kinase C." J Biol Chem **262**(2): 772-777.

Houslay, M. D. (2010). "Underpinning compartmentalised cAMP signalling through targeted cAMP breakdown." Trends Biochem Sci **35**(2): 91-100.

Houslay, M. D. and D. R. Adams (2003). "PDE4 cAMP phosphodiesterases: modular enzymes that orchestrate signalling cross-talk, desensitization and compartmentalization." Biochem J **370**(Pt 1): 1-18.

Houslay, M. D. and D. R. Adams (2010). "Putting the lid on phosphodiesterase 4." Nat Biotechnol **28**(1): 38-40.

Houslay, M. D., G. S. Baillie and D. H. Maurice (2007). "cAMP-Specific phosphodiesterase-4 enzymes in the cardiovascular system: a molecular toolbox for generating compartmentalized cAMP signaling." Circ Res **100**(7): 950-966.

Houslay, M. D., P. Schafer and K. Y. Zhang (2005). "Keynote review: phosphodiesterase-4 as a therapeutic target." Drug Discov Today **10**(22): 1503-1519.

Huai, Q., Y. Liu, S. H. Francis, J. D. Corbin and H. Ke (2004). "Crystal structures of phosphodiesterases 4 and 5 in complex with inhibitor 3-isobutyl-1-methylxanthine suggest a conformation determinant of inhibitor selectivity." J Biol Chem **279**(13): 13095-13101.

Huang, L. J., K. Durick, J. A. Weiner, J. Chun and S. S. Taylor (1997). "D-AKAP2, a novel protein kinase A anchoring protein with a putative RGS domain." Proc Natl Acad Sci U S A **94**(21): 11184-11189.

Huang, L. J., K. Durick, J. A. Weiner, J. Chun and S. S. Taylor (1997). "Identification of a novel protein kinase A anchoring protein that binds both type I and type II regulatory subunits." J Biol Chem **272**(12): 8057-8064.

Hutchinson, J. A., N. P. Shanware, H. Chang and R. S. Tibbetts (2011). "Regulation of ribosomal protein S6 phosphorylation by casein kinase 1 and protein phosphatase 1." J Biol Chem **286**(10): 8688-8696.

Impey, S., S. R. McCorkle, H. Cha-Molstad, J. M. Dwyer, G. S. Yochum, J. M. Boss, S. McWeeney, J. J. Dunn, G. Mandel and R. H. Goodman (2004). "Defining the CREB regulon: a genome-wide analysis of transcription factor regulatory regions." Cell **119**(7): 1041-1054.

Jiang, J. K., K. Ghoreschi, F. Deflorian, Z. Chen, M. Perreira, M. Pesu, J. Smith, D. T. Nguyen, E. H. Liu, W. Leister, S. Costanzi, J. J. O'Shea and C. J. Thomas (2008). "Examining the chirality, conformation and selective kinase inhibition of 3-((3R,4R)-4-methyl-3-(methyl(7H-pyrrolo[2,3-d]pyrimidin-4-yl)amino)piperidin-1-y l)-3-oxopropanenitrile (CP-690,550)." J Med Chem **51**(24): 8012-8018.

Jimenez, J. L., C. Punzon, J. Navarro, M. A. Munoz-Fernandez and M. Fresno (2001). "Phosphodiesterase 4 inhibitors prevent cytokine secretion by T lymphocytes by inhibiting nuclear factor-kappaB and nuclear factor of activated T cells activation." J Pharmacol Exp Ther **299**(2): 753-759.

Jin, S. L. and M. Conti (2002). "Induction of the cyclic nucleotide phosphodiesterase PDE4B is essential for LPS-activated TNF-alpha responses." Proc Natl Acad Sci U S A **99**(11): 7628-7633.

Johnson, M., I. Zaretskaya, Y. Raytselis, Y. Merezhuk, S. McGinnis and T. L. Madden (2008). "NCBI BLAST: a better web interface." Nucleic Acids Res **36**(Web Server issue): W5-9.

Jubb, H., A. P. Higueruelo, A. Winter and T. L. Blundell (2012). "Structural biology and drug discovery for protein-protein interactions." Trends Pharmacol Sci **33**(5): 241-248.

Kamenetsky, M., S. Middelhaufe, E. M. Bank, L. R. Levin, J. Buck and C. Steegborn (2006). "Molecular details of cAMP generation in mammalian cells: a tale of two systems." J Mol Biol **362**(4): 623-639.

Kapiloff, M. S., N. Jackson and N. Airhart (2001). "mAKAP and the ryanodine receptor are part of a multi-component signaling complex on the cardiomyocyte nuclear envelope." J Cell Sci **114**(Pt 17): 3167-3176.

Kasai, H. and O. H. Petersen (1994). "Spatial dynamics of second messengers: IP3 and cAMP as long-range and associative messengers." Trends Neurosci **17**(3): 95-101.

Katsarou-Katsari, A., A. Filippou and T. C. Theoharides (1999). "Effect of stress and other psychological factors on the pathophysiology and treatment of dermatoses." Int J Immunopathol Pharmacol **12**(1): 7-11.

Kehoe, J. W., N. Velappan, M. Walbolt, J. Rasmussen, D. King, J. Lou, K. Knopp, P. Pavlik, J. D. Marks, C. R. Bertozzi and A. R. Bradbury (2006). "Using phage display to select antibodies recognizing post-translational modifications independently of sequence context." Mol Cell Proteomics **5**(12): 2350-2363.

Kemp, B. E., D. J. Graves, E. Benjamini and E. G. Krebs (1977). "Role of multiple basic residues in determining the substrate specificity of cyclic AMP-dependent protein kinase." J Biol Chem **252**(14): 4888-4894.

Khalaileh, A., A. Dreazen, A. Khatib, R. Apel, A. Swisa, N. Kidess-Bassir, A. Maitra, O. Meyuhas, Y. Dor and G. Zamir (2013). "Phosphorylation of ribosomal protein S6 attenuates DNA damage and tumor suppression during development of pancreatic cancer." Cancer Res **73**(6): 1811-1820.

Kohler, D., P. Birk, K. Konig, A. Straub, T. Eldh, J. C. Morote-Garcia and P. Rosenberger (2011). "Phosphorylation of vasodilator-stimulated phosphoprotein (VASP) dampens hepatic ischemia-reperfusion injury." PLoS One **6**(12): e29494.

Krause, M., E. W. Dent, J. E. Bear, J. J. Loureiro and F. B. Gertler (2003). "Ena/VASP proteins: regulators of the actin cytoskeleton and cell migration." Annu Rev Cell Dev Biol **19**: 541-564.

Krieg, J., A. R. Olivier and G. Thomas (1988). "Analysis of 40S ribosomal protein S6 phosphorylation during the mitogenic response." Methods Enzymol **164**: 575-581.

Krueger, G. G., R. G. Langley, C. Leonardi, N. Yeilding, C. Guzzo, Y. Wang, L. T. Dooley, M. Lebwohl and C. P. S. Group (2007). "A human interleukin-12/23 monoclonal antibody for the treatment of psoriasis." N Engl J Med **356**(6): 580-592.

Kwak, H. J., J. S. Song, J. Y. Heo, S. D. Yang, J. Y. Nam and H. G. Cheon (2005). "Roflumilast inhibits lipopolysaccharide-induced inflammatory mediators via suppression of nuclear factor-kappaB, p38 mitogen-activated protein kinase, and c-Jun NH2-terminal kinase activation." J Pharmacol Exp Ther **315**(3): 1188-1195.

Landry, Y., N. Niederhoffer, E. Sick and J. P. Gies (2006). "Heptahelical and other G-protein-coupled receptors (GPCRs) signaling." Curr Med Chem **13**(1): 51-63.

Lee, D. C., D. F. Carmichael, E. G. Krebs and G. S. McKnight (1983). "Isolation of a cDNA clone for the type I regulatory subunit of bovine cAMP-dependent protein kinase." Proc Natl Acad Sci U S A **80**(12): 3608-3612.

Li, X., G. S. Baillie and M. D. Houslay (2009). "Mdm2 directs the ubiquitination of beta-arrestin-sequestered cAMP phosphodiesterase-4D5." J Biol Chem **284**(24): 16170-16182.

Li, X., R. MacLeod, A. J. Dunlop, H. V. Edwards, N. Advant, L. C. Gibson, N. M. Devine, K. M. Brown, D. R. Adams, M. D. Houslay and G. S. Baillie (2009). "A scanning peptide array approach uncovers association sites within the JNK/beta arrestin signalling complex." FEBS Lett **583**(20): 3310-3316.

Li, X., S. Vadrevu, A. Dunlop, J. Day, N. Advant, J. Troeger, E. Klussmann, E. Jaffrey, R. T. Hay, D. R. Adams, M. D. Houslay and G. S. Baillie (2010). "Selective SUMO modification of cAMP-specific phosphodiesterase-4D5 (PDE4D5) regulates the functional consequences of phosphorylation by PKA and ERK." Biochem J **428**(1): 55-65.

Lidqvist, M., O. Nilsson, J. Holmgren, C. Hall and C. Fermer (2008). "Phage display for site-specific immunization and characterization of high-risk human papillomavirus specific E7 monoclonal antibodies." J Immunol Methods **337**(2): 88-96.

Linn, H., K. S. Ermekova, S. Rentschler, A. B. Sparks, B. K. Kay and M. Sudol (1997). "Using molecular repertoires to identify high-affinity peptide ligands of the WW domain of human and mouse YAP." Biol Chem **378**(6): 531-537.

Lipworth, B. J. (2005). "Phosphodiesterase-4 inhibitors for asthma and chronic obstructive pulmonary disease." Lancet **365**(9454): 167-175.

Lira, E. C., D. A. Goncalves, E. S. L. T. Parreiras, N. M. Zanon, I. C. Kettelhut and L. C. Navegantes (2011). "Phosphodiesterase-4 inhibition reduces proteolysis and atrogenes expression in rat skeletal muscles." Muscle Nerve **44**(3): 371-381.

Liu, J., M. Chen and X. Wang (2000). "Calcitonin gene-related peptide inhibits lipopolysaccharide-induced interleukin-12 release from mouse peritoneal macrophages, mediated by the cAMP pathway." Immunology **101**(1): 61-67.

Lovatt, M., A. Filby, V. Parravicini, G. Werlen, E. Palmer and R. Zamoyska (2006). "Lck regulates the threshold of activation in primary T cells, while both Lck and Fyn contribute to the magnitude of the extracellular signal-related kinase response." Mol Cell Biol **26**(22): 8655-8665.

Lowes, M. A., A. M. Bowcock and J. G. Krueger (2007). "Pathogenesis and therapy of psoriasis." Nature **445**(7130): 866-873.

Lugnier, C., T. Keravis, A. Le Bec, O. Pauvert, S. Proteau and E. Rousseau (1999). "Characterization of cyclic nucleotide phosphodiesterase isoforms associated to isolated cardiac nuclei." Biochim Biophys Acta **1472**(3): 431-446.
Lundblad, J. R., R. P. Kwok, M. E. Laurance, M. L. Harter and R. H. Goodman (1995). "Adenoviral E1A-associated protein p300 as a functional homologue of the transcriptional co-activator CBP." Nature **374**(6517): 85-88.
Lynch, M. J., G. S. Baillie and M. D. Houslay (2007). "cAMP-specific phosphodiesterase-4D5 (PDE4D5) provides a paradigm for understanding the unique non-redundant roles that PDE4 isoforms play in shaping compartmentalized cAMP cell signalling." Biochem Soc Trans **35**(Pt 5): 938-941.
Ma, X. T., X. J. Zhang, B. Zhang, Y. Q. Geng, Y. M. Lin, G. Li and K. F. Wu (2004). "Expression and regulation of interleukin-23 subunits in human peripheral blood mononuclear cells and hematopoietic cell lines in response to various inducers." Cell Biol Int **28**(10): 689-697.
Malik, B., S. R. Price, W. E. Mitch, Q. Yue and D. C. Eaton (2006). "Regulation of epithelial sodium channels by the ubiquitin-proteasome proteolytic pathway." Am J Physiol Renal Physiol **290**(6): F1285-1294.
Malmberg, A. B., E. P. Brandon, R. L. Idzerda, H. Liu, G. S. McKnight and A. I. Basbaum (1997). "Diminished inflammation and nociceptive pain with preservation of neuropathic pain in mice with a targeted mutation of the type I regulatory subunit of cAMP-dependent protein kinase." J Neurosci **17**(19): 7462-7470.
Man, H. W., P. Schafer, L. M. Wong, R. T. Patterson, L. G. Corral, H. Raymon, K. Blease, J. Leisten, M. A. Shirley, Y. Tang, D. M. Babusis, R. Chen, D. Stirling and G. W. Muller (2009). "Discovery of (S)-N-[2-[1-(3-ethoxy-4-methoxyphenyl)-2-methanesulfonylethyl]-1,3-dioxo-2,3-dihy dro-1H-isoindol-4-yl] acetamide (apremilast), a potent and orally active phosphodiesterase 4 and tumor necrosis factor-alpha inhibitor." J Med Chem **52**(6): 1522-1524.
Manning, B. D., A. R. Tee, M. N. Logsdon, J. Blenis and L. C. Cantley (2002). "Identification of the tuberous sclerosis complex-2 tumor suppressor gene product tuberin as a target of the phosphoinositide 3-kinase/akt pathway." Mol Cell **10**(1): 151-162.
Mannino (1971). "Chronic disease reports in the morbidity and mortality weekly report (MMWR)." Epidemiol Bull **10**(2): 6-9.

Marchmont, R. J. and M. D. Houslay (1980). "A peripheral and an intrinsic enzyme constitute the cyclic AMP phosphodiesterase activity of rat liver plasma membranes." Biochem J **187**(2): 381-392.

Mason, A. R., J. Mason, M. Cork, G. Dooley and H. Hancock (2013). "Topical treatments for chronic plaque psoriasis." Cochrane Database Syst Rev **3**: CD005028.

Mason, A. R., J. M. Mason, M. J. Cork, H. Hancock and G. Dooley (2013). "Topical treatments for chronic plaque psoriasis of the scalp: a systematic review." Br J Dermatol **169**(3): 519-527.

Mayr, B. and M. Montminy (2001). "Transcriptional regulation by the phosphorylation-dependent factor CREB." Nat Rev Mol Cell Biol **2**(8): 599-609.

McCann, F. E., A. C. Palfreeman, M. Andrews, D. P. Perocheau, J. J. Inglis, P. Schafer, M. Feldmann, R. O. Williams and F. M. Brennan (2010). "Apremilast, a novel PDE4 inhibitor, inhibits spontaneous production of tumour necrosis factor-alpha from human rheumatoid synovial cells and ameliorates experimental arthritis." Arthritis Res Ther **12**(3): R107.

McPhee, I., S. J. Yarwood, G. Scotland, E. Huston, M. B. Beard, A. H. Ross, E. S. Houslay and M. D. Houslay (1999). "Association with the SRC family tyrosyl kinase LYN triggers a conformational change in the catalytic region of human cAMP-specific phosphodiesterase HSPDE4A4B. Consequences for rolipram inhibition." J Biol Chem **274**(17): 11796-11810.

Menter, A., A. Gottlieb, S. R. Feldman, A. S. Van Voorhees, C. L. Leonardi, K. B. Gordon, M. Lebwohl, J. Y. Koo, C. A. Elmets, N. J. Korman, K. R. Beutner and R. Bhushan (2008). "Guidelines of care for the management of psoriasis and psoriatic arthritis: Section 1. Overview of psoriasis and guidelines of care for the treatment of psoriasis with biologics." J Am Acad Dermatol **58**(5): 826-850.

Meyuhas, O. (2008). "Physiological roles of ribosomal protein S6: one of its kind." Int Rev Cell Mol Biol **268**: 1-37.

Miki, K. and E. M. Eddy (1998). "Identification of tethering domains for protein kinase A type Ialpha regulatory subunits on sperm fibrous sheath protein FSC1." J Biol Chem **273**(51): 34384-34390.

Mongillo, M., T. McSorley, S. Evellin, A. Sood, V. Lissandron, A. Terrin, E. Huston, A. Hannawacker, M. J. Lohse, T. Pozzan, M. D. Houslay and M. Zaccolo (2004). "Fluorescence resonance energy transfer-based analysis of cAMP

dynamics in live neonatal rat cardiac myocytes reveals distinct functions of compartmentalized phosphodiesterases." Circ Res **95**(1): 67-75.
Moore, C. E., J. Xie, E. Gomez and T. P. Herbert (2009). "Identification of cAMP-dependent kinase as a third in vivo ribosomal protein S6 kinase in pancreatic beta-cells." J Mol Biol **389**(3): 480-494.
Mountz, J. D. (2002). "Significance of increased circulating proteasome in autoimmune disease." J Rheumatol **29**(10): 2027-2030.
Muller, F. U., J. Neumann and W. Schmitz (2000). "Transcriptional regulation by cAMP in the heart." Mol Cell Biochem **212**(1-2): 11-17.
Navarro, J., C. Punzon, J. L. Jimenez, E. Fernandez-Cruz, A. Pizarro, M. Fresno and M. A. Munoz-Fernandez (1998). "Inhibition of phosphodiesterase type IV suppresses human immunodeficiency virus type 1 replication and cytokine production in primary T cells: involvement of NF-kappaB and NFAT." J Virol **72**(6): 4712-4720.
Nestle, F. O., D. H. Kaplan and J. Barker (2009). "Psoriasis." N Engl J Med **361**(5): 496-509.
Nikolaev, V. O., M. Bunemann, L. Hein, A. Hannawacker and M. J. Lohse (2004). "Novel single chain cAMP sensors for receptor-induced signal propagation." J Biol Chem **279**(36): 37215-37218.
Nikolaev, V. O., S. Gambaryan, S. Engelhardt, U. Walter and M. J. Lohse (2005). "Real-time monitoring of the PDE2 activity of live cells: hormone-stimulated cAMP hydrolysis is faster than hormone-stimulated cAMP synthesis." J Biol Chem **280**(3): 1716-1719.
Nikolaev, V. O. and M. J. Lohse (2006). "Monitoring of cAMP synthesis and degradation in living cells." Physiology (Bethesda) **21**: 86-92.
Nilsson, K. and C. Sundstrom (1974). "Establishment and characteristics of two unique cell lines from patients with lymphosarcoma." Int J Cancer **13**(6): 808-823.
Noren, K. A. and C. J. Noren (2001). "Construction of high-complexity combinatorial phage display peptide libraries." Methods **23**(2): 169-178.
Ohtsubo, K., T. Yamada, L. Zhao, T. F. Jin, S. Takeuchi, H. Mouri, K. Yamashita, K. Yasumoto, N. Fujita, H. Kitagawa, T. Ohta, H. Ikeda and S. Yano (2014). "Expression of Akt kinase-interacting protein 1, a scaffold protein of the PI3K/PDK1/Akt pathway, in pancreatic cancer." Pancreas **43**(7): 1093-1100.

Okamoto, M., H. Takemori and Y. Katoh (2004). "Salt-inducible kinase in steroidogenesis and adipogenesis." Trends Endocrinol Metab **15**(1): 21-26.
Ollivier, V., G. C. Parry, R. R. Cobb, D. de Prost and N. Mackman (1996). "Elevated cyclic AMP inhibits NF-kappaB-mediated transcription in human monocytic cells and endothelial cells." J Biol Chem **271**(34): 20828-20835.
Ozdamar, S. O., D. Seckin, B. Kandemir and A. Y. Turanli (1996). "Mast cells in psoriasis." Dermatology **192**(2): 190.
Page, C. P. and D. Spina (2011). "Phosphodiesterase inhibitors in the treatment of inflammatory diseases." Handb Exp Pharmacol(204): 391-414.
Pande, J., M. M. Szewczyk and A. K. Grover (2010). "Phage display: concept, innovations, applications and future." Biotechnol Adv **28**(6): 849-858.
Papp, K. A., R. Kaufmann, D. Thaci, C. Hu, D. Sutherland and P. Rohane (2013). "Efficacy and safety of apremilast in subjects with moderate to severe plaque psoriasis: results from a phase II, multicenter, randomized, double-blind, placebo-controlled, parallel-group, dose-comparison study." J Eur Acad Dermatol Venereol **27**(3): e376-383.
Parravicini, V., M. Gadina, M. Kovarova, S. Odom, C. Gonzalez-Espinosa, Y. Furumoto, S. Saitoh, L. E. Samelson, J. J. O'Shea and J. Rivera (2002). "Fyn kinase initiates complementary signals required for IgE-dependent mast cell degranulation." Nat Immunol **3**(8): 741-748.
Parry, G. C. and N. Mackman (1997). "Role of cyclic AMP response element-binding protein in cyclic AMP inhibition of NF-kappaB-mediated transcription." J Immunol **159**(11): 5450-5456.
Pathan E, A. S., Van-Rossen L "Efficacy and safety of apremilast, an oral phosphodiesterase 4 inhibitor, in ankylosing spondylitis." Ann Rheum Dis. In press.
Perera, G. K., P. Di Meglio and F. O. Nestle (2012). "Psoriasis." Annu Rev Pathol **7**: 385-422.
Phan, J., Z. Li, A. Kasprzak, B. Li, S. Sebti, W. Guida, E. Schonbrunn and J. Chen (2010). "Structure-based design of high affinity peptides inhibiting the interaction of p53 with MDM2 and MDMX." J Biol Chem **285**(3): 2174-2183.
Platzer, C., E. Fritsch, T. Elsner, M. H. Lehmann, H. D. Volk and S. Prosch (1999). "Cyclic adenosine monophosphate-responsive elements are involved in the transcriptional activation of the human IL-10 gene in monocytic cells." Eur J Immunol **29**(10): 3098-3104.

Polymeropoulos, E. E., Hofgen, N. (1997). "Quantitative Structure-Activity Relationships." **16**(3): 231-234.

Ponsioen, B., J. Zhao, J. Riedl, F. Zwartkruis, G. van der Krogt, M. Zaccolo, W. H. Moolenaar, J. L. Bos and K. Jalink (2004). "Detecting cAMP-induced Epac activation by fluorescence resonance energy transfer: Epac as a novel cAMP indicator." EMBO Rep **5**(12): 1176-1180.

Press, N. J. and K. H. Banner (2009). "PDE4 inhibitors - a review of the current field." Prog Med Chem **47**: 37-74.

Rehmann, H., B. Prakash, E. Wolf, A. Rueppel, J. de Rooij, J. L. Bos and A. Wittinghofer (2003). "Structure and regulation of the cAMP-binding domains of Epac2." Nat Struct Biol **10**(1): 26-32.

Rennard, S. I., N. Schachter, M. Strek, K. Rickard and O. Amit (2006). "Cilomilast for COPD: results of a 6-month, placebo-controlled study of a potent, selective inhibitor of phosphodiesterase 4." Chest **129**(1): 56-66.

Resh, M. D. (1998). "Fyn, a Src family tyrosine kinase." Int J Biochem Cell Biol **30**(11): 1159-1162.

Ritchlin, C., S. A. Haas-Smith, D. Hicks, J. Cappuccio, C. K. Osterland and R. J. Looney (1998). "Patterns of cytokine production in psoriatic synovium." J Rheumatol **25**(8): 1544-1552.

Robichaud, A., P. B. Stamatiou, S. L. Jin, N. Lachance, D. MacDonald, F. Laliberte, S. Liu, Z. Huang, M. Conti and C. C. Chan (2002). "Deletion of phosphodiesterase 4D in mice shortens alpha(2)-adrenoceptor-mediated anesthesia, a behavioral correlate of emesis." J Clin Invest **110**(7): 1045-1052.

Rothe, A., R. J. Hosse and B. E. Power (2006). "In vitro display technologies reveal novel biopharmaceutics." FASEB J **20**(10): 1599-1610.

Roux, P. P., D. Shahbazian, H. Vu, M. K. Holz, M. S. Cohen, J. Taunton, N. Sonenberg and J. Blenis (2007). "RAS/ERK signaling promotes site-specific ribosomal protein S6 phosphorylation via RSK and stimulates cap-dependent translation." J Biol Chem **282**(19): 14056-14064.

Ruf, M. T., A. Andreoli, P. Itin, G. Pluschke and P. Schmid (2014). "Ribosomal protein S6 is hyperactivated and differentially phosphorylated in epidermal lesions of patients with psoriasis and atopic dermatitis." Br J Dermatol **171**(6): 1533-1536.

Ruvinsky, I., N. Sharon, T. Lerer, H. Cohen, M. Stolovich-Rain, T. Nir, Y. Dor, P. Zisman and O. Meyuhas (2005). "Ribosomal protein S6 phosphorylation is a determinant of cell size and glucose homeostasis." Genes Dev **19**(18): 2199-2211.

Sachs, B. D., G. S. Baillie, J. R. McCall, M. A. Passino, C. Schachtrup, D. A. Wallace, A. J. Dunlop, K. F. MacKenzie, E. Klussmann, M. J. Lynch, S. L. Sikorski, T. Nuriel, I. Tsigelny, J. Zhang, M. D. Houslay, M. V. Chao and K. Akassoglou (2007). "p75 neurotrophin receptor regulates tissue fibrosis through inhibition of plasminogen activation via a PDE4/cAMP/PKA pathway." J Cell Biol **177**(6): 1119-1132.

Sadana, R. and C. W. Dessauer (2009). "Physiological roles for G protein-regulated adenylyl cyclase isoforms: insights from knockout and overexpression studies." Neurosignals **17**(1): 5-22.

Saito, Y. D., A. R. Jensen, R. Salgia and E. M. Posadas (2010). "Fyn: a novel molecular target in cancer." Cancer **116**(7): 1629-1637.

Salmond, R. J., J. Emery, K. Okkenhaug and R. Zamoyska (2009). "MAPK, phosphatidylinositol 3-kinase, and mammalian target of rapamycin pathways converge at the level of ribosomal protein S6 phosphorylation to control metabolic signaling in CD8 T cells." J Immunol **183**(11): 7388-7397.

Salmond, R. J., A. Filby, I. Qureshi, S. Caserta and R. Zamoyska (2009). "T-cell receptor proximal signaling via the Src-family kinases, Lck and Fyn, influences T-cell activation, differentiation, and tolerance." Immunol Rev **228**(1): 9-22.

Sample, V., L. M. DiPilato, J. H. Yang, Q. Ni, J. J. Saucerman and J. Zhang (2012). "Regulation of nuclear PKA revealed by spatiotemporal manipulation of cyclic AMP." Nat Chem Biol **8**(4): 375-382.

Samrao, A., T. M. Berry, R. Goreshi and E. L. Simpson (2012). "A pilot study of an oral phosphodiesterase inhibitor (apremilast) for atopic dermatitis in adults." Arch Dermatol **148**(8): 890-897.

Schafer, P. (2012). "Apremilast mechanism of action and application to psoriasis and psoriatic arthritis." Biochem Pharmacol **83**(12): 1583-1590.

Schafer, P. H., A. Parton, L. Capone, D. Cedzik, H. Brady, J. F. Evans, H. W. Man, G. W. Muller, D. I. Stirling and R. Chopra (2014). "Apremilast is a selective PDE4 inhibitor with regulatory effects on innate immunity." Cell Signal **26**(9): 2016-2029.

Schafer, P. H., A. Parton, A. K. Gandhi, L. Capone, M. Adams, L. Wu, J. B. Bartlett, M. A. Loveland, A. Gilhar, Y. F. Cheung, G. S. Baillie, M. D. Houslay, H.

W. Man, G. W. Muller and D. I. Stirling (2010). "Apremilast, a cAMP phosphodiesterase-4 inhibitor, demonstrates anti-inflammatory activity in vitro and in a model of psoriasis." Br J Pharmacol **159**(4): 842-855.

Schett, G., V. S. Sloan, R. M. Stevens and P. Schafer (2010). "Apremilast: a novel PDE4 inhibitor in the treatment of autoimmune and inflammatory diseases." Ther Adv Musculoskelet Dis **2**(5): 271-278.

Schett G, W. J., Papp K (2009). "Apremilast is active in the treatment of rheumatoid arthritis." Arthritis Rheum **60**: 510.

Schett G, W. J., Papp K, Joos R, Rodrigues JF, Vessey AR, Hu C, and d. V. K. Stevens R (2012). "Oral apremilast in the treatment of active psoriatic arthritis: results of a multicenter, randomized, double-blind, placebocontrolled study." Arthritis Rheum **64**: 3156–3167.

Schudt, C., S. Winder, M. Eltze, U. Kilian and R. Beume (1991). "Zardaverine: a cyclic AMP specific PDE III/IV inhibitor." Agents Actions Suppl **34**: 379-402.

Seldon, P. M., P. J. Barnes, K. Meja and M. A. Giembycz (1995). "Suppression of lipopolysaccharide-induced tumor necrosis factor-alpha generation from human peripheral blood monocytes by inhibitors of phosphodiesterase 4: interaction with stimulants of adenylyl cyclase." Mol Pharmacol **48**(4): 747-757.

Sengupta, R., T. Sun, N. M. Warrington and J. B. Rubin (2011). "Treating brain tumors with PDE4 inhibitors." Trends Pharmacol Sci **32**(6): 337-344.

Serezani, C. H., M. N. Ballinger, D. M. Aronoff and M. Peters-Golden (2008). "Cyclic AMP: master regulator of innate immune cell function." Am J Respir Cell Mol Biol **39**(2): 127-132.

Sheibanie, A. F., I. Tadmori, H. Jing, E. Vassiliou and D. Ganea (2004). "Prostaglandin E2 induces IL-23 production in bone marrow-derived dendritic cells." FASEB J **18**(11): 1318-1320.

Sidhu, S. S. (2000). "Phage display in pharmaceutical biotechnology." Curr Opin Biotechnol **11**(6): 610-616.

Siuciak, J. A. (2008). "The role of phosphodiesterases in schizophrenia : therapeutic implications." CNS Drugs **22**(12): 983-993.

Smith, G. P. and V. A. Petrenko (1997). "Phage Display." Chem Rev **97**(2): 391-410.

Souness, J. E., D. Aldous and C. Sargent (2000). "Immunosuppressive and anti-inflammatory effects of cyclic AMP phosphodiesterase (PDE) type 4 inhibitors." Immunopharmacology **47**(2-3): 127-162.

Souness, J. E., M. Griffin, C. Maslen, K. Ebsworth, L. C. Scott, K. Pollock, M. N. Palfreyman and J. A. Karlsson (1996). "Evidence that cyclic AMP phosphodiesterase inhibitors suppress TNF alpha generation from human monocytes by interacting with a 'low-affinity' phosphodiesterase 4 conformer." Br J Pharmacol **118**(3): 649-658.

Souness, J. E., C. Maslen, S. Webber, M. Foster, D. Raeburn, M. N. Palfreyman, M. J. Ashton and J. A. Karlsson (1995). "Suppression of eosinophil function by RP 73401, a potent and selective inhibitor of cyclic AMP-specific phosphodiesterase: comparison with rolipram." Br J Pharmacol **115**(1): 39-46.

Spano, J. P., J. O. Bay, J. Y. Blay and O. Rixe (2005). "Proteasome inhibition: a new approach for the treatment of malignancies." Bull Cancer **92**(11): E61-66, 945-952.

Sparks, A. B., J. E. Rider, N. G. Hoffman, D. M. Fowlkes, L. A. Quillam and B. K. Kay (1996). "Distinct ligand preferences of Src homology 3 domains from Src, Yes, Abl, Cortactin, p53bp2, PLCgamma, Crk, and Grb2." Proc Natl Acad Sci U S A **93**(4): 1540-1544.

Spina, D. (2003). "Phosphodiesterase-4 inhibitors in the treatment of inflammatory lung disease." Drugs **63**(23): 2575-2594.

Spina, D. (2008). "PDE4 inhibitors: current status." Br J Pharmacol **155**(3): 308-315.

Steiner, A. L., D. M. Kipnis, R. Utiger and C. Parker (1969). "Radioimmunoassay for the measurement of adenosine 3',5'-cyclic phosphate." Proc Natl Acad Sci U S A **64**(1): 367-373.

Stevens, C., Y. Lin, B. Harrison, L. Burch, R. A. Ridgway, O. Sansom and T. Hupp (2009). "Peptide combinatorial libraries identify TSC2 as a death-associated protein kinase (DAPK) death domain-binding protein and reveal a stimulatory role for DAPK in mTORC1 signaling." J Biol Chem **284**(1): 334-344.

Stork, P. J. and J. M. Schmitt (2002). "Crosstalk between cAMP and MAP kinase signaling in the regulation of cell proliferation." Trends Cell Biol **12**(6): 258-266.

Sturgill, T. W., L. B. Ray, E. Erikson and J. L. Maller (1988). "Insulin-stimulated MAP-2 kinase phosphorylates and activates ribosomal protein S6 kinase II." Nature **334**(6184): 715-718.

Sunahara, R. K. and R. Taussig (2002). "Isoforms of mammalian adenylyl cyclase: multiplicities of signaling." Mol Interv **2**(3): 168-184.

Sutherland, E. W. and T. W. Rall (1958). "Fractionation and characterization of a cyclic adenine ribonucleotide formed by tissue particles." J Biol Chem **232**(2): 1077-1091.

Suzuki, T., K. T. J, R. Ajima, T. Nakamura, Y. Yoshida and T. Yamamoto (2002). "Phosphorylation of three regulatory serines of Tob by Erk1 and Erk2 is required for Ras-mediated cell proliferation and transformation." Genes Dev **16**(11): 1356-1370.

Takahashi, N., T. Tetsuka, H. Uranishi and T. Okamoto (2002). "Inhibition of the NF-kappaB transcriptional activity by protein kinase A." Eur J Biochem **269**(18): 4559-4565.

Takio, K., S. B. Smith, E. G. Krebs, K. A. Walsh and K. Titani (1984). "Amino acid sequence of the regulatory subunit of bovine type II adenosine cyclic 3',5'-phosphate dependent protein kinase." Biochemistry **23**(18): 4200-4206.

Tanaka, T., H. D. Halicka, X. Huang, F. Traganos and Z. Darzynkiewicz (2006). "Constitutive histone H2AX phosphorylation and ATM activation, the reporters of DNA damage by endogenous oxidants." Cell Cycle **5**(17): 1940-1945.

Tasken, K. and E. M. Aandahl (2004). "Localized effects of cAMP mediated by distinct routes of protein kinase A." Physiol Rev **84**(1): 137-167.

Tasken, K., B. S. Skalhegg, K. A. Tasken, R. Solberg, H. K. Knutsen, F. O. Levy, M. Sandberg, S. Orstavik, T. Larsen, A. K. Johansen, T. Vang, H. P. Schrader, N. T. Reinton, K. M. Torgersen, V. Hansson and T. Jahnsen (1997). "Structure, function, and regulation of human cAMP-dependent protein kinases." Adv Second Messenger Phosphoprotein Res **31**: 191-204.

Taylor, S. S., C. Kim, D. Vigil, N. M. Haste, J. Yang, J. Wu and G. S. Anand (2005). "Dynamics of signaling by PKA." Biochim Biophys Acta **1754**(1-2): 25-37.

Theoharides, T. C. (1990). "Mast cells: the immune gate to the brain." Life Sci **46**(9): 607-617.

Theoharides, T. C. (1996). "The mast cell: a neuroimmunoendocrine master player." Int J Tissue React **18**(1): 1-21.

Theoharides, T. C. and D. E. Cochrane (2004). "Critical role of mast cells in inflammatory diseases and the effect of acute stress." J Neuroimmunol **146**(1-2): 1-12.

Tompa, P. (2012). "On the supertertiary structure of proteins." Nat Chem Biol **8**(7): 597-600.

Torphy, T. J. (1998). "Phosphodiesterase isozymes: molecular targets for novel antiasthma agents." Am J Respir Crit Care Med **157**(2): 351-370.

Uretsky, B. F., T. Generalovich, P. S. Reddy, R. B. Spangenberg and W. P. Follansbee (1983). "The acute hemodynamic effects of a new agent, MDL 17,043, in the treatment of congestive heart failure." Circulation **67**(4): 823-828.

Valjent, E., J. Bertran-Gonzalez, H. Bowling, S. Lopez, E. Santini, M. Matamales, A. Bonito-Oliva, D. Herve, C. Hoeffer, E. Klann, J. A. Girault and G. Fisone (2011). "Haloperidol regulates the state of phosphorylation of ribosomal protein S6 via activation of PKA and phosphorylation of DARPP-32." Neuropsychopharmacology **36**(12): 2561-2570.

van Kuijk, A. W., P. Reinders-Blankert, T. J. Smeets, B. A. Dijkmans and P. P. Tak (2006). "Detailed analysis of the cell infiltrate and the expression of mediators of synovial inflammation and joint destruction in the synovium of patients with psoriatic arthritis: implications for treatment." Ann Rheum Dis **65**(12): 1551-1557.

Van Parijs, L. and A. K. Abbas (1998). "Homeostasis and self-tolerance in the immune system: turning lymphocytes off." Science **280**(5361): 243-248.

Versari, D., J. Herrmann, M. Gossl, D. Mannheim, K. Sattler, F. B. Meyer, L. O. Lerman and A. Lerman (2006). "Dysregulation of the ubiquitin-proteasome system in human carotid atherosclerosis." Arterioscler Thromb Vasc Biol **26**(9): 2132-2139.

Versteeg, G. A., R. Rajsbaum, M. T. Sanchez-Aparicio, A. M. Maestre, J. Valdiviezo, M. Shi, K. S. Inn, A. Fernandez-Sesma, J. Jung and A. Garcia-Sastre (2013). "The E3-ligase TRIM family of proteins regulates signaling pathways triggered by innate immune pattern-recognition receptors." Immunity **38**(2): 384-398.

Vo, V. A., J. W. Lee, J. Y. Kim, J. H. Park, H. J. Lee, S. S. Kim, Y. S. Kwon and W. Chun (2014). "Phosphorylation of Akt Mediates Anti-Inflammatory Activity of 1-p-Coumaroyl beta-D-Glucoside Against Lipopolysaccharide-Induced Inflammation in RAW264.7 Cells." Korean J Physiol Pharmacol **18**(1): 79-86.

Wachtel, H. (1982). "Characteristic behavioural alterations in rats induced by rolipram and other selective adenosine cyclic 3', 5'-monophosphate phosphodiesterase inhibitors." Psychopharmacology (Berl) **77**(4): 309-316.

Wang, H., Y. Liu, Y. Chen, H. Robinson and H. Ke (2005). "Multiple elements jointly determine inhibitor selectivity of cyclic nucleotide phosphodiesterases 4 and 7." J Biol Chem **280**(35): 30949-30955.

Wang, H., M. S. Peng, Y. Chen, J. Geng, H. Robinson, M. D. Houslay, J. Cai and H. Ke (2007). "Structures of the four subfamilies of phosphodiesterase-4 provide insight into the selectivity of their inhibitors." Biochem J **408**(2): 193-201.

Weichhart, T. and M. D. Saemann (2008). "The PI3K/Akt/mTOR pathway in innate immune cells: emerging therapeutic applications." Ann Rheum Dis **67 Suppl 3**: iii70-74.

Williams, J. J. and T. M. Palmer (2012). "Unbiased identification of substrates for the Epac1-inducible E3 ubiquitin ligase component SOCS-3." Biochem Soc Trans **40**(1): 215-218.

Willoughby, D. and D. M. Cooper (2008). "Live-cell imaging of cAMP dynamics." Nat Methods **5**(1): 29-36.

Wong, W. and J. D. Scott (2004). "AKAP signalling complexes: focal points in space and time." Nat Rev Mol Cell Biol **5**(12): 959-970.

Wool, I. G. (1996). "Extraribosomal functions of ribosomal proteins." Trends Biochem Sci **21**(5): 164-165.

Woolley, D. E. (2003). "The mast cell in inflammatory arthritis." N Engl J Med **348**(17): 1709-1711.

Xu, R. X., A. M. Hassell, D. Vanderwall, M. H. Lambert, W. D. Holmes, M. A. Luther, W. J. Rocque, M. V. Milburn, Y. Zhao, H. Ke and R. T. Nolte (2000). "Atomic structure of PDE4: insights into phosphodiesterase mechanism and specificity." Science **288**(5472): 1822-1825.

Yang, H. B., X. Yang, J. Cao, S. Li, Y. N. Liu, Z. W. Suo, H. B. Cui, Z. Guo and X. D. Hu (2011). "cAMP-dependent protein kinase activated Fyn in spinal dorsal horn to regulate NMDA receptor function during inflammatory pain." J Neurochem **116**(1): 93-104.

Yang, J., J. A. Drazba, D. G. Ferguson and M. Bond (1998). "A-kinase anchoring protein 100 (AKAP100) is localized in multiple subcellular compartments in the adult rat heart." J Cell Biol **142**(2): 511-522.

Yang, J. H., R. K. Polanowska-Grabowska, J. S. Smith, C. W. t. Shields and J. J. Saucerman (2014). "PKA catalytic subunit compartmentation regulates contractile and hypertrophic responses to beta-adrenergic signaling." J Mol Cell Cardiol **66**: 83-93.

Yeo, M. G., H. J. Oh, H. S. Cho, J. S. Chun, E. E. Marcantonio and W. K. Song (2011). "Phosphorylation of Ser 21 in Fyn regulates its kinase activity, focal adhesion targeting, and is required for cell migration." J Cell Physiol **226**(1): 236-247.

Yu, R., J. Zhong, M. Li, X. Guo, H. Zhang and J. Chen (2013). "PACAP induces the dimerization of PAC1 on the nucleus associated with the cAMP increase in the nucleus." Neurosci Lett **549**: 92-96.

Zaccolo, M., F. De Giorgi, C. Y. Cho, L. Feng, T. Knapp, P. A. Negulescu, S. S. Taylor, R. Y. Tsien and T. Pozzan (2000). "A genetically encoded, fluorescent indicator for cyclic AMP in living cells." Nat Cell Biol **2**(1): 25-29.

Zaccolo, M. and T. Pozzan (2002). "Discrete microdomains with high concentration of cAMP in stimulated rat neonatal cardiac myocytes." Science **295**(5560): 1711-1715.

Zambon, A. C., L. Zhang, S. Minovitsky, J. R. Kanter, S. Prabhakar, N. Salomonis, K. Vranizan, I. Dubchak, B. R. Conklin and P. A. Insel (2005). "Gene expression patterns define key transcriptional events in cell-cycle regulation by cAMP and protein kinase A." Proc Natl Acad Sci U S A **102**(24): 8561-8566.

Zeller, E., H. J. Stief, B. Pflug and M. Sastre-y-Hernandez (1984). "Results of a phase II study of the antidepressant effect of rolipram." Pharmacopsychiatry **17**(6): 188-190.

Zhang, H. T. (2009). "Cyclic AMP-specific phosphodiesterase-4 as a target for the development of antidepressant drugs." Curr Pharm Des **15**(14): 1688-1698.

Zhang, K. Y., G. L. Card, Y. Suzuki, D. R. Artis, D. Fong, S. Gillette, D. Hsieh, J. Neiman, B. L. West, C. Zhang, M. V. Milburn, S. H. Kim, J. Schlessinger and G. Bollag (2004). "A glutamine switch mechanism for nucleotide selectivity by phosphodiesterases." Mol Cell **15**(2): 279-286.

Zolk, O., C. Schenke and A. Sarikas (2006). "The ubiquitin-proteasome system: focus on the heart." Cardiovasc Res **70**(3): 410-421.

Zurita, A. J., W. Arap and R. Pasqualini (2003). "Mapping tumor vascular diversity by screening phage display libraries." J Control Release **91**(1-2): 183-186.